OSU

SUBSURFACE ELECTROMAGNETIC TARGET CHARACTERIZATION AND IDENTIFICATION

Luen Charm Chan

LEVEL

AD A072491

The Ohio State University

ElectroScience Laboratory

Department of Electrical Engineering
Columbus, Ohio 43212

Technical Report 784722-3

Contract DAAK70-77-C-0114

June 1979

APPROVED FOR PUBLIC RELEASE:
DISTRIBUTION UNLIMITED.

Department of the Army
U.S. Army Mobility Equipment Research and Development Command
Fort Belvoir, Virginia 22060

NOTICES

When Government drawings, specifications, or other data are used for any purpose other than in connection with a definitely related Government procurement operation, the United States Government thereby incurs no responsibility nor any obligation whatsoever, and the fact that the Government may have formulated, furnished, or in any way supplied the said drawings, specifications, or other data, is not to be regarded by implication or otherwise as in any manner licensing the holder or any other person or corporation, or conveying any rights or permission to manufacture, use, or sell any patented invention that may in any way be related thereto.

DISCLAIMER NOTICE

Unclassified

SECURITY CLASSIFICATION OF THIS PAGE (When Data Entered)

REPORT DOCUMENTATION PAGE

READ INSTRUCTIONS BEFORE COMPLETING FORM

1. REPORT NUMBER

2. GOVT ACCESSION NO.

3. RECIPIENT'S CATALOG NUMBER

4. TITLE (and Subtitle)

6 SUBSURFACE ELECTROMAGNETIC TARGET CHARACTERIZATION AND IDENTIFICATION,

5. TYPE OF REPORT & PERIOD COVERED

~~Technical Report~~

6. PERFORMING ORG. REPORT NUMBER

14 ESL-784722-3

7. AUTHOR(s)

10 Luen Charm/Chan

8. CONTRACT OR GRANT NUMBER(s)

DAAK70-77-C-0144

9. PERFORMING ORGANIZATION NAME AND ADDRESS

The Ohio State University ElectroScience Laboratory, Department of Electrical Engineering, Columbus, Ohio 43212

10. PROGRAM ELEMENT, PROJECT, TASK AREA & WORK UNIT NUMBERS

Project #A131/E036/77 7A130270

11. CONTROLLING OFFICE NAME AND ADDRESS

Department of the Army, U.S. Army Mobility Equipment Research and Development Command, Fort Belvoir, Virginia 22060

12. REPORT DATE

April 1979

13. NUMBER OF PAGES

259

14. MONITORING AGENCY NAME & ADDRESS (if different from Controlling Office)

12 276 p.

15. SECURITY CLASS. (of this report)

Unclassified

15a. DECLASSIFICATION/DOWNGRADING SCHEDULE

16. DISTRIBUTION STATEMENT (of this Report)

15 DAAK70-77-C-0114

DISTRIBUTION STATEMENT A

Approved for public release; Distribution Unlimited

17. DISTRIBUTION STATEMENT (of the abstract entered in Block 20, if different from Report)

11 Jun 79

APPROVED FOR PUBLIC RELEASE: DISTRIBUTION UNLIMITED.

18. SUPPLEMENTARY NOTES

The material contained in this report is also used as a dissertation submitted to the Department of Electrical Engineering, The Ohio State University as partial fulfillment for the degree Doctor of Philosophy.

19. KEY WORDS (Continue on reverse side if necessary and identify by block number)

Subsurface radar	Prony's method
Impulse source	Predictor-correlator
Crossed-dipole antenna	Digital processor
Mine-like target	Microcomputer
Complex natural resonances	

20. ABSTRACT (Continue on reverse side if necessary and identify by block number)

A method for subsurface radar target characterization and identification is described. This method characterizes subsurface radar targets by their complex natural resonances which are extracted directly from their backscattered time-domain waveforms. The difference equation coefficients associated with the complex resonances are then used in the predictor-correlator for target identification. Both the characterization and identification processes are extensively tested with real radar measurements and found to yield practical target identification performance. The target identification process is simple and involves→

DD FORM 1 JAN 73 1473 EDITION OF 1 NOV 65 IS OBSOLETE

Unclassified

SECURITY CLASSIFICATION OF THIS PAGE (When Data Entered)

402 251

2.

only simple algebraic operations. Based on the identification process, a "first-generation" microcomputer identification radar system is implemented for target identification in real time. This radar system is found to yield practical identification performance.

ACKNOWLEDGMENTS

The author wishes to express his appreciation to his graudate adviser Professor D.L. Moffatt, and former graudate adviser Professor L. Peters, Jr. for their guidance during the course of this work and for their thorough reading of the original draft of the dissertation. A debt of gratitude is owed to the other member of the reading committee, Professor A.A. Ksienski, for his critical review of the text. Special thanks are also due the author's colleagues, Mr. C.W. Davis, III for his consultations and helpful suggestions; Mr. R. Gaglianello for his help in the implementation of the microcomputer target identification system. Above all, the author wants to express his deepest appreciations to his wife Shu Mee whose seemingly endless patience, understanding and help made this experience of disseration writing much easier.

The material contained in this report is also used as a dissertation submitted to the Department of Electrical Engineering, The Ohio State University as partial fulfillment for the degree Doctor of Philosophy.

TABLE OF CONTENTS

LIST OF TABLES

Table		Page

Table | Page

Table		Page

LIST OF FIGURES

Figure		Page

Figure | Page

Figure		Page

CHAPTER I
INTRODUCTION

A. Research Goals

Subsurface radar detection and identification of geological and man-made structures is an area of current importance. Examples are: location of utility pipes such as plastic and metallic gas pipes and water pipes[1,2,3], location of voids and tunnels[4], anthropology mapping[5], and possible exploration of energy sources such as oil, gas and coal. Yet, almost all of the work done in this area was directed toward target detection. Few attempted the problem of target identification. Subsurface target identification is a problem far more severe than the identification of aerospace targets by conventional radars where the target can literally be seen and the class of false targets is limited in scope. Underground there are varities of unknown false or undesired targets to complicate the task. Furthermore, the medium involved, i.e., the ground, is usually lossy, inhomogeneous and, most of all, electrically weather-dependent. These problems, together with the presence of the air-ground interface makes the task of subsurface target identification truly formidable. It is for these reasons that, to date, there is no single technique or system capable of identifying subsurface targets in real time.

In this study, a technique for subsurface target identification is developed and extensively tested with real radar measurements collected using a video pulse radar[1-4] under different conditions (i.e., different ground conditions, different antennas, etc.). This technique is implemented with a "first-generation" microcomputer system to demonstrate the feasibility of real-time subsurface target identification.

The technique used in this study characterizes subsurface targets by their complex natural resonances[7-11], which are extracted directly from the processed time domain waveforms via Prony's Method[12-15]. A predictor-correlator[40] uses the difference equation coefficients associated with these complex resonances as discriminants to generate a correlation coefficient for target identification. This characterization and identification method is attractive for it characterizes the response of a target by a set of complex numbers which is independent of the pulse radar location. Furthermore, the complex resonances and the difference equation coefficients are pre-determined, thus, only simple algebraic operations are involved in calculating the correlation coefficient for a real-time identification decision.

B. Related Research in Subsurface Target Characterization and Identification

Electromagnetic techniques have been used successfully for many years for probing the earth. Keller and Freschnecht[25] give an excellent summary of these procedures. A recent summary of subsurface probing techniques is given in a report by D.C. Gates, et al.[26].

Perhaps the earliest documentation of a subsurface electronagnetic radar system is contained in a patent issued in 1937 in which an electrical analog of seismic systems is described[16]. There is, however, no mention of successful implementation of such a radar. There have been attempts to use bistatic radar configurations of this type but the results have generally not been highly successful[17,18]. The reason, recognized by Horton[19], is that the tail of the pulse coupled directly from the transmit to the receive antenna occurs "just at the time when the maximum of the reflected pulse (from a buried target) must be accurately timed. This coincidence tends to ruin the measurement".

A significant result in video pulse technology is described in a patent by Lerner in which a video pulse system is used for more moderate depths[20]. Lerner's scheme differed from the earlier patent in that the same antenna was used for both transmitting and receiving. Lerner introduced a combination of TR, ATR and Hybrids to separate the transmitted pulse and the received target signal.

In this study, a crossed-dipole antenna system is used to incorporate this function into the antenna itself, i.e., transmit-receive isolation is achieved by isolating the antennas themselves. The crossed dipole is an orthogonal dipole pair, one horizontal dipole for transmission and another orthogonal horizontal dipole for reception, which provides substantial reduction of the primary (directly coupled) signal on the receiving antenna. Many measurements have been made on a variety of shallow targets (less than 15 m) using these concepts[1-4,21,22]. Targets include geological structures such as faults, joints, sink holes and man-made structures such as pipes. A commercial unit for pipe detection based upon the research and design work at the ElectroScience Laboratory, and designated as Terrascan, is being produced by Microwave Associates Inc.[6]. The pulse radar used in this study for subsurface target identification is a Terrascan-like radar system.

A major reason for the success of the characterization and identification procedures discussed in this dissertation lies in the improvements in the antenna system. The original cross-type antenna structure developed at the ElectroScience Laboratory for subsurface radar applications was basically a crossed bowtie geometry wrapped aroung a sphere[21], but this was subject to noise. The crossed bowtie

evolved into various planar crossed-dipole arrangements as used by Moffatt[4]. These arrangements were, however, too awkward for use in real-time on-location target identification. Later, Young[1,3] introduced the loaded folded dipole geometry of the Terrascan system. Tribuzi[66] improved this by introducing the loaded folded bowtie configuration. Wald[59] further improved the electrical characteristics of this structure by eliminating part of the supporting structure. He also constructed the small antenna used in a later part of this dissertation for identification of mines. The design of the smaller antenna was dictated by the results obtained in this dissertation since its purpose was to shift the antenna resonance to more nearly coincide with those of the mine-like target.

One of the first studies initiated in the development of the pulse radar system with the crossed-dipole antenna for subsurface target detection and identification was the detection and identification of TDMB mines[28-35]. This study included efforts in the development of antenna systems and techniques to extract the characteristic spectra of the electromagnetic fields scattered by the TDMB mine. In 1970, Sullivan[21] investigated the feasibility of using the characteristic real-frequency resonances of subsurface targets in the identification of simple buried objects. The system used in Sullivan's study was a video pulse radar with a crossed-polarized antenna system. A similar system using crossed dipoles was later used by Moffatt, et al.[4] in the probing of man-made and geological subsurface targets. The subsurface video pulse radar system was then modified and developed to be the existing Terrascan system in a study to detect gas pipes[1-3]. To automate the Terrascan system for automatic target identification, Chan[22] investigated a matched filter technique for automatic identification of plastic pipes using a Terrascan-like radar system.

Other methods have been employed in the detection and identification of subsurface targets. In particular, various techniques of Pattern recognition[37-39] were used by Echard, et al. for the detection and identification of buried mines[36].

This study investigated the possibility of using in situ target complex natural resonances to characterize and identify subsurface targets. The basic method was first introduced by Hill[40] in the detection of targets near the surface of the earth, and later used by Chan, et al.[23,48-50] in the characterization and identification of subsurface targets.

C. Structure of This Report

The structure of this report is as follows:

In chapter II, the basic radar measurement procedure is persented. In addition, preliminary signal processing is discussed since certain preprocessing does improve the target identification results.

In Chapter III, we present a method for extracting from response data records (i.e., the time-domain waveforms) the complex natural resonances associated with the targets. This method, known as Prony's method, is outlined and applied to extract target resonances from the backscattered waveforms in the time domain.

In Chapter IV, the predictor-correlator method for target identification is discussed and applied to the waveforms collected in this study. Detail identification statistics are given.

In Chapter V, the effects of radar bandwidth on the characterization and identification method are studied.

In Chapter VI, the effects of target size and depth on the characterization and identification method are discussed.

In Chapter VII, we direct attention to the detecion and identification of mine-like targets in practical situations. Improvements on the pulse radar system are made for the implementation of a portable, real-time on-location subsurface target identification radar.

In Chapter VIII, we discuss the implementation of the subsurface identification radar as a microcomputer system. Detailed prodecures of the implementation are presented. Real-time target identification results using the microcomputer system are given.

In Chapter IX, a method for automatic tuning of the identification radar to the ground condition in real time is discussed. This method is simple and can be easily incorporated into the microcomputer system for real-time subsurface target identification.

In Chapter X, major achievements accomplished in this work are summarized. Conclusions and recommendations are made.

CHAPTER II
MEASURED AND PROCESSED WAVEFORMS FROM THE SUBSURFACE TARGETS

A. Objectives

The objectives of this chapter are the following:

1. To give a description of the subsurface pulse radar and the subsurface targets selected for this study and to summarize the procedures taken to measure the backscattered waveforms from these targets. Raw (unprocessed) waveforms from the targets are shown.

2. To summarize the signal-processing techniques used to partially suppress noise and clutter in the raw waveforms. Processed waveforms are given.

B. Subsurface Electromagnetic Video Pulse Radar System

The video pulse radar system used to collect measurements for this study basically consists of three components: the energy source, the antenna system for signal transmitting and receiving and the receiver for signal processing. The design of these components is dictated by the electrical properties of the ground, the depth of the target of interest as well as the target, clutter and noise characteristics. A picture of the Terrascan-like subsurface pulse radar used in this study together with a basic block diagram is shown in Figure 1. The basic components are: the impulse generator, the crossed-dipole antenna system and the receiver. Basic operation is as follows. The impulse generator transmits short pulses of energy through the transmit antenna into the ground. The presence of a target scatters the incident energy toward the receive antenna. This scattered energy is received as a sampled time-domain waveform for target characterization and identification.

In the current study a short video pulse of approximately 150 ps duration (at 3 dB points) and a nominal 1000V peak amplitude was used (see Figure 2). This pulse duration is much shorter than those used in conventional radar practice. Furthermore, a conventional radar has a few percent bandwidth about its carrier

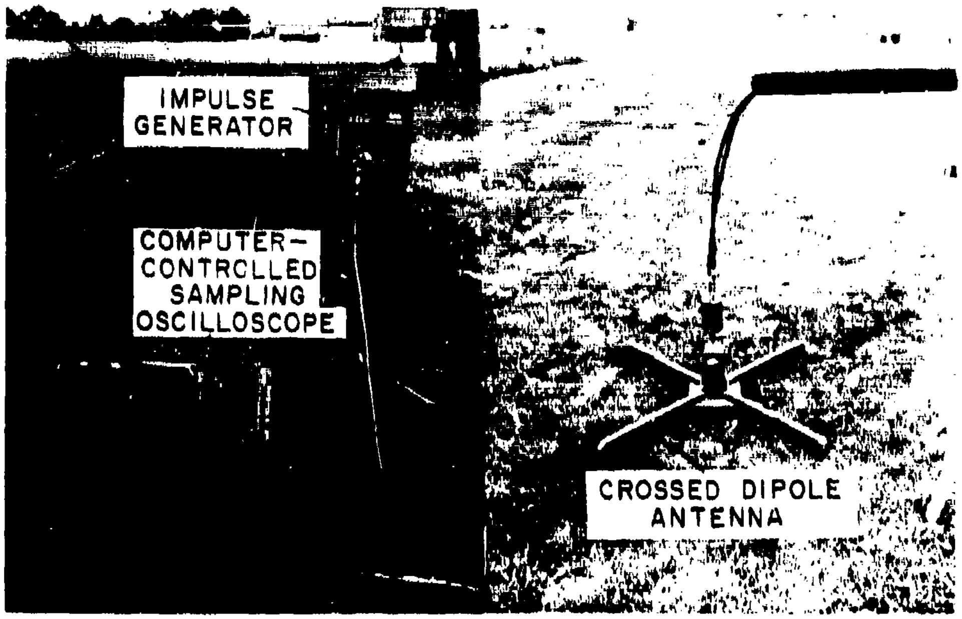

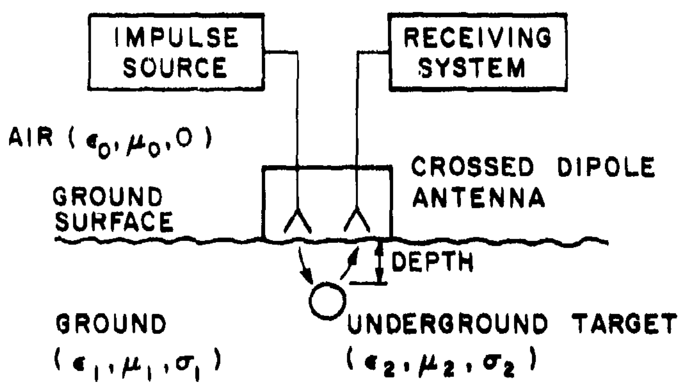

Figure 1. The subsurface pulse radar and its block diagram.

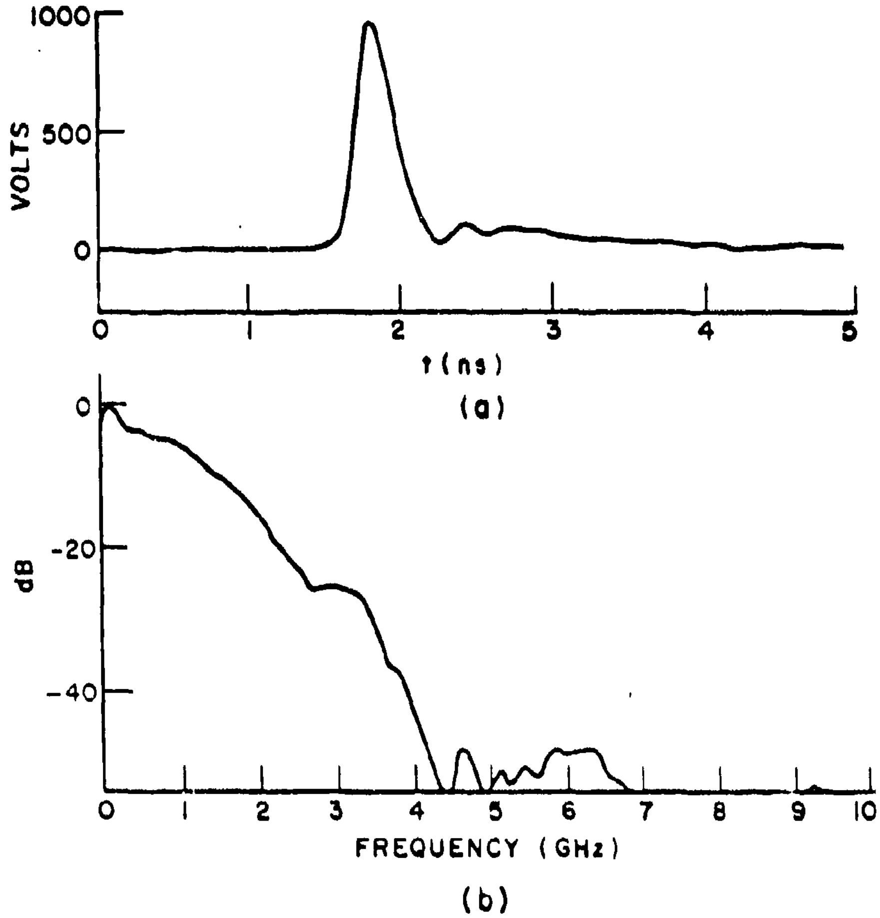

Figure 2. Characteristics of the impulse source in time and frequency domain.

frequency whereas this video pulse output spectrum spreads from essentially dc (repetition rate = 256 Hz) to beyond 3 GHz. It is this broad band of frequencies inherent in this narrow pulse that makes target identification a possibility, i.e., the scattered fields from the targets can be sampled over a very broad frequency band and each sample contains information about the targets. The use of such a narrow pulse also has a second substantial advantage for the detection and identification of shallow targets, in that the transmitted pulse magnitude has fallen to a low value before the pulse reflected from the target returns to the antenna. This "time isolation" effectively minimizes the width of the radar "dead zone" and enables the scattered pulse to be observed over a wide time span. A second form of isolation exists in the choice of the antenna system. The pulse radar uses a pair of crossed, loaded, folded dipoles with 0.6m (2 feet) long arms lying flush with the ground surface (see Figure 1). The crossed-dipole antenna system achieves substantial isolation between transmit and receive antennas. For a perfectly orthogonal pair and no target perturbation, the transmitted pulse would not be observed on the receive antenna. In practice, antenna isolation on the order of 60 dB below the nominal pulser voltage is achieved routinely. Such isolation further minimizes the width of the "dead zone" and is essential for shallow-depth target identification. The dipoles are heavily loaded, with both resistors and incorporated absorber in the antenna to reduce multiple reflections and consequently reduce pulse distortion caused by the antenna. The crossed-dipole antenna system has two additional advantages for the identification of subsurface targets. First, being a cross-polarized system it is insensitive to reflections from layers which are parallel to the antenna arms. An important example is the ground surface whose reflection of the incident pulse energy would produce extraneous signals in other non-orthogonal systems. Second, received waveforms obtained from objects which have no symmetry with respect to the antenna arms go through a polarity reversal as the crossed-dipole antenna system is rotated (about its vertical axis) by 90°. This feature represents a valid method by which a target can be separated from an extended no-target echo which is introduced by multiple reflections on the antenna structure[3].

Typical raw time-domain waveforms received with the antenna oriented at 0° and at 90° over the center of a plastic mine-like target are shown in Figure 3. Several waveform features can be described. The first sharp impulsive-type portion of the waveform is due to direct coupling between the transmit and receive antennas. From the amplitude of the coupling signal and the pulser output, it

---

*A smaller antenna (0.15 m) is later used for a more specific purpose of mine identification.

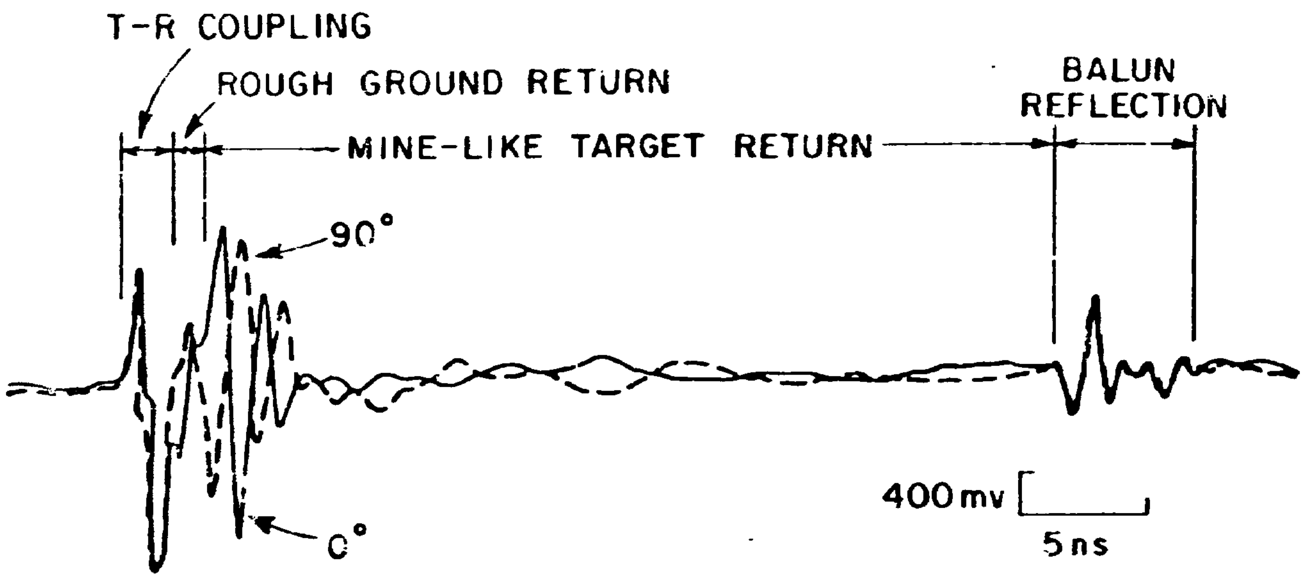

Figure 3. Typical raw waveform received by the pulse radar system.

is seen that about 60 dB isolation is achieved. Note that this signal does not change significantly with antenna orientation and thus can be removed by forming the difference of the two waveforms. The coupling signal is a source of clutter but it is also useful as a time reference for target depth and range, since it occurs at essentially the time the source impulse is radiated from the feed terminals of the transmit antenna. The next feature of the waveform beyond the impulse is the random clutter due to the ground surface irregularities directly beneath the antenna. Because of the short duration of the impulse and good antenna design, this clutter feature dies out in a few nanoseconds. Thus, only a small portion of the clutter overlaps the return from the mine-like target. The signal from the mine-like target appears to be rather strong. Furthermore, it reverses polarity when the antenna is rotated by 90°, thus, its amplitude will double in the difference waveform. The mine-like target signal extends through a time window of approximately 30 ns and falls to a negligible level at the time the balun reflection occurs. The balun is necessary for connecting the unbalanced impulse generator to the balanced dipole antenna. The impedance mismatch at this connection is the source of the balun reflection. The balun reflection limits the width of the reflectionless time window of the system. In the present system, the width of the reflectionless time window is 36.5 ns, which turned out to be wide enough for the identification of the shallow subsurface targets considered in this study. For a wider window, one can lengthen the delay cable at the balun-antenna connection. One can also greatly suppress the effects of the balun reflection by shortening the length of the delay cable at the balun-antenna connection. In this case, the balun reflection would occur in the time region where the target signal is much higher in amplitude. In a later section, we describe a smaller antenna which was used for improved target identification performance. This small antenna was built with the delay cable shortened and the balun structure placed almost at the antenna feed points. The balun reflection can be completely eliminated if a balanced pulser is made available in the future. Elimination of the balun would also yield a narrower transmitted pulse due to less cable loss and dispersion.

An unprocessed time-domain waveform is present in the receiver for target characterization and identification. The structure of the receiver basically consists of a sampling oscilloscope for signal reception, a signal-processing unit for clutter and noise reduction and a unit for target characterization and identification. In this study, because of the flexibility it offered, a general-purpose digital computer was first used to control the sampling oscilloscope and to implement the processing, characterization and identification units. After all of the target characterization and identification procedures had been established, much of the flexibility was discarded and a relatively simple system designed for target detection and identification. Such a system was implemented with a microcomputer for target identification in real time. Discussion of the microcomputer system is presented in Chapter VIII.

C. The Subsurface Targets

Five targets of similar size were buried at the same depth of 5 cm (2 inches, measured from the ground surface to the nearest target surface). Figure 4 shows the geometry of the targets.

All targets were buried in the backyard of the ElectroScience Laboratory at points where the ground is known to be relatively undisturbed (i.e., free of other objects). The average dc conductivity within 30 cm (12 inches) of the ground surface measured at the target sites ranged from 30 mS/m for wet ground to about 20 mS/m for dry ground and 10 mS/m for icy ground. The relative dielectric constant measured at approximately 100 MHz ranged from 25 for wet ground to 16 for dry ground and 9 for icy ground.

Since a goal of this study was to achieve separation of a mine-like target from other (false) targets using radar data, a major effort was directed toward the study of the mine-like target. The method of identification developed here can easily be adapted to systems in which other targets are considered as desired targets or targets to be separated.

Backscattered waveforms were obtained using the subsurface pulse radar system. Measurements were made at different ground locations with respect to the various targets. Locations of the antenna center for these measurements are shown as dots in Figure 5. At each location two backscattered waveforms were obtained using two different antenna orientations, one of which was a 90° rotation with respect to the other. A standard antenna orientation used in obtaining the measurements is shown in Figure 5. Measurements were obtained with the antenna center vertically above the center and edges of the targets. Beyond the target edges, measurements were made at the regular interval of 15 cm (6 inches).

Data accumulation was started in early June 1977 and continued through early April 1979. During this period the ground condition changed from wet to dry and to icy. Data were obtained for each ground condition to gauge the effects of the changing ground condition on the characterization and identification of the subsurface targets.

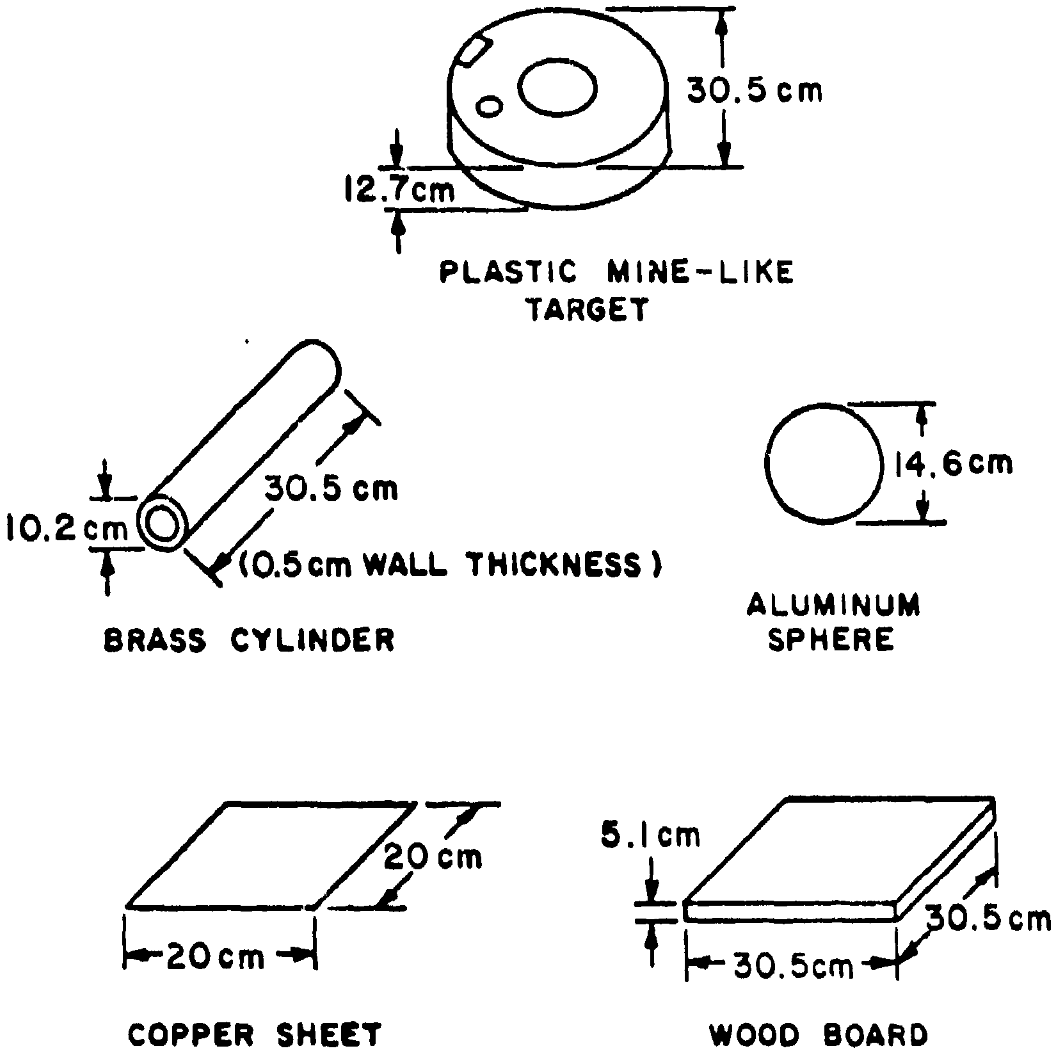

Figure 4. Physical characteristics of the subsurface targets.

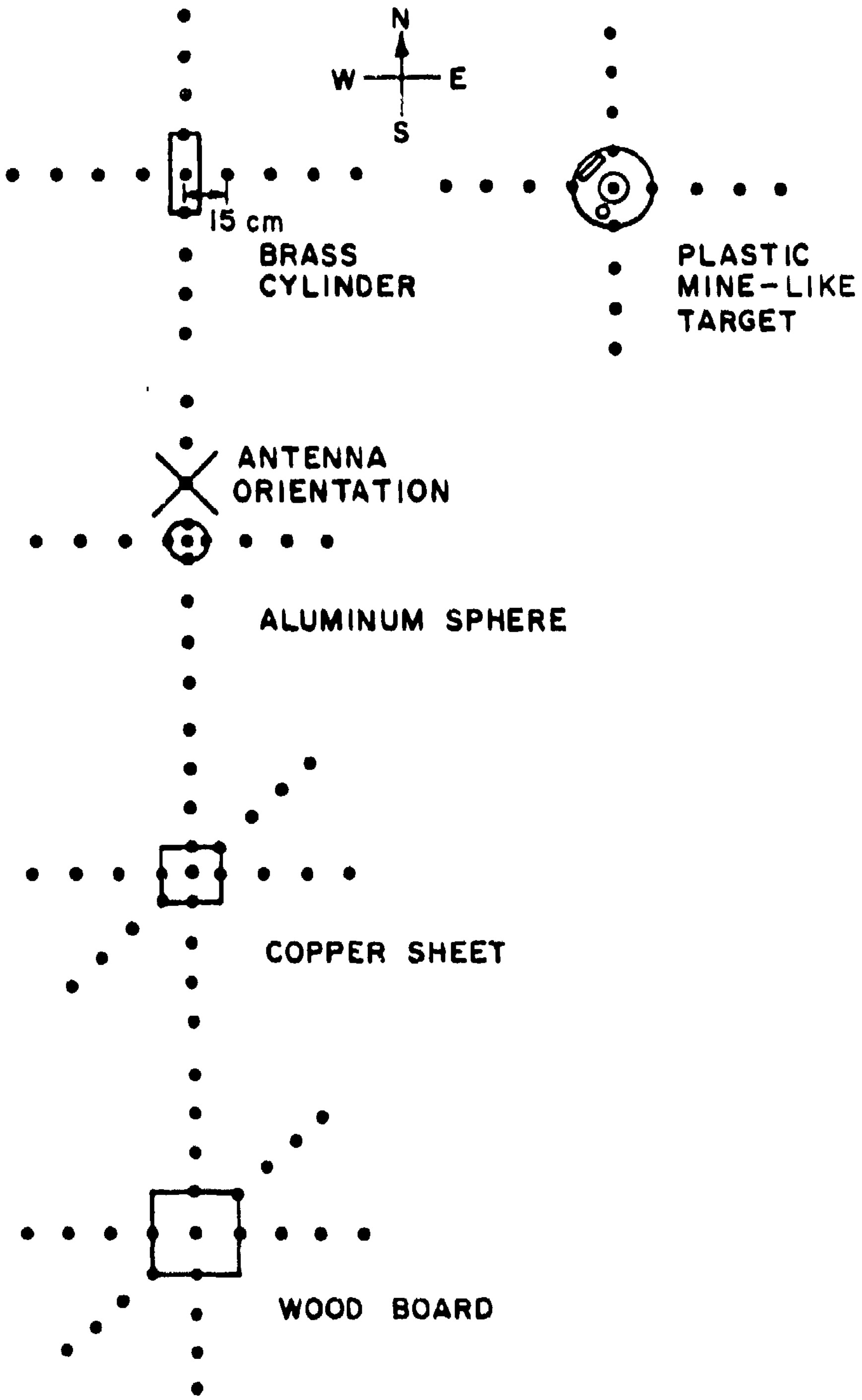

Figure 5. Measurement locations and antenna orientation.

D. Raw Measured Waveforms

All waveforms collected by the Terrascan-like radar used in this study consist of 256 samples in a time window of 50 ns. The (hardware) basic sampling period T_B is 0.2 ns, giving a sampling frequency of 5.12 GHz*.

There are three possible classes of signals present in these raw waveforms.

1. Noise: noise refers to extraneous signals which are not in any way related to the radar source signal. Examples are thermal noise, interference, etc.

2. Clutter: clutter refers to extraneous signals which are related to the radar source. Examples are transmit-receive coupling, reflection from ground surface irregularities, and echoes from objects other than the desired target.

3. Desired Signal: desired signal refers to echoes of the incident source energy from the desired target.

For shallow targets the desired signal may include direct reflections from the target and multiple reflections between the target and the antenna. Since the antenna is so near the target, the antenna radiation mechanisms and the target scattering mechanisms may not be distinct.

Noise and clutter are the extraneous signals that the signal-processing unit is designed to suppress under certain conditions.

The scattered fields from the targets, both desired and undesired, plus noise and clutter produce a signal at the terminals of the receive antenna. In most conventional receivers noise is reduced by the introduction of filters. For broad-band signals this is not possible but noise is reduced substantially by averaging a number of received waveforms. In general, however, for this antenna system even in our local urban environment where many strong interfering signals exist, the voltage pulse caused by the scatterer is clearly visible on the oscilloscope. In the subsurface pulse radar system, due to the low sensitivity of the antenna system to above-

---

*Waveforms collected by the microcomputer system consist of 128 samples in a time window of 25 ns. The microcomputer system is discussed in Chapter VIII.

ground disturbances, the noise level is inherently low. Furthermore, it was found that a simple arithmetic averaging process is an effective means for reducing noise[22,24]. This means of course that the noise is not target-induced.

Typical average raw waveforms are shown in Figure 6. The second waveform (---) in each figure is obtained by rotating the antenna by 90°. If the observed signal is caused by direct coupling between the transmit and receive antenna (T-R coupling), the signal would not be changed by this rotation. On the other hand if the signal is caused by any external scatterer, a polarity reversal is observed. These raw waveforms illustrate the various classes of signals. Figure 6-a shows a no-target waveform which is a received waveform with no target (desired or undesired) present within the radar range. Such a waveform, after averaging, contains clutter only. Figure 6-b shows a waveform from the desired mine-like target. In this waveform, the T-R coupling and the ground surface clutter occur early in time and because of the shallow target depth a certain portion of the desired signal is overlapped by the clutter. It is these extraneous signals that various signal-processing techniques are designed to suppress. Figure 6-c shows a waveform from the brass cylinder.

E. Processed Waveforms

Before proceeding to the target identification algorithms, a certain amount of preprocessing of the data is desirable. This is essential here since the goal is to obtain the purest scattering data possible for target characterization. These steps are made possible by the availability of a computer in the measuring system. The data processing will not all be essential in a field system to detect and identify such targets. It is envisioned that any such preprocessing that may be required can be done in a microcomputer which will be a part of the final system. The preprocessing here included:

1. Arithmetic averaging: this process forms the arithmetic average of ten raw waveforms at the same antenna location and orientation.

2. Amplitude shift: any dc drift in the waveforms is corrected by adjusting the base line.

3. Gating: the time regions before the T-R antenna coupling and after the first balun reflection are replaced by a straight line at zero level. The resulting "effective" time window (same for all waveforms) is 36.5 ns wide (186 samples).

4. Time shift: the effective time window is shifted to the same time region for all waveforms.

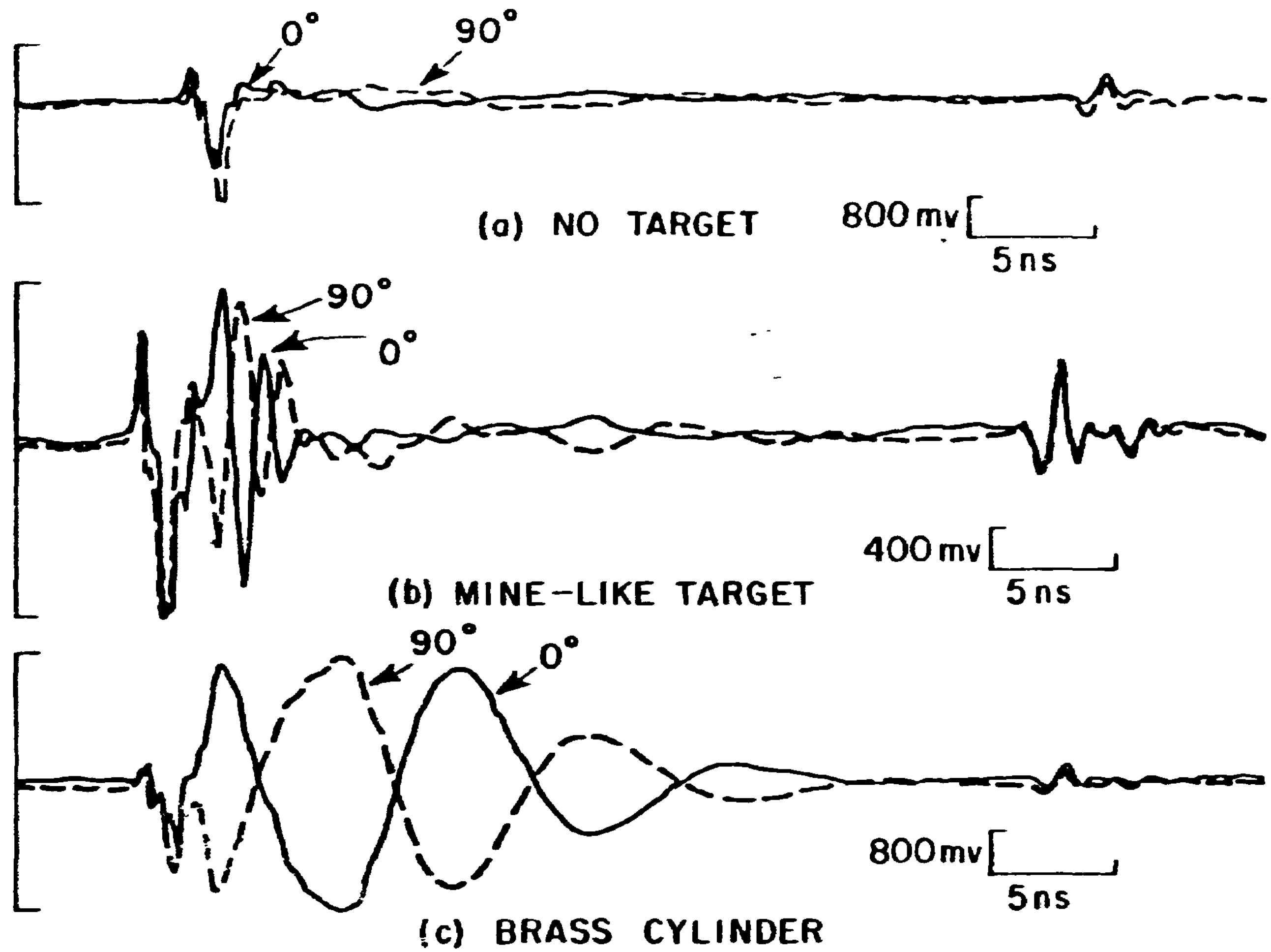

Figure 6. Typical average raw waveforms from the subsurface targets.

5. <u>90°-rotation difference technique</u>: this process forms the difference between two average, shifted and gated waveforms from the same antenna location but with different antenna orientations of which one is 90° rotation with respect to the other.

6. <u>Multistation averaging</u>: this process forms the arithmetic average of all the difference waveforms (5. above) from the antenna locations which present identical relative geometry between antenna and target.

These processed waveforms are considered to be relatively noise and clutter-free. Furthermore, they contain only the back-scattered information from the individual targets since the ground of the target sites was undisturbed (free of other objects) and relatively smooth. These processed waveforms are to be used only to establish the parameters of identification system. They are not used for the identification of an unknown target.

A set of processed waveforms and their Fast Fourier Transforms (FFT)[64] for the mine-like target at various antenna locations in a wet ground is shown in Figures 7 and 8. Typical waveforms for the other targets are shown in Figures 9 and 10.

The following important generalizations with regard to these waveforms are made:

1. All time-domain waveforms exhibit transient behavior in the late-time region where only the natural response of the target exists. This transient behavior is of prime importance, and, as will be shown in Chapter III, dictates the characterization and identification method for these targets.

2. The strong peaks in the FFT's of the waveforms indicate the possible existence of resonance behavior in the back-scattered waveforms. These peaks may be a good approximate measure of the imaginary parts of the complex resonances of the targets in situ. Note that while the time-domain waveforms from different antenna locations over the mine-like target change noticeably, the locations of the strong peaks in their FFT's stay relatively unchanged (see the vertical dotted lines in Figure 8), indicating the complex natural resonances of the target are excitation invariant. This was anticipated and is the most attractive feature of the target characterization scheme.

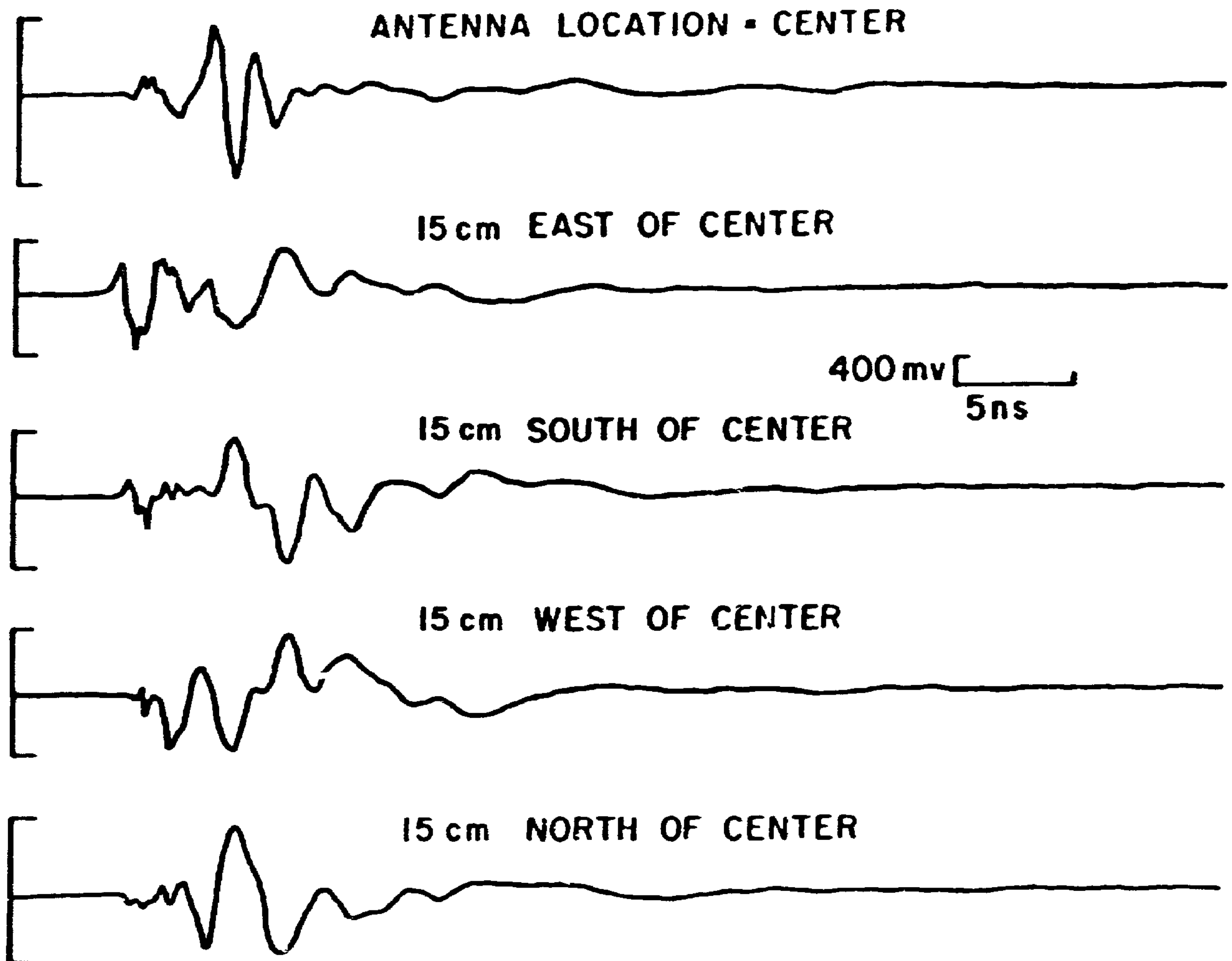

Figure 7. Processed waveforms from the mine-like target at different antenna locations in wet ground.

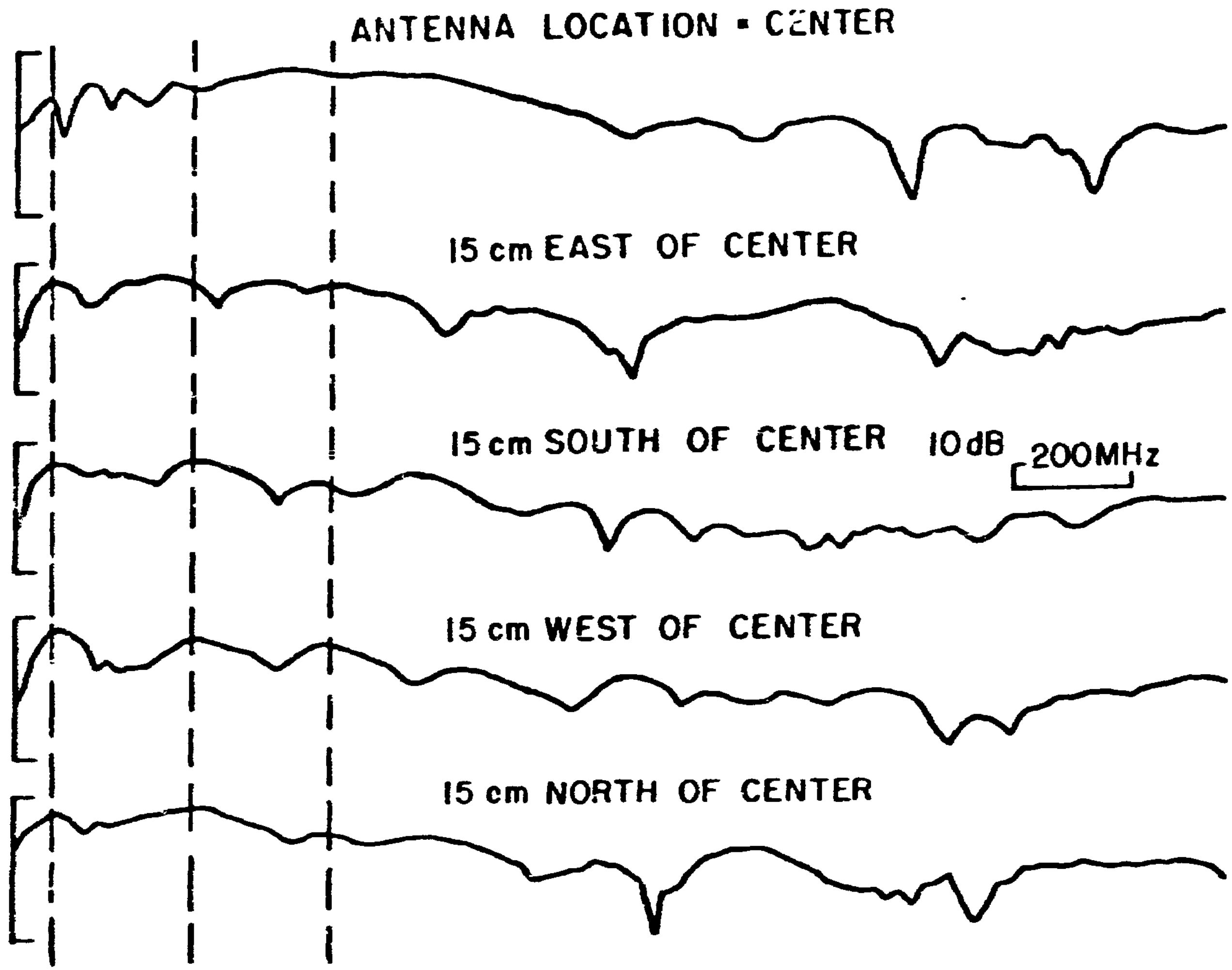

Figure 8. FFT of the processed waveforms from the mine-like target.

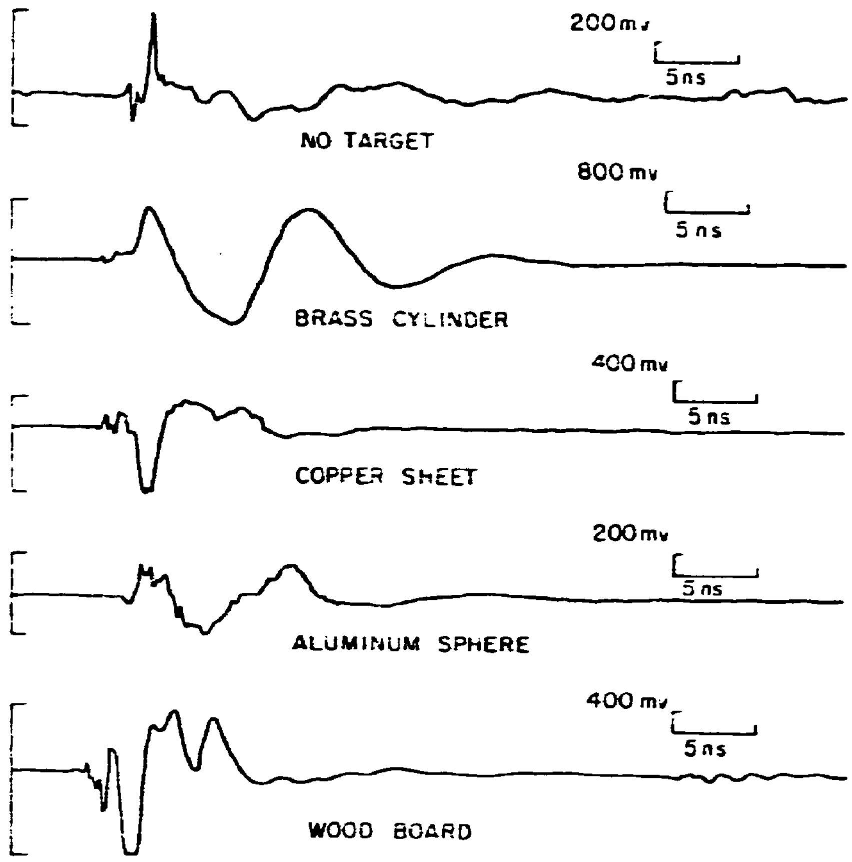

Figure 9. Processed waveforms from the other subsurface targets.

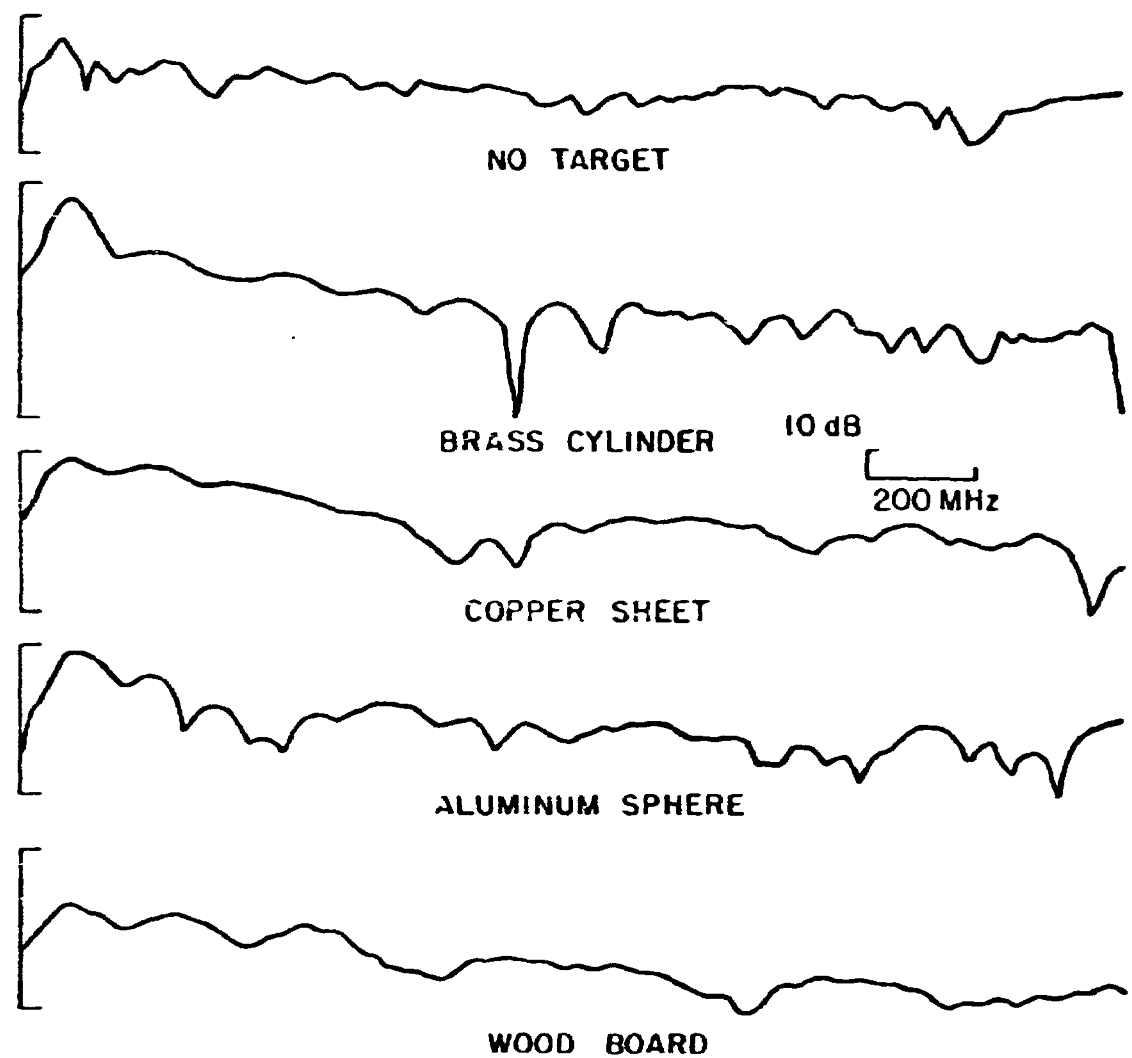

Figure 10. FFT of the processed waveforms from the other subsurface targets.

3. For the waveforms given in Figures 7 and 9 the signal level of the cylinder is the highest while the signal level of the sphere is the lowest. As a reasonable quantitative parameter for comparison of signal and clutter levels, the following definition of signal-to-clutter ratio (S/C) was used in this study.

$$\frac{S}{C} \triangleq \frac{E_T}{\bar{E}_{NT}} = \frac{E_M - \bar{E}_{NT}}{\bar{E}_{NT}} \tag{1}$$

where

E_T is the energy of the target signal,

E_M is the energy of the measured waveform, and

$\bar{E}_{NT}$ is the statistical mean energy of the ensemble of clutter or no-target waveforms used to estimate $\bar{E}_{NT}$. In this study, we considered only single-target situations, hence a collection of 51 no-target measurements taken at various locations in the vicinity of the target site was used as the ensemble of clutter waveforms.

The Energy of a waveform was defined and estimated as follows.

$$E \triangleq \frac{\sum_{t=t_s}^{t_e} r^2(t)}{(t_e - t_s)/T_B} \quad ; \; t = iT_B \tag{2}$$

where $r(t)$ is the waveform under consideration and t_s, t_e are the start and stop-time of the interval of interest. In this study t_s was taken to be the time at which the absolute maximum of the waveform occurred and t_e was taken to be the time at which the balun reflection occurred. The reasons for these choices of t_s and t_e are given in later chapters.

The mean clutter level was evaluated as

$$\bar{E}_{NT} = \frac{\sum_{i=1}^{51} \sum_{t=t_{si}}^{t_{ei}} \left(r_{NTi}^2(t)/(t_{ei} - t_{si})/T_B \right)}{51} \tag{3}$$

where $r_{NTi}(t)$ is the ith no-target waveform in the ensemble and t_{si}, t_{ei} are the start and stop time, respectively of the ith no-target waveform.

Using the above definitions, the signal-to-clutter ratio at various antenna locations over the 5cm deep targets were evaluated and are given in Figure 11. It was found that the signal-to-clutter ratio for the mine-like target ranged from 0.21 to 3.50 depending on the antenna location and orientation*. The brass cylinder and the wood board targets had the highest and lowest signal-to-clutter ratios, respectively.

The three items mentioned above: the transient behavior, the complex natural resonances and the signal level of the backscattered waveforms are of prime importance in subsurface target identification. Their dependence on changing ground conditions complicates the identification process. Any practical subsurface target identification algorithm must be able to adapt to this changing condition and identify the desired target in a wide range of, if not all, ground conditions. A comparison between the brass cylinder waveform in dry and icy ground given in Figure 12 clearly shows the effects of changing ground condition. Although both waveforms exhibit similar transient behavior, the time intervals between the zero crossings are different, indicating a shift in the locations of the target resonances. The amplitudes of the two waveforms are also different.

The FFT's of the backscattered waveforms indicate that the strongest frequency concentration is at about 70 MHz, furthermore, almost all signal energy is in the 0-500 MHz frequency band. This "system bandwidth" is of great significance in subsurface target identification for it dictates the number of target resonances and the magnitude of the corresponding residues in the backscattered waveforms.

In the next chapter we attempt to characterize the various subsurface targets by approximating their processed backscattered waveforms with a finite complex exponential series with the complex exponents being the complex natural resonances of the targets. A method for extracting these resonances directly from the time-domain waveforms will be presented. Results from the application of this method are given.

---

*S/C depends also on the ground condition. The estimates given in Figure 11 was based on a set of measurements obtained in a relatively dry ground condition over a time period of several days. Furthermore, S/C at symmetric locations are assumed equal. $S/C \cong 0$ when $E_M \cdot E_{NT}$.

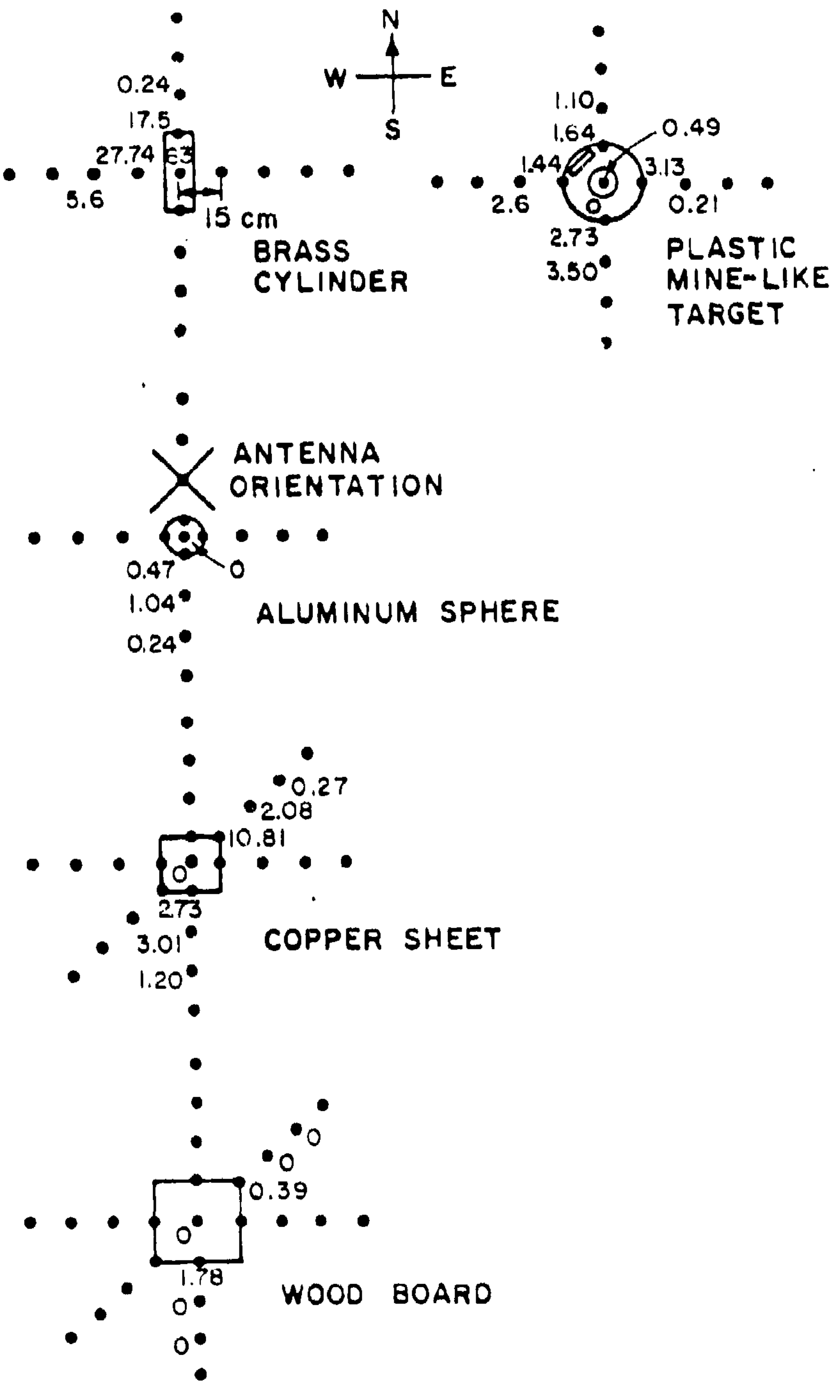

Figure 11. Signal-to-clutter ratio estimates of the waveforms from the subsurface targets at different antenna locations.

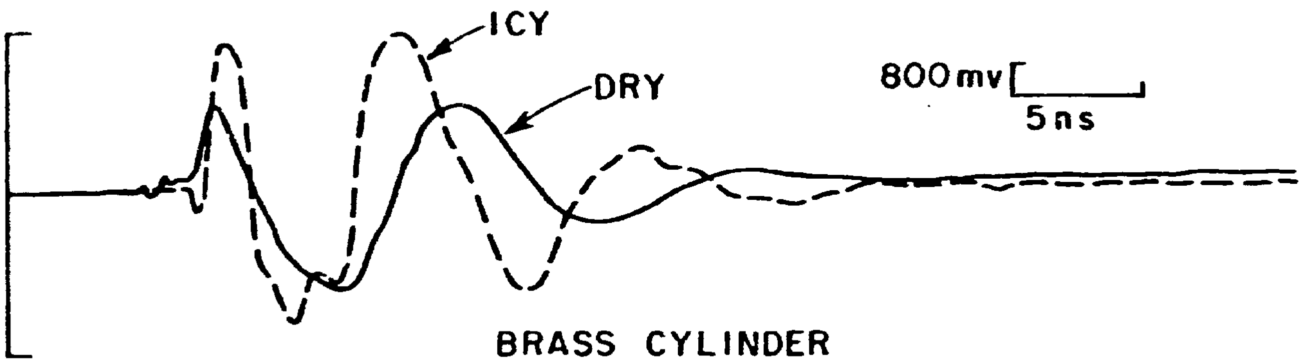

Figure 12. Processed waveforms from the brass cylinder in dry and icy ground.

CHAPTER III
CHARACTERIZATION OF SUBSURFACE TARGETS BY THEIR COMPLEX NATURAL RESONANCES

A. Objectives

This chapter summarizes a study of the characterization of subsurface targets by their complex natural resonances. A method for extracting the resonances from the processed backscattered waveforms is derived for completeness. The method is known as Prony's method [12-15] and, when applied to measured data, it is extremely sensitive to the values of its parameters. An approach to solve certain of these problems will be presented. Prony's method is applied to the processed backscattered waveforms and an analysis of the resulting resonances is focused on the following:

1. The excitation invariance of the complex natural resonances of the individual targets with respect to antenna location.

2. The degree of distinction between the complex natural resonances of the different targets.

3. The effects of changing ground condition on the location of the complex natural resonances.

B. Complex Natural Resonances

The concept of using complex natural resonances for target characterization is developed from the fact that all finite-size objects have resonances that depend on their physical characteristics such as size, shape and composition as well as the medium surrounding the object. These resonances, however, are independent of the excitation[40]. As a useful but inexact analogy, in circuit theory, the form of the transient response of a lumped linear circuit may be determined from the knowledge of the resonances and the corresponding residues of the response function in the complex frequency plane. The actual transient response of the circuit is then simply a summation of all the residues multiplied by the inverse transforms of the resonances. In 1965, Kennaugh and Moffatt[41] generalized the impulse response concept to include the distributed parameter scattering problems and suggested that a lumped circuit representation, at low

frequencies or long time, was possible. Later, similar and more formal representations have been designated as the Singularity Expansion Method (SEM)[7-8]. This hypothesis is generally supported by the fact that typical transient response waveforms, such as those shown in Chapter II, appear to be dominated by a few exponentially damped sinusoids. Based on this concept, a subsurface target can be characterized by a set of complex natural resonances which is independent of the location and orientation of the crossed-dipole antenna. These resonances, however, are dependent on ground condition. Such a characterization is attractive for it catalogs a target by a small set of complex numbers.

The backscattered waveforms from the subsurface targets received by the pulse radar system are good approximations to the impulse responses of the targets. Furthermore, they appear to be dominated by a few exponentially damped sinusoids, and thus can be represented as

$$r(t) = \sum_{n=1}^{N} a_i \, e^{s_i t} \tag{4}$$

where $r(t)$ is the received transient waveform, s_i's are the complex resonant frequencies or pole locations in the complex frequency plane. These have, by common usage in this representation, become designated as complex resonances or more simply as resonances. These various terms will be used for s_i in this document. a_i's are the corresponding residues and N is the number of complex resonances within the frequency band of the radar system. The corresponding expression in the complex frequency domain is

$$\mathcal{L}[r(t)] = \sum_{i=1}^{N} \frac{a_i}{(s-s_i)} \tag{5}$$

where $\mathcal{L}[\ ]$ is the Laplace transform operator[42] and s is the complex frequency. Note that the resonances are not dependent on antenna location and orientation however, the residues are.

In order to exploit Equation (4), it is necessary to first determine the values of the complex natural resonances of the targets. The method used here extracts the resonances of a target directly from its transient response. This method is known as Prony's method, which was first derived by Prony in 1795[12], and was later suggested by Van Blaricum, et al., for extracting the pole singularities of transient waveforms in 1975[14].

C. Derivation of Prony's Method

In discrete form, Equation (4) can be written as

$$r(KT_B) = \sum_{i=1}^{N} a_i \, e^{s_i KT_B} \quad , \quad K = 0,1,2\cdots \tag{6}$$

where K is the sampling index and T_B is the basic hardware sampling period of our measurement system (see Chapter II). For an exact solution of the 2N unknowns a_i and s_i, we can set up 2N (nonlinear) equations by using 2N sample values of $r(KT_B)$. Prony's method uses 2N uniform samples, and

$$r(nT) = \sum_{i=1}^{N} a_i \, e^{s_i nT} \quad ; \quad n = 0,1,2\cdots, M = 2N-1 \tag{7}$$

where T, the Prony interval, is the interval between the samples used along the waveform. In general, N itself also represents an unknown which is usually fixed by a trial and error process.* If no waveform interpolation is exercised, T is equal to integer multiples of T_B. Writing out Equation (7), we have 2N equations

$$\left.\begin{aligned}
r_0 &= a_1 + a_2 \cdots && + a_N \\
r_1 &= a_1 z_1 + a_2 z_2 \cdots && + a_N z_N \\
r_2 &= a_1 z_1^2 + a_2 z_2^2 + \cdots && + a_N z_N^2 \\
&\;\;\vdots \\
r_M &= a z_1^M + a_2 z_2^M + \cdots && + a_N z_N^M
\end{aligned}\right\} \tag{8}$$

where

$$r_n = r(nT)$$

and

$$z_i = e^{s_i T} \quad .$$

---

*N represents the number of target resonances which are excited by interrogating frequencies within the "system bandwidth".

Equation (8) is a set of nonlinear equations in the z_i's. Let $z_1, z_2 \cdots z_N$ be the roots of the algebraic equation

$$\alpha_0 + \alpha_1 z^1 + \alpha_2 z^2 + \cdots \alpha_N z^N = 0 \tag{9}$$

so that the left hand side of Equation (9) is equal to the product

$$(z-z_1)(z-z_2) \cdots (z-z_N) = 0 \quad , \tag{10}$$

that is,

$$\sum_{m=0}^{N} \alpha_m z^m = \prod_{i=1}^{N} (z-z_i) = 0 \quad . \tag{11}$$

Thus, if we can evaluate α_m, then z_i can be obtained by a simple factorization of an Nth degree polynomial. To solve for α_m, we obtain from Equations (7) and (8)

$$\sum_{m=0}^{N} \alpha_m r_{K+m} = \sum_{m=0}^{N} \alpha_m \left(\sum_{i=1}^{N} a_i z_i^{K+m} \right) \quad ; \; K = 0,1,2 \cdots M-N \quad .$$

Interchanging the order of the summation yields

$$\sum_{m=0}^{N} \alpha_m r_{K+m} = \sum_{i=1}^{N} a_i z_i^k \left(\sum_{m=0}^{N} \alpha_m z_i^m \right) \quad .$$

From Equation (11), we see that the summation inside the parenthesis of the above equation is zero, thus, we arrive at the desired linear homogeneous difference equation

$$\sum_{m=0}^{N} \alpha_m r_{K+m} = 0 \quad ; \quad K = 0,1,2 \cdots M-N \quad . \tag{12}$$

Thus, the sample values of r(t) satisfy an Nth order linear homogeneous difference equation. This difference equation is commonly referred to as the Prony difference equation.

The Prony difference equation is linear and homogeneous, and can be used to solve for the N+1 coefficients, i.e., α_m's. In the classical Prony's method, these coefficients are obtained by setting $\alpha_N = 1$ and solving the resulting matrix equation by matrix inversion that is,

$$AB = C \tag{13}$$

where

$$A = \begin{bmatrix} r_0 & r_1 & r_2 & \cdots & r_{N-1} \\ r_1 & r_2 & r_3 & \cdots & r_N \\ \cdot & & & & \\ \vdots & & & & \\ r_{M-N} & r_{M-N+1} & r_{M-N+2} & \cdots & r_{M-1} \end{bmatrix}$$

$$B = \begin{bmatrix} \alpha_0 \\ \alpha_1 \\ \cdot \\ \vdots \\ \alpha_{N-1} \end{bmatrix} \quad \text{and} \quad C = - \begin{bmatrix} r_N \\ r_{N+1} \\ \vdots \\ r_M \end{bmatrix} \quad .$$

Note that for $M=2N-1$, A is a square symmetric circulant matrix and is readily invertable. Standard computer routines such as GELG[43] can be used to do the matrix inversion. Once the α_m's are determined, the next step is to solve for the N values of z_i. These z_i's are obtained by finding the roots of Equation (11). The N roots are complex numbers and because $r(t)$ is real, these complex numbers appear in complex conjugate pairs. The polynomial root finding process can be easily performed by using standard routines such as Muller[44,45].

It is now trivial to obtain the poles s_i. Since the roots of Equation (11) were defined by Equation (8), the poles are simply

$$s_i = \frac{1}{T} \ln(z_i) \quad . \tag{14}$$

The final step in Prony's method is to determine the value of the residues a_i. To do this, we simply solve the matrix equation embodied in Equation (8). In matrix form this set of equations is written as

$$DE = F \tag{15}$$

where

$$D = \begin{bmatrix} 1 & 1 & \cdots & 1 \\ z_1 & z_2 & \cdots & z_N \\ z_1^2 & z_2^2 & \cdots & z_N^2 \\ \vdots & \vdots & & \vdots \\ z_1^{N-1} & z_2^{N-1} & \cdots & z_N^{N-1} \end{bmatrix}$$

$$E = \begin{bmatrix} a_1 \\ a_2 \\ \vdots \\ a_N \end{bmatrix} \quad \text{and} \quad F = \begin{bmatrix} r_0 \\ r_1 \\ \vdots \\ r_{N-1} \end{bmatrix}$$

where now the only unknowns are the elements of the residue matirx E.

The above derivation of Prony's method is valid only when all natural resonances present are simple poles. For multiple-order poles, a slight modification is necessary in solving for the residues. The derivation of Prony's method for multiple-order poles is given in Appendix A for completeness. However, in this study we have not found it necessary to postulate multiple-order poles.

In summary, Prony's method solves for the complex natural resonances (poles) and the corresponding residues associated with the back-scattered time-domain waveforms from a system of nonlinear equations (Equation (8)) by breaking it down into three simple steps:

(1) Solve for the values of α_m's of the linear Equation (13) by matrix inversion.

(2) Solve for the poles by factoring the polynomial of Equation (11).

(3) Solve for the residues from the linear Equation (15) by matrix inversion.

The derivation of Prony's method is simple enough. However, its application to the measured backscattered waveforms is a much more complicated process. The following section outlines some of the difficulties.

D. Clutter and/or Noise in Prony's Method

Prony's method has been found to be extremely sensitive to clutter and/or noise. Its ability to extract the complex natural resonances of a waveform accurately is severely inhibited by the presence of clutter and noise[46-48]. Since Prony's method is an interpolation process (otherwise referred to as curve fitting), in the presence of clutter and/or noise, it will give a set of poles which fit the noisy transient response but will not necessarily represent the complex natural resonances of the target. Various signal-processing techniques have been applied to reduce the effect of clutter and/or noise in Prony's method[46-48], with the most commonly used being the least-square error technique. With it, Equation (13) in the previous section is solved in the least-square sense. In this case, M samples are used in lieu of 2N samples where $M>2N$. Thus, the matrix A becomes rectangular, and Equation (13) is solved by the pseudo-inverse technique

$$A^T A B = A^T C \tag{16}$$

or

$$\Phi B = D \tag{17}$$

where

$$\Phi = A^T A$$

and

$$D = A^T C \quad .$$

Since Φ is the signal covariance matrix, it is real, symmetric and positive definite, and is thus readily invertible to yield the value of α_m's.

A second technique applied to reduce noise in Prony's method was brought about by the observation that, in solving for the N+1 α_m's in the M homogeneous Equations (13), we can, instead of setting $\alpha_N=1$, require that the Euclidean norm of the α vector be 1, i.e.,

$$\sum_{m=0}^{N} \alpha_m^2 = 1 \quad . \tag{18}$$

Such an approach leads to the eigenvalue method[48,49,52].

Instead of setting the leading coefficient $\alpha_N=1$, we can of course set any of the N+1 coefficients to 1 in solving for the α_m's of Equation (10). Such a constraint leads to the interpolation version of Prony's method[51,52].

The classical Prony's method, the eigenvalue method and the interpolation version of Prony's method were all considered in this study. For completeness, derivations of the eigenvalue method and the interpolation version of Prony's method are given in Appendix B.

Numerous other signal-processing techniques have been applied [46-47], thus far, however, no completely satisfactory result has been reported using measured data. In the following section a systematic procedure that is giving good results for the present data is outlined. This procedure was used in extracting the complex natural resonances of the processed backscattered waveforms in Chapter II and yielded our best results to date. As we will see, the procedure does indeed provide satisfactory target separation.

The problem is really one of linear prediction and is prominant in many diverse disciplines[53]. No general solution has yet emerged and the acceptability of a given method really depends upon the application. It is interesting however that minimizing the total squared error (actual vs estimate) in some sense is a common starting point. Yet this in no way optimizes the resonance locations. For our purpose because the resonance locations need not be found in real time, present methods are adequate if not completely satisfying. A real need is to compile and translate all of the various methods already being used. Such a tutorial unified review would be invaluable but is beyond the scope of the present effort. We can of course easily incorporate any new techniques into the identification scheme.

E. Applying Prony's Method to the Processed Measured Backscattered Waveforms

In applying Prony's method, one approach is to pre-determine the following parameters:

1. N, the number of poles to be extracted from the waveform. Van Blaricum[14,15,47] suggested a method which relies on the fact that the (N+1)th eigenvalue of the matrix should equal σ^2, the variance of the additive gaussian stationary and uncorrelated noise. Such a method does not seem practical for our measured data in which the clutter seems to be nonstationary (transient).

2. T, the Prony interval. Obviously, undersampling (T too large) will almost surely bring aliased results. It was also found that oversampling produces extraneous high frequency poles.

3. t_s, t_e the start and stop time of the fitting interval. t_s must lie in the time region where the forced response portion of the backscattered waveform has ended and t_e must lie in the region where clutter/noise effects are not dominant.

4. M, the number of sample points used in the fitting process. M determines the amount of overspecification on the system of Equations (13).

In the presence of clutter and/or noise, it was found that the accuracy of the extracted resonances was found to be extremely sensitive to the values of the above five parameters[48]. For the method to yield an accurate solution, we have to find the "right" set of values for these parameters. The approach developed in this study is to vary these parameters (over a reasonable range) and assume that the "right" values of the parameters corresponding to the "desired" resonances are those that allow the closest approximation to the measured waveform in the time domain. That is, a calculated waveform is developed from the resonances and residues found, and this waveform is compared to the original waveform point by point over the fitting interval $[t_s, t_e]$ and the total squared error found. The solution which affords the smallest total squared error is considered to be the "desired" solution. This approach is used to find the coefficients of the difference equation but once done for a target needs not be repeated for target-separation purposes. It is conceivable that such a searching procedure can be lengthy. Furthermore, ranges of the parameters are dependent on the waveform being processed. However, with a little experience, one can usually minimize them. The ranges of these parameters in this sutdy were fixed as follows:

1. The number of "significant" peaks in the Fast Fourier Transform of the waveforms is usually a good measure of N and since the number of "significant" peaks is between 2 and 7 in all waveforms considered, the range of N was chosen to be from 4 to 14 (we assumed that one peak corresponded to at most two poles).

2. Shannon's sampling theorem constrains the maximum value of T, while the bandwidth of the radar system (<500 MHz) constrains the minimum value of T.* The values of T were chosen to be $3T_B$, $5T_B$ $\cdots$ $10T_B$ corresponding to minimum and maximum Nyquist frequencies of 256 MHz and 768 MHz, respectively.

---

*Frequencies beyond the system bandwidth contains noise only unless we attempt some spectral estimation techniques. The approach may be worthy of study when studying "deeper" targets.

3. The values of t_s were chosen to be t_{max}, $(t_{max}+2T_B)$, $(t_{max}+4T_B)$ $\cdots$ $(t_{max}+8T_B)$ where t_{max} is the time at which the absolute maximum of the waveform occurs. It was found that such a choice ensured a decaying nature in almost all the waveforms considered. t_e was chosen to to be the time at which the balun reflection occurs (see Chapter II).

4. Since a vastly oversized M would result in an unstable solution from Prony's method[13,15,48], the values of M were chosen to be 2N, 3N, $\cdots$ 6N.

Each set of values of the five parameters (N,T,t_s,t_e,M) will give a set of complex resonances when Prony's method is applied to a waveform. This set of complex resonances maximizes the fit between the approximated waveform $r_A(t)$ and the measured waveform $r(t)$ in the interval $[t_s,t_s+(M-1)T]$ with the sampling interval of T. For all complex resonances resulting from all possible sets of (N,T,t_s,t_e,M) in the chosen range, the "desired" set of complex resonances is chosen to be the one which minimizes the total normalized point-by-point squared error ε over the error-calculating interval. The error ε, which will be henceforth referred to as mean-square error, is defined as

$$\varepsilon = \left(\sum_t (r(t)-r_A(t))^2\right) \Big/ \left(\sum_t (r^2(t)+r_A^2(t))\right) \quad ; \quad t=iT_B \; . \tag{19}$$

In this study, $r(t)$ was taken to be the processed measured waveform and the approximated waveform $r_A(t)$ was generated via the method of linear prediction[53], where

$$r_A(t+m_oT) = \sum_{\substack{m=0 \\ m\neq m_o}}^{N} \frac{-\alpha_m}{\alpha_{m_o}} r_M(t+mT) \quad . \tag{20}$$

In Equation (20), $r_A(t)$ and $r_M(t)$ are the approximated and the processed measured waveform, respectively, the α_m's are the difference equation coefficients obtained from the Prony's method, and m_o is an index chosen for suppression of clutter and noise effects. In this study, m_o was chosen to be the coefficient of maximum magnitude. With Equation (20), the mean-square error ε can be expressed as

$$\varepsilon = \frac{\sum\limits_{t=t_s+m_oT}^{t_e-NT+m_oT} \frac{1}{\alpha_{m_o}^2}\left(\sum\limits_{m=0}^{N}\alpha_m r_M(t+mT)\right)^2}{\sum\limits_{t=t_s+m_oT}^{t_e-NT+m_oT}\left(r_A^2(t)+r_M^2(t)\right)} \quad ; \; t = iT_B \quad . \tag{21}$$

From Equations (12) and (21), we note that the mean-square error ε is zero when the measured waveform is free of clutter/noise and is perfectly characterized by Equation (4). The error should be small when $r_M(t)$ is closely approximated by Equation (4).

The choice of the above error criterion is related to the form of the correlation coefficient chosen in the target identification algorithm of Chapter IV, in such a way that minimization of ε results in the maximization of the correlation coefficient.

With the above search procedure, Prony's method and its variations were applied to the processed waveforms to extract their complex natural resonances. Results are shown in the next section.

F. The Extracted Resonances of the Subsurface Targets

The locations of extracted resonances of the mine-like target at different antenna locations in icy ground are plotted in Figure 13 (here only poles in the upper left half s plane are shown, details are given in Appendix C). From Figure 13, we make the following observations:

1. The extracted resonances tend to form "clusters". Some possible clusters are shown in Figure 13. The formation of these clusters are based on the obviousness of clustering of the resonances and the known fact that the accuracy in determining the real part of the extracted resonance is normally poor. A cluster can contain at most one pole extracted from a waveform. Poles with residues which are three orders down in magnitude compared to the maximum residue are discarded. Poles which are remote from the clustered groups are excluded. Beyond an obvious weighing dictated by the actual pole locations no real significance should be attached to the shape of the closed contour surrounding each cluster.

2. Only a small number of clusters or resonances are present.

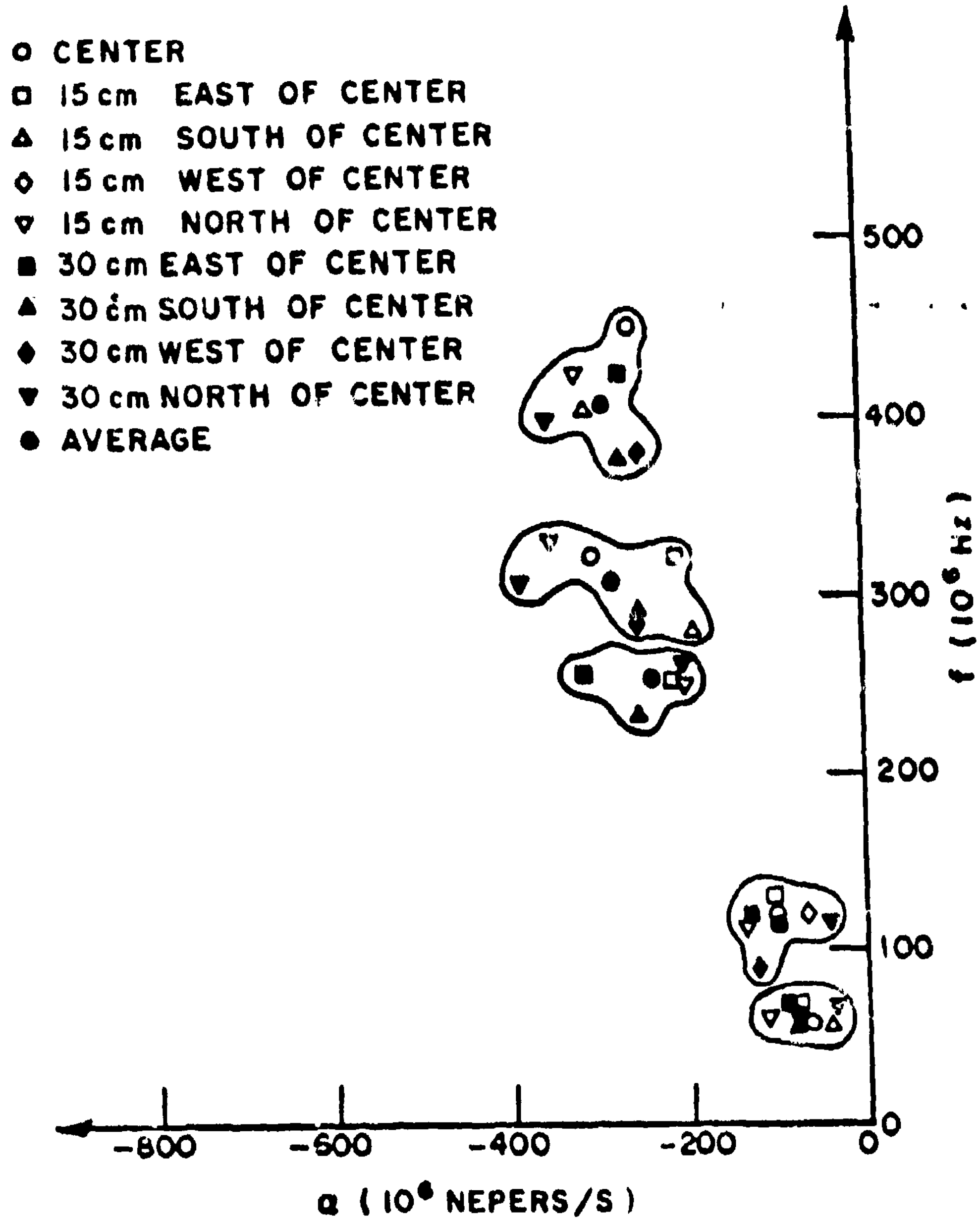

Figure 13. Location of the extracted resonances of the mine-like target at different antenna locations in icy ground.

3. The variation in the real parts of the resonances within a cluster is generally greater than the variation in their imaginary parts. There is at least one more major factor, besides the ever-present clutter/noise, that causes such variations, namely, the target-antenna interactions. At the shallow depth of 5 cm, for most antenna locations considered, the targets are in the near field of the antennas for the entire bandwidth (< 500 MHz) of our radar system.

4. An additional factor contributes to the variations in the extracted resonances from the mine-like target, namely, its complex structure. This target possesses the most complex structure of all targets considered.

5. The phenomenon of certain resonance(s) being weakly excited in certain radar aspects is evident. The weakly excited resonances were not extracted.

6. As expected, the residues are aspect dependent. This becomes evident by noting the variations of the magnitude of the residues of the poles in the clusters (See Appendix C).

7. The mean-square error ε is small ($\leq .01$, see Appendix C) in all cases considered, meaning that the finite sum of complex exponentials fits the measured waveforms well. This is a necessary condition for our identification algorithm whose correlation coefficient is defined to be unity minus the mean-square error ε.

In this study, a subsurface target was characterized by the set of average extracted resonances. Averaging was performed over all the extracted resonances in each cluster. For the mine-like target, the average extracted resonances are shown as solid dots in Figure 13. Parameters such as the variation from the average of each pole within the cluster is not meaningful because of its causes which include, besides the effects of clutter and noise, the possible variations in the pole excitation at the various antenna locations and orientations. Slight pole variations due to the variations in the antenna locations and orientations is possible for the finite exponential sum representation of the target's transient response is only an approximation and that the targets considered are located in the closed vicinity of the radar system.

The extracted resonances shown in Figure 13 were obtained using classical Prony's method (i.e., $\alpha_N=1$). Classical Prony's method was found to extract poles with tighter clusterings among the results given by other methods under the constraint $\alpha_m=1, m=0,1\cdots,N$[52]. The eigenvalue method provided results similar to those given by the

Classical Prony's method. Thus, no clear cut choice of method was discernable. Accordingly, the extracted resonances shown in this dissertation were the results of either of these two methods.

In order to see the effects of the changing ground condition on the location of the extracted resonances, the average resonances of the mine-like target in different ground conditions are tabulated in Table 1 and are plotted in Figure 14. From Figure 14, we see that there were five (pairs) extracted resonances. The imaginary parts of the extracted resonances were relatively insensitive to changes in ground condition. This seems to imply the resonances of the mine-like target are internal resonances. This also means that the target identification scheme when applied to this target will be relatively insensitive to ground conditions.

The implications of the fact that there were five (pairs) resonances extracted from the mine-like target waveforms is significant. It means that this target can now be characterized by a finite-order system.

Not all the extracted resonances are related to the scattering mechanisms of the mine-like target. In fact, the lowest resonance was found to be the antenna resonance of the system. This becomes particularly clear when we study the resonances extracted from the mine-like target waveforms collected with a 12m long antenna. By gating out the late-time portion of the backscattered waveform from the mine-like target received by the 12m long antenna, we effectively eliminated the resonance of the antenna created by the finite length of the antenna arms. Thus, poles extracted from these waveforms are all target-related. A typical such backscattered waveform in the time domain is shown in Figure 15, The short time window (compared to the 0.6m long antenna waveforms of Figures 7) of the waveform indicates the absence of any low frequency content. The average extracted resonances from the mine-like target waveforms received by the 12m long antenna at various locations are shown in Figure 16. A quick comparison with the extracted resonances from the 0.6m long antenna waveforms reveals the fact that the resonance with imaginary part of approximately 60 MHz is the antenna resonance. Thus, for the system with the 0.6m long antenna, four (pairs) target resonances were present in the received waveforms. The antenna resonance was extracted from almost every waveform of all targets considered.

In contrast to the case of the plastic mine-like target, the brass cylinder was found to possess external resonances. Table 2 lists the average extracted resonances of the brass cylinder in various ground conditions. Locations of these resonances are also plotted in Figure 17. From Figure 17 we see the following effects of the changing ground condition on the extracted resonances of the brass cylinder. First, the antenna resonance is insensitive to changes in the ground condition. This may be attributed to the fact that the

arms of the crossed-dipole antenna were not in electrical contact with the ground surface. Second, the imaginary parts of the three higher-order* resonances increased significantly when the ground changes from dry to icy. This is to be expected, because the resonances of the brass cylinder are external resonances. The increase in the imaginary parts of these external resonances indicated a decrease in the value of the dielectric constant of the ground. Third, the real part of the three higher-order resonances generally decreased as the ground changed from dry to icy, indicating that icy ground in this case was more lossy. The increase in loss seemed to be the reason for the absence of the real cylinder pole in icy ground.

The average extracted resonances of the aluminum sphere, copper sheet and wood board are tabulated in Table 3. From Table 3 we see that the antenna resonance is present in the waveforms of all targets. Note that the extracted resonances of the five targets considered lay in the same general region of the complex frequency plane and are only marginally separated. Such is expected to some extent because all targets considered have (again marginally) similar sizes. Such marginal level of distinction in the poles is expected to present difficult tests for the identification algorithm. Furthermore the number of resonances for the various targets are also close (4 to 5 pairs); this further tests our identification method.

The location of the target resonances are related to the scattering mechanisms of the target. For subsurface targets, these relationships are complicated by the presence of the air-ground interface, the ground condition and the characteristics of the transient antenna system. For shallow targets the near-field effects and the target-antenna interactions further complicate the picture. In this dissertation, we do not intend to explore these relationships. Instead, we proceed to use the extracted resonances for identification of the various subsurface targets. In the next chapter, a basic identification algorithm will be given and identification results using the extracted resonances as the discriminants will be presented.

---

*Order here denotes increasing imaginary part.

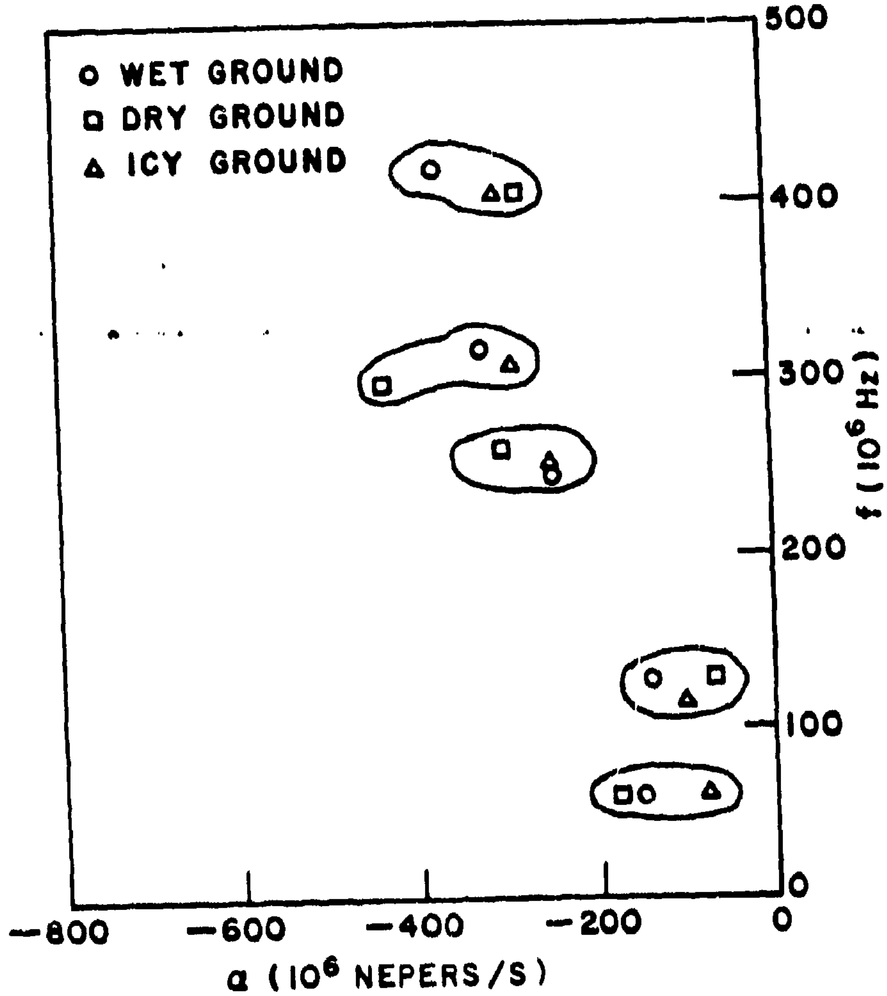

Figure 14. Locations of the average extracted resonances of the mine-like target in different ground conditions.

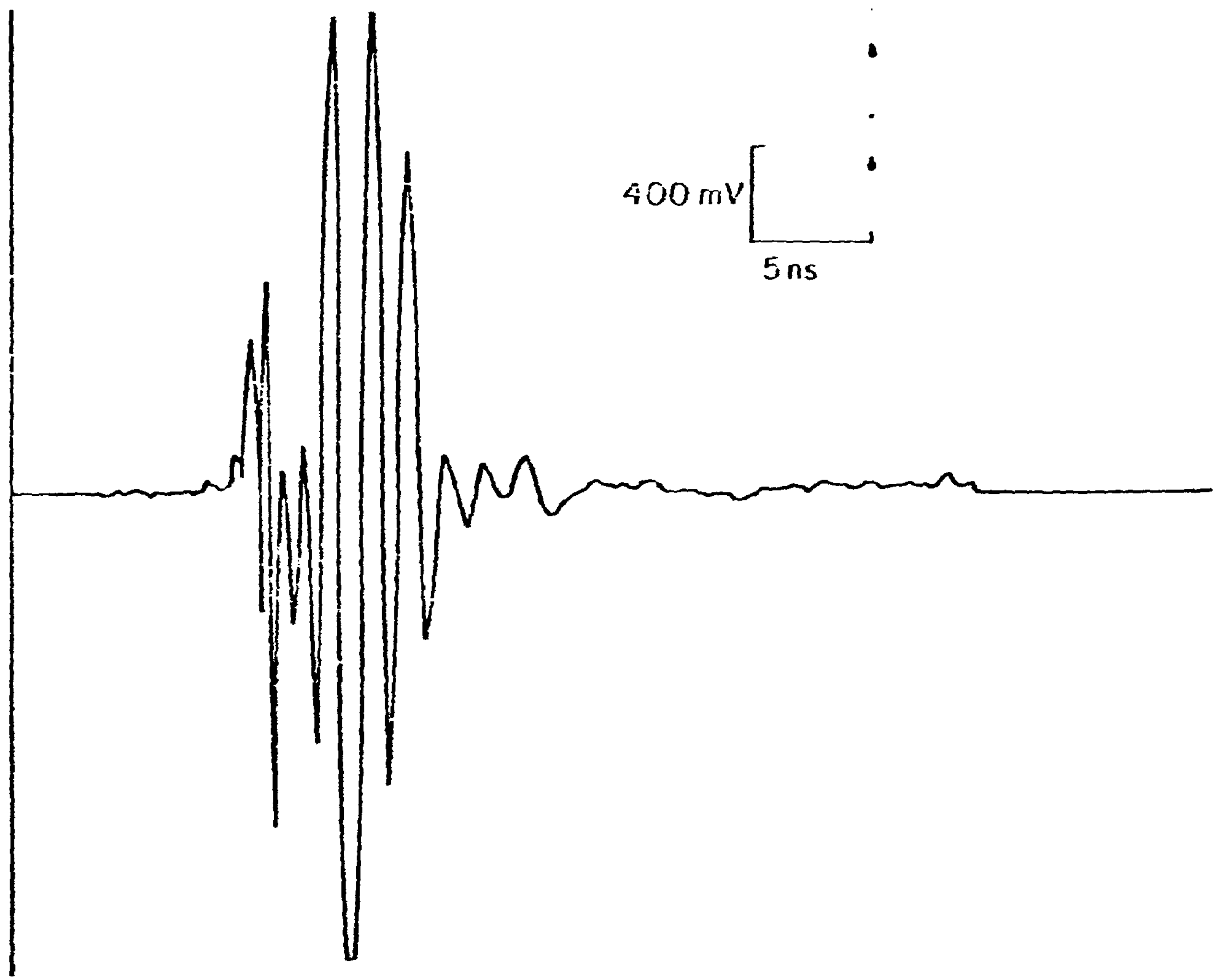

Figure 15. A typical backscattered waveform received by the 12m long antenna from the mine-like target.

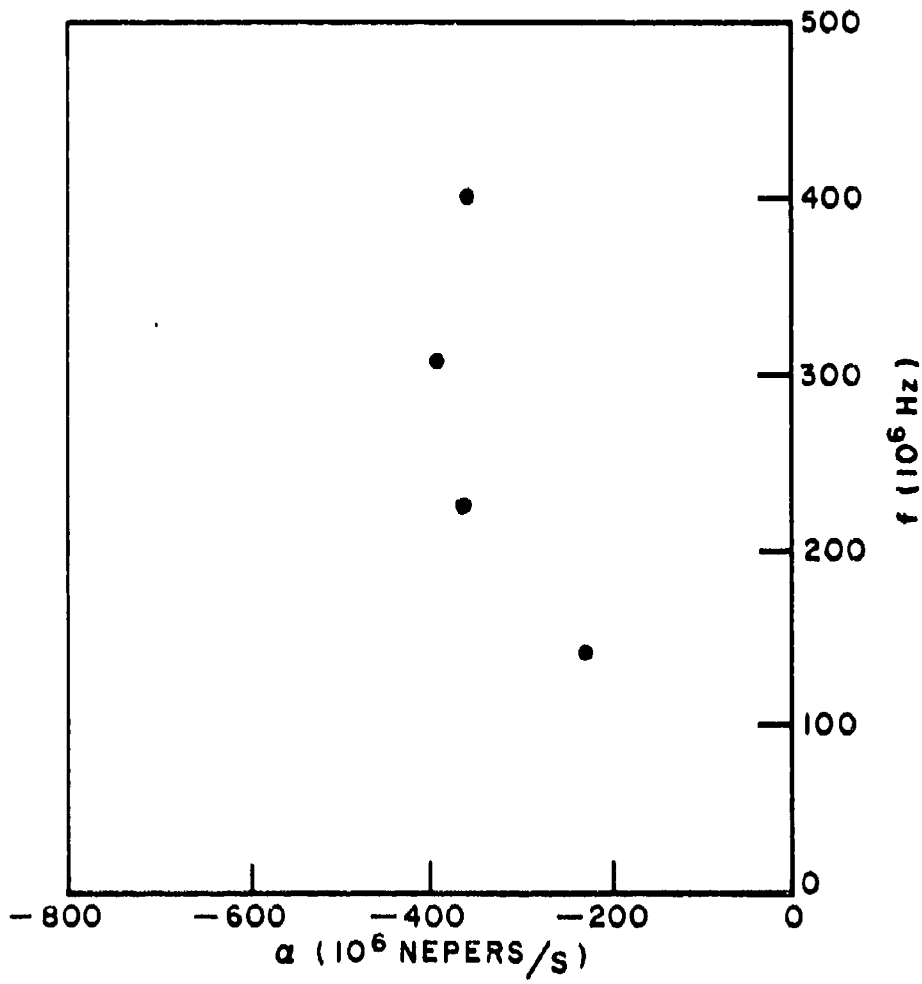

Figure 16. Average extracted resonances from the mine-like target waveforms received by the 12m long antenna.

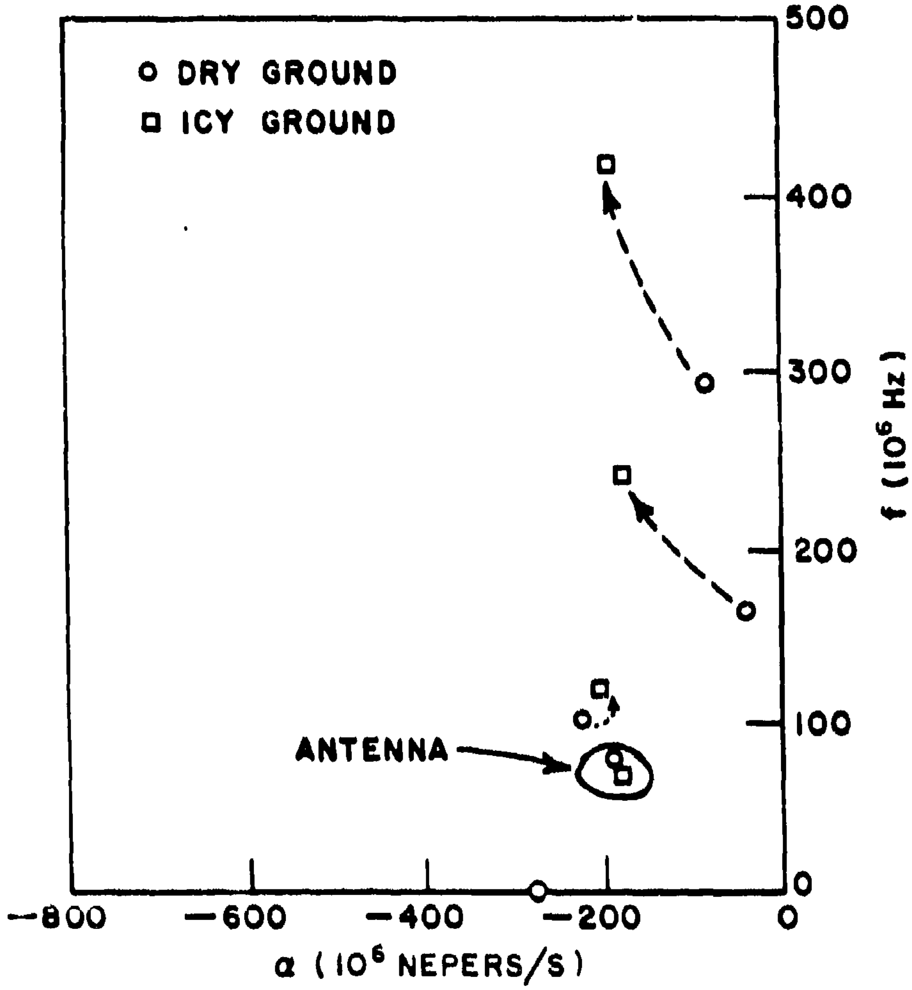

Figure 17. Average extracted resonances of the brass cylinder in different ground conditions.

TABLE 1
AVERAGE EXTRACTED RESONANCES OF THE MINE-LIKE TARGET IN DIFFERENT GROUND CONDITIONS

ICY GROUND		DRY GROUND		WET GROUND	
POLE REAL PART*	POLE IMAG PART*	POLE REAL PART	POLE IMAG PART	POLE REAL PART	POLE IMAG PART
-.7493116E8	±.6347621E8	-.1755790E9	±.5769154E8	-.1502978E8	±.6074772E8
-.9981995E8	±.1146405E9	-.6843569E8	±.1287960E9	-.1339401E9	±.1286094E8
-.2416503E9	±.2535799E9	-.3048629E9	±.2609797E9	-.2434968E9	±.2418420E9
-.2809195E9	±.3074791E9	-.4321735E9	±.2957980E9	-.3207980E9	±.3180883E9
-.2885261E9	±.4076659E9	-.2797264E9	±.4037985E9	-.3661906E9	±.4218155E9

*Real and Imaginary parts of the extracted resonances shown in Tables 1, 2 and 3 are in Nepers/s and Hz, respectively.

TABLE 2

AVERAGE EXTRACTED RESONANCES OF THE BRASS CYLINDER IN DIFFERENT GROUND CONDITIONS

ICY GROUND		DRY GROUND		WET GROUND	
POLE REAL PART	POLE IMAG PART	POLE REAL PART	POLE IMAG PART	POLE REAL PART	POLE IMAG PART
		-.2769107E9	.0000000		
-.1754246E9	±.7320464E8	-.1904656E9	±.7836537E8	-.1514337E8	±.6581380E8
-.1993071E9	±.1208164E9	-.2233100E9	±.9971379E8	-.2173419E9	±.9414942E8
-.1763301E9	±.2462725E9	-.0480810E9	±.1681942E9	-.2332553E9	±.2106191E9
-.1882724E9	±.4224952E9	-.0701791E9	±.2964066E9	-.6256987E8	±.3249909E9

TABLE 3

AVERAGE EXTRACTED RESONANCES OF THE ALUMINUM SPHERE, COPPER SHEET AND THE WOOD BOARD

ALUMINUM SPHERE DRY GROUND		COPPER SHEET DRY GROUND		WOOD BOARD WET GROUND	
POLE REAL PART	POLE IMAG PART	POLE REAL PART	POLE IMAG PART	POLE REAL PART	POLE IMAG PART
-.157154E9	±.6774348E8	-.1542518E9	±.6444038E8	-.1017222E9	±.6758739E8
-.9679531E8	±.1115148E9	-.1801754E9	±.9524389E8	-.5267251E8	±.1368924E9
-.2448631E9	±.3035603E9	-.2092095E9	±.1634348E9	-.1346969E9	±.1986688E9
-.5818507E8	±.3973762E9	-.2065430E9	±.2889621E9	-.2283739E9	±.2903170E9
				-.1330163E9	±.4125691E9

CHAPTER IV
THE PREDICTOR-CORRELATOR IDENTIFIER

A. Objectives

This chapter summarizes the target identification procedure based on the predictor-correlator identification method[40,9-11]. A detailed analysis on the predictor-correlator is presented. Identification performances based on real radar measurements are given.

Processing for target identification using the predictor-correlator consists of comparing a measured waveform from an unknown target with a calculated waveform produced using the resonances of a known desired target. The procedure is as follows:

1. Preprocessing: The preprocessor attempts to suppress clutter and noise. For "single-look"* identification, the following preprocessing steps are taken:

   a. Arithmetic Averaging (see Chapter II).

   b. Amplitude Shift (see Chapter II).

   c. Time Shift (see Chapter II).

   d. 90°-rotation Difference (see Chapter II).

   e. Filtering: It was found that with the system under discussion, almost all of the target signal energy resided in the 0-500 MHz region (see Chapter II), thus, to suppress out-of-band clutter and noise a low-pass trapezodal filter with the transfer function shown in Figure 18 was inserted into the preprocessing unit. Various critical frequencies were tested, the ones shown in Figure 18 yielded the best identification performance.

---

* i.e., Identification based on a single radar observation

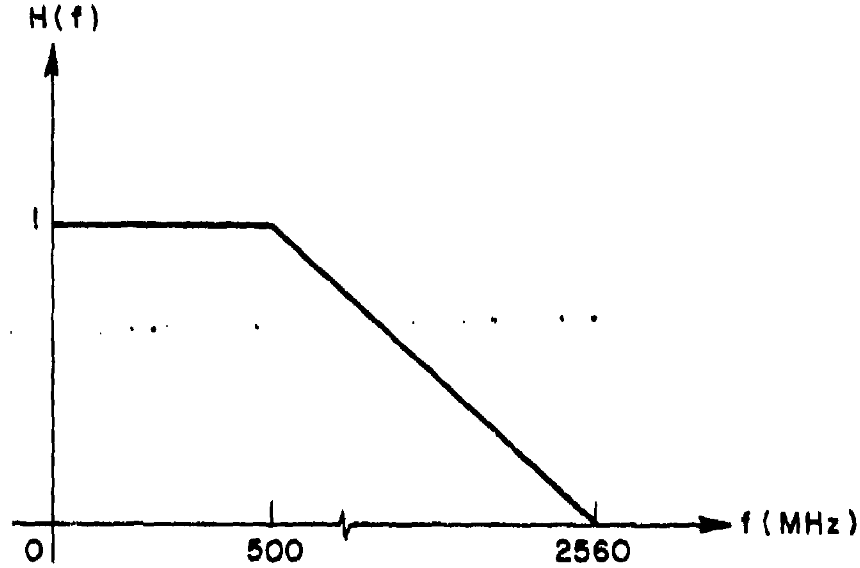

Figure 18. Transfer function of the pre-processor filter used in the 0.6m long antenna system for target identification.

For design flexibility, the filtering processes were performed in the frequency domain with the Fast Fourier Transform (FFT) package available in the digital computer system library. The only goal of the filtering operation is to remove the out-of-band frequency contents without adding any extraneous frequencies to the spectrum of the target response. The trapezoidal filter structure is a digital filter and was used here because of its linear phase characteristics and the availability of the FFT package in the digital computer. The FFT package allows tremendous flexibilities in digital filter design. It is important to note that the use of the trapezoidal filter here was not meant to be "optimum". More extensive study may well yield a better filter structure.

2. Detection: The detector performs a screening operation for the predictor-correlator identifier by rejecting as undesired-target waveforms those waveforms whose parameters are not within the desired ranges. The parameters considered in this study were:

a. Waveform energy (as defined in Chapter II).

b. Peak timing of the waveform.

c. Peak amplitude of the waveform

The desired ranges of the detection parameters were determined by studying the ranges of these parameters of the desired-target waveforms. Examples illustrating the choosing of the detection parameters are given in Section F of this chapter.

3. Prediction: Predict the calculated waveform using the Prony difference equation.

4. Correlation: Calculate the correlation coefficient for threshold identification by comparing the processed and the calculated waveforms. The correlation coefficient is defined to be unity minus the normalized total squared error.

This approach assumes that the poles and the difference equation coefficients for the desired target have previously been obtained. Thus, only simple algebraic operations are involved in calculating the correlation coefficient for an identification decision.

B. The Predictor

The predictor generates the calculated waveform. With the complex natural resonances and a chosen value of T, the coefficients α_m's of the Prony difference equation (see Equation (12)) can be determined via Equation (11). Thus, for one value of T, we can generate a calculated waveform by one of the following methods:

1. One-step prediction:

$$r_C(t+NT,T) = \sum_{m=0}^{N-1} -\alpha_m r_M(t+mT) \tag{22}$$

or

2. Interpolation:

$$r_C(t+m_oT,T) = \sum_{\substack{m=0 \\ m\neq m_o}}^{N} \frac{-\alpha_m}{\alpha_{m_o}} r_M(t+mT) \tag{23}$$

where

$$t = t_s + nT_B \quad , \quad n=0,1,2\cdots$$

and

$$T = iT_B \quad , \qquad i=1,2,\cdots$$

$r_c(t,T)$ and $r_M(t,T)$ are the calculated and processed measured waveform, respectively. t_s is the start-time (see Chapter II and III). The parameter m_0 is an index chosen for suppression of clutter and noise effects. In this study the interpolation method was used and m_0 was chosen to be the coefficient of maximum magnitude. By comparing Equations (22), (23) and (12) we note that when the measured waveform is from the desired target, $r_c(t)$ and $r_M(t)$ are equal and hence perfectly correlated. Note that one calculated waveform is constructed at each chosen value of T and the same measured waveform is used to construct calculated waveforms for all chosen values of T.

The one-step prediction method was first used by Hill who applied it to the detection and identification of targets (above ground) near the half space[40]. This method was then modified by Moffatt, et al.[9] to become the interpolation method for improved performance in clutter/noise. The predictor uses past values of the measured waveforms only, while the interpolator uses both past and future values and, together with its normalization process, was found to perform better in the presence of clutter/noise.

C. The Correlator

The correlation coefficient, formed by comparing the calculated and the processed measured waveform, is a function of T.

$$\rho(T) = 1 - \frac{\sum\limits_{t=t_s+m_0T}^{t_e-NT+m_0T} [r_c(t,T)-r_M(t)]^2}{\sum\limits_{t=t_s+m_0T}^{t_e-NT+m_0T} (r_c^2(t,T)+r_M^2(t))} \tag{24}$$

where the start-time t_s is taken to avoid the forced response of the backscattered waveform, while the stop-time t_e is taken to avoid the low-amplitude signal at the tail end of the waveform. In this study t_s was taken to be the time the absolute maximum of the waveform occurs, while t_e was taken to be the time the balun reflection occurs.

Equation (24) can be rewritten as

$$\rho(T) = \frac{\sum_{t=t_s+m_oT}^{t_e-NT+m_oT} 2r_c(t,T)r_M(t)}{\sum_{t=t_s+m_oT}^{t_e-NT+m_oT} (r_c^2(t,T)+r_M^2(t))} \quad . \tag{25}$$

We note that the numerator of the quotient in Equation (25) is the cross-correlation between the calculated and processed measured waveforms. The nominal range of $\rho(T)$ is $-1 \leq \rho(T) \leq 1$, and

$$\rho(T) = +1 \text{ when } r_c(t) = + r_M(t) \quad . \tag{26}$$

The quotient term in Equation (24) is identical to the mean-square error ε in Equation (21) when the approximated waveform $r_A(t)$ in the Prony process is equal to the calculated waveform $r_c(t)$. Thus,

$$\rho(T) = 1 - \varepsilon \quad . \tag{27}$$

The importance of Equation (27) lies in the fact that it ties the characterization and the identification processes together in such a way that optimization of one process (e.g., minimum ϵ) will lead to the optimization of the other (maximum $\rho(T)$). Therefore, the evaluation of optimum values of the parameters (N,T,t_s,t_e,M) in the characterization process leads also to optimum values in the identification process. This is rather significant in the evaluation of $\rho(T)$.

From Equations (24) and (25), we see that the interval in the error calculation is from t_s+m_oT to t_e-NT+m_oT, giving an error interval size of t_e-t_s-NT. Thus, the size of the error interval decreases as T increases.

D. The Predictor-Correlator as a Filter

In order to understand the operation of the predictor-correlator identifier, it is helpful to consider the identifier as a linear time-invariant filter.

From Equations (21) and (24), we see that, an instantaneous error e can be defined as

$$e(t+m_oT) = r_M(t+m_oT) - r_c(t+m_oT) = \sum_{m=0}^{N} \frac{\alpha_m}{\alpha_{m_o}} r_M(t+mT) \quad . \tag{28}$$

Thus, the instantaneous error e can be interpreted as the output of a Finite impulse response (FIR) filter[54-56] with the filter coefficients α'_m where

$$\alpha'_m = \frac{\alpha_m}{\alpha_{m_o}} \quad . \tag{29}$$

Note that although the filtering operation is based on the sampling interval T, the instantaneous error exists at the sampling period of T_B, where T is taken to be multiples of T_B. In the Z domain [54-56], the instantaneous error is given by

$$E(Z) = Z^{-N+m_o} \sum_{i=0}^{k-1} Z^{\frac{i}{k}} C(Z)R_M(Z) \tag{30}$$

where

$E(Z)$ = Z transform of the instantaneous error, based on T

$C(Z) = \sum_{m=0}^{N} \frac{\alpha_{N-m}}{\alpha_{m_o}} Z^{-m}$, is the Z transform of the filter coefficient sequence.

$R_M(Z)$ = Z transform of the processed measured waveform

and

$T = KT_B$, $K = 1,2,\cdots$.

The product $C(Z)R_M(Z)$ in Equation (30) is the filtering operation in the Z domain. Since the Z transform is based on the sampling interval T, thus this product term alone results in samples only at the sampling intervals of T in the time domain. The weighed sum operation (weighed by $Z^{i/k}$) fills the time interval between these samples with samples at finer sampling interval of T_B, and thus assures a better error waveform resolution. The presence of the factor Z^{-N+m_o} is to make sure that the starting point of the instantaneous error be consistent with that stated in the definition of the instantaneous error for the case of the interpolation method.

Using Equations (11), we rewrite Equation (30) as

$$E(Z) = \frac{1}{\alpha_{m_o}} Z^{-N+m_o} \sum_{i=0}^{k-1} Z^{\frac{i}{k}} R_M(Z) \prod_{j=1}^{N} (1-Z^{-1}Z_j) \tag{31}$$

where $Z_j = e^{s_j T}$ are the locations of the desired-target resonances in the Z plane, s_j are the complex resonances in the s plane and N is the number of complex resonances of the desired target. Note that the locations of the complex resonances in the Z plane are functions of the sampling interval T.

From Equations (24-31), we make the following important observations:

1. The mean-square error ε is the normalized energy of the instantaneous error e. ε is directly related to e as follows.

$$\varepsilon = \frac{\sum\limits_t e^2(t)}{\sum\limits_t e^2(t) + 2\sum\limits_t r_M^2(t) - 2\sum\limits_t r_M(t)e(t)} \tag{32}$$

where the summations in Equation (32) are taken over the error interval. The lower and upper bounds of the mean-square error ε are given by Equation (33)

$$\frac{1}{1 + \frac{2}{x} - \frac{2}{\sqrt{x}}} \geq \varepsilon \geq \frac{1}{1 + \frac{2}{x} + \frac{2}{\sqrt{x}}} \tag{33}$$

where

$$x \triangleq \frac{\sum\limits_t e^2(t)}{\sum\limits_t r_M^2(t)}$$

and the summations are again taken over the error interval.

The error bounds are plotted as a function of x in Figure 19. From Figure 19, the following observations are made:

a. ε is bounded as follows :

$$2 \geq \varepsilon \geq 0 .$$

$$\varepsilon = 2 \text{ when } e(t) = 2r_M(t) \text{ and} \tag{34}$$

$$\varepsilon = 0 \text{ when } e(t) = 0 .$$

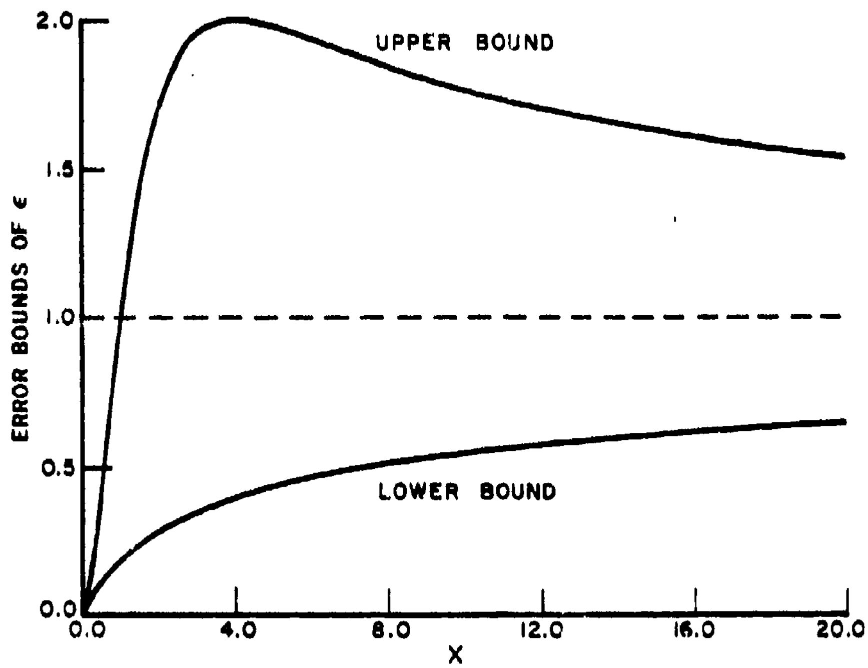

Figure 19. Bounds of the mean-square error ε.

b. The lower bound of ε increases monotonically as the energy of the instantaneous error ε'* increases. ε approaches 1 as ε' approaches infinity.

c. The upper bound of ε increases monotonically from 0 to 2 as ε' increases from 0 to the value of

$$4\sum_t r_M^2(t)/((t_e-t_s)/T_B) \quad .$$

At this ε' value, ε attains its maximum upper bound of 2. The upper bound of ε decreases from 2 to 1 as ε' increases to infinity. Although the upper bound of ε does not increase monotonically as ε' increases from 0 through its entire range, the lower bound does. Thus, it is reasonable to say that large ε' generally means large ε.

2. The difference between the one-step prediction and the interpolation method lies in the filter gain normalization factor $1/\alpha_{m_0}$. In the one-step prediction method, $\alpha_N=1$, thus, the possibility of larger-than-one filter coefficients α_m exists. Such filter coefficients would of course amplify clutter and noise effects. In the interpolation method, α_{m_0} is the difference equation coefficient of maximum magnitude. Thus, no filter coefficient can have value larger than one.

3. For the desired target, $R_M(t)$ is given by the Z transform of Equation (4) and thus Equation (30) can be written as

$$E(Z) = \frac{1}{\alpha_{m_0}} Z^{-N+m_0} \sum_{i=0}^{k-1} Z^{\frac{i}{k}} \left[\sum_{m=1}^{N_1} \frac{a_m}{(1-Z^{-1}Z_m)} \right] \prod_{j=1}^{N} (1-Z^{-1}Z_j)$$

$$= \frac{1}{\alpha_{m_0}} Z^{-N+m_0} \sum_{i=0}^{k-1} Z^{\frac{i}{k}} \frac{Q(Z)}{\prod_{m=1}^{N_1} (1-Z^{-1}Z_m)} \prod_{j=1}^{N} (1-Z^{-1}Z_j) \qquad (35)$$

---

*
$$\varepsilon' \stackrel{\Delta}{=} \sum_{t=t_s+m_0T}^{t_e-NT+m_0T} e^2(t)/((t_e-t_s)/T_B)$$

where N_1 is the number of complex resonances present in the waveform and, N is the number of all possible complex resonances of the desired target present within the radar bandwidth and used for target identification purposes. Since certain target resonances may not be excited for some radar locations and orientations, N_1 and N are not necessarily equal. Q(Z) is a polynomial of order N_1 in Z^{-1}.

From Equation (33), we see that the predictor-correlator identification process is basically a pole-removal process. Furthermore, the process of pole removal is performed by putting zero's at the locations of the poles.

In the case of $N_1=N$,

$$E(Z) = \frac{1}{\alpha_{m_o}} Z^{-N+m_o} \sum_{i=0}^{k-1} Z^{\frac{i}{K}} Q(Z) \qquad (36)$$

Thus

$$e(nT_B) = \frac{1}{\alpha_{m_o}} q(nT_B) = 0 \text{ for } nT_B \geq m_oT \qquad (37)$$

where

$$q(nT_B) = \mathcal{Z}^{-1}\left[Z^{-N+m_o} \sum_{i=0}^{k-1} Z^{\frac{i}{K}} Q(Z)\right]$$

where $\mathcal{Z}^{-1}[\ ]$ is the inverse Z transform operation. Since Q(Z) is a polynomial of order N in Z^{-1}, $q(nT_B)$ is zero for $nT_B \geq m_oT$ [54-56]. Thus, the instantaneous error $e(nT_B)$ is zero for $nT_B \geq m_oT$ and the mean-square error would also be zero in this time region. The above derivation is based on the assumption that the resonance time region of the waveform starts at t=0. Since the resonance region of the waveforms considered in this study is assumed to start at $t=t_s$, the mean-square error would be zero for $t \geq t_s+m_oT$. This is the lower limit of the error-calculation intervals as defined in Equations (21) and (24).

In the case of $N_1<N$,

$$E(Z) = \frac{1}{\alpha_{m_o}} Z^{-N+m_o} \sum_{i=0}^{k-1} Z^{\frac{i}{K}} Q(Z) \prod_{j=1}^{N-N_1} (1-Z^{-1}z_j) \qquad (38)$$

Thus

$$e(nT_B) = q'(nT_B) \tag{39}$$

where

$$q'(nT_B) = \mathcal{Z}^{-1}\left[Z^{-N+m_o} \sum_{i=0}^{k-1} Z^{\frac{i}{k}} Q(Z) \prod_{j=1}^{N-N_1} (1-Z^{-1}Z_j)\right] \quad . \tag{40}$$

Since $Q(Z)$ is of degree N_1 in Z^{-1}, thus $q'(nT_B)$ is again zero for $nT_B \geq m_oT$. Thus putting the number of all possible extracted resonances of the desired target in the identifier assures a zero error and thus a unity correlation coefficient for the desired target waveforms from all radar locations and orientations. If not all possible extracted resonances are used for target identification, the possibility of $N_1 > N$ exists and in this case,

$$E(Z) = \frac{1}{\alpha_{m_o}} Z^{-N+m_o} \sum_{i=0}^{k} Z^{\frac{i}{k}} \frac{Q(Z)}{\prod_{i=1}^{N_1-N} (1-Z^{-1}Z_i)} \quad . \tag{41}$$

The instantaneous error has poles in its Z transform, causing it to be a waveform of infinite duration [54-56]. Thus, a large mean-square error could occur for a desired-target waveform, possibly causing the correlation coefficient to be much less than one.

4. For an undesired target, the instantaneous error depends on the processed waveform $r_M(t)$ as well as the locations of the zero's in the identifier. Small error could result only in the cases where the undesired-target waveform is closely characterized by a set of complex resonances which are approximately equal to the desired-target resonances (i.e., the zeros in the identifier). In the one-pole case where,

$$R_M(Z) = \frac{1}{1-Z^{-1}Z_1}$$

$$C(Z) = (1-Z^{-1}Z_2) \tag{42}$$

where $R_M(Z)$, the Z transform of the measured waveform is assumed to have only one pole at Z_1 with residue 1. $C(Z)$, the identification filter is assumed to consist of a zero at Z_2. The error can be expressed as

$$E(Z) = \frac{1}{\alpha_{m_o}} Z^{-N+m_o} \sum_{i=0}^{k-1} Z^{\frac{i}{k}} \frac{1}{(1-Z^{-1}Z_1)} (1-Z^{-1}Z_2) \tag{43}$$

$$= Z^{-N+m_o} \sum_{i=0}^{k-1} Z^{\frac{i}{k}} \left[\frac{1}{\alpha_{m_o}} - \frac{1}{\alpha_{m_o}} (Z_1-Z_2) \frac{Z^{-1}}{1-Z^{-1}Z_1} \right] .$$

Thus,

$$\varepsilon' = \left[\frac{||Z_1-Z_2||}{\alpha_{m_o}} \right]^2 \sum_t r_M^2(t)/((t_e-t_s)/T_B) \tag{44}$$

where $||\cdot||$ denotes complex magnitude. Hence the total squared error ε' is directly proportional to the magnitude square of the difference between the locations of the pole and the zero.

In a two-pole case where

$$R_M(Z) = \frac{1}{1-Z^{-1}Z_1} + \frac{1}{1-Z^{-1}Z_1^*}$$

$$C(Z) = (1-Z^{-1}Z_2)(1-Z^{-1}Z_2^*) \tag{45}$$

where [ ]* denotes complex conjugation. The error can be expressed as

$$E(Z) = \frac{1}{\alpha_{m_o}} Z^{-N+m_o} \sum_{i=0}^{k-1} Z^{\frac{i}{k}} \left[\left(\frac{1}{1-Z^{-1}Z_1} + \frac{1}{1-Z^{-1}Z_1^*} \right) (1-Z^{-1}Z_2)(1-Z^{-1}Z_2^*) \right] \tag{46}$$

or

$$E(Z) = \frac{1}{\alpha_{m_0}} Z^{-N+m_0} \sum_{i=0}^{k-1} Z^{\frac{i}{k}} \left\{ (1-Z^{-1}Z_2^*) + (1-Z^{-1}Z_2) + \right.$$
$$+ Z^{-1}\left[\frac{(Z_1-Z_2)}{1-Z^{-1}Z_1} + \frac{(Z_1^*-Z_2^*)}{1-Z^{-1}Z_1^*}\right] +$$
$$\left. + Z^{-2}\left[\frac{(Z_1-Z_2)Z_2}{1-Z^{-1}Z_1} + \frac{(Z_1^*-Z_2^*)Z_2^*}{1-Z^{-1}Z_1^*}\right]\right\}. \quad (47)$$

The total square error ε' is independent of the first two terms on the right hand side of Equation (47). Furthermore, the inverse Z transform of the last two terms are given by [54]

$$\zeta^{-1}\left[Z^{-1}\left(\frac{Z_1-Z_2}{1-Z^{-1}Z_1} + \frac{Z_1{}^*Z_2{}^*}{1-Z^{-1}Z_1{}^*}\right)\right] = ||Z_1-Z_2||e^{\alpha_1(t-T)} \times$$
$$\times \cos[\omega_1(t-T) + \theta_1] \quad (48)$$

and

$$\zeta^{-1}\left[Z^{-2}\left(\frac{(Z_1-Z_2)Z_2}{1-Z^{-1}Z_1} + \frac{(Z_1^*-Z_2^*)Z_2^*}{1-Z^{-1}Z_1^*}\right)\right]$$
$$= ||Z_1-Z_2||\;||Z_2||\;e^{\alpha_1(t-2T)} \times$$
$$\times \cos[\omega_1(t-2T)+\theta_1+\theta_2] \quad (49)$$

where θ_1 and θ_2 are the arguments of the complex numbers (Z_1-Z_2) and Z_2, respectively.

From Equations (47) and (48), we see that

$$e(t) = \frac{1}{\alpha_{m_0}} ||Z_1-Z_2||e^{\alpha_1(t-T)} \left\{\cos[\omega_1(t-T)+\theta_1] + \right.$$
$$+ ||Z_2||e^{-\alpha_1 T} \cos[(\omega_1(t-T)+\theta_1) +$$
$$\left. + (\omega_1 T+\theta_2)]\right\} \quad . \quad (50)$$

Thus, the instantaneous error depends on the following three items:

a. The amplitude factor $||Z_1-Z_2||^2 = e^{2\alpha_1 T} + e^{2\alpha_2 T} - 2e^{(\alpha_1+\alpha_2)T}\cos(\omega_1-\omega_2)T$, where $s_2=\alpha_2+j\omega_2$ is the location of the zero of the filter in the s plane,

b. The factor $2e^{-\alpha_1 T}||Z_2|| = 2e^{-(\alpha_1-\alpha_2)T}$,

c. The phase term $\omega_1 T+\theta_2=(\omega_1+\omega_2)T$.

All of the above three items are dependent on the sampling interval T. Thus, in designing the identification radar, the value(s) of T should be chosen to maximize ε' by considering its dependence on the above three items. In maximizing ε', we note the following guidelines:

a. Small values* of T result in $||Z_1-Z_2||$ approaching zero. This causes ε' to approach zero. Thus, small T values offer no identification capability.

b. Large values** of T also result in $||Z_1-Z_2||$ approaching zero. Thus, large T values offer no identification capability.

c. Intermediate value of T should be chosen to satisfy the following conditions as closely as possible:

   i. $e^{2\alpha_1 T}$ $e^{2\alpha_2 T}$ and $e^{(\alpha_1+\alpha_1)T}$ approach 1 ,

   ii. $(\omega_1-\omega_2)T$ approaches $\pm\pi$,

   iii. $(\omega_1+\omega_2)$ approaches 2π ,

   iv. To prevent severe aliasing effects, we require that $\pi \geq \omega_1 T$ and $\omega_2 T$.

---

* Small T in this case means that the quantity $(\omega_1-\omega_2)T$ approaches 0 and the quantities $e^{\alpha_1 T}$, $e^{\alpha_2 T}$ and $e^{(\alpha_1+\alpha_2)T}$ approach 1.

**Large T in this case means that the quantities $e^{2\alpha_1 T}$, $e^{2\alpha_2 T}$ and $e^{(\alpha_1+\alpha_2)T}$ approach 0.

Conditions i. and ii. maximize the amplitude factor $||Z_1-Z_2||$. Conditions i. and iii. make sure that the second term in Equation (50) is maximized and has the same sign as the first term. Conditions ii. and iii. require that $2\pi \geq \omega_2 T \geq \pi$.* Condition i. requires that T be as small as possible. These, together with condition iv indicate that a reasonable compromise is to choose T such that $\omega_2 T=\pi$.

Although the above analysis is based on a two-pole system, for system of more than two poles, the above results are expected to be reasonably valid when ω_1 is taken to be the imaginary part of the dominant pole of the measured waveform to be identified and ω_2 is taken to be the imaginary part of the zero of the identification filter which is closest to the dominant pole. In practical target identifications situations, the waveforms from the desired as well as the undesired targets almost always contain more than two poles (see Chapter III). Furthermore, the dominance of the resonances of the undesired target is generally unknown. Thus, for better identification performance, it is advisable to base the identification decision-making process on more than one value of T. Based on the analysis in this section, the smallest "effective" value of T is in the neighborhood of T_N where

$$T_N = \frac{\pi}{\omega_M} = \frac{1}{2f_M} \quad , \tag{51}$$

and $\omega_M=2\pi f_M$ is the maximum imaginary part of the desired-target resonances. In applying the criterion given by Equation (51) to choose the values of T for target identification, the word neighborhood should be emphasized and taken to mean that, although the single value of T for optimum target-separation performance cannot be found without the complete knowledge of the undesired-target waveform, the value $T=T_N$ should give reasonable, if not the optimum performance. Furthermore, for target identification based on more than one value of T, the region of T values chosen should contain T_N.

The analysis presented in this section are generally supported by the identification results obtained in this study. Identification results are shown in Section F of this chapter.

---

* It is assumed that $\omega_2 > \omega_1$. Note that the design of the low-pass filter in the preprocessor of the identification radar assures that frequencies higher than ω_2 will be highly attenuated. Thus, $\omega_2 > \omega_1$ is a valid assumption.

L. The Identification Algorithm

In this study, a "single-look" identification algorithm was used. An identification decision was made for every measured backscattered waveform. The identification algorithm was one of threshold identification based on the values of $\rho(T)$ evaluated at different values of T, and the average value of $\rho(T)$ denoted by $\langle\rho(T_0)\rangle$. Thus, the decision algorithm was

$$
\left.\begin{array}{ll}
\text{"Desired Target" when} & \left\{\begin{array}{l} \rho(T_{0i}) \geq \rho_{THi} \text{ for } i=1 \ \underline{\text{and}}\ 2 \cdots \underline{\text{and}}\ I \\ \underline{\text{and}}\ \langle\rho(T_0)\rangle \triangleq \dfrac{\sum_{i=1}^{I} \rho(T_{0i})}{I} \geq \rho_{THA} \end{array}\right. \\
\text{"Undesired Target" when} & \left\{\begin{array}{l} \rho(T_{0i}) < \rho_{THi} \text{ for } i=1 \ \underline{\text{or}}\ 2 \cdots \underline{\text{or}}\ I \\ \underline{\text{or}}\ \langle\rho(T_0)\rangle < \rho_{THA} \end{array}\right.
\end{array}\right\} . \tag{52}
$$

ρ_{THi} is the identification threshold for $\rho(T)$ at the T value of T_{0i}. T_{0i}'s are the values of T chosen for optimum identification performance. ρ_{THA} is the identification threshold for the average of $\rho(T)$ taken over all the values of T_{0i}. Thus, for a single measured waveform, we evaluate its correlation function $\rho(T)$ at all chosen values of T_{0i} and compare the values $\rho(T_{0i})$ and $\langle\rho(T_0)\rangle$ to ρ_{THi} and ρ_{THA}, respectively for an identification decision. Figure 20 illustrates the decision-making process. In Figure 20, the value of the $\rho(T)$ curve represented by "dots" at $T_{01}, T_{02} \cdots T_{05}$ as well as $\langle\rho(T_0)\rangle$ are greater than their corresponding thresholds hence, the targets it represents is by decision a "desired" target. The $\rho(T)$ curve represented by "boxes" has at least one of the values $\rho(T_{0i})$ or $\langle\rho(T_0)\rangle$ below its corresponding threshold, thus, the target it represents is by decision an "undesired" target.

T_{0i}'s are the value of T chosen for optimum identification performance. The values of T_{0i} are closely related to the value of the resonances of the desired target and Equation (51). Details concerning the values of T_{0i}'s will be further discussed in the next section. In Equation (52), quotation marks are used to signify a decision, i.e., "Desired target" is by decision a desired target while in reality it could be an undesired target (in case of false alarm).

The identification algorithm given in Equation (52) reduces to its simplest form when only one value of T_{0i} is considered. In this case, the identification algorithm is

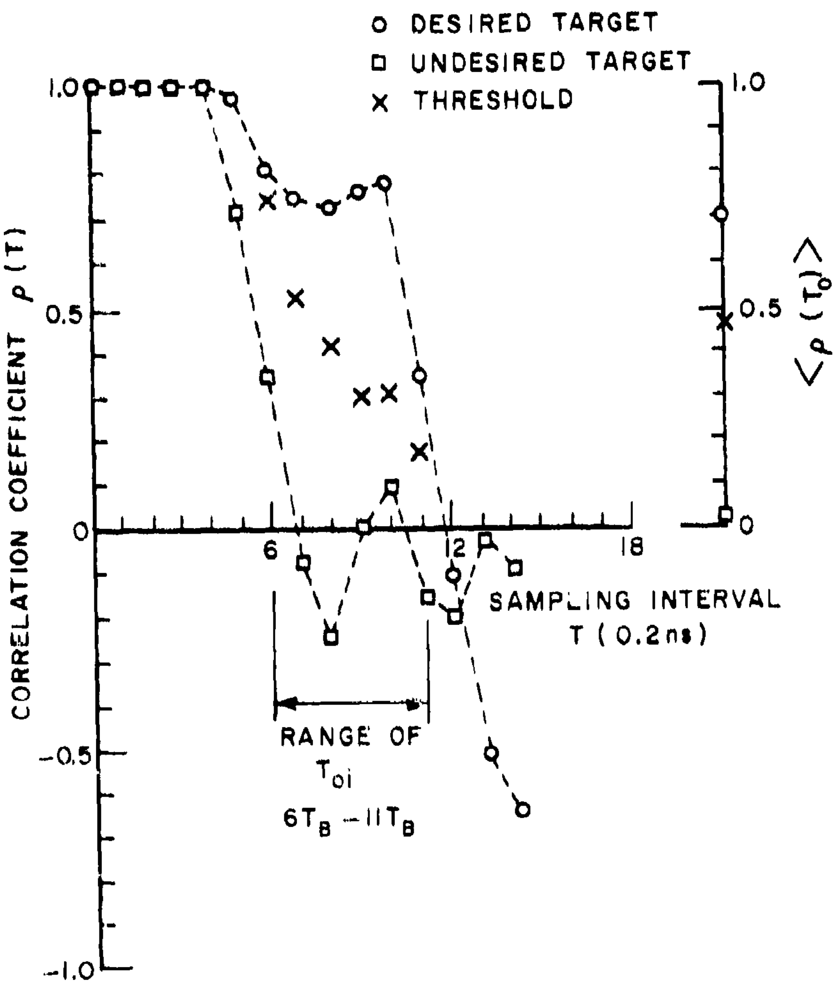

Figure 20. The decision-making process for the multiple-threshold identification algorithm.

$$\text{"Desired target" when } \rho(T_0) > \rho_{TH}$$
$$\text{"Undesired target" when } \rho(T_0) < \rho_{TH} \; . \qquad (53)$$

In the following section, the predictor-correlator identification method is applied to the processed waveforms. Identification performance will be presented and discussed.

F. Performance of the Predictor-Correlator Identifier

In order to demonstrate the effectiveness of the predictor-correlator, a set of identification performance based on a single value of $\rho(T)$ were obtained by applying the predictor-correlator alone (i.e., without the filter and the detector) to the difference waveforms. Identification results based on multiple values of $\rho(T)$ and with the filter and detector operations inserted will be presented late in this section. Identification performance was characterized by a $\rho(T)$ curve. Typical $\rho(T)$ curves are shown in Figure 21. In this case, the identifier was set to identify the mine-like target in a wet ground condition.

From Figure 21, we find that typical $\rho(T)$ curves have the following features:

1. The value of $\rho(T)$ is approximately 1 for small values of T. This is true for $\rho(T)$ of both the desired and undesired targets. This region of T has no identification capability.

2. The region of T_0 where "optimal" identification performance occurs is in the immediate neighborhood of T_N where t_M is given by Equation (51). In this case for identification of the mine-like target in a wet ground condition. The resonances of the mine-like target as given in Table 1c was used. Thus, f_M = 420 MHz, corresponding to the rounded T_N value of 6 T_B (or 1.2 ns). For the $\rho(T)$ curves given in Figure 21, the region of T_0 is from 6 T_B to 11 T_B. This result supported the observations made in Section D of this chapter. The fact that the region of effective values of T contained values larger than T_N indicated that the dominant pole(s) in the copper sheet waveform had imaginary parts lower than 420 MHz.

3. The value of $\rho(T)$ fluctuates when T is much larger than T_N ($T > 2T_N$). This region of T has no identification capability. Besides the reason given in Section D of this chapter, this can also be attributed to the following.

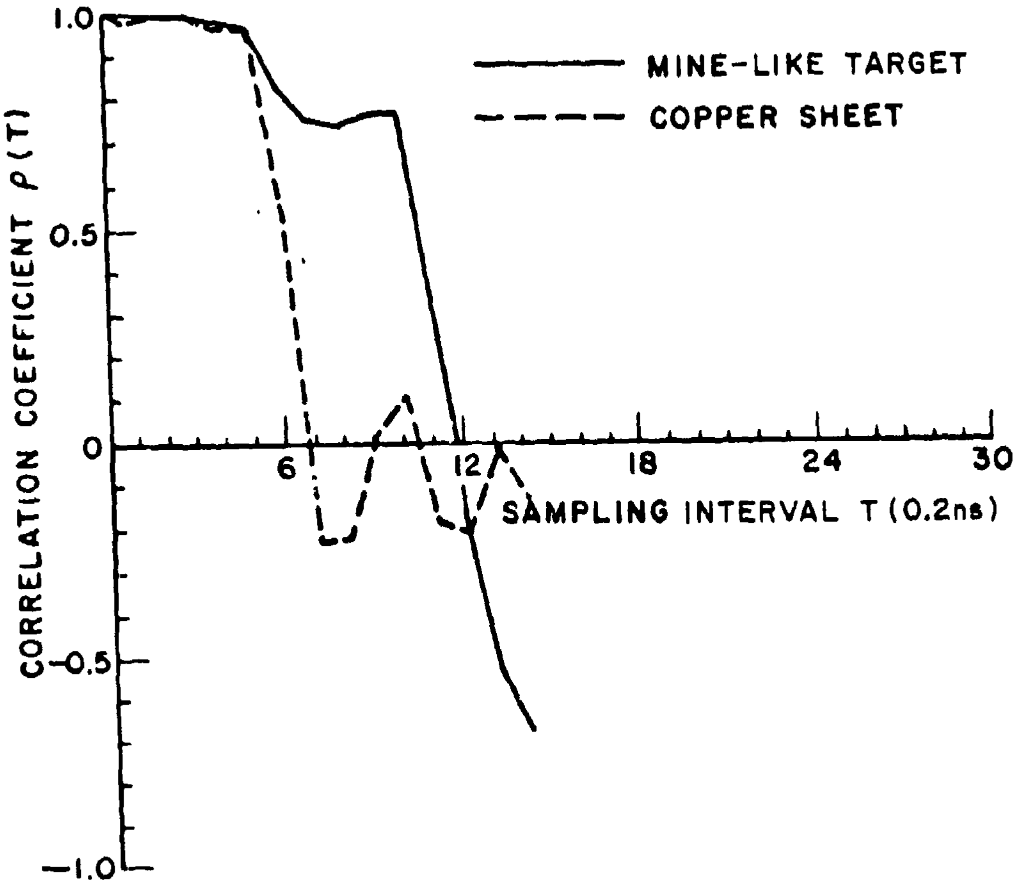

Figure 21. Typical ρ(T) curves for the identification of the mine-like target in wet ground.

First, aliasing of the high frequency zeros in the identifier makes these zeros ineffective. Second, the size of the error interval of the error ϵ decreases as T increases, for the number of instantaneous error samples used in the calculation of ϵ decreases. Third, because of the large value of T, only the tail end of the measured waveform is used in the calculation of ϵ. This region of the measured waveform has low signal level.

The above features of the $\mu(T)$ curves were generally observed in almost all cases considered. The significance of these features is that optimal identification performance occurs in a confined range of T values in the immediate neighborhood of T_N. Hence one knows a priori the value or range of values of T on which to base the implementation of the radar system. These features are again demonstrated in the $\mu(T)$ curves given in Figures 22 and 23 for the identification of the mine-like target and the brass cylinder in dry ground, respectively.

In this study, the criterion for optimum identification performance was to require perfect identification of desired-target returns, and thus optimal performance was the one with the lowest false alarm probability obtained by varying T. Single-look identification and false alarm probabilities are estimated in a frequency of occurrence sense. Thus,

$$P_I = \frac{N_2}{N_1} \tag{54}$$

$$P_{FA} = \frac{N_4}{N_3} \tag{55}$$

where

P_I = Probability of identification

P_{FA} = Probability of false alarm

and

N_1 = Total number of desired-target waveforms within the identification range.

N_2 = Number of desired-target signals which are correctly identified within the identification range.

N_3 = Total number of other-target waveforms.

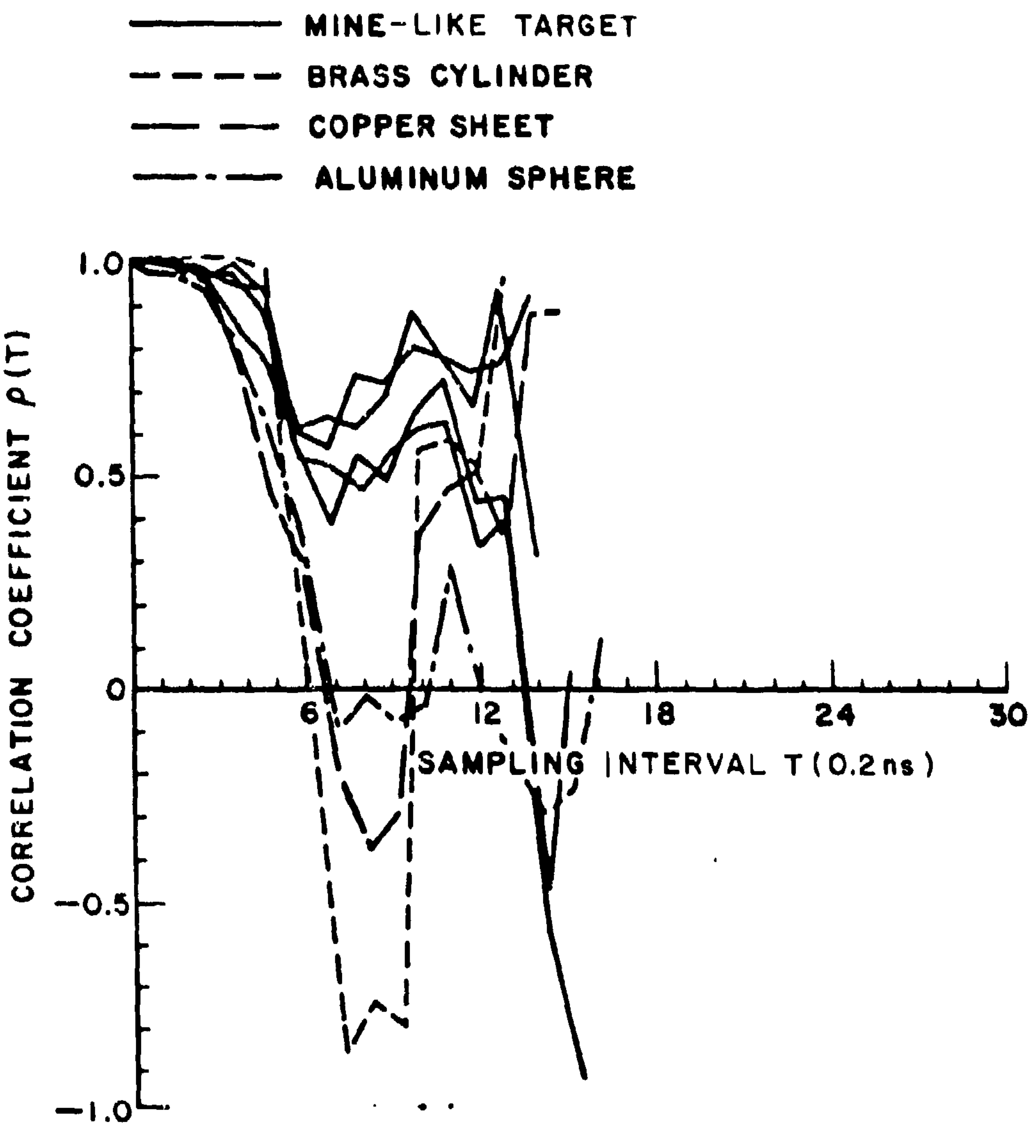

Figure 22. Typical ρ(T) curves for the identification of the mine-like target in dry ground.

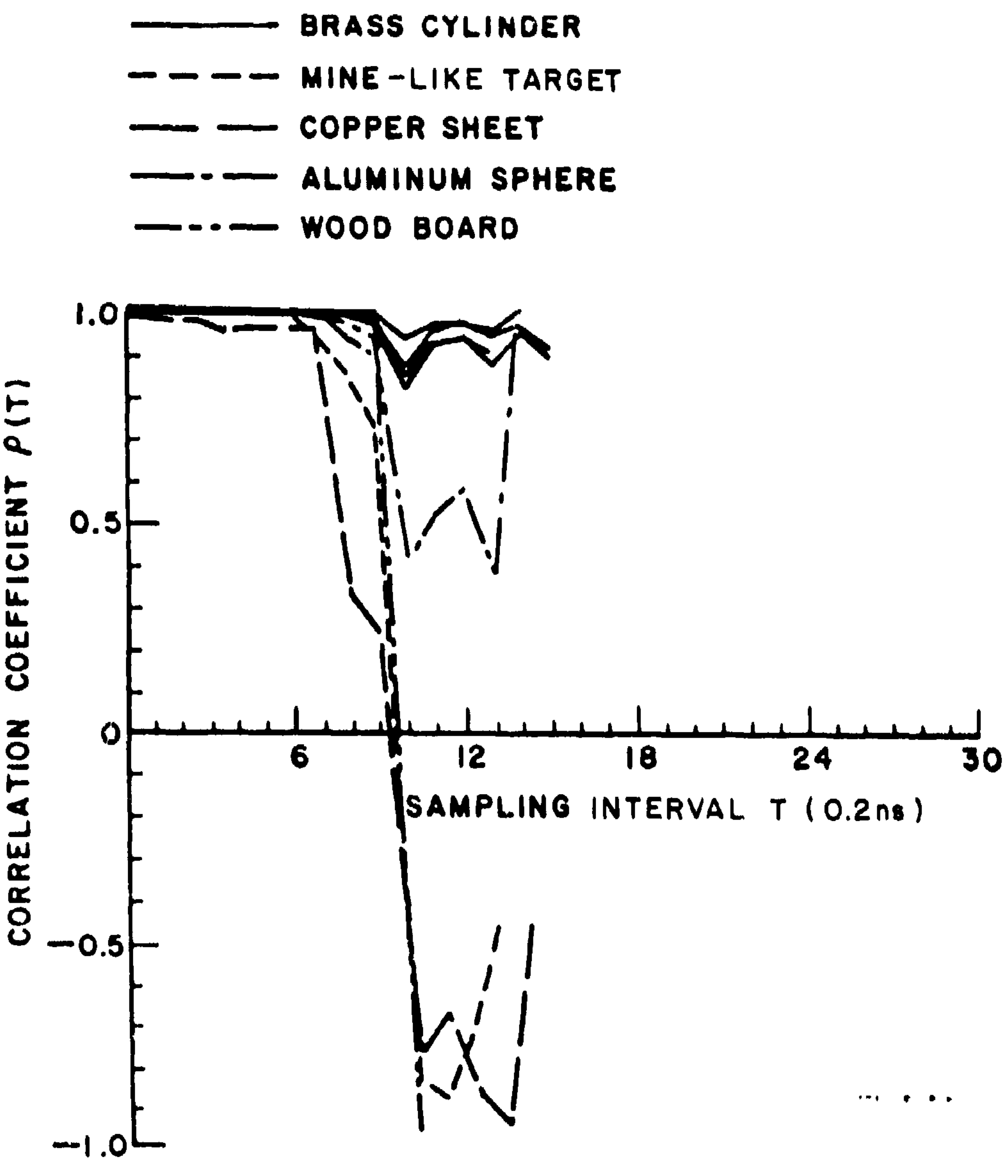

Figure 23. Typical ρ(T) curves for the identification of the brass cylinder in dry ground.

N_4 = Number of other-target waveforms which are mistaken to be desired-target waveforms.

Note that N_3, N_4 basically determine the accuracy or "confidence interval"[65] of the above estimates of the identification statistics.

To see the degree of separation between the mine-like target and other subsurface targets, consider the distribution of correlation coefficients shown in Figure 24. In this case, the system is set to identify the mine-like target in wet ground. From Figure 24, we see that, for P_I = 100%, and $T_O = 9T_B$, the minimum separation margin between the mine-like target and other targets is 0.93 in the value of $\rho(T_O)$. In this case, for an identification performance estimate of P_I = 100%, P_{FA} = 0% one can set the identification threshold ρ_{TH} at a value ranging from -0.26 to 0.167. The maximum value of ρ_{TH} is 0.167. The correlation coefficients for the mine-like target shown in Figure 24 include only cases measured within the identification range R_{ID}. In this study, identification range is the radar range measured from the center of the target. Correlation coefficients for the other targets include all cases measured.

A summary of optimal single-look identification performance is given in Table 4 (for details, see Appendix E). Estimates of P_I = 100%, P_{FA} = 0% identification performance were obtained for the identification range of 30 cm measured from the center of the mine-like target and the brass cylinder.

This set of identification performance basically established the fact that the predictor-correlator identification method worked in its simplest form and with a minimum amount of preprocessing. However, in a practical system, one would prefer to have the filter and detector inserted for better performance in more severe clutter/noise environment provided that the amount of time taken to perform these operations are not too large to make them non-cost-effective. Furthermore, the multiple-threshold algorithm would also provide better performance.

In target identification with detection and multiple-threshold operations, the ranges of the detection parameters, i.e., waveform energy, peak timing and peak magnitude must be chosen. Furthermore, the values of T_{Oi} as well as the identification thresholds ρ_{THi} and ρ_{THA} must be determined. In this study, these parameters were experimentally determined via the following procedure:

1. The ranges of the detection parameters were chosen to be the ranges of these parameters of the waveforms measured from the desired target within the identification range.

2. Choose the range of T_{Oi} values based on the conditions given in Section D of this chapter.

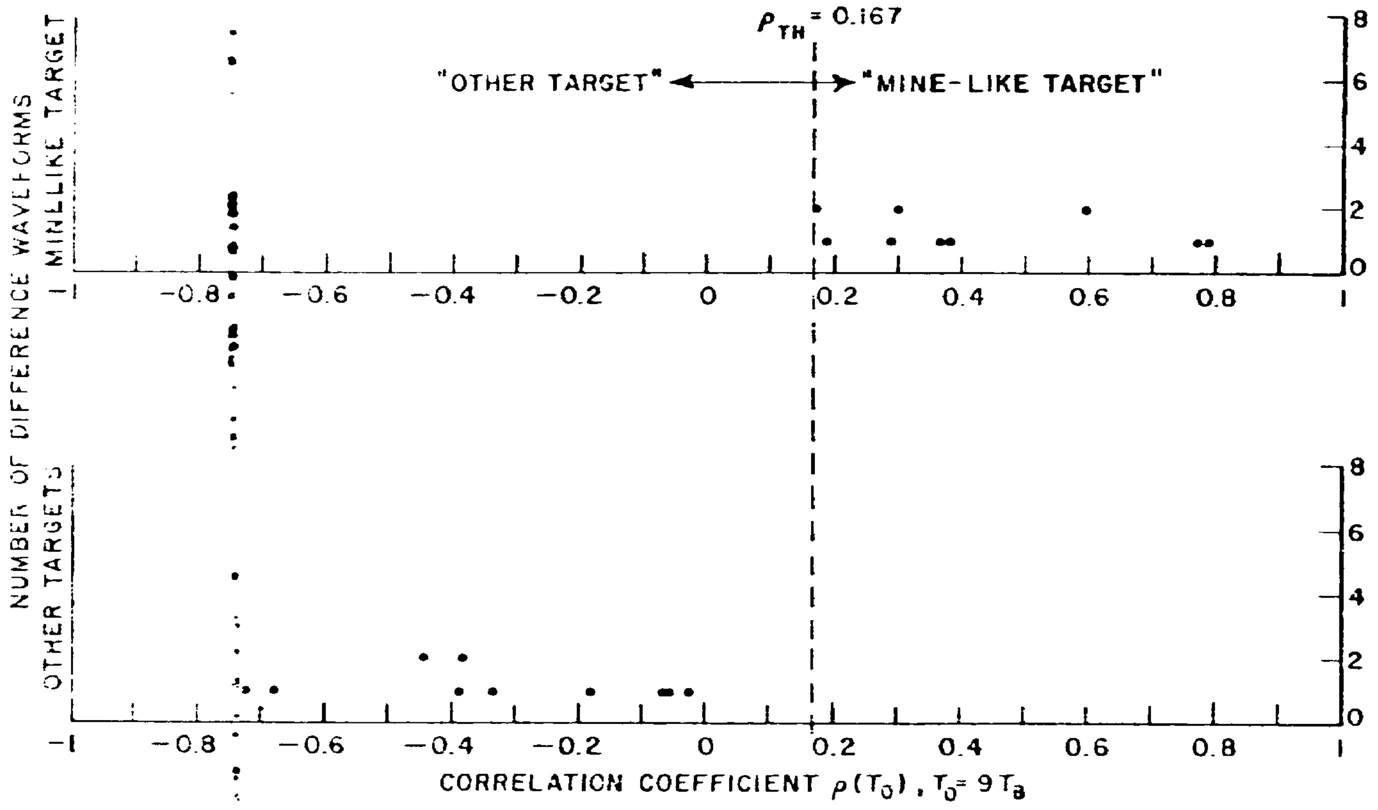

Figure 24. Distribution of correlation coefficients for the identification of the mine-like target in wet ground. R_{ID}=30 cm.

TABLE 4
SUMMARY OF SINGLE-LOOK IDENTIFICATION PERFORMANCE
OF THE SHORT-CABLE SYSTEM .
P_I=100% For All Cases

DESIRED TARGET	GROUND CONDITION	T_o	ρ_{TH}	R_{ID} (cm)	P_{FA}	NUMBER OF WAVEFORMS	
						DESIRED TARGET	UNDESIRED TARGET
MINE-LIKE TARGET	WET	$7T_B$-$9T_B$	.183	30	0%	12	12
MINE-LIKE TARGET	DRY	$7T_B$-$9T_B$	.483	15	0%	5	3
MINE-LIKE TARGET	ICY	$7T_B$-$9T_B$	.423	30	0%	9	9
BRASS CYLINDER	ICY	$5T_B$-$7T_B$	.675	30	0%	9	9

*PERFORMANCE FOR R_{ID}=30 cm WAS NOT OBTAINED IN THIS CASE.

R_{ID} = IDENTIFICATION RANGE, MEASURED FROM CENTER OF TARGET

3. Choose the identification thresholds to be the minimum values of $\rho(T_{oi})$ and $\rho(T_o)$ evaluated from the desired-target waveforms measured within the identification range.

An example is given below to clarify the above procedure. From the waveforms measured from a mine-like target in a wet ground condition, we evaluated their detection parameters (as tabulated in Table 5) and determined the minimum and maximum of these parameters. The ranges of these parameters were used as the desired ranges of the detection parameters in the detector. With the extracted resonances from the measured waveforms (as given in Table 6), and the conditions given in Section D of this chapter, we chose the range of T_{oi} values to be from (T_N-T_B) to $2T_N$. In this case f_M=428 MHz, thus

$$T_N = \left[\frac{1}{2\times428\times10^6}\right]^* = 5T_B$$

* [ ] denotes greatest integer.

TABLE 5
DETERMINING THE DETECTION PARAMETERS FOR IDENTIFICATION
OF THE MINE-LIKE TARGET IN A WET GROUND CONDITION.
R_{ID}=30 cm

ANTENNA LOCATION / PARAMETERS	C	15 cm,S	30 cm,S	15 cm,N	30 cm,N	15 cm,E	30 cm,E	15 cm,W	30 cm,W	MINIMUM	MAXIMUM
t_{max}*	37	27	29	38	69	46	71	60	67	27	69
m_{max}**	1.63418	3.99696	2.35840	2.65925	1.78342	1.70874	1.18873	2.74239	1.88786	1.18873	3.99696
E_M***	.12784	.57531	.68460	.33775	.25890	.22767	.10616	.20658	20827	.12784	.68460

* t_{max} = peak timing, in units of T_B

** m_{max} = peak magnitude, in units of 200 mV

*** E_M = waveform energy, in units of $(200\ mV)^2$.
Definition of E_M is given in Chapter II

TABLE 6
AVERAGE EXTRACTED RESONANCES OF THE MINE-LIKE TARGET IN A WET GROUND CONDITION

POLE (REAL)*	POLE (IMAG)
-1.71536397E8	±6.1601933 E7
-5.73125538E7	±1.32122486E8
-2.87494683E8	±2.27030133E8
-1.82908509E8	±3.07411043E8
-9.76454733E7	±4.28447900E8

*Real and imaginary parts of the extracted poles are in nepers/s and Hz, respectively.

With the values of T_{0i}, we evaluate the values of $\rho(T_{0i})$ and $<\rho(T_0)>$ for the all measured desired-target waveforms. The minimum of these values are chosen to be the identification thresholds. This is illustrated in Table 7.

Table 8 summarizes a set of single-look identification performance based on the additional preprocessing and the multiple-threshold algorithm. Note that the size of the ensembles of waveforms considered indicates a better estimate of the identification statistics. In obtaining this set of identification performance, the region of T_0 values was chosen to be from (T_N-T_B) to $2T_N$. Details concenring the identification results are given in Appendix E.

The identification statistics discussed so far were obtained with the identifier "tuned" to the right ground condition, e.g., the wet-ground resonances of the mine-like target were used to identify the mine-like target in that wet ground condition. If the identifier is not tuned, identification performance will degrade, e.g., for the waveforms considered in Table 4, when the dry-ground resonances were used to identify the mine-like target in wet ground, performance degraded to P_I=90%, P_{FA}=16.6%. Methods for on-location calibration of the ground condition and automatic tuning of the identification radar to ground condition is currently being pursued. One method is based on the backscattered waveforms from thin wires measured using the same pulse radar system. On-location calibration of the ground condition and automatic tuning of the identifier to the ground condition are discussed in Chapter IX.

TABLE 7
DETERMINING THE IDENTIFICATION THRESHOLDS FOR THE MINE-LIKE TARGET IN A WET GROUND CONDITION.
R_{ID}=30 cm

ANTENNA LOCATION $\rho(T_{oi})$	C	15 cm,S	30 cm,S	15 cm,N	30 cm,N	15 cm,E	30 cm,E	15 cm,W	30 cm,W	MINIMUM $=\rho(T_{oi})$
$\rho(4T_B)$	.984	.948	.975	.996	.996	.971	.998	.934	.997	.948
$\rho(5T_B)$	.920	.667	.739	.927	.905	.943	.808	.635	.846	.667
$\rho(6T_B)$	.128	-.0871	-.209	.0331	.642	.530	.240	.354	.218	-.209
$\rho(7T_B)$	.490	.243	.377	.348	.573	.453	.390	.258	.269	.243
$\rho(8T_B)$	.606	-.0615	.099	.0880	.589	.522	.351	.150	.271	-.0615
$\rho(9T_B)$	.924	-.118	.200	.227	.716	.639	.402	.820	.681	-.118
$\rho(10T_B)$	.878	.224	.0566	.291	.177	.413	.609	.547	.880	.224
$\rho(T_o)$	.70442	.25937	.31965	.41568	.65683	.63864	.54245	.52819	.59555	.25937

Identification is degraded when the radar frequencies do not properly span the target resonances. This is demonstrated in Chapter V.

TABLE 8
SUMMARY OF SINGLE-LOOK IDENTIFICATION PERFORMANCE OF THE SHORT-CABLE SYSTEM BASED ON ADDITIONAL PREPROCESSING AND MULTIPLE-THRESHOLD ALGORITHM.
P_I=100% For All Cases

DESIRED TARGET	GROUND CONDITION	T_{oi}	ρ_{THi}	ρ_{THA}	R_{ID} (cm)	P_{FA}	NUMBER OF WAVEFORMS: DESIRED TARGET	NUMBER OF WAVEFORMS: UNDESIRED TARGET
MINE-LIKE TARGET	WET,1	$4T_B$	.948	.25937	30	0%	9	70
		$5T_B$	.667					
		$6T_B$	-.209					
		$7T_B$	.243					
		$8T_B$	-.0615					
		$9T_B$	-.118					
		$10T_B$	.224					
MINE-LIKE TARGET	WET,2	$5T_B$	.445	.30050	30	5.7%	9	70
		$6T_B$	-.488					
		$7T_B$	.127					
		$8T_B$	.243					
		$9T_B$	.289					
		$10T_B$	.221					
		$11T_B$	.436					
		$12T_B$	-.259					

TABLE 8 (Cont.)

BRASS CYLINDER	WET	$5T_B$ $6T_B$ $7T_B$ $8T_B$ $9T_B$ $10T_B$ $11T_B$ $12T_B$	.610 .510 .614 .386 -.139 .543 .389 .691	.34073	30	.97%	9	103
ALUMINUM SPHERE	WET	$5T_B$ $6T_B$ $7T_B$ $8T_B$ $9T_B$ $10T_B$ $11T_B$ $12T_B$	.197 .481 .600 -.106 .218 .189 .103 .341	.42942	37	6.12%	8	98

CHAPTER V
EFFECTS OF RADAR BANDWIDTH ON THE CHARACTERIZATION AND IDENTIFICATION OF SUBSURFACE TARGETS

A. Introduction

The target resonances present in the backscattered waveforms depend on the bandwidth of the radar system. Target resonances residing near the band edge(s) or outside the bandwidth of the radar system are either weakly excited or not excited at all. Thus, when the radar bandwidth is reduced, the number of target resonances present in the backscattered waveforms will decrease accordingly. In this study, a set of data was obtained with an additional 200 m of connecting cables(RG-8) inserted in the system to keep the equipment indoors during inclement weather. These cables acted as a low-pass filter with attenuation of 30 dB at 400 MHz and thus reduced the radar bandwidth. Such bandwidth reduction was found to degrade identification performance for certain subsurface targets under consideration.

B. Processed Waveforms Obtained With the Long-Cable System

Typical processed waveforms obtained with the long-cable system are shown in Figure 25. A quick comparison between the waveforms in Figures 7, 9 and 25 indicates the severe loss of high frequency in the waveforms of the mine-like target and wood board. Furthermore, there was a significant loss of signal amplitude for all waveforms.

C. Extracted Resonances

The average extracted resonances of the long-cable waveforms from the subsurface targets are given in Tables 9 and 10. A comparison between the extracted resonances in Tables 3 and 9, 10 indicates a general loss of high-frequency resonances in the long-cable waveforms. The loss of high-frequency content causes the high frequency resonances to be either weakly excited or not excited at all. A comparison between the resonances extracted from the two sets of mine-like target waveforms (as plotted in Figure 26) shows that, in the long-cable system, the resonance of the mine-like target at 300 MHz was not excited, while the resonance at 400 MHz was only weakly excited.

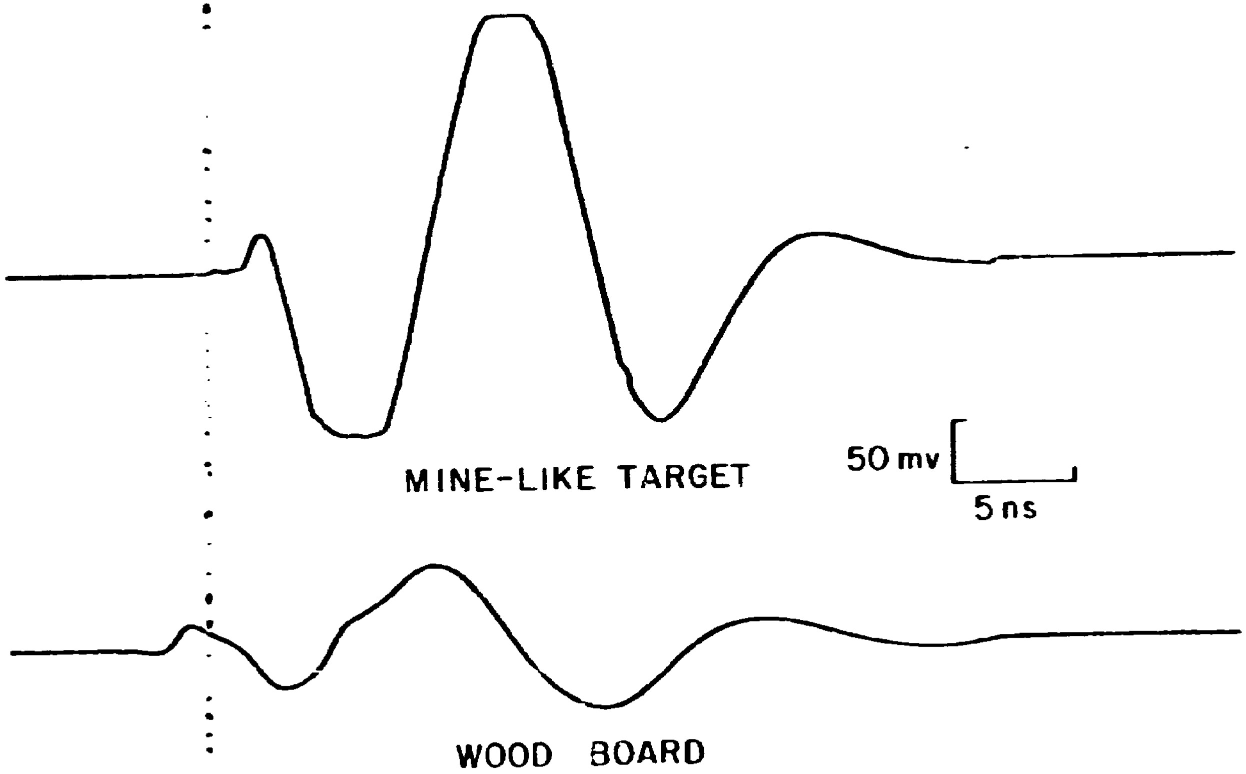

Figure 25. Typical long-cable processed waveforms from the mine-like target and the wood board.

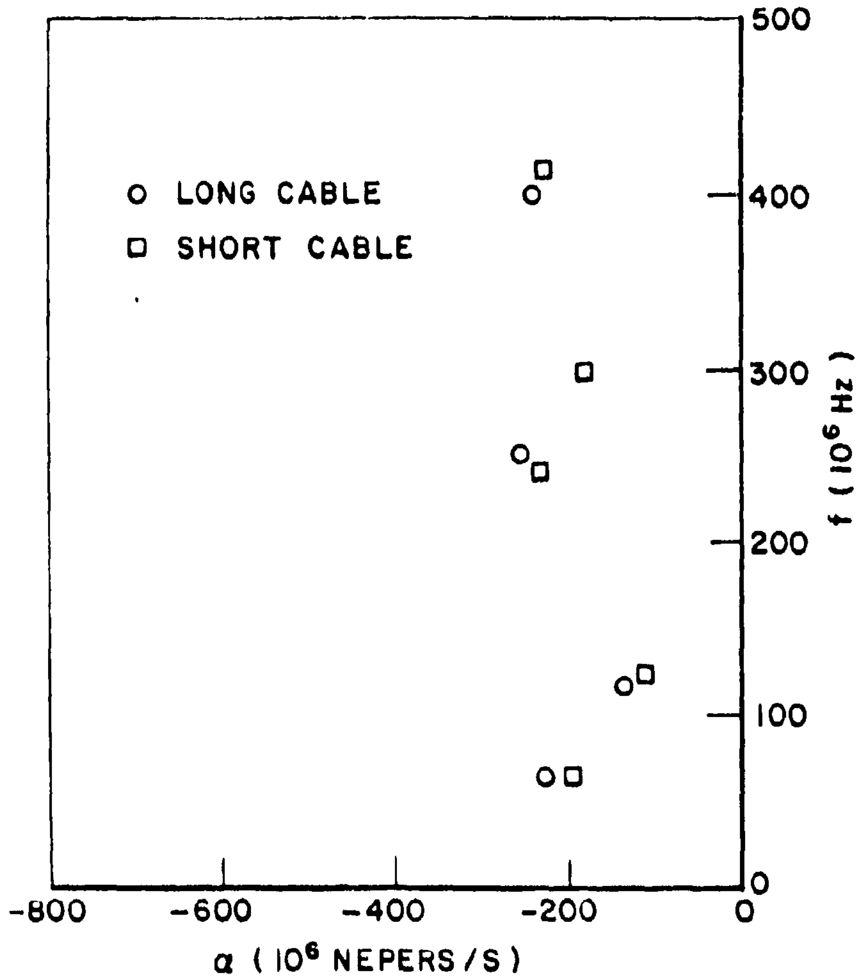

Figure 26. Average extracted resonances from the long and short-cable mine-like target waveforms.

TABLE 9

AVERAGE EXTRACTED RESONANCES OF THE MINE-LIKE TARGET AND THE BRASS CYLINDER IN THE LONG-CABLE SYSTEM

MINE-LIKE TARGET DRY GROUND		BRASS CYLINDER DRY GROUND	
POLE REAL PART (NEPERS/s)	POLE IMAG PART (Hz)	POLE REAL PART (NEPERS/s)	POLE IMAG PART (Hz)
-.2212043E9	±.6866711E8	-.2769107E9	±.0000000
-.1330764E9	±.1213923E9	-.1904636E9	±.7836537E8
-.2593455E9	±.2503563E9	-.2233100E9	±.9971379E8
-.2429505E9	±.4063677E9	-.0430810E9	±.1681942E9
		-.0701791E9	±.2964066E9

TABLE 10

AVERAGE EXTRACTED RESONANCES OF THE ALUMINUM SPHERE, COPPER SHEET AND THE WOOD BOARD IN THE LONG-CABLE SYSTEM

ALUMINUM SPHERE DRY GROUND		COPPER SHEET DRY GROUND		WOOD BOARD WET GROUND	
POLE REAL PART (NEPERS/s)	POLE IMAG PART (Hz)	POLE REAL PART (NEPERS/s)	POLE IMAG PART (Hz)	POLE REAL PART (NEPERS/s)	POLE IMAG PART (Hz)
-.1393208E9	±.6465970E8	-.1850247E9	±.6443022E8	-.1267105E9	±.5738908E8
-.1709803E9	±.1078600E9	-.2442978E9	±.8136559E8	-.1282961E9	±.8721573E8
-.46776075E9	±.2148951E9	-.3748783E9	±.1701710E9	-.1931582E9	±.1958087E9
-.2322153E9	±.3146104E9	-.3748783E9	±.2733628E9	-.1301331E9	±.2682561E9
				-.2503479E9	±.3415180E9

D. Target Identification Performance

Single-look identification performance is summarized in Table 11.* As expected, identification performance degraded. The drastic degradation in the performance for the identification of the mine-like target and the wood board clearly demonstrated the importance of high frequencies for the identification of these two targets.

TABLE 11
SUMMARY OF SINGLE-LOOK IDENTIFICATION PERFORMANCE OF THE LONG-CABLE SYSTEM. ADDITIONAL CABLE LENGTH=200 m. P_I=100% For All Cases

DESIRED TARGET	GROUND CONDITION	T_0	ρ_{TH}	R_{ID} (cm)	P_{FA}	NUMBER OF WAVEFORMS	
						DESIRED TARGET	UNDESIRED TARGET
MINE-LIKE TARGET	DRY	$7T_B$	.675	30	33.55%	9	152
BRASS CYLINDER	DRY	$10T_B$	.600	30	4.49%	9	156
ALUMINUM SPHERE	DRY	$10T_B$	.867	52	9.29%	12	140
COPPER SHEET	DRY	$9T_B$	.964	40	4.35%	11	138
WOOD BOARD	WET	$7T_B$	.823	45	23.98%	11	138

The importance of the high-frequency resonances of the mine-like target stems from the fact that its high-frequency resonances are dominant (see residues of target resonances in Appdenix C). An attempt to identify this target without strongly exciting its dominant resonances results in the poorer identification performance. To improve target identification performance, the radar must be able to transmit and receive more high-frequency energy in the vicinity of these high-order resonances. The short-cable system discussed previously represented an improvement over the long-cable system. However, much more

*This set of identification results was obtained based on threshold identification with one value of T_0 and without detection and filtering.

improvement can be made in the various components of the pulse radar system to provide a better "match" between the system bandwidth and the bandwidth in which the dominant target resonances reside. One of these components is the antenna system.

For the identification of the plastic mine-like target, the crossed-dipole antenna with arm length of 0.6 m (2 feet) did not provide a "good" match between the radar system bandwidth and the bandwidth of the target resonances. The extracted resonances shown in Figure 14 indicated that the antenna resonance was not even near the high-order resonances of the mine-like target. Such mismatch of bandwidths results in the low level of correlation coefficients as tabulated in Table 8. For better characterization and identification of the mine-like target, the frequency of the antenna resonance needs to be increased. One easy way to accomplish such increase is to reduce the size of the antenna. In this study, a smaller crossed-dipole antenna with arm length of 0.15 m (0.5 feet) was built to provide a better match of bandwidths for the identification of the mine-like target. Mine identification is the subject of Chapter VII.

In the next chapter, we study the effects of target depth and size on the characterization and identification of subsurface targets.

CHAPTER VI
EFFECTS OF TARGET DEPTH AND SIZE ON THE CHARACTERIZATION AND IDENTIFICATION OF SUBSURFACE TARGETS

A. Introduction

To study the effects of target size and depth on the characterization and identification technique, two sets of targets were buried (see Figures 27 and 28). The first set consisted of a series of different-size brass cylinders buried at different depths. The second set consisted of a series of different-length 0.3125 cm (1/8-inch) diameter thin brass wires buried at the depth of 5 cm (2 inches). Backscattered waveforms were obtained using the subsurface pulse radar at various antenna locations. Locations of the antenna center are shown as dots in Figures 27 and 28.

B. Processed Waveforms

Processed waveforms from the cylinder and the wire targets are shown in Figures 29-31. From these waveforms, the following observations are made:

1. All these waveforms exhibited some transient behavior, signifying the possible existence of one or more natural resonances.

2. A comparison between the brass cylinder waveforms shown in Figures 9 and 29 indicates that the signal level of the waveform from the brass cylinder at 5 cm depth was approximately 12 dB higher than that of the waveform from the brass cylinder at 30 cm depth. This signified a propagation loss of over 10 dB per 30 cm (1 foot).

3. A burst of signal energy appeared in the early-time portion of the waveforms from the brass cylinders at 90 and 150 cm depth. This was caused by a phenomenon known as the "Trench effect"[22].

   Rain, snow and evaporation changed the moisture content of the ground and the distribution of moisture was perturbed by the Trench walls. At times during the course of a year the ground in the trench was found by direct measurement to be drier and at other times wetter

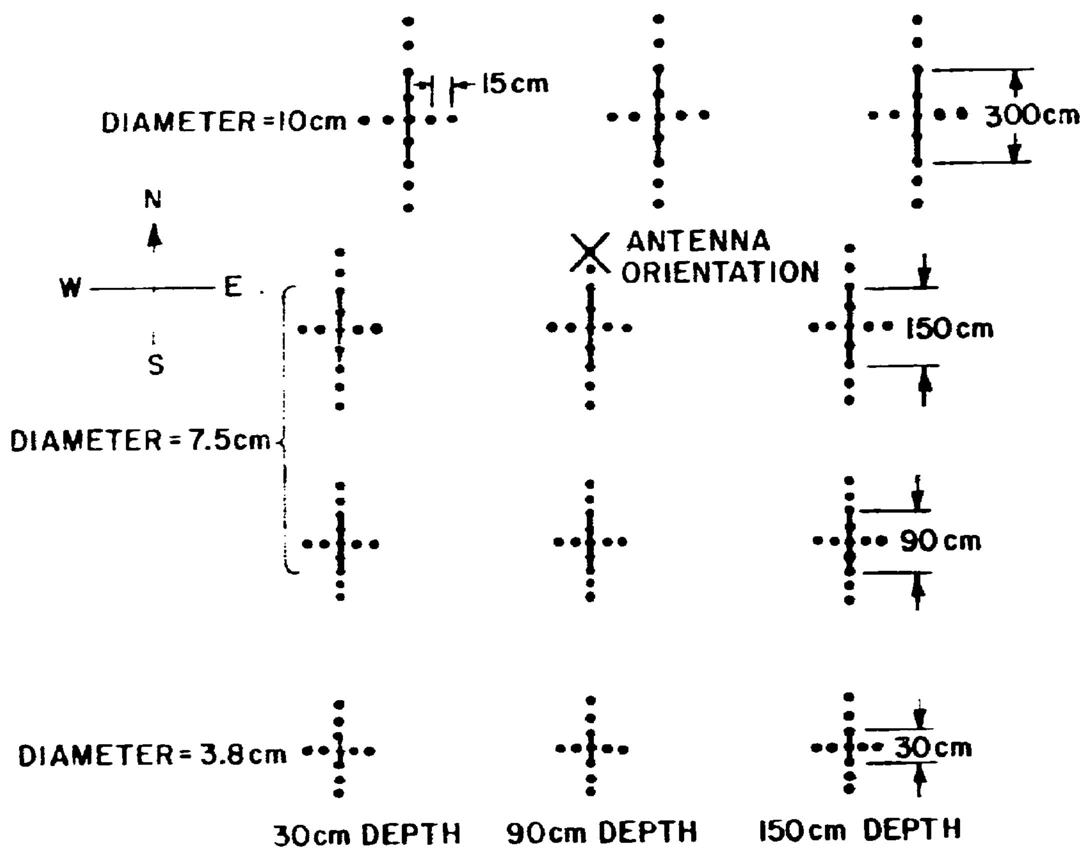

Figure 27. Layout of the buried cylinders.

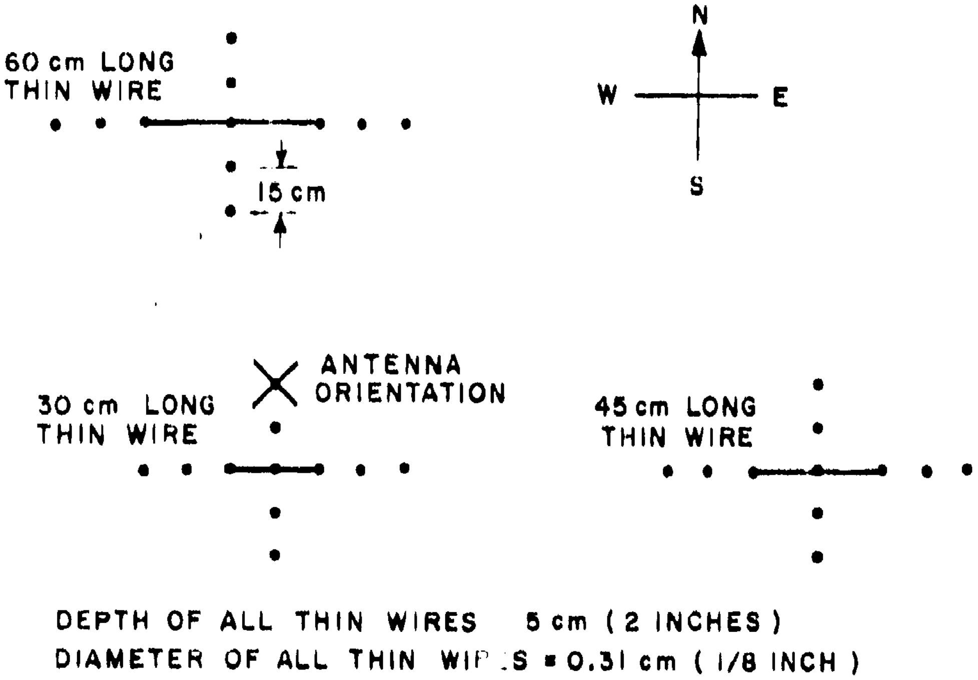

Figure 28. Layout of the buried thin wires.

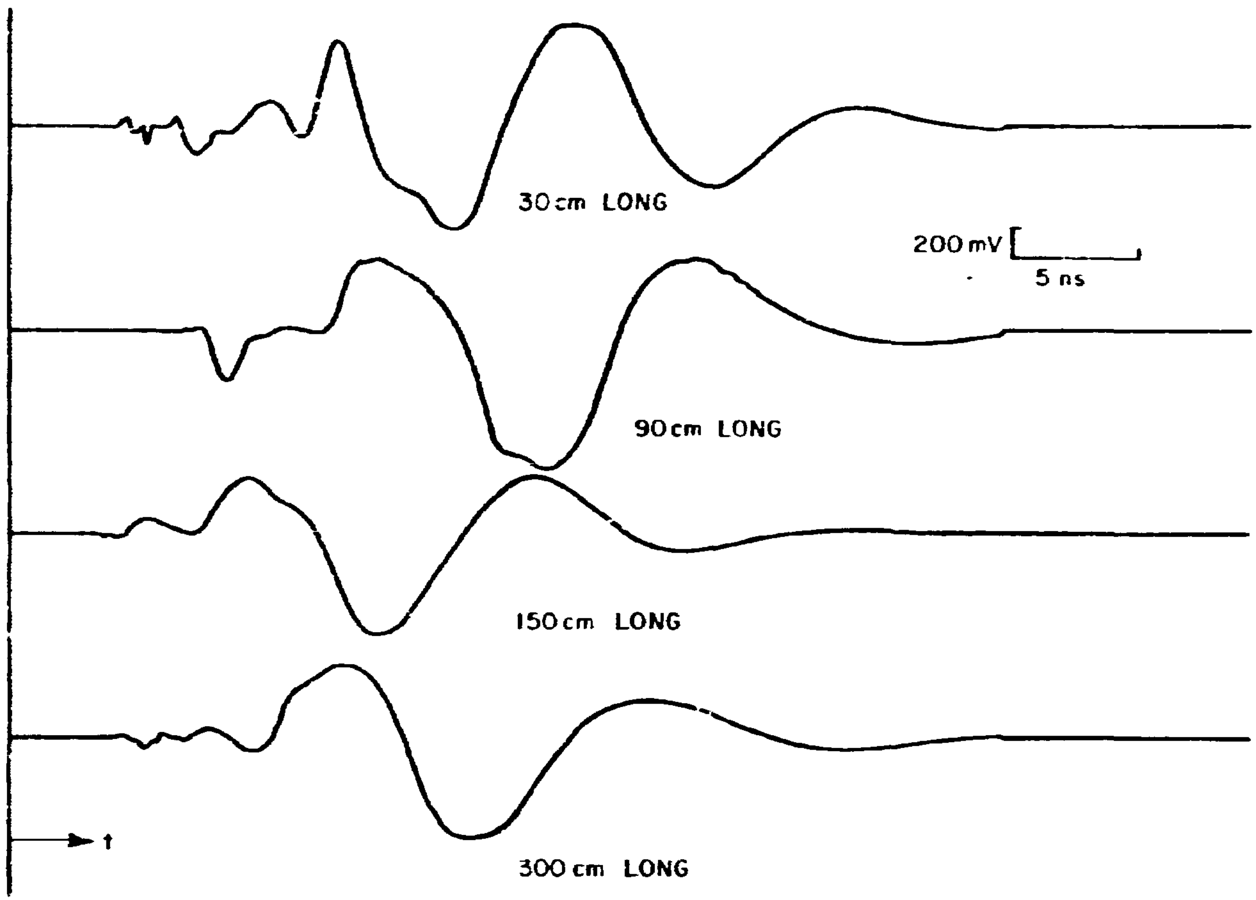

Figure 29. Processed waveforms from the different-size cylinders at 30 cm depth.

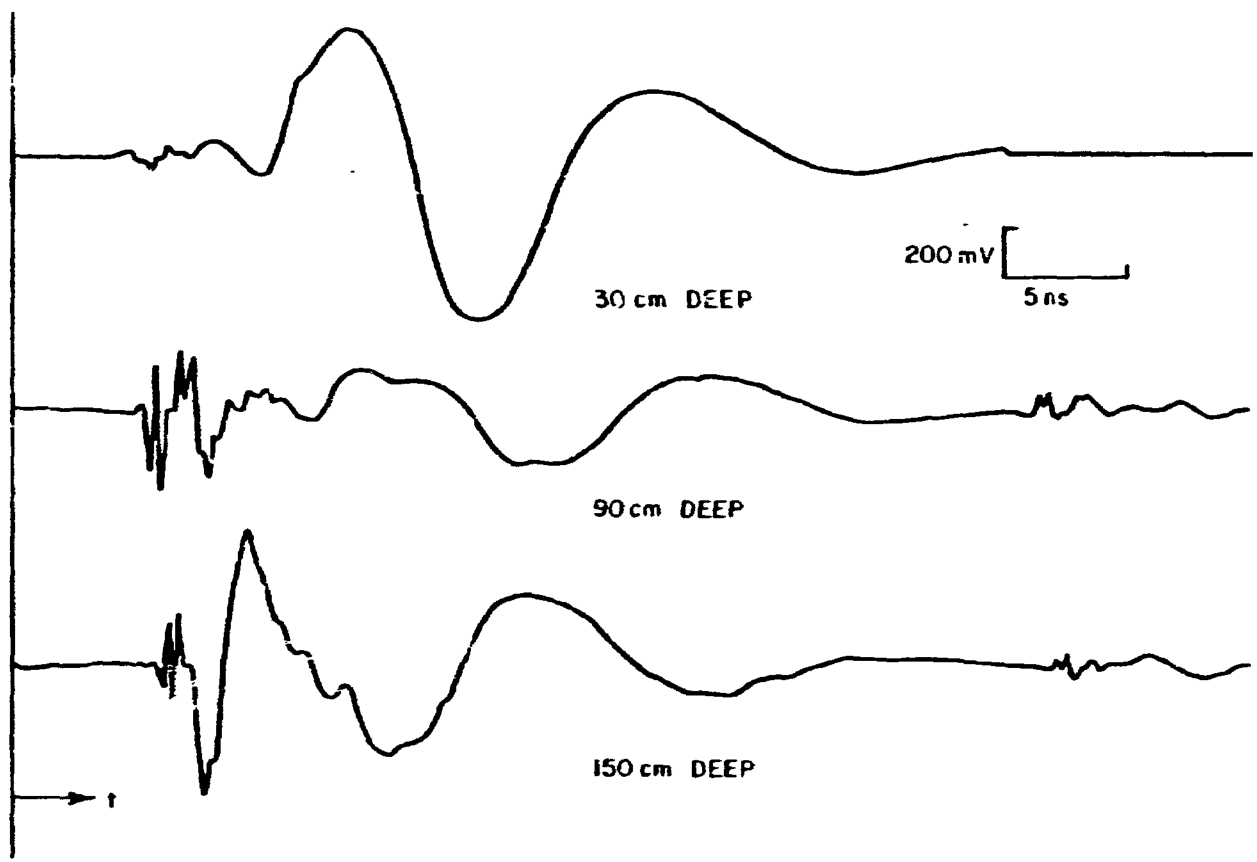

Figure 30. Processed waveforms from the 300cm long cylinder at different depths.

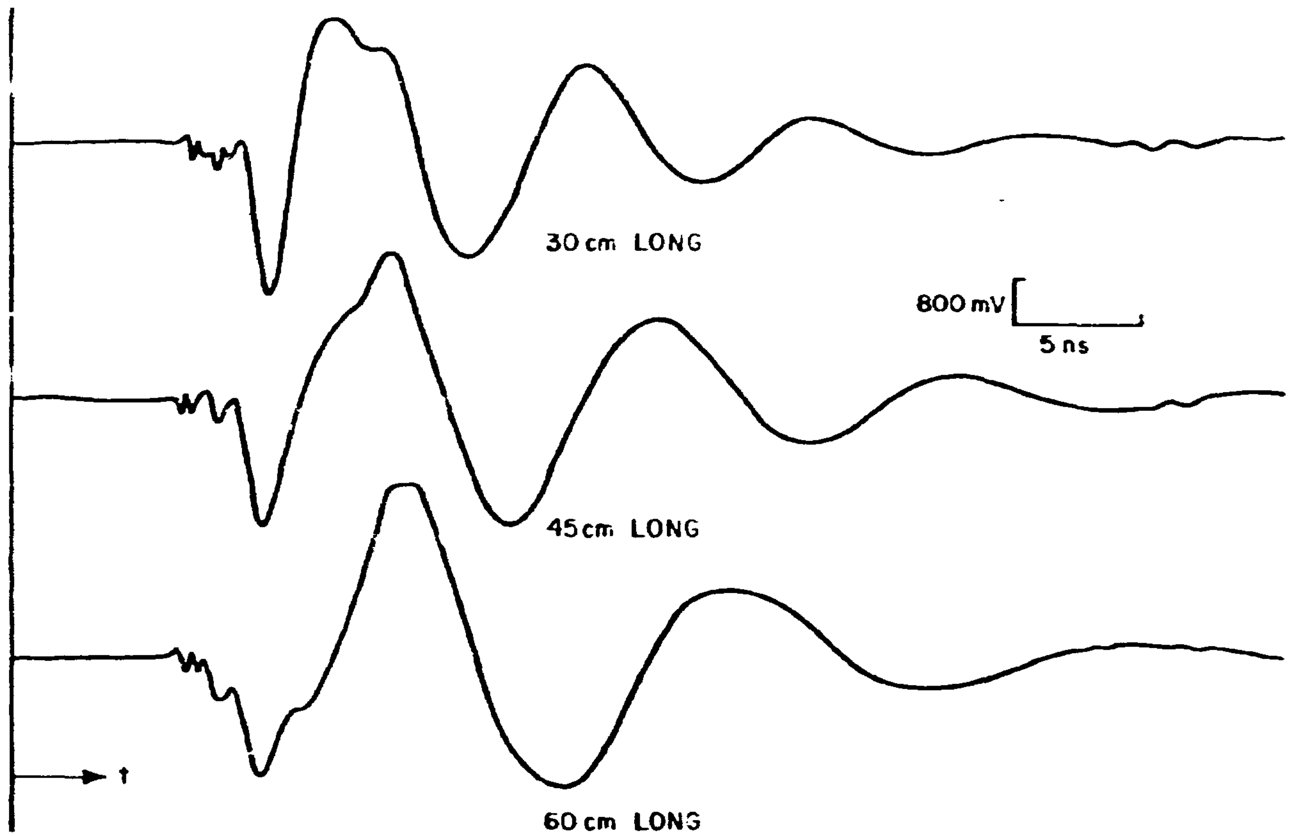

Figure 31. Processed waveforms from the different-size thin wires at 5 cm depth.

than the ground outside the trench. Thus, the trench became a scatterer. The trench signal obscured the cylinder signal and made the task of target identification difficult.

4. Careful study of the waveforms of Figure 31 from the thin wires indicated that the time interval between zero crossings increased according to the increase in the wire size. Such phenomenon was not observed in the cylinder waveforms.

C. The Extracted Resonances

1. Effects of target depth

To see the effects of depth on the complex resonances, the average extracted resonance of the 30cm long cylinders at different depths are shown in Figure 32. From these resonances, we make the following observations:

a. The high-frequency content in the backscattered waveforms was highly attenuated as target depth increases. The highest-order resonance which was present in the 5 and 30cm deep cylinder waveforms was absent from the waveforms of the deeper cylinders.

b. All resonances with imaginary parts smaller than 400 MHz were present in the cylinder waveforms of all depths.

c. The lowest-order resonance was the antenna resonance (0.6m long antenna). This resonance was present in almost all the waveforms of all targets at all depths collected using this antenna.

d. The imaginary part of the target resonances of the brass cylinder occurred in integer multiples of the imaginary part of the lowest-order target resonance. This seemed to suggest that the extracted resonance of the brass cylinder were caused by the multiple scattering mechanisms along the length of the cylinder only (i.e., the dipole mode)[21], the creeping-wave modes were not present in the waveforms. The absence of the creeping wave type resonances was further emphasized when we compared the extracted resonances of the same-size thin wire at the depth of 5 cm to the cylinder resonances (see Figure 32). The same lower-order resonances were extracted. This proved the absence of the creeping-wave modes, for the creeping-wave modes of the thin wires have resonant frequencies which are too high to be present inside the bandwidth of our radar system. The absence of the creeping-wave modes is attributed to the high loss suffered by the creeping waves as it traveled around the circumference, and the cross-polarization effects of the crossed-dipole antenna system.

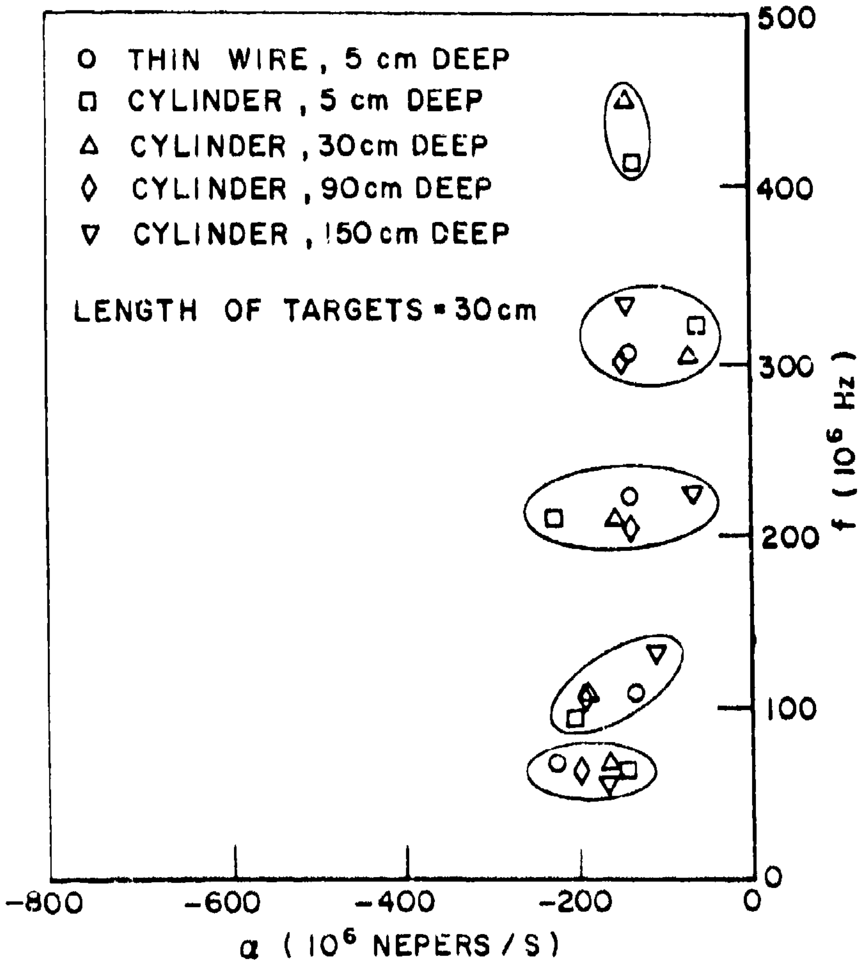

Figure 32. Average extracted resonances of the 30cm long cylinders at different depths.

With the absence of the creeping-wave type resonances, from the point of view of the target resonances, the thin wire and the cylinder are indistinguishable. Separation of these two targets is possible only when discriminants other than the lower resonances are used. One such possible discriminant is the forced response of the back-scattered waveforms which contains information about the profile area of the target[48].

e. The fact that the extracted resonances of the 30cm long cylinder are related solely to the length of the cylinder suggests the use of these resonances to estimate the parameters of the ground. If we consider these resonances to be an approximation to the resonances of the same-size cylinder in a homogeneous medium illuminated by a plane wave, the imaginary parts of these resonances can be approximated by Equation (54)[21]

$$f_n = n \frac{c}{2L\sqrt{\epsilon_r}} \quad ; \quad n = 1,2,3\cdots \tag{54}$$

where L is the physical length of the cylinder, c is the speed of light in free space and ϵ_r is the relative dielectric constant of the medium. Using Equation (54) and the extracted resonances of the 30cm long cylinder as given in Figure 32 the relative dielectric constant is estimated to be approximately 20 at the resonant frequency of approximately 100 MHz. This estimate agrees closely with the estimate from other methods currently being investigated in the ElectroScience Laboratory[58].

The complex resonances of the 30cm long cylinders and thin wire relate very simply to their physical size. This simple relationship disappears when the size of the target increases beyond a certain threshold. This is demonstrated in the following discussion.

2. Effects of target size

As target size increases, we expect the target resonances to be lower in frequency. Such expectation turns out to be warranted when we consider the extracted resonances of the different-size thin wires at the depth of 5 cm as shown in Figure 33. Again, the imaginary parts of target resonances occur in simple multiples of the imaginary parts of the lowest-order target resonance, and as the length of the wire increases up to 60 cm, the frequency decreases according to its size. This expectation turns out to be unwarranted when the length of the cylinder increases to over 90 cm at the depth of 30 cm.

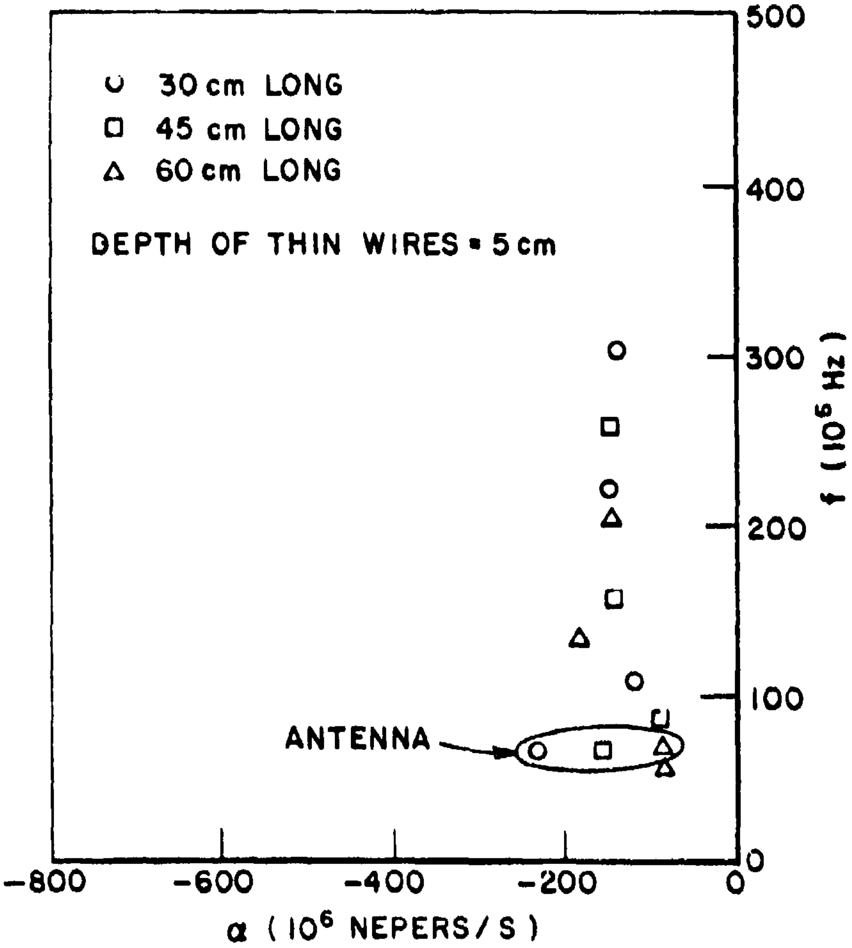

Figure 33. Average extracted resonances of the different-size thin wires at 5 cm depth.

Extracted resonances of the different-size cylinders at the depth of 30 cm are shown in Figure 34.

Although resonances of the large-size targets are no longer related to their sizes in simple form, however, there are still resonances present in the backscattered waveforms. Hence identification of these targets is still possible. Some identification results are presented in the next section.

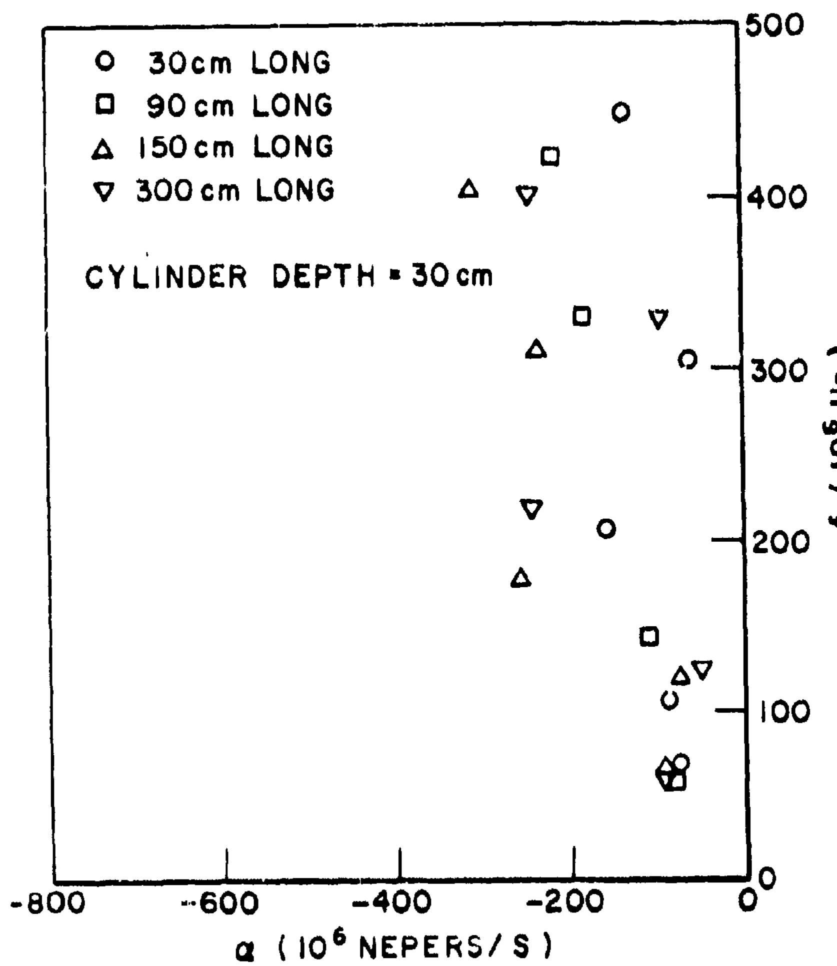

Figure 34. Average extracted resonances of the different-size cylinders at 30 cm depth.

D. Target Identification

Some single-look identification performance results are given in Table 12. Based on these results, the following observations are made:

1. All false alarm probabilities were less than 8%. In some cases, estimates of P_I=100%, P_{FA}=0% were obtained.

2. Identification range decreased as target depth increased.

In the next chapter we focus our attention on the detection and identification of mine-like targets in more extensive and practical situations. Improvements over the Terrascan-like pulse radar are made for the implementation of a portable on-location real-time subsurface target identification radar.

TABLE 12
SUMMARY OF SINGLE-LOOK IDENTIFICATION PERFORMANCE FOR THE BRASS CYLINDERS OF DIFFERENT SIZES
P_I=100% For All Cases

BRASS CYLINDER		R_{ID} (cm)		P_{FA}	NUMBER OF WAVEFORMS	
LENGTH (cm)	DEPTH (cm)	South-North	East-* West		DESIRED TARGET	UNDESIRED TARGET
30	30	30	30	3.08%	11	65
90	30	60	30	7.25%	9	69
150	30	105	30	0%	17	65
300	30	150	30	0%	9	65
300	90	150	15	7.9%	7	38
300	150	150	15	0%	9	33

*See Figure 27.

CHAPTER VII
ELECTROMAGNETIC MINE DETECTION AND IDENTIFICATION

A. Objectives

This chapter focuses on the detection and identification of mine-like targets. First a second model of the mine-like target was buried at the same depth of 5 cm. Measurements were obtained over the two isolated mine-like targets for comparison and identification. Second, to simulate a realistic mine identification situation a set of waveforms was obtained over a section of a rough road in which numerous false targets existed. These false targets were caused by the debris existing in the old country-style road, and thus represented a set of realistic false targets in a mine field. The set of rough road measurement was used for evaluation of "typical" false-target discrimination. Third, a small antenna of arm length 0.15 m (0.5 foot) was built and used to provide better characterization and identification of the mine-like target. Performance of the small-antenna system is presented and discussed.

B. A Second Model of the Mine-Like Target

Typical processed waveforms from the two mine-like targets at the same relative antenna-target geometry are shown in Figure 35. There are minor differences in these two waveforms. This can be attributed to the minor difference in the structure of these two targets, clutter and the difference in the ground conditions at the two target locations. Complex natural resonances of the two models of the mine-like target were extracted from their backscattered waveforms using Prony's method. The average extracted resonances of the two models are shown in Figure 36. Again the slight difference in the locations of these two sets of resonance is attributed to the possible slight difference in the structure of the two models, clutter and the difference in the ground conditions at the two target sites.

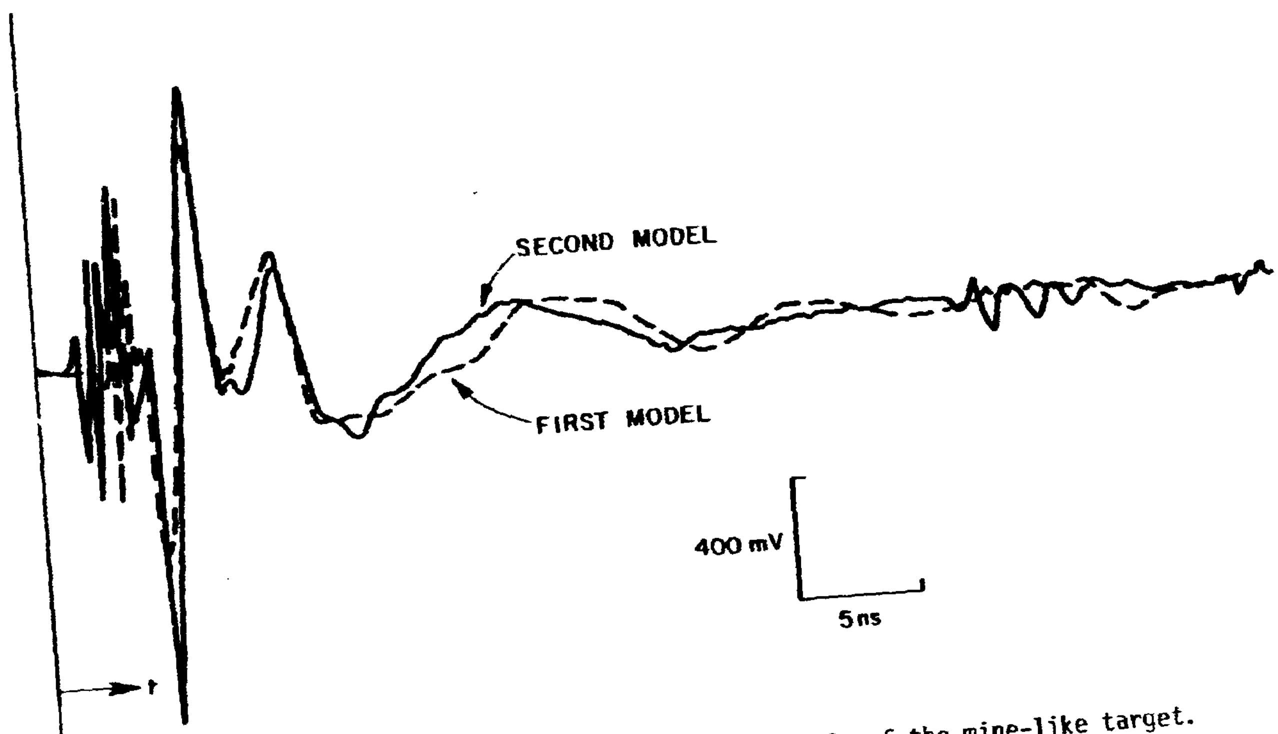

Figure 35. Processed waveforms from the two models of the mine-like target.

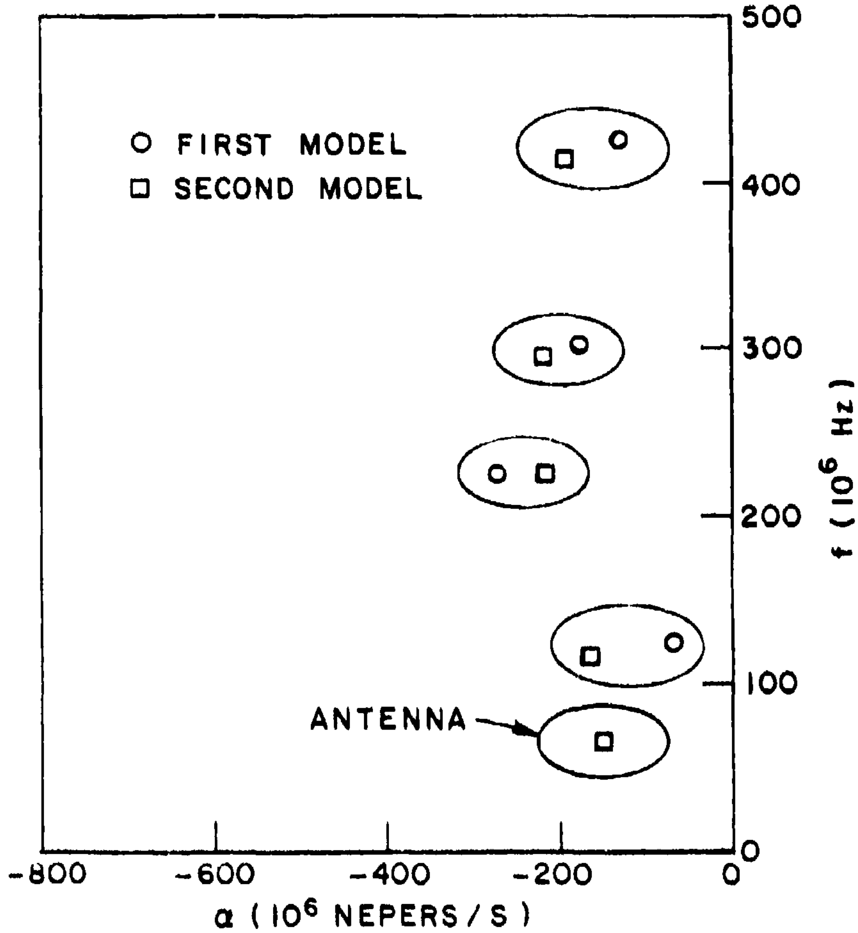

Figure 36. Average extracted resonances of the two mine-like targets.

C. False Target Measurements in the Rough Road

A set of 53 (difference) waveforms was collected over 53 locations in a 40m section of a rough road adjacent to the Electro-Science Laboratory. These echoes were probably a result of debris existing in this old country-style road. There were numerous such false targets observed. Pictures of the rough road is shown in Figure 38.

The measurement locations were chosen to ensure significant false-target signal levels for a more realistic and difficult test of the identification method. Figure 38 shows a typical false-target waveform.

D. Mine Identification

The predictor-correlator identification method was applied to the waveforms from the two mine-like targets and the rough road-bed for identification of the two mine-like targets and false-target discrimination. Single-look identification statistics are given in Table 13.

This set of identification statistics basically established the fact that the predictor-correlator identification method did indeed successfully identify different models of the mine-like target at different locations. Furthermore the method successfully separated the mine-like target from the set of false targets which were typical of the false targets found in a realistic mine field.

The pulse radar system discussed so far represented a workable (and successful) mine identification system, however two obvious improvements could be made. First, there was the bandwidth mismatch problem (as discussed in Chapter V) that resulted in low-level values of the correlation coefficient. The bandwidth mismatch problem could be corrected by introducing an antenna system with a higher-frequency antenna resonance. Second, the size of the crossed-dipole antenna (1.2 m (4 feet) maximum dimension) was a bit too large for a practical mine identification system. There existed a single solution to the two problems mentioned above. This solution was the reduction in the antenna size. Since the 0.6m long (arm length) antenna had a reson ance at 65 MHz, a 0.15m (0.5 foot) long antenna would have a resonance at 260 MHz which was close to the mid-frequency of the resonance bandwidth. A crossed-dipole of 0.15 m arm length was therefore built for improved mine identification performance[59]. Performance of this antenna on the identification of the mine-like target is discussed in the next section.

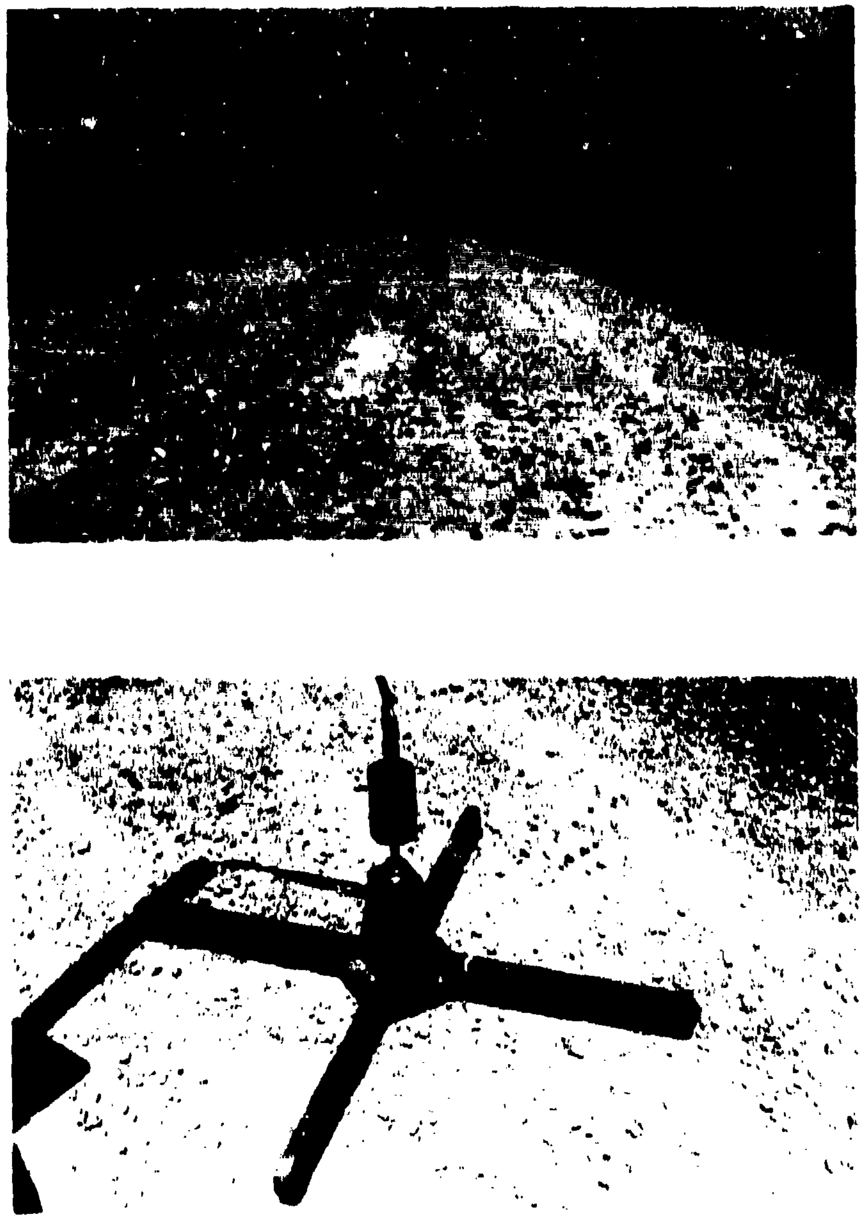

Figure 37. The rough road for false-target measurements.

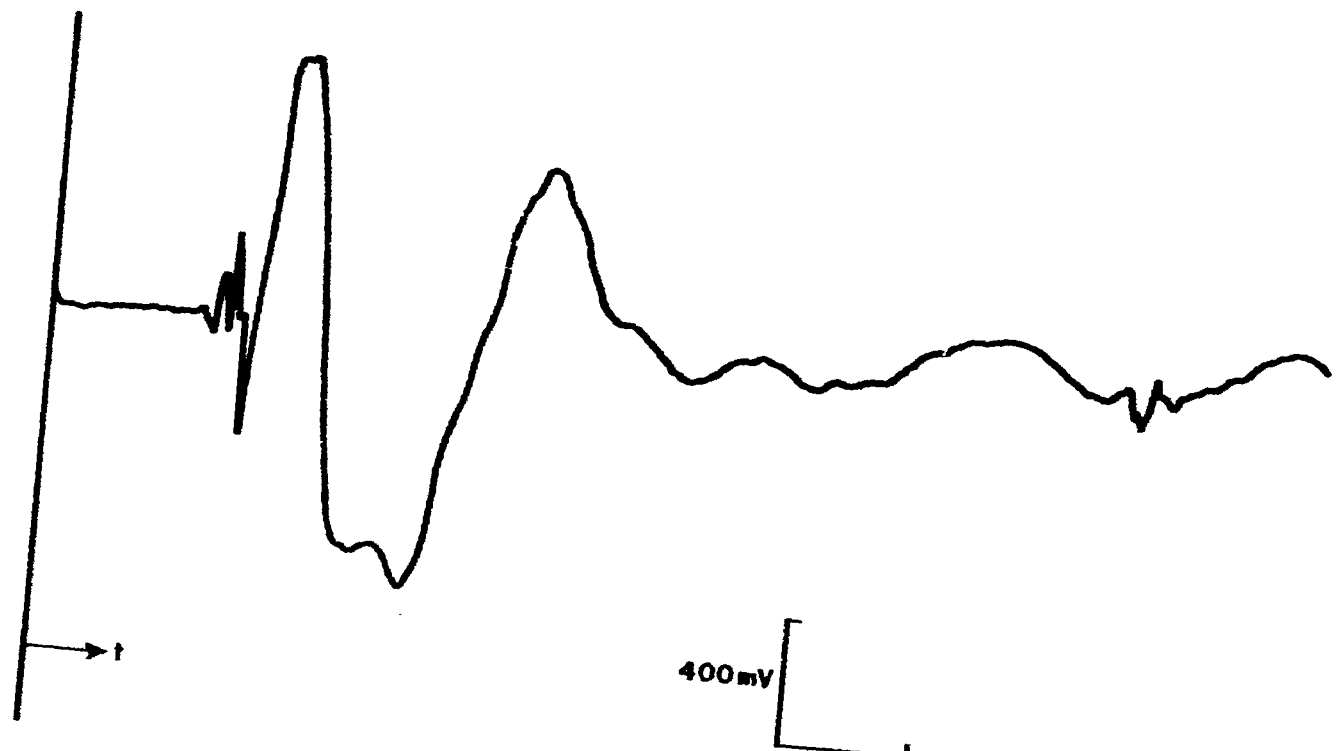

Figure 38. Processed waveform from a typical false target in the rough road.

TABLE 13
SINGLE-LOOK IDENTIFICATION STATISTICS: THE FIRST AND SECOND MODEL OF THE MINE-LIKE TARGET VS THE FALSE TARGETS IN THE ROUGH ROAD-BED.
P_I=100%

DESIRED TARGET	GROUND CONDITION	T_{oi}	ε_{THi}	ε_{THA}	R_{ID} (cm)	P_{FA}	NUMBER OF WAVEFORMS	
							DESIRED TARGET	UNDESIRED TARGET
		$4T_B$	.948					
		$5T_B$	.667					
MINE-LIKE TARGET	WET,1	$6T_B$	-.209	.25937	30	1.85%	9	53
FIRST MODEL		$7T_B$	.243					
		$8T_B$	-.0615					
		$9T_B$	-.118					
		$10T_B$	.224					
		$5T_B$	.445					
		$6T_B$	-.488					
MINE-LIKE TARGET	WET,2	$7T_B$	.127	.30050	30	3.70%	9	53
SECOND MODEL		$8T_B$	.243					
		$9T_B$	.289					
		$10T_B$	.221					
		$11T_B$	.436					
		$12T_B$	-.259					

E. A Small Antenna for Improved Performance in Mine Identification

A picture of the small crossed-dipole antenna is shown in Figure 39. This antenna was used to obtain a set of measurements over the 5cm deep targets. Typical processed waveforms are shown in Figure 40. For comparison purposes, Figure 41 shows the processed waveforms obtained using the 0.6m long antenna over the same target locations From Figures 40 and 41, we note the following improvements obtained using the 0.15m long antenna. First, the 0.15m long antenna offers a gain of at least 6 dB in target signal level. Second, the level of the no-target signal obtained using the 0.15m long antenna is generally lower. Third, the time interval of the target signals obtained using the 0.15m long antenna is only half as long. This reduction in interval size would effectively reduce the computation time for evaluating the correlation coefficient by a factor of two.

Due to the minimization of the length of the inter-connecting cables at the balun-antenna connection of the small antenna, the balun reflection exists in the early-time portion of the waveform. In this region, the primary target signal level is much higher than the level of the balun reflection. This severely suppresses the effects of the balun reflection. The decrease in cable length is also a contributing factor to the 6 dB gain in signal level. With the balun reflection moved in, the stop-time t_e of the error-calculating interval in the Prony's and the predictor-correlator identification processes had to be changed. In this study, the choice of t_e for the small-antenna system was based on the resonances of the mine-like target. The value of t_e was chosen to yield an error interval of size equal to five times the period of the lowest imaginary part of the target resonances (125 MHz). This resulted in the t_e value of t_s+100T_B.

Figures 42-44 shows more waveforms and their FFT's obtained using the 0.15m long antenna. From the FFT's of the waveforms, it is found that most energy resided in the frequency region of 100 M to 500 MHz with the most dominant frequency in the region of about 300 MHz (as compared to 70 MHz for the 0.6m long antenna).

The set of waveforms obtained with the small antenna over the 5cm deep targets was processed for pole extraction and identification of the mine-like target. Average complex resonances of the mine-like target extracted from these waveforms are shown in Figure 45. For comparison purposes, the extracted resonances from the mine-like target waveforms obtained with the 0.6m long antenna in a similar ground condition are also shown in Figure 45. The locations of the target resonances from both antennas were almost identical. However, the imaginary part of the antenna resonance increased by a factor of 4 when the length of the antenna arm was reduced from 0.6 m to 0.15 m.

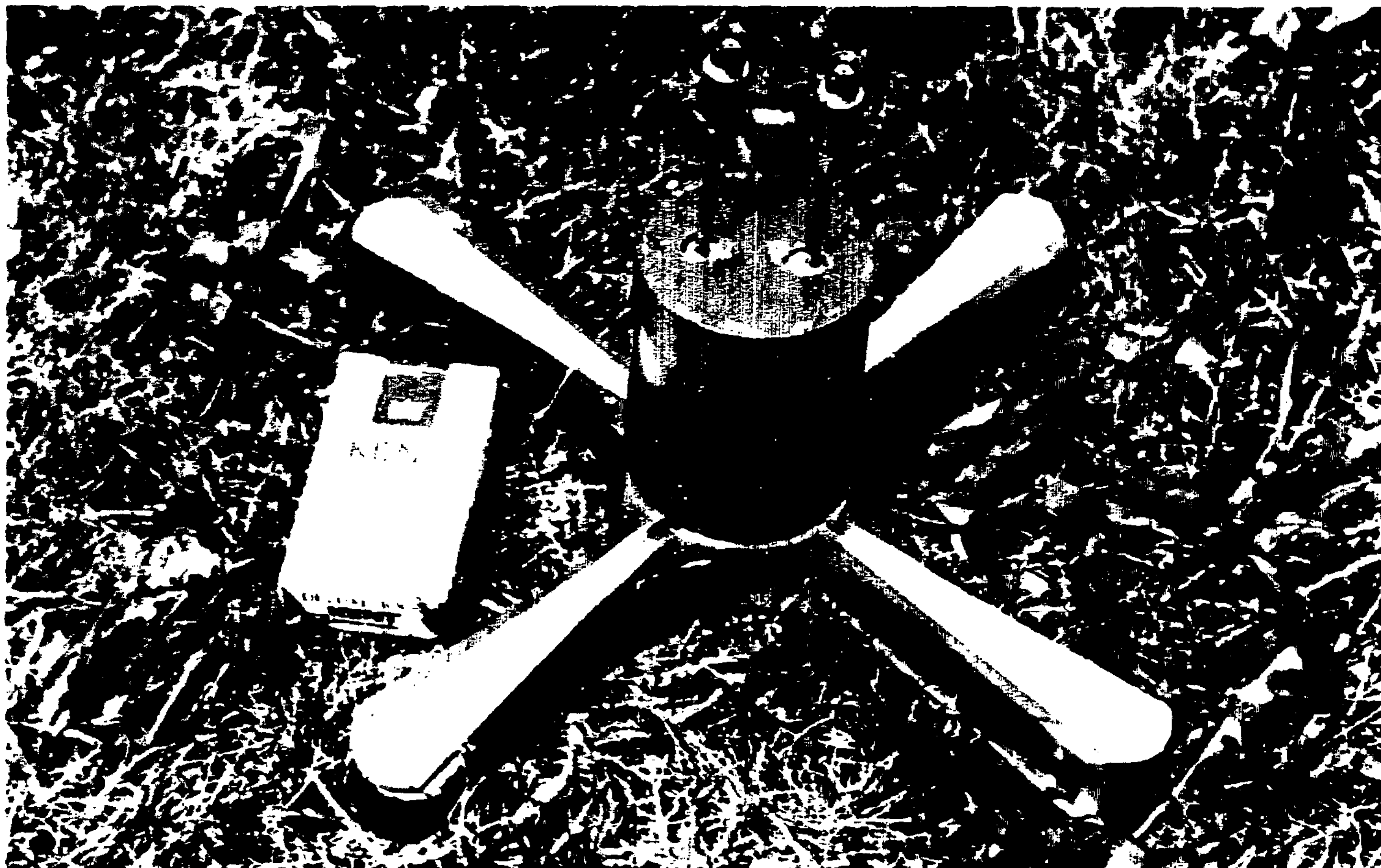

Figure 39. The small crossed-dipole antenna for improved mine identification performance.

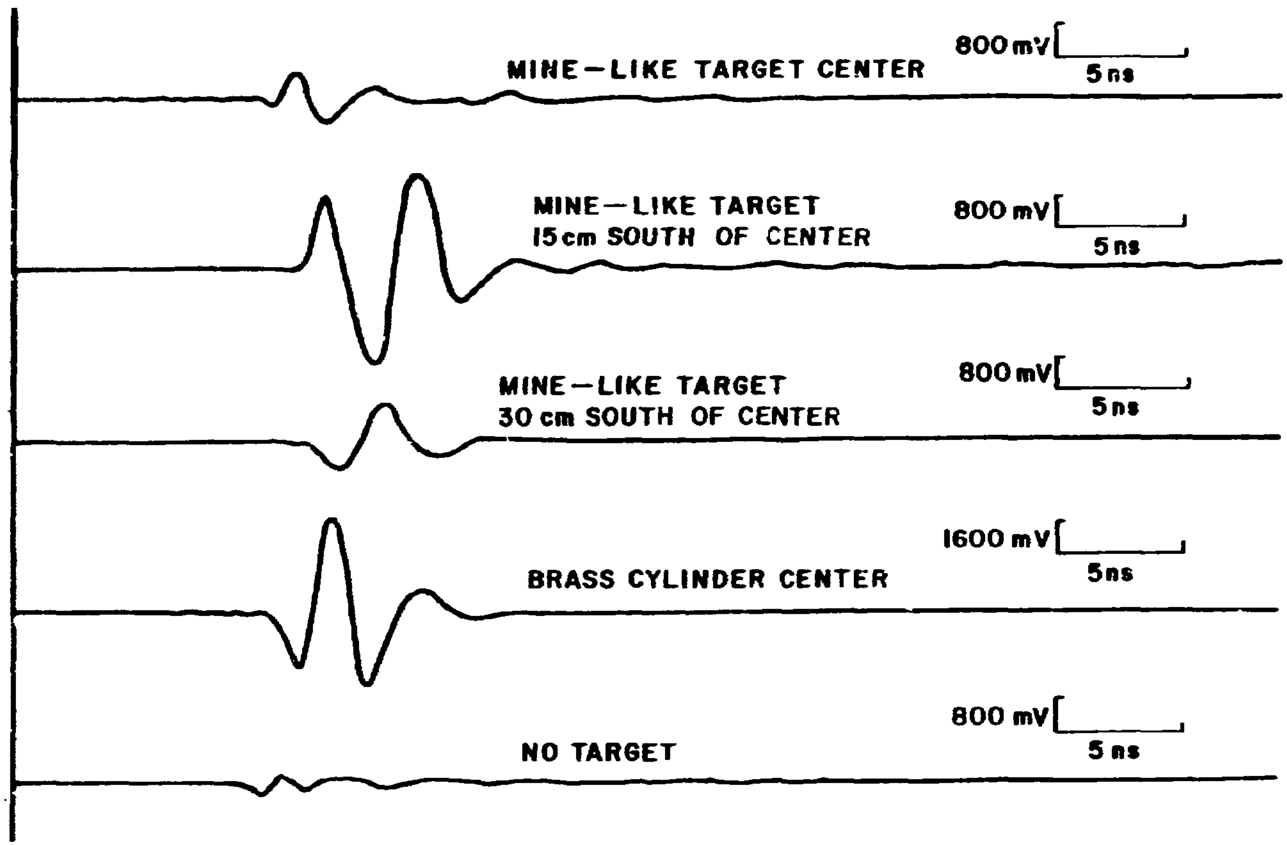

Figure 40. Processed small-antenna waveforms from the 5cm ceep subsurface targets.

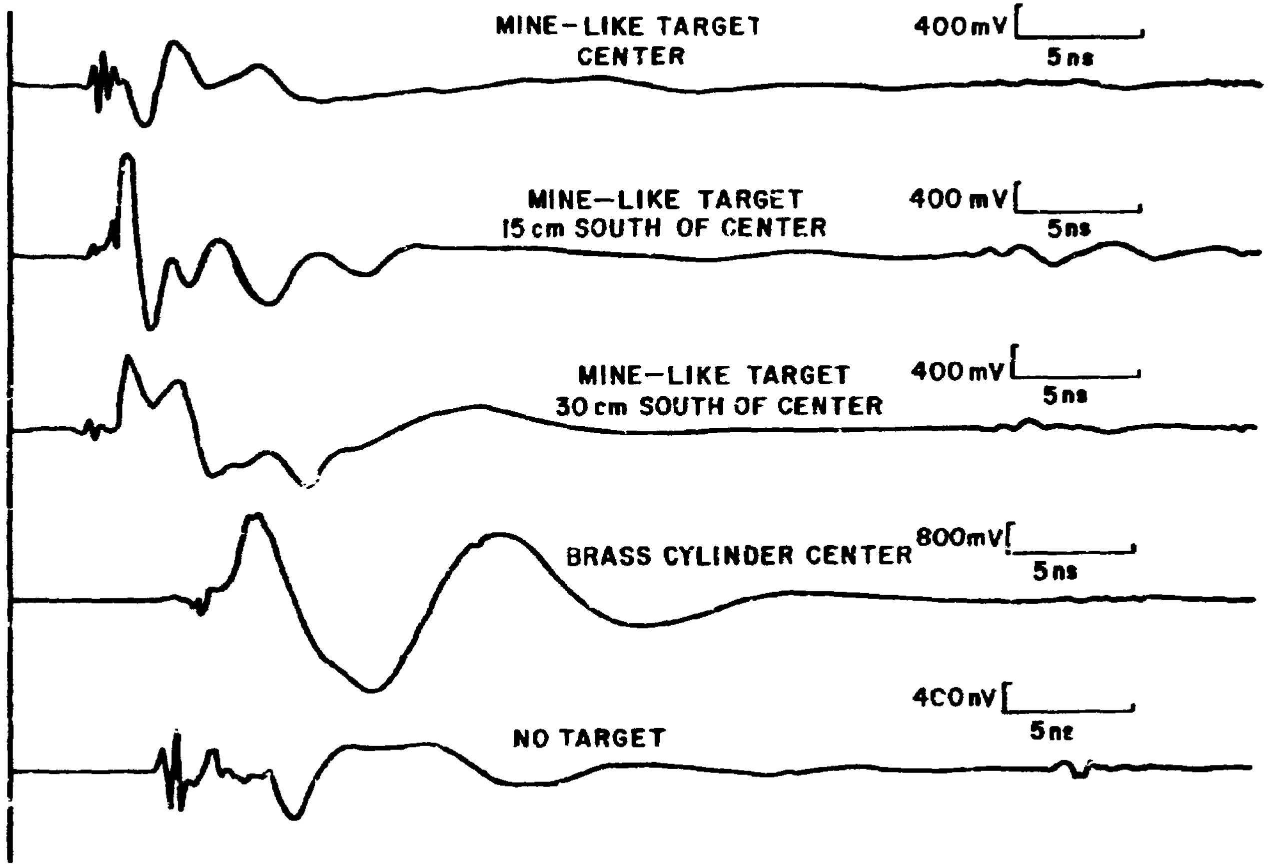

Figure 41. Processed waveforms from 5cm deep targets measured using the 0.6m long antenna.

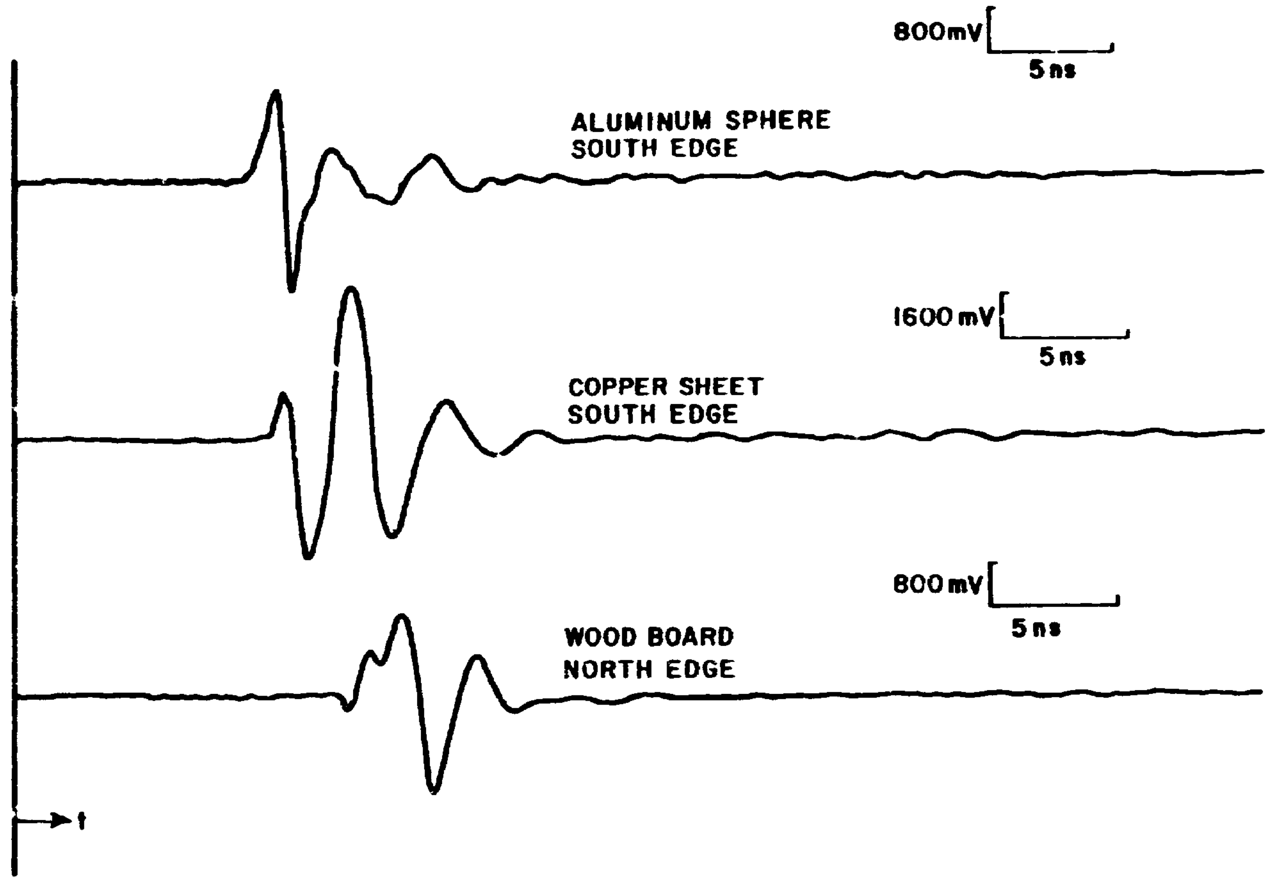

Figure 42. Additional processed small-antenna waveforms from the 5cm deep targets.

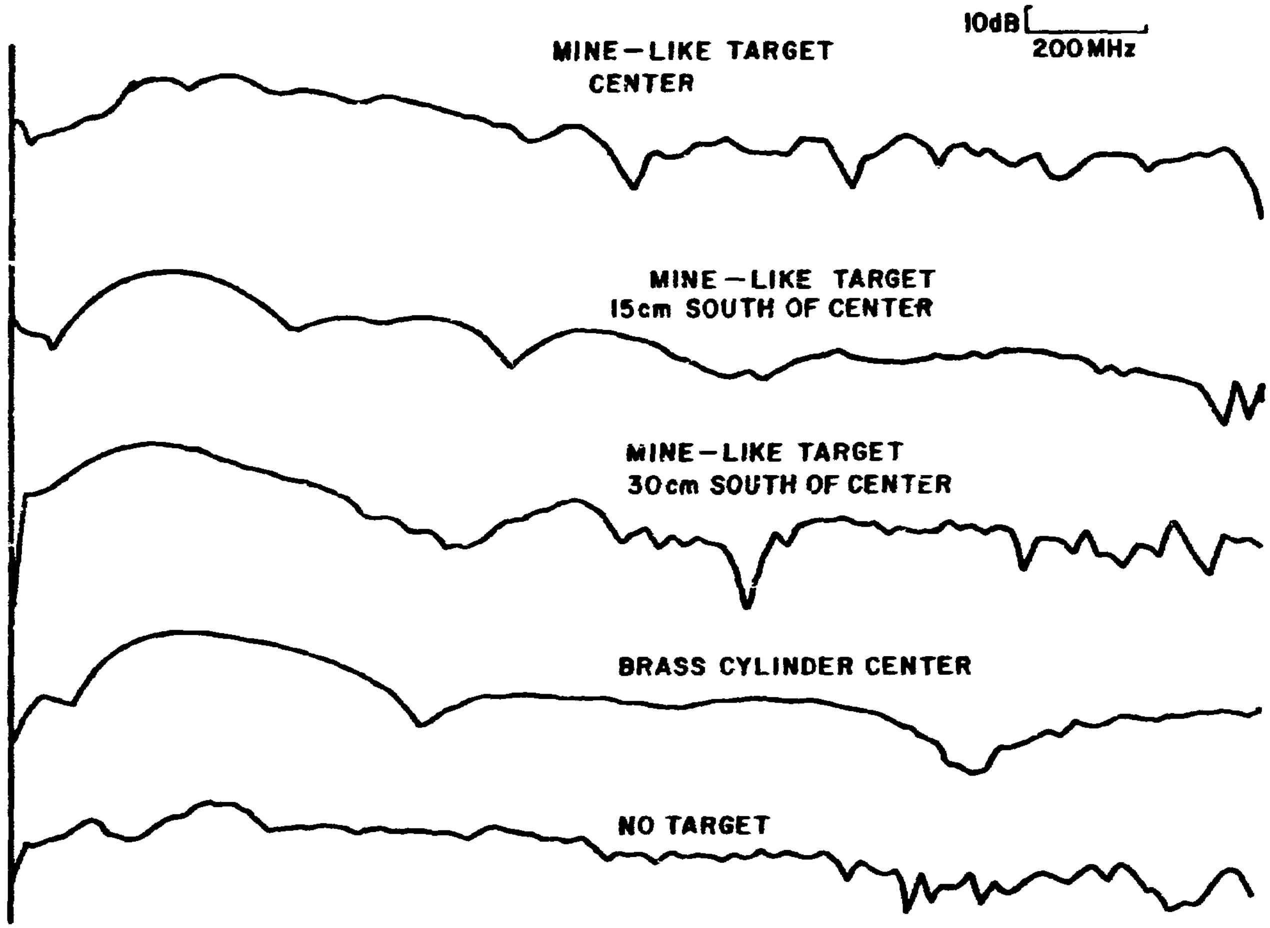

Figure 43. FFT of the small-antenna waveforms shown in Figure 40.

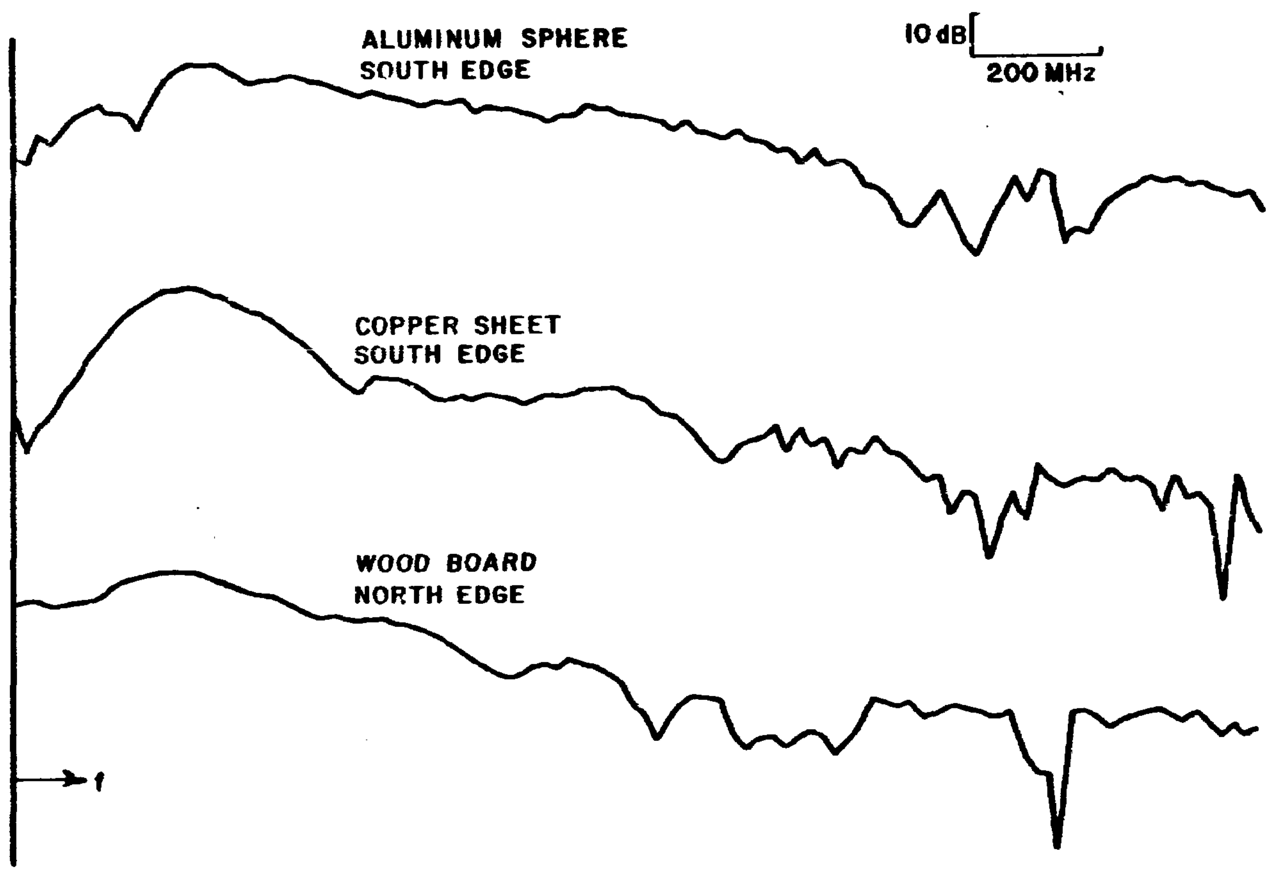

Figure 44. FFT of the small-antenna waveforms shown in Figure 42.

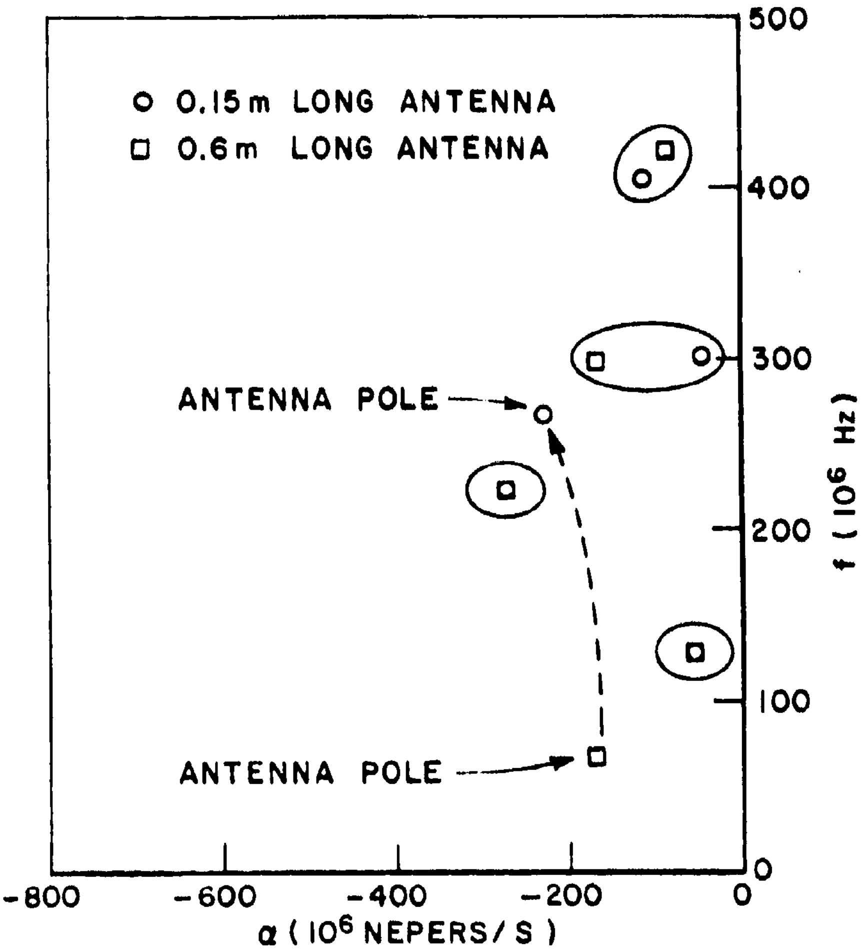

Figure 45. Average extracted resonances from the mine-like target waveforms taken using the 0.15m and the 0.6m long antennas in similar ground conditions.

Complex resonances of the various 5cm deep targets are shown in Figure 46. The antenna resonance was present in almost all target waveforms measured. The complex resonances of these targets were in the same general area of the complex frequency plane as the antenna resonance. This was expected to present a difficult test to the identifier.

Single-look identification statistics obtained using the small antenna in identification of the mine-like target is shown in Table 14. Typical $\rho(T)$ curves are shown in Figure 47. From Table 14 and Figure 47, the following observations are made:

1. Target identification performance estimates based on the extracted resonances of the mine-like target was P_I=100%, P_{FA}=1.72% within a 30 cm radius of target center. Within a 45 cm radius, identification performance was P_I=100%, P_{FA}=6.90%. This set of statistics was obtained with an ensemble of 13 mine-like target and 58 false-target waveforms. These performances represented an improvement over the performance obtainable with the 0.6m long antenna. The 0.6m long antenna system was unable to identify the mine-like target in a distance of more than 30 cm from the target center.

2. In addition to the range improvement, a quick comparison between the identification statistics given in Tables 8 and 14 indicates that the level of $\rho(T)$ values for the mine-like target were generally improved. It is expected that this will produce improved identification in the presence of greater amounts of clutter. It has already been observed that target identification in the presence of clutter has been improved.

3. The region of T_O values for optimum identification performance was in the neighborhood of T_N=6T_B. However, this region of T_O values was shifted toward small T_O values. This was attributed to the shift to dominance of to the high-frequency poles due to the shift in the antenna resonance. Note that the region of T_O included T_N.

   Because of the change in the bandwidth of the small-antenna system a band-pass filter was used in the preprocessor of the identifier to suppress out-of-band clutter and noise. The transfer function of the band-pass filter is shown in Figure 48.

In the next chapter, we discuss the implementation of the small-antenna mine identification system as a microcomputer system. Target identification performance will be given.

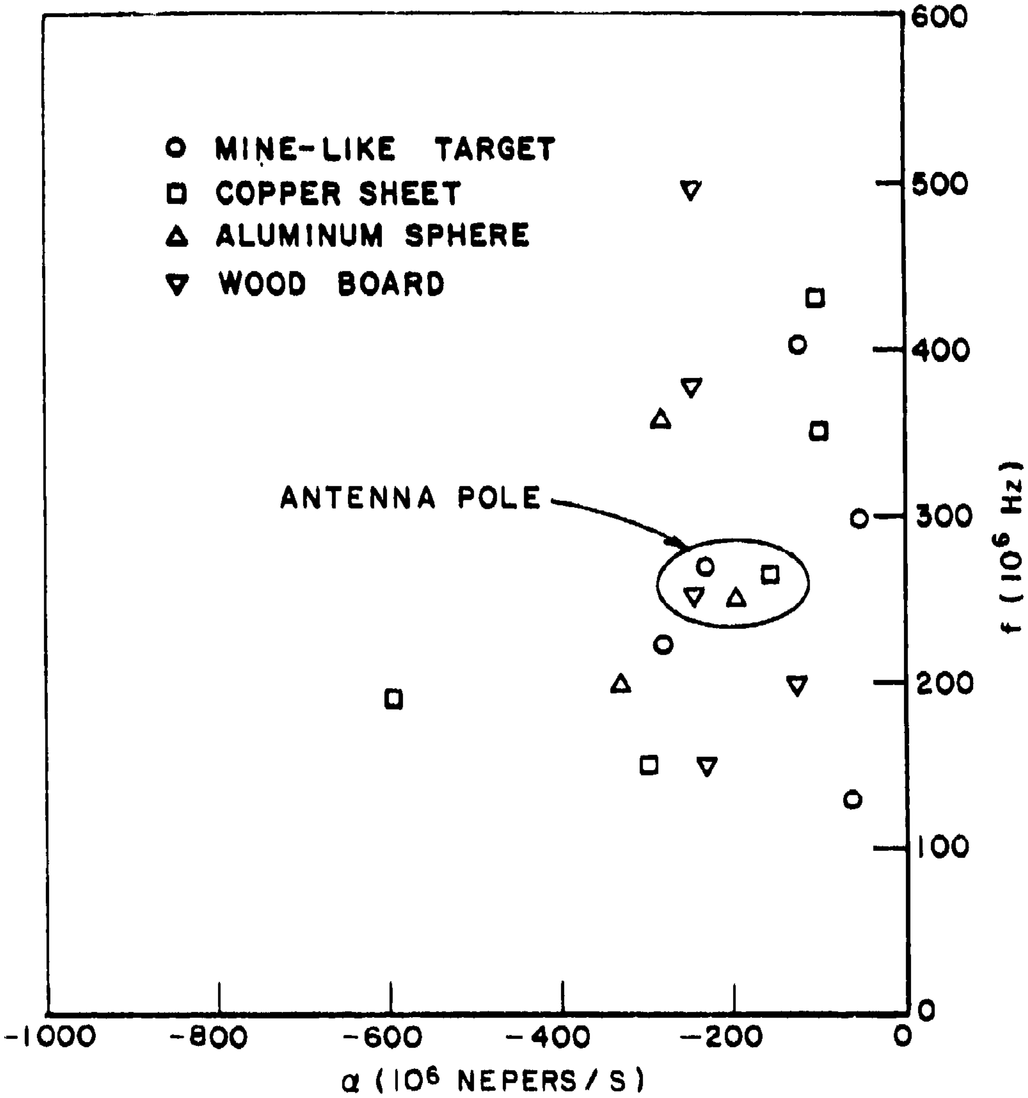

Figure 46. Average extracted resonances from the waveforms of the 5cm deep targets obtained with the small antenna.

TABLE 14
SINGLE-LOOK IDENTIFICATION PERFORMANCE FOR IDENTIFICATION OF THE MINE-LIKE TARGET WITH THE SMALL-ANTENNA SYSTEM.
$P_I=100\%$

DESIRED TARGET	GROUND CONDITION	T_{oi}	ρ_{THi}	ρ_{THA}	P_{FA} $R_{ID}=30$ cm	P_{FA} $R_{ID}=45$ cm	NUMBER OF WAVEFORMS: DESIRED TARGET $R_{ID}=30$ cm	NUMBER OF WAVEFORMS: DESIRED TARGET $R_{ID}=45$ cm	NUMBER OF WAVEFORMS: UNDESIRED TARGET
		$4T_B$	.615						
		$5T_B$	.166						
MINE-LIKE TARGET	WET	$6T_B$	.615	.59436	1.72%	6.90%	9	13	58
		$7T_B$	.456						
		$8T_B$	.420						

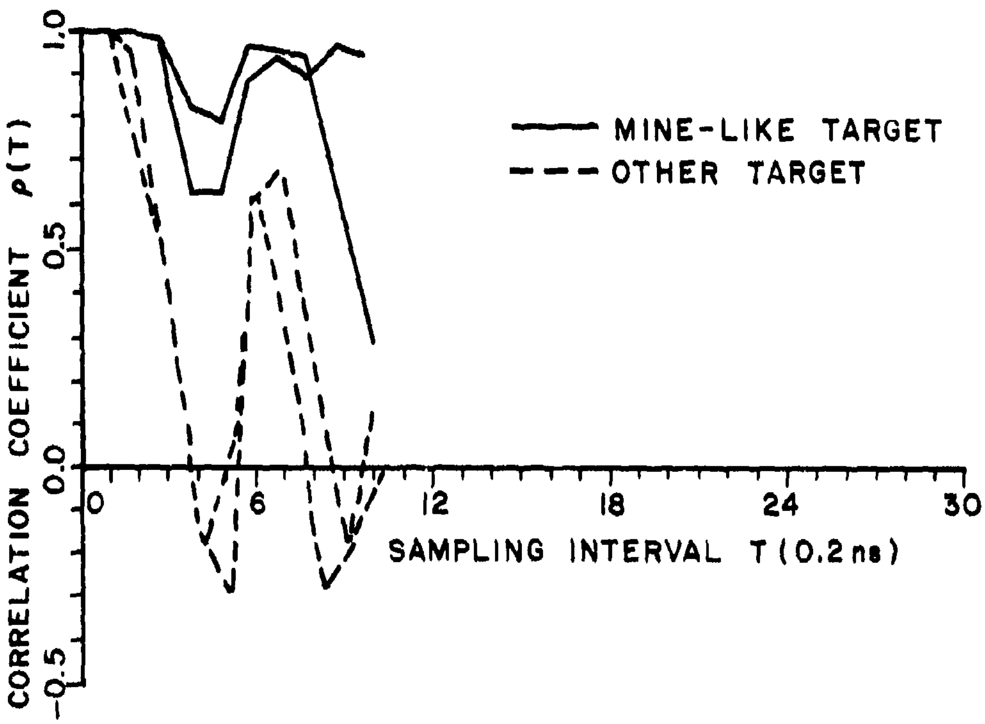

Figure 47. Typical ρ(T) curves for the identification of the mine-like target using the small-antenna system.

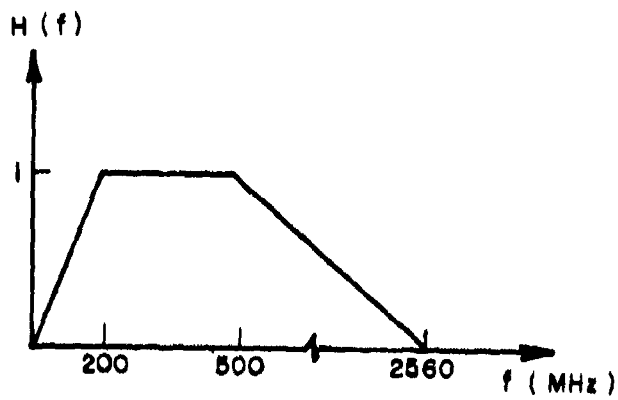

Figure 48. Transfer function of the preprocessor filter used in the small-antenna system for target identification.

CHAPTER VIII
A MICROCOMPUTER SYSTEM FOR REAL-TIME ON-LOCATION SUBSURFACE TARGET IDENTIFICATION

A. Objectives

This chapter discusses the implementation of the pulse radar identification system as a microcomputer system for real-time on-location identification of subsurface targets. The identification radar is implemented with an SDK-80 microcomputer[60] in conjunction with the Terrascan. The processing algorithms are stored in the system as microprograms. Arithmetic operations are performed by a hardware arithmetic processing unit and data can be recorded by a cassette recorder. Thus the microcomputer system can serve either as a real-time identification system or as a data-recording system.

B. Structure of the Microcomputer Target Identification System

The basic structure of the microcomputer target identification system is shown in Figure 49. The major components and their corresponding functions are the following:

1. Terrascan System: the raw backscattered waveform is received by the crossed-dipole antenna in analog form. This analog waveform is sampled by the Terrascan system which essentially serves as a sampling oscilloscope and provides various flexibilities such as gain, time delay, and dc offset to the waveform. The sampled raw waveform is displayed on the neon display and then fed to the analog board as a discrete-time signal.

2. Analog Board: besides converting the sampled raw waveform to digital form using an 8-bit A/D converter, the analog board provides a keyboard for inputting to the microcomputer system. Various operating modes of the microcomputer system are initiated through the command codes entered from the keyboard. The analog board also provides 6 LED display lights for displaying echoes of the input command codes, various system operating information, and important

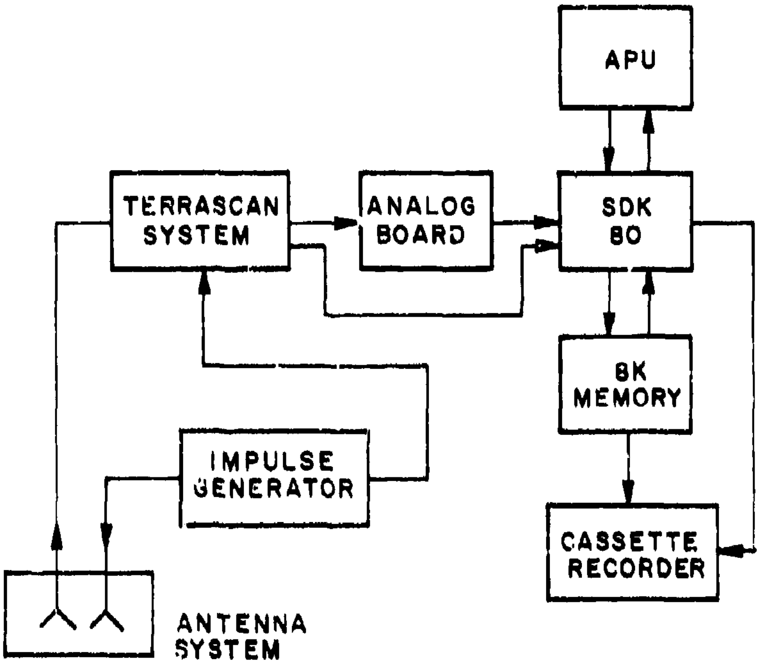

Figure 49. Block diagram of the microcomputer system for on-location subsurface target identification in real time.

information concerning the received waveform (such as peak timing, peak values, etc.).

3. SDK-80: this is the microcomputer unit. All operating system programs, signal-preprocessing, detection and identification and data-recording operations are stored as microprograms in the SDK-80[60]. These microprograms are executed when the proper commands are entered from the keyboard. The SDK-80 is an 8-bit machine running at a clock rate of 2 MHz.

4. Arithmetic Processing Unit (APU): the hardware arithmetic processing unit is interfaced to the SDK-80 microcomputer for high-speed arithmetic calculations. The APU provides various flexibilities such as floating-point or fixed-point arithmetic, single or double precision, function (such as trigonometric functions, etc.) generations, etc.

5. Memory Board: 8K memory bytes (8 bits/byte) for data storage.

6. Cassette Recorder: used for data recording

Similar systems had been built and documented under different studies[67] at the ElectroScience Laboratory. Except for the addition of the hardware arithmetic processing unit, the system developed and implemented in this dissertation has basically the same design and hardware. Thus, only the details concerning the APU are given in Appendix I. Details concerning the other modules of the microcomputer system are well documented in various reports[67].

C. Implementation of the Microcomputer System for Subsurface Target Identification

Pictures of the microcomputer system and its components are shown in Figures 50 and 51. Two major operations, namely target identification and data recording were implemented in the microcomputer system. The target identification process performed by the microcomputer is outlined in Figure 52. All processes except the automatic tuning process have been implemented. The tuning process is discussed in Chapter IX. In short, when the target identification mode is being executed, the Terrascan samples the received analog waveform, displays and feeds it to the analog board for A/D conversion. The digital waveform is then fed to the memory board where the average waveform is formed. The average waveform goes to the preprocessing unit for reduction in clutter/noise. This preprocessed waveform arrives at the detector for a screening operation. The detector screens out waveforms whose energy, peak timing and peak amplitude are out of the desired ranges. The "in-range" waveform would then be fed to the predictor-correlator for target identification. "Out-of-range" waveforms are considered as "undesired-target" waveforms. The correlation coefficients and the processed waveforms are stored in the 8K memory which is transferred to the cassette recorder when filled. For target identification based on the predictor-correlator method, only the difference equation coefficients corresponding to the desired target need to be stored in the microcomputer for the evaluation of $\rho(T)$, the complex resonances are not stored. For multiple-threshold identification, a set of coefficients corresponding to each chosen value of T_{0i} needs to be stored. Note that these coefficients depend on ground condition, thus, for on-location subsurface target identification in real time, an automatic tuning process is necessary. Automatic tuning of the identification radar to the ground condition is discussed in Chapter IX.

A list of executable commands and their detailed descriptions are given in Table 31 of Appendix I.

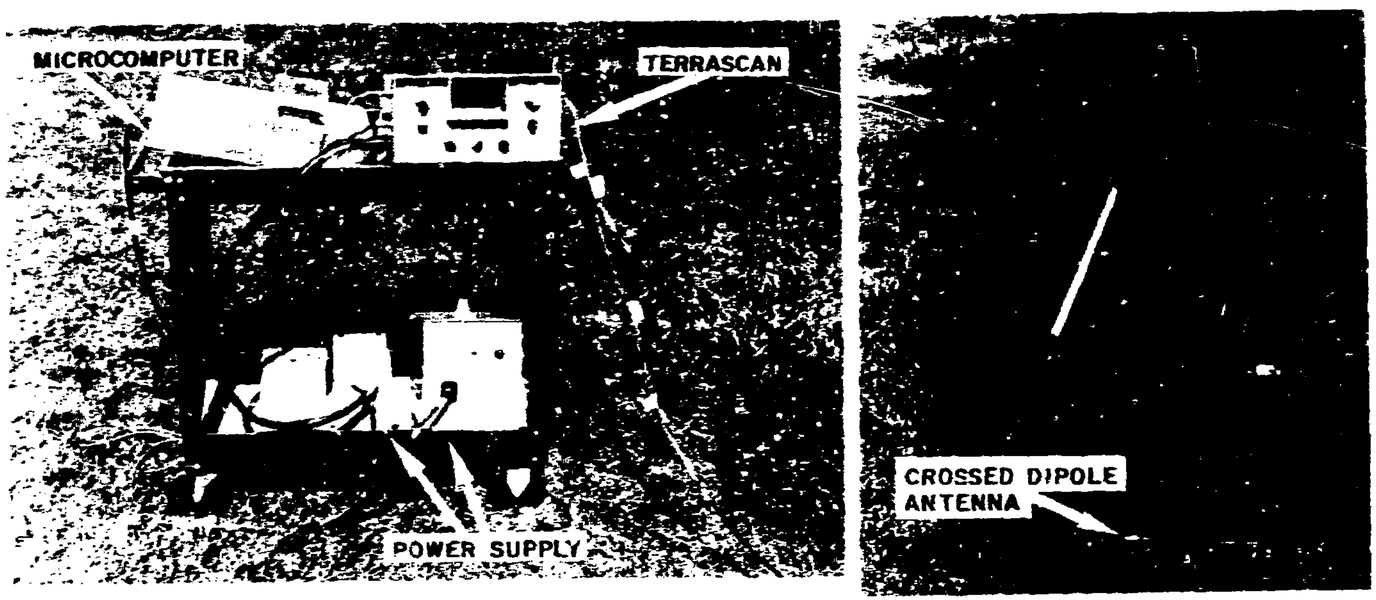

Figure 50. Picture of the microcomputer target identification system.

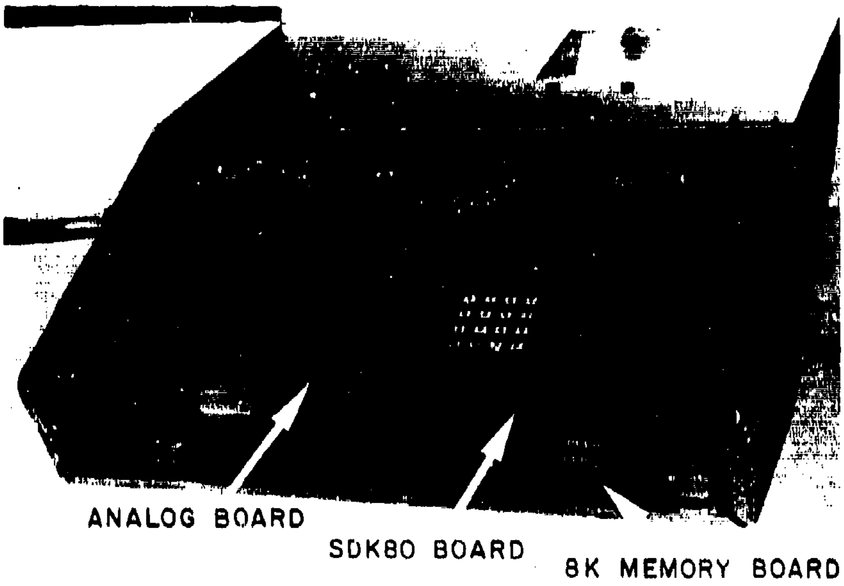

(a) THE MICROCOMPUTER

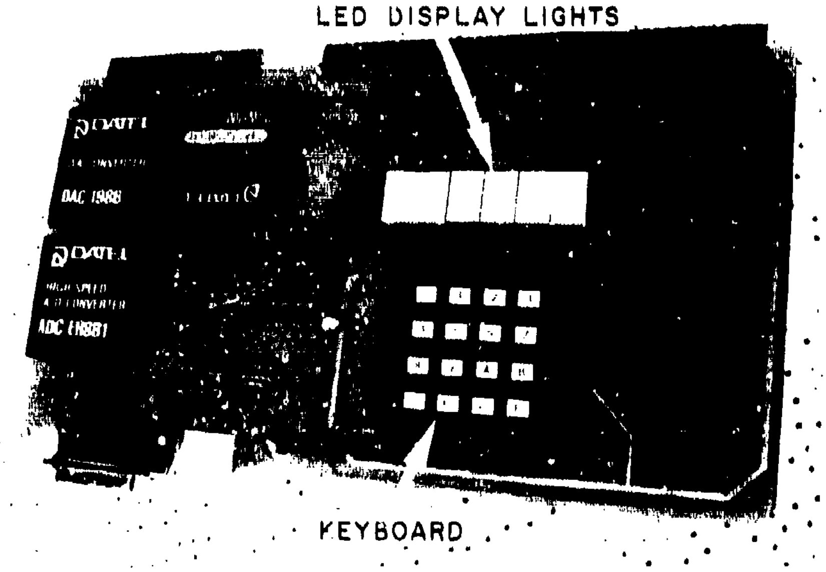

(b) THE ANALOG BOARD

Figure 51. The microcomputer and its components.

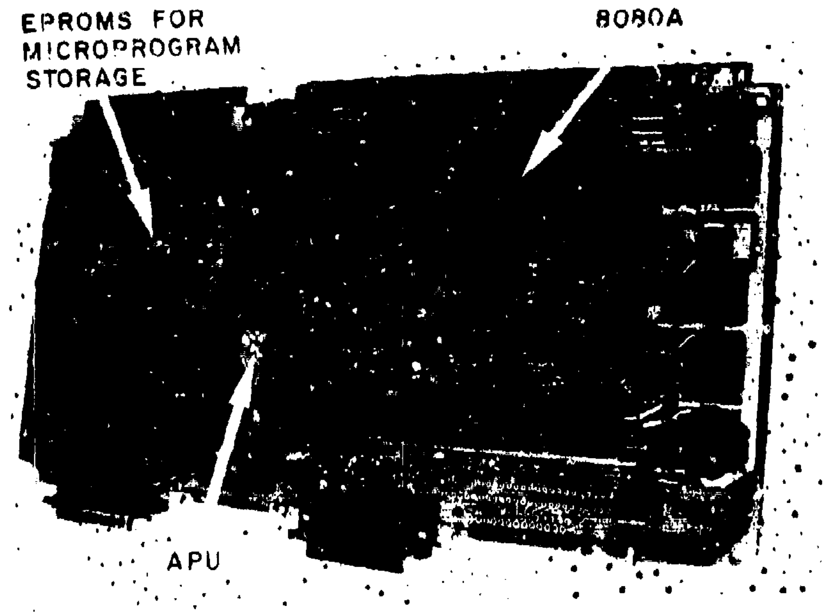

(c) THE SDK80 BOARD

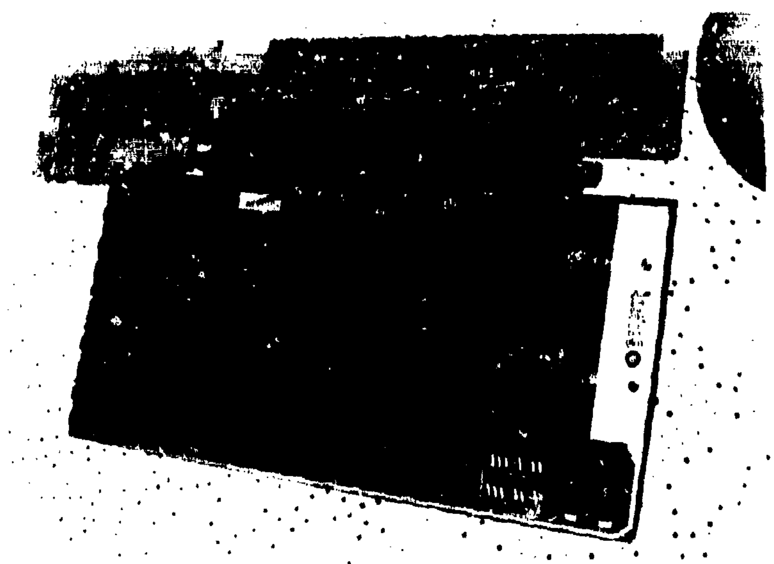

(d) THE 8K MEMORY BOARD

Figure 51 (cont'd). The microcomputer and its components.

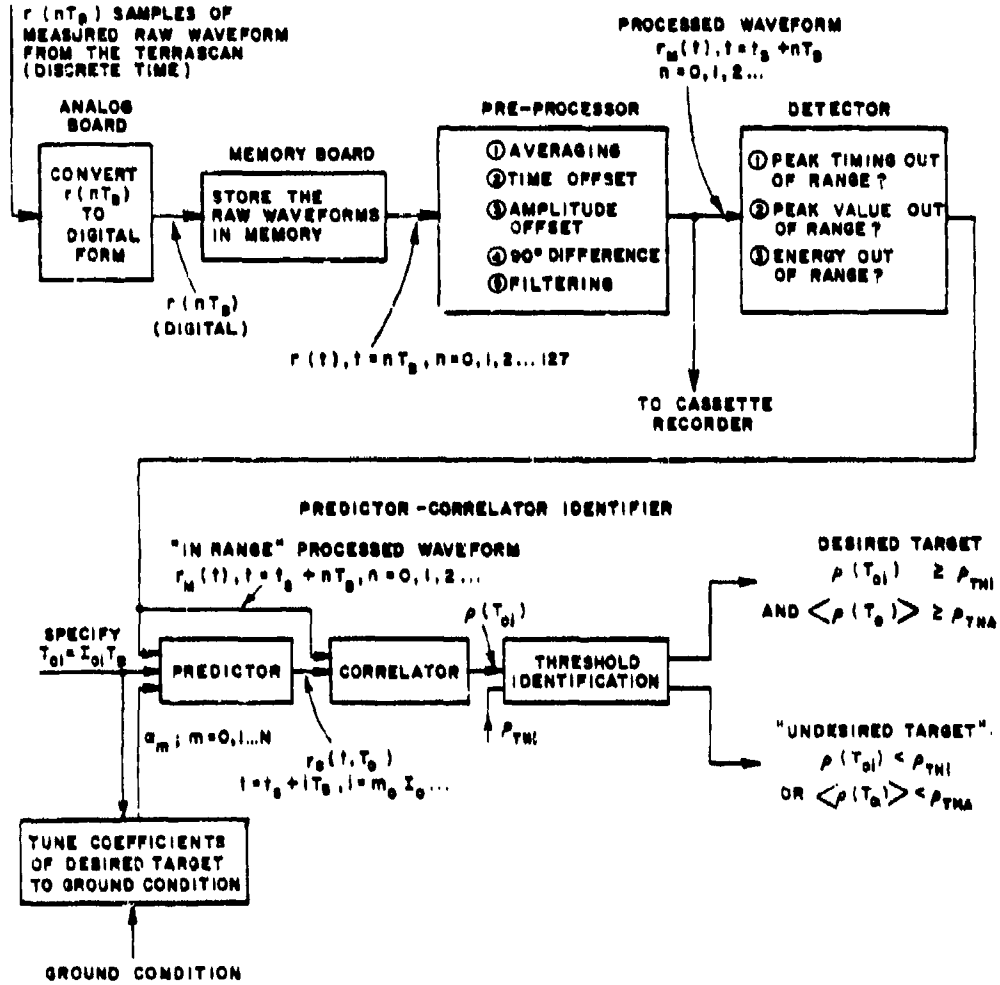

Figure 52. The identification process implemented in the microcomputer system.

The following notes with regard to the implementation of the microcomputer identification system are important:

1. Due to hardware constraints in the Terrascan, a waveform obtained with the microcomputer system contained only 128 data points. The waveforms obtained with the digital computer controlled system contained 256 data points. Thus, we were faced with possible loss of resolution in time (i.e., a larger sampling period must be used in order for 128 samples to cover a 50 ns time window) or frequency (i.e., smaller time window must be used). Careful study of the small-antenna waveforms from the mine-like target revealed the fact that the energy of practically all waveforms resided in a time window of 25 ns (see Figure 40). Hence, by choosing a time window for 25 ns and 128 samples for the mine identifier, both time and frequency resolution were maintained.

2. Besides frequency and time resolution of the waveforms, the other important considerations are data precision, flexibility and speed. In this system, double-precision floating-point* arithmetic is used to perform the major calculations such as the evaluation of the correlation coefficient $\rho(T)$ and the FIR filtering in the preprocessing unit. The floating-point format offers large dynamic range, flexibility and ease of implementation. The function-generation capability (such as trigonometric functions, transcendental functions, etc., are available for floating-point numbers only) of the APU provides tremendous flexibilities in the implementation of digital signal processing techniques. These, together with the fact that scaling operation is not needed for floating-point operations, makes the floating-point format an ideal choice for a "first-generation" computer system. The tremendous amount of scaling operations in the fixed-point calculations makes the calculations difficult to track and furthermore, the great amount of scaling often causes loss in data precision. The trade-off in using the floating-point format is the computing speed. Floating-point operations usually take more computing time than the corresponding fixed-point operations. Furthermore, the 25-bit mantissa offers less "nominal" data precision than the 32-bit fixed-point formated number. With the choice of data format, we now estimate the computing time needed for an identification decision. The major areas requiring significant amount of computations are the following:

*Floating-point number in this system is represented by a 7-bit exponent and a 25-bit mantissa.

a. Arithmetic averaging

This process forms the arithmetic average of N_1 raw waveforms from the same antenna location and orientation for reduction of noise. Here, the major part of the computation time goes to the sampling of the N_1 waveforms. The sampling time Δt is inversely proportional to the repetition frequency of the radar source, i.e., the impulse generator, and

$$\Delta t = \frac{N_1 \cdot N_2}{R_F} \tag{55}$$

where

N_1 = number of waveforms required to form the average,

N_2 = number of samples in a waveform, and

R_F = repetition frequency of the impulse generator.

In the present system, N_1=10, N_2=128 and R_F=256. Thus Δt=5 seconds. If the repetition frequency can be increased to 10 KHz*, Δt will be decreased to 0.125 second.

b. 90°-difference

This process forms the difference between two waveforms from two antenna orientations (one of which is a 90° rotation from the other) at the same antenna location. The differencing operation basically increases the sampling time by a factor of 2. In the final system applications, this process is probably not needed. At any rate, the antenna rotation process will represent a major time factor.

c. Calculation of $\rho(T)$

This process evaluates the correlation coefficient $\rho(T)$ at all chosen values of T_{0i}'s for multiple-threshold identification. Note that with the choice of floating-point format, the expression for $\rho(T)$ given in Equation (24) can be manipulated for minimum computation time. In floating-point calculations, due to the shifting of exponents required for the add/subtract operations, the amount of time required to perform an add/subtract operation can be larger than that required for a multiply/divide operation. Table 15 lists the computation time required by the APU to perform each of the four basic floating-point arithmetic operations. The maximum difference in the average computation time for the four operations are less than 23% of the minimum

---

*This is believed to be within state-of-the-art technology.

TABLE 15
COMPUTATION TIME REQUIRED BY THE APU TO PERFORM THE FLOATING-POINT ARITHMETIC OPERATIONS

FLOATING POINT OPERATION	NUMBER OF CLOCK CYCLES*		
	MINIMUM	MAXIMUM	AVERAGE**
ADD	56	350	203
SUBTRACT	58	352	205
MULTIPLY	168	168	168
DIVIDE	171	171	171

* 1 clock cycle = 500 ns
**AVERAGE = (MINIMUM+MAXIMUM)/2

average computation time. Thus it seems reasonable to manipulate the expression for $\rho(T)$ to minimize the total number of operations. Based on the above criterion, the following expression for $\rho(T)$ is implemented in the predictor-correlator of the microcomputer system for target identification.

$$\rho(T) = 1 - \frac{\sum_{t=t_s+m_oT}^{t_c-NT+m_oT} e^2(t)}{\sum_{t=t_s+m_oT}^{t_c-NT+m_oT} r_M(t)(r_M(t)-e(t)) + \sum_{t=t_s+m_oT}^{t_c-NT+m_oT} e^2(t)} \tag{56}$$

where

$$e(t) = r_M(t)-r_c(t) \quad .$$

The number of aritimetic operations required to evaluate $\rho(T)$ at a T value of T_{oi} is given in Table 16.

TABLE 16
NUMBER OF ARITHMETIC OPERATIONS REQUIRED TO EVALUATE $\rho(T)$ OF EQUATION (56) AT THE VALUE OF $T=T_{oi}$

OPERATION	NUMBER OF OPERATIONS
ADD	$(N+2)(M-NI_{oi})-1$
SUBTRACT	$M-NI_{oi}$
MULTIPLY	$(N+1)(M-NI_{oi})+1$
DIVIDE	1

In Table 16,

N = number of resonances of the desired target used for identification purposes,

$M = (t_e-t_s+T_B)/T_B$, and

$I_{oi} = T_{oi}/T_B$.

Note that $M-NI_{oi}$ is the number of instantaneous error samples in the error interval.

With the small antenna system and for mine identification, N=10, M=101, I_{oi}=4,5,6,7 and 8 (see Chapter VII). The total computation time ranges from 0.26 seconds to 0.64 seconds with an average of 0.45 seconds.

d. The filtering operation in the preprocessor

Because of the unavailability of the FFT package in the microcomputer system, the digital filtering operation in the preprocessor was performed in the time domain via the following relationship[55,56]

$$r_M(nT_B) = \sum_{i=1}^{N'} h(iT_B)r_1(nT_B-iT_B) \qquad (57)$$

where

$r_M(nT_B)$ = the processed filtered waveform,

$r_1(nT_B)$ = the processed unfiltered waveform,

$h(iT_B)$ = impulse response of the digital filter, and

N' = order of the digital filter.

The impulse response of the digital bandpass filter given in Figure 47 was obtained by taking the inverse FFT of the digital filter transfer function. This impulse response and transfer function are shown in Figures 53a and b, respectively. Using this time-domain filter, a set of identification results was obtained using the in-house computer for the identification of the mine-like target based on the small-antenna waveforms previously obtained (see Chapter VII). Identical estimates of identification performance were obtained (i.e., P_I= 100%, P_{FA}=1.72% for R_{ID}=30 cm, and P_I=100%, P_{FA}=6.90% for R_{ID}=45 cm).

The time-domain filter shown in Figure 53b is a FIR filter with a large order of N'=128. Thus, tremendous computation time will be consumed in the filtering operation if it is to be impelemented in the microcomputer system. To save computation time, the order of this FIR filter was lowered to 37 by using a "windowing" technique with a Kaiser window[55,56,61]. The Kaiser window, the "windowed" impulse response of the filter and the FFT of the windowed impulse response are shown in Figure 53c-e. Identification performance estimates obtained using the in-house computer with this windowed filter was P_I=100%, P_{FA}=8.62% for R_{ID}=45 cm. Thus, performance only slightly degraded. This filter was incorporated into the microcomputer system for real-time identification of the mine-like target. The windowed time-domain filter has 37 coefficients and is symmetric about its center. Based on Equation (57) and Table 15, the average time required for the filtering operation on a small-antenna waveform is 0.5 seconds (vs 2 seconds for the unwindowed filter). The digital filter can be replaced by an analog filter placed at the front end of the receiver in the final identification system.

e. Detection

Operations performed in the detection include peak detection, energy calculations, etc.

f. Execution of computer instructions

The amount of time taken for execution of the computer instructions depends on the efficiency of the microprogram written.

In summarizing, the amount of time required for an identification decision in the identification of the mine-like target with the existing small-antenna microcomputer system is estimated to be approximately 11 seconds with 0.45 seconds of average predictor-correlating time.

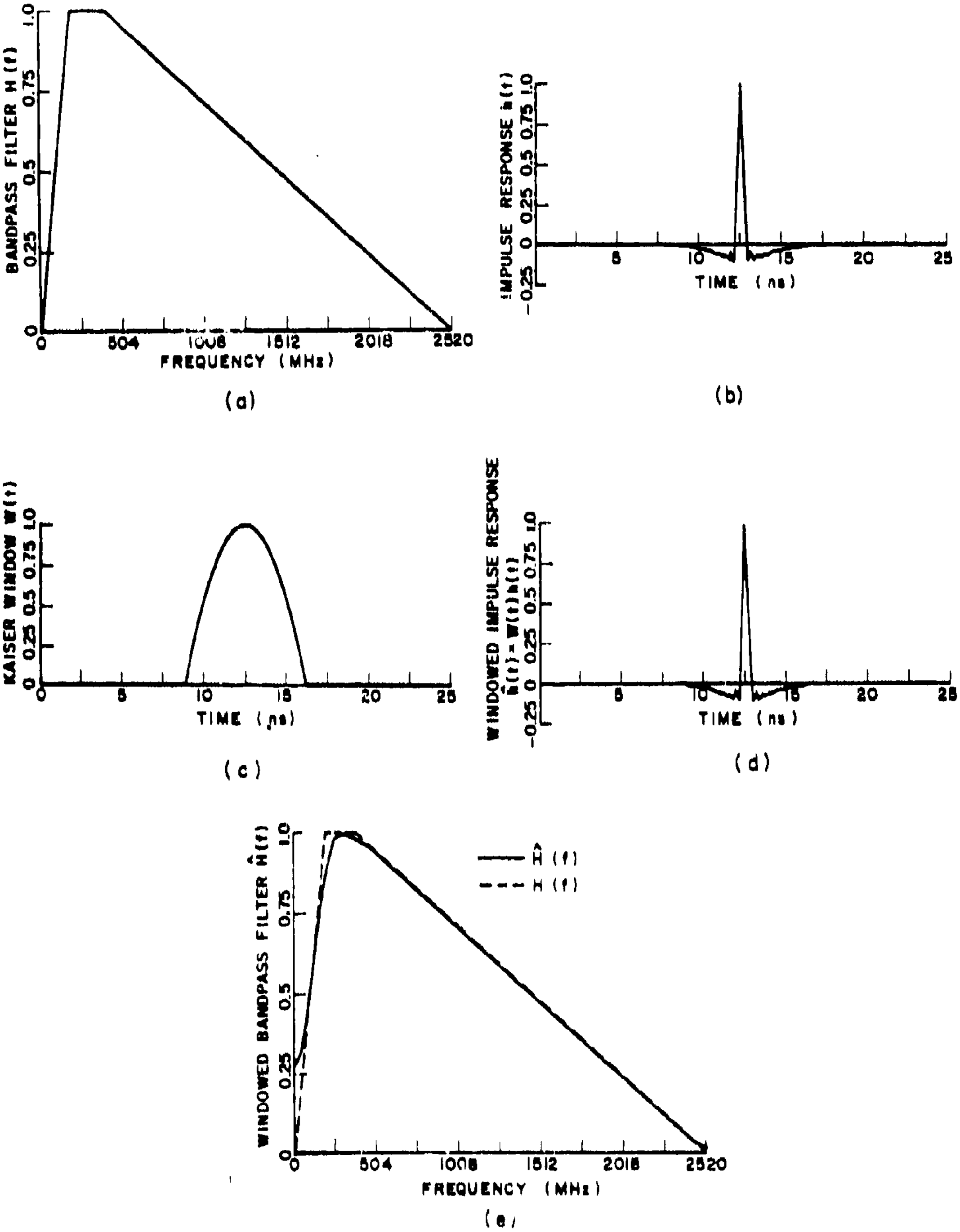

Figure 53. Design of the preprocessor FIR filter for target identification with the small-antenna microcomputer system.

The decision time goes down drastically to about 0.7 seconds if the repetition frequency of the pulser can be increased to 10 KHz, and the filtering operation in the preprocessor can be performed with an analog filter. Using state-of-the-art technology, both these conditions can be easily met.

Based on the simulated identification results obtained with the microcomputer conditions (i.e., 128 samples per waveform, FIR filtering), the microcomputer identification system is expected to identify the mine-like target with the same level of performance as the results previously presented in this dissertation.

D. Calibration of the Microcomputer Target Identification System

Calibration of the microcomputer system includes the following:

1. Time scale

The time scale was calibrated by comparing two waveforms from the same target. One of the waveforms was obtained with a fixed length of cable added to the system. The time window was calibrated at 25 ns. However, the impedance mismatch at the trigger pick-off circuitory of the Terrascan limited the reflectionless time window to 20 ns (see Figure 54). The secondary reflections caused by this impedance mismatch occurred at a time which was 20 ns from the transmit-receive coupling. This reduction in the size of the reflectionless time window was later found to limit the identification range of the radar system.

2. Amplitude scale

Operations performed in the detector required accurate calibration of the peak amplitude, peak timing as well as the energy of the mine-like target waveforms. These calibrations were performed by collecting a set of waveforms over the mine-like target and tabulating the various detection thresholds based on the set of waveforms

3. On-location ground condition

On-location ground-condition calibration is discussed in Chapter IX. At the present time, the in-situ complex resonances of the mine-like target waveforms were obtained by analyzing the waveforms collected in 2. using Prony's method. The difference equation coefficients associated with these resonances were then used for real-time target identification. Real-time identification performance of the microcomputer system is discussed in the next section.

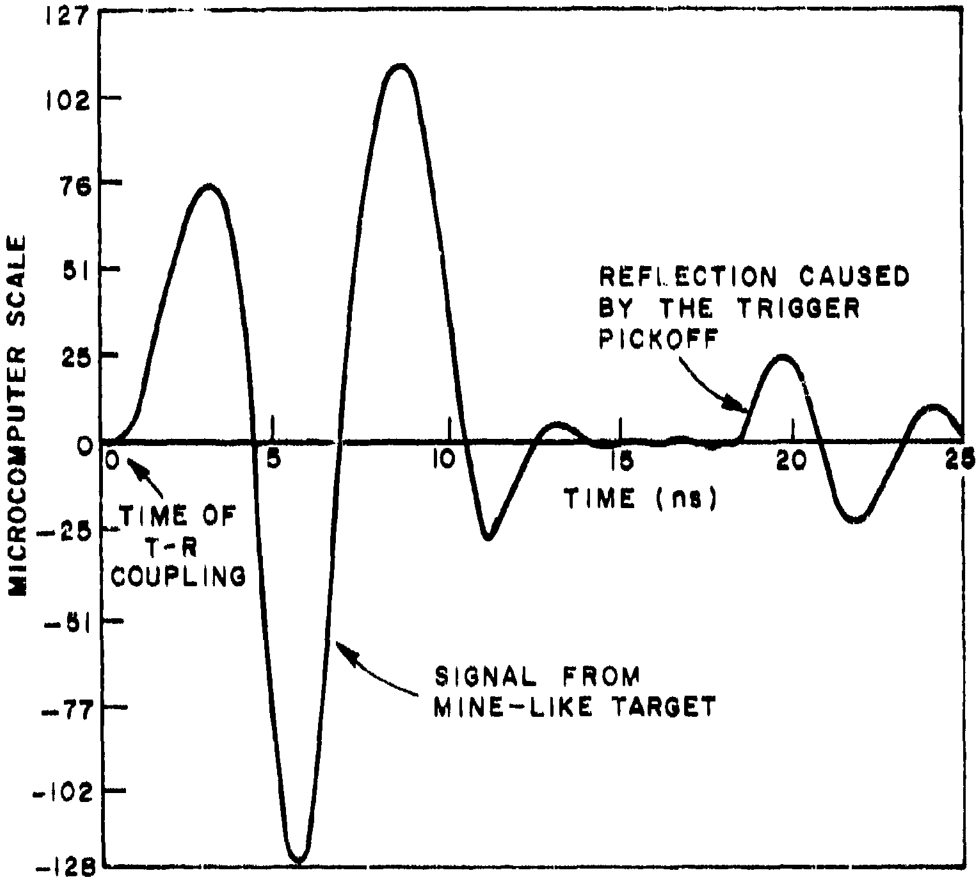

Figure 54. Typical processed mine-like target waveform received by the microcomputer system.

E. Real-Time Identification Performance of the Microcomputer Target Identification System

1. Identification performance

Two sets of identification data were obtained for the identification of the mine-like target in two different ground conditions. The first set was obtained using the poles and thresholds as given in Tables 27 and 30 of Appendix G for real-time identification of the mine-like target. Real-time identification performance of P_I=100% and P_{FA}=0% was obtained for R_{ID}=30 cm (based on 9 mine-like target waveforms and 21 other-target waveforms). It was found that, for R_{ID}=45 cm identification performance degraded to P_I=12%, P_{FA}=0%. This reduction in identification range was attributed to the presence of the unwanted reflections from the trigger pick-off in the latter portion of the time window.

The second set of identification data was obtained under a different and rapidly changing ground condition. A set of measurements over the mine-like target was collected over a lightly wet ground for calibrating the ground condition, target resonances, and the various detection and identification thresholds. However, there were rapid weather changes between the time of data analysis (for calibrations) and real-time identification. There was heavy rainfall during the interim period, and in one day, even a moderate snow storm. These drastic weather changes altered the ground condition, and with the system tuned to the previously calibrated conditions, it was found that the level of the correlation coefficients for the mine-like target waveforms was generally lowered. Hence to ensure a 100% identification probability, the identification thresholds had to be lowered. Thus, with an untuned system and using lower threshold values (see Appendix I for details), a set of real-time identification data was obtained. Identification data based on 17 mine-like target and 13 other-target waveforms were P_I=100% and P_{FA}=0% for R_{ID}=30 cm. Thus, lowering the threshold values seems to be an effective means to counter the problem of uncertain ground conditions for this penetrable "desired target". This aspect of the system warrants a detailed future investigation.

2. Speed

The two sets of identification data discussed in the above subsection were obtained with N_1 (the number of raw waveforms required to form an average waveform) set equal to 8. Thus, for a pulse repetition rate of 256 Hz, the amount of time required for the microcomputer system to form an average difference waveform was 8 seconds. The amount of time taken for the correct identification of the mine-like target was clocked at approximately 2.5 seconds. Thus, the total real-time for a correct identification of the mine-like target was approximately 10.5 seconds. The amount of time required for false-target or no-target discrimination was less than 10.5 seconds. In the

implementation of later generations of this identification system, it is expected that, the identification speed will drastically increase with the increase in pulse repetition rate, decrease in N_1, elimination of the 90° difference operation, and more efficient microprograms.

3. Precision

To find the precision of the correlation coefficients calculated in the microcomputer system, correlation coefficients were calculated for a waveform using the microcomputer system. These correlation coefficients were then compared to those calculated by the in-house computer system for the same waveform. It was found that, the two sets of results differed in the 10th bit of the mantissa of the floating-point formatted numbers. No error was observed in the exponents. Thus, using the 25-bit floating-point format of the APU resulted in a 0.1% truncated error in the correlation coefficients. This is expected to have little effect on the identification performance.

F. Possible Future Improvements on the Microcomputer System

In addition to the impedance mismatch at the trigger pick-off circuitory of the Terrascan, a few other aspects of the microcomputer system can be modified to improve identification performance.

1. The sampling system in the Terrascan

The Terrascan system was originally designed for low-frequency operation (i.e., frequencies less than 200 MHz), as such its sampling system is therefore slow. The slow sampling system causes loss in high-frequency content of the received waveforms. Figure 55 shows two waveforms, one received by the Terrascan and the other by a faster sampling system, from the same target at the same antenna location and orientation. The loss of high-frequency content in the waveform received by the Terrascan system is quite apparent.

With the identification performance obtained thus far using the microcomputer system, the high-frequency loss in the Terrascan sampling system does not seem to affect identification performance for the identification of the mine-like target considered in this study. However, such high-frequency loss will almost surely degrade performance when the system is used to identify smaller mines.

2. The dynamic range in signal level

The microcomputer system currently uses an 8-bit A/D converter to convert the received analog waveforms to digital form. This results in a 48 dB dynamic range in signal level. For the identification of low-level signals the dynamic range needs to be increased.

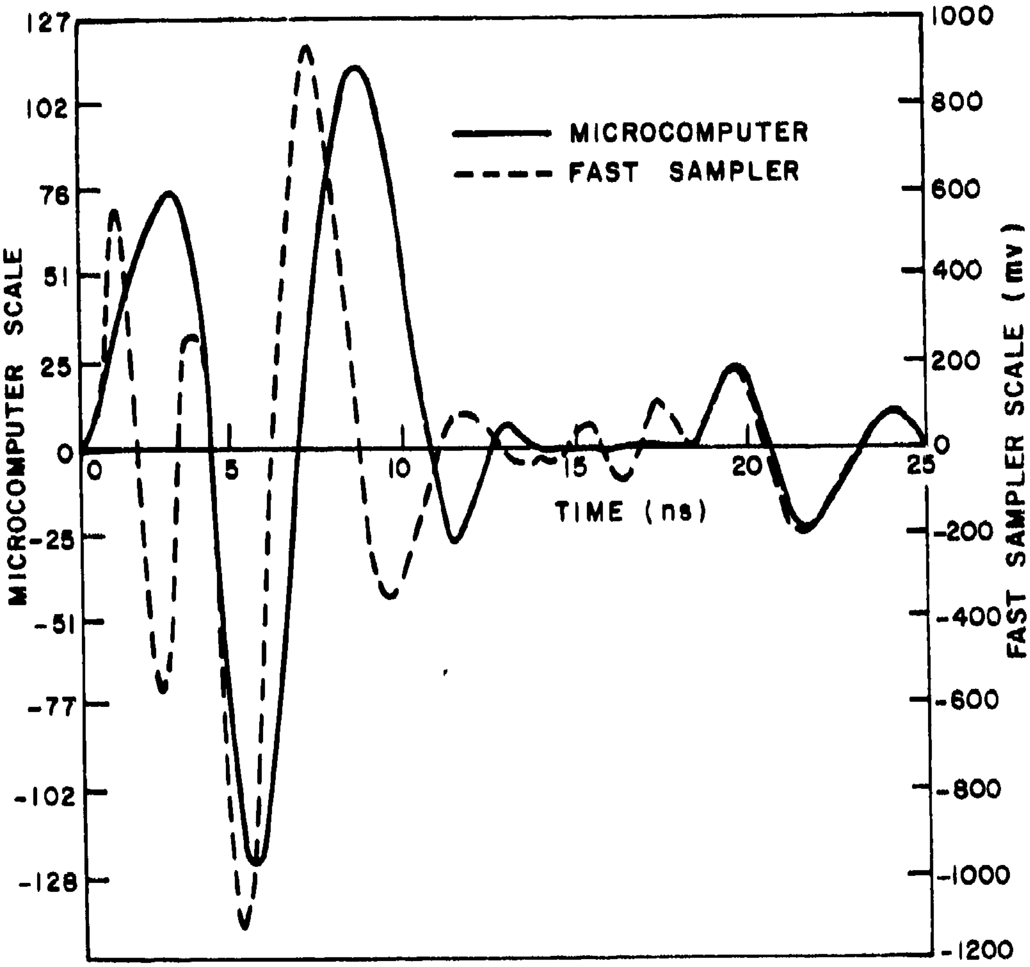

Figure 55. Processed mine-like target waveforms received by the microcomputer and the fast sampling system.

3. Gain control of the Terrascan

The gain control of the Terrascan system offers a limited range of gains in large discrete steps. Such large discrete steps may result in large truncation error.

In summarizing, a microcomputer system has been implemented for real-time subsurface target identification. Real-time single-look identification performance of P_I=100% and P_{FA}=0% for R_{ID}=30 cm was obtained with a total of 26 mine-like target waveforms and 34 other-target waveforms for the identification of the mine-like target in different ground conditions. The amount of time required for a correct identification of the mine-like target was approximately 10.5 seconds. The amount of time required for a correct other-target or no-target discrimination was less than 10.5 seconds.

The microcomputer system built in this study was intended to be a "first-generation" system. Many possible modifications of the system were recommended in this chapter for better identification speed, data precision, and identification performance. The most important modification is the process of automatic tuning of the radar system to the on-location ground condition. This is the topic of Chapter IX.

CHAPTER IX
A METHOD FOR REAL-TIME ON-LOCATION TUNING OF THE IDENTIFICATION RADAR TO THE GROUND CONDITION

A. Objectives

The importance of tuning the radar system to the ground condition was illustrated in Chapter IV. An un-tuned subsurface identification radar system yielded degraded performance. This chapter discusses a possible method for automatic tuning of the radar system to the ground condition. Emphasis is on the simplicity of the method and the possibility of incorporating such method into the microcomputer system for on-location target identification in real time.

B. The Use of Backscattered Waveforms From Thin Wires to Estimate The Ground Parameters

The backscattered waveforms from the buried thin wires as shown in Chapter VII possess the following properties which are useful in the calibration of ground conditions:

1. The waveforms contain complex natural resonances which are related to the ground parameters in a simple fashion.

2. The wire waveforms are of high amplitude, thus the estimate of the resonances will be accurate.

3. The lowest-order target resonance of the thin wires are the most dominant. (See Appeidix J). This implies that the thin wire waveforms can be closely characterized by a single resonance. Thus,

$$r_M(t) = 2a_1 \, e^{\alpha_1(t-t')} \cos\omega_1(t-t') \tag{58}$$

where

$r_M(t)$ = processed waveform ,

$s_1 = \alpha_1 + j\omega_1$ = complex resonance,

a_1 = residue associated with s_1, and

t' = start time of the transient signal from the wire.

For a thin wire, the first resonance can be approximated by Equation (58)

$$\alpha_1 = -\frac{\sigma}{2\varepsilon} - 0.0828\frac{\pi c}{\sqrt{\varepsilon_r}L} \tag{59}$$

$$\omega_1 = 0.9251\frac{\pi c}{\sqrt{\varepsilon_r}L}$$

where

σ = ground conductivity (homogeneous medium assumed),

ε = ground permittivity ,

c = speed of light in free space ,

ε_r = relative dielectric constant of the ground, and

L = length of wire .

The complex natural resonance given by Equation (59) is a good approximation to the first natural mode of a thin wire with a length/diameter ratio of 100 buried in a homogeneous medium of good dielectric (i.e., medium with a small loss tangent of $\sigma/\omega\varepsilon \ll 1$)[52,69]. Here, it is used to estimate the ground parameters based on the waveforms from the buried thin wires and is found to yield reasonable results.

Since the waveform is dominated by a single resonance, the values of α_1 and ω_1 can be easily estimated from the decaying envelope and the peak timing at two samples of the waveform, thus, the ground parameters can be estimated via the following equations:

$$\varepsilon_r = \left[\frac{0.9251(t_1-t_0)C}{2L}\right]^2$$

and (60)

$$\sigma = 2\varepsilon\left[(t_1-t_0)^{-1}\ln\frac{r_M(t_0)}{r_M(t_1)} - 0.0828\frac{\pi c}{L\sqrt{\varepsilon_r}}\right]$$

where $r(t_0)$ and $r(t_1)$ are the sample values of the measured waveform at time t_0 and t_1, respectively.* All other parameters are as previously defined.

Using Equation (60), the ground parameters represented by the waveform shown in Figure 56 are estimated to be ϵ_r=14 and σ=24 mS/m.** These estimates are found to be very close to the estimates obtained suing different techniques currently being investigated in another study at the ElectroScience Laboratory[58]. The method outlined in Equation (60) is attractive, for it uniquely characterizes the ground condition by two sample values of a thin-wire waveform.

C. Automatic Tuning of the Identification Radar to the Ground Condition

The knowledge of the ground parameters basically solves the automatic ground-condition tuning problem for the real-time identification of simple targets such as the brass cylinder and the aluminum sphere whose resonances are related to the ground parameters in a known analytical fashion[21,63]. However, it does not solve the tuning problem for the real-time identification of plastic mines, for the analytic relations between the complex natural resonances of the plastic mine-like target and the ground parameters are not known. To date, the characterization of targets, should it be free-space or subsurface targets, is a relatively new research problem. Furthermore, research efforts have mostly been concentrated in the characterization of perfectly conducting targets only. Characterization of dielectric targets such as the plastic mine-like target with complex natural resonances via analytical method has not been previously treated. This could be achieved but it represents a substantial research effort beyond the scope of the present study. In this study we suggest solving the automatic tuning problem for identification of mines experimentally with the procedure outlined as follows:

Step 1: Estimate the ground parameter by using the method outlined by Equation (60).

---

* Equation (60) is valid only when $r_M(t_0)$ and $r_M(t_1)$ are both non-zero and that $\omega_1(t_1-t_0)=2n\pi$ where $n=1,2,3\cdots$.

** Note that these estimates are, of course, accurate only at ω_1. Furthermore, the loss tangent, based on the estimated values of ϵ_r and σ, is found to be 0.252.

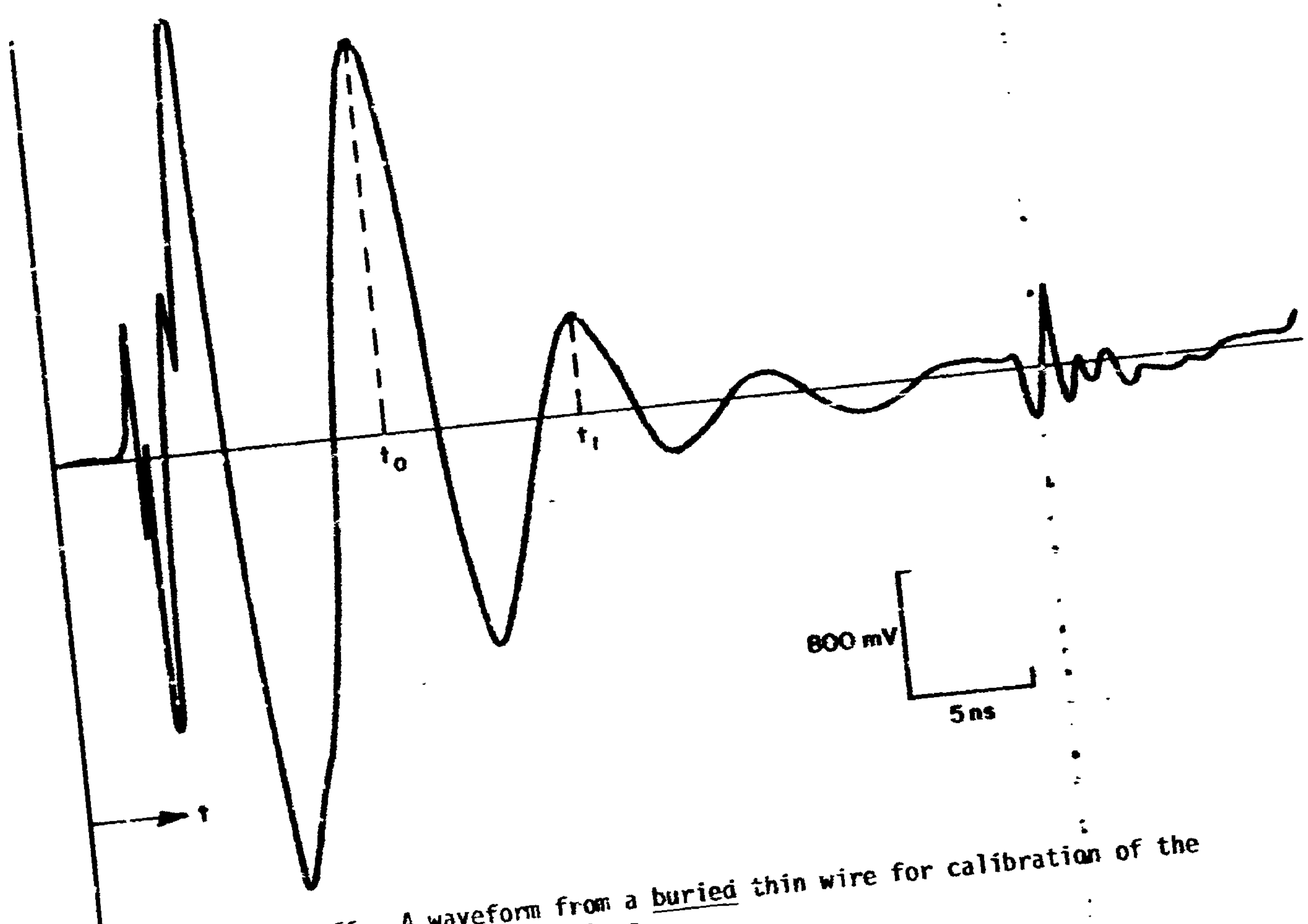

Figure 56. A waveform from a buried thin wire for calibration of the ground parameters.

Step 2: Determine the loci of the complex resonances of the mine-like target experimentally as the ground parameters vary. Ground parameters can be controlled by using different kinds of soils, or by increasing the moisture and salt content of the ground. Thus, the loci of the natural resonances (or the coefficients α_m's) can be determined as a function of t_1-t_0, $r_M(t_0)$, and $r_M(t_1)$ and stored in ROM's in the microcomputer identification system for on-location target identification in real time.

To make the above method even more attractive and practical, the thin wire does not have to be buried for ground-condition characterization. Figure 57 shows waveforms obtained from a thin wire laying at different locations on the surface of the ground.* Again, the waveform is dominated by one (pair) resonance and thus, the ground condition is uniquely characterized by the values and timing of two sample points of the waveform. In the case of the on-surface wire however, because of the fact that part of the wire is in the air, the ground parameters are no longer estimated accurately by Equation (60). Nevertheless, the unique information about the ground condition is assumed to be contained in the two samples of the waveform. Thus far, this assumption is found to be valid. The on-surface wire waveforms given in Figure 55 indicate different decaying envelopes and zero-crossing intervals for different ground conditions.

The method of ground-condition tuning outlined above amounts to an extensive experimental effort and is planned for the future.

---

* The wire has to be in good contact with the ground.

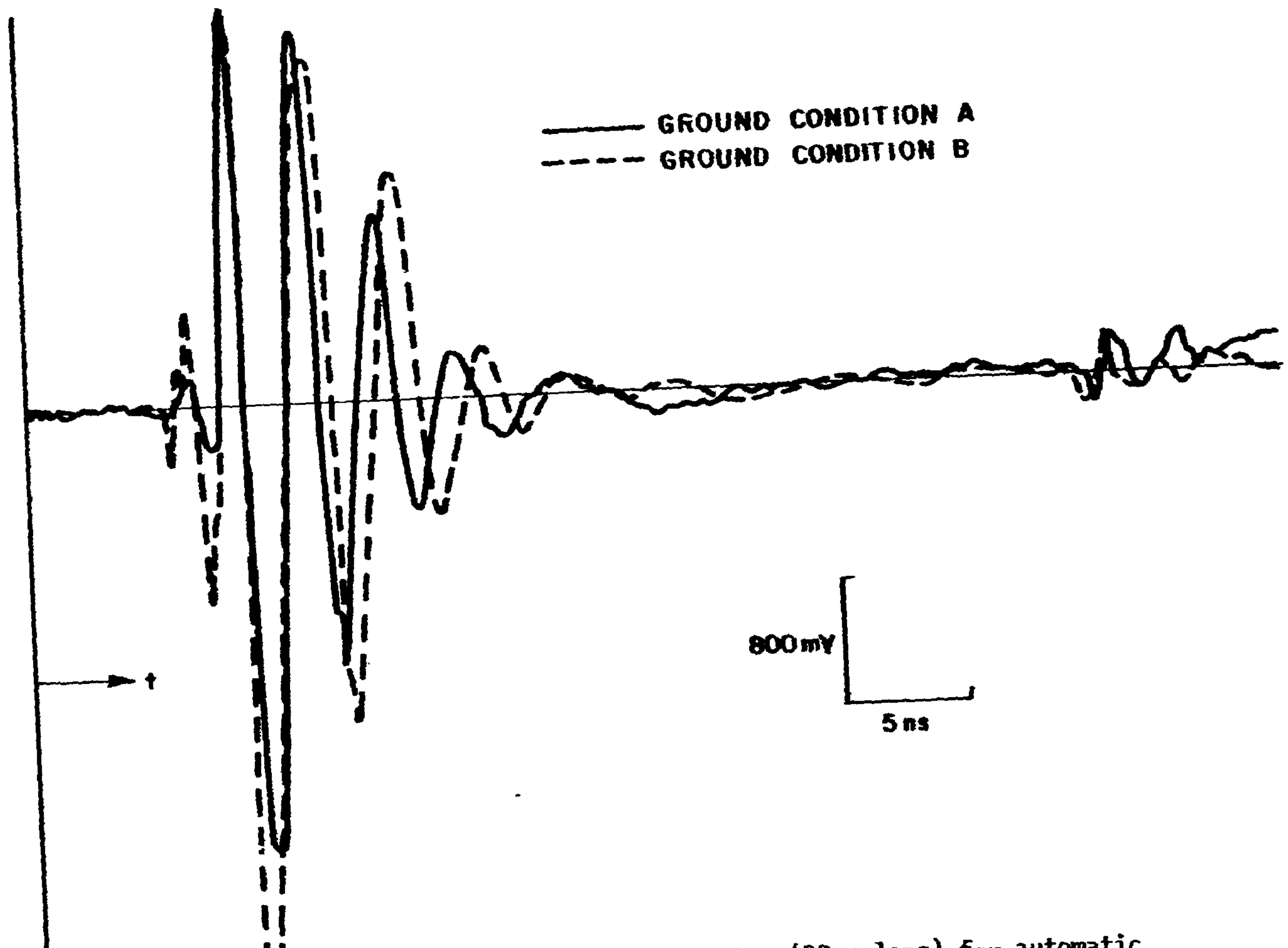

Figure 57. Waveforms from an on-surface thin wire (30cm long) for automatic tuning of the subsurface radar to ground condition.

CHAPTER X
SUMMARY, CONCLUSIONS AND RECOMMENDATIONS

A. Summary

At the time research in this report was initiated, the claim that electromagnetic signals were impractical for subsurface exploration because of attenuation had already been refuted. References in this report contain additional evidence refuting this claim. We demonstrate that the received signals from objects beneath the surface of the earth can also be interpreted intelligently. That is, that much more than simple ray tracing with a postulated reflection coefficient at some depth is possible. We show conclusively, using real subsurface probing data, that the target can be identified. It is emphasized that the identification is not simply a seismic-type map subject to interpretation and qualification by the observer but an actual processing scheme which inquires as to the presence of a particular target. We also stress that the methods developed in this dissertation are field-oriented and operate in real time. The paragraphs below itemize the specific progress which has been made.

The predictor-correlator method for characterizing and identifying subsurface targets was studied and extensively tested using real radar measurements obtained with a Terrascan-type subsurface pulse radar. Measurements were obtained over three sets of targets. The first set consisted of five similar-size targets including a plastic mine-like target, a brass cylinder, an aluminum sphere, a copper sheet and a wood board. These targets were buried at a depth of 5 cm (2 inches). The second set consisted of a series of different-size (maximum dimension varies from 30 cm to 300 cm) brass cylinders buried at different depths (depth varies from 30 cm to 150 cm). The third set consisted of a series of thin wires buried at the depth of 5 cm (2 inches). The method of characterization and identification uses the complex natural resonances as the discriminants for the identifier and the method of linear prediction for evaluation of the correlation coefficients for threshold identification. The complex natural resonances of the desired target are determined a priori and the difference equation coefficients related to these resonances are stored in the identification system for real-time on-location target identification. The identification process is simple and involves only simple algebraic operations.

The characterization and identification methods were found to be successful and a "first-generation" microcomputer system was built for on-location identification of mines in real time. A simple method for automatic tuning of the identification radar to the ground condition was suggested. This method is simple to use and can easily be incorporated into the microcomputer system for real-time target identification purposes. The significant findings are:

1. The identification method was extensively tested, with measurements over the subsurface targets, and found to be extremely successful. Single-look identification statistics for the identification of the mine-like target in different ground conditions were estimated to be P_I=100%, P_{FA}=2.25% for R_{ID}=30 cm over an ensemble of 55 mine-like target waveforms and 222 other-target waveforms.* The S/C of the ensemble of mine-like target waveforms ranged from 0.21 to 3.5.

2. A microcomputer system was implemented for real-time subsurface target identification using the techniques developed in this study. Single-look identification statistics for the identification of the mine-like target were estimated to be P_I=100%, P_{FA}=0% for R_{ID}=30 cm over an ensemble of 30 mine-like target waveforms and 30 other-target waveforms. The amount of time required for a correct identification of the mine-like target was 10.5 seconds, a correct discrimination of an other-target or no-target required less time.

3. Identification performance degraded when the radar system was not tuned to the right ground condition

4. Identification performance degraded when the radar frequencies did not properly span the target resonances.

5. Single-look identification performance was characterized by a correlation coefficient vs. sampling interval ($\rho(T)$) curve. Optimal identification performance occurred when the sampling interval T was in the immediate neighborhood of T_N (see Equation (51)). Thus, one knows a priori the value or the region of values of the sampling interval needed for design and implementation of the identification radar.

---

* Identification statistics given here is estimated from the ensemble of all mine-like target waveforms collected using the Terrascan-like systems.

6. All subsurface targets considered were characterized by a small and finite number (5 pairs or less) of resonances. These resonances were invariant with respect to radar location.

7. The resonances of the plastic mine-like target were found to be internal resonances, with their imaginary parts independent of ground condition. The resonances of the brass cylinder were found to be external resonances; both their imaginary and real parts were dependent on ground conditions.

8. The extracted resonances of the brass cylinders were found to be the dipoles modes along the length of the cylinder. Furthermore, they closely approximated the resonances of the same target buried in a homogeneous medium with plane-wave illumination. This discovery suggested a good way to estimate the ground parameters (see Section VII-B).

9. The high-frequency content of the backscattered waveforms was highly attenuated as target depth increased. Identification range decreased as target depth increased.

10. Up to a certain threshold, the frequency of the target resonances decreased according to the increase in target size, and target resonances depended solely on the scattering mechanisms of the targets. Beyond the threshold, increase in target size did not warrant the decrease in the frequency of the resonances. In this case, target resonances would depend on the scattering mechanisms as well as other quantities such as the antenna pattern, etc.

The significant contributions of this report are:

1. The problem of applying Prony's Method to real radar measurements for extraction of the complex resonances was considered as one of parameter optimization. This approach yielded legitimate target resonances from waveforms with S/C as low as 0.21 (see Chapter III).

2. The predictor-correlator method was extensively tested with real radar measurements, and found to yield practical single-look identification performance. Furthermore, it was found that there existed a limited range of T values in which optimum identification performance occurred. (See Chapter IV).

3. A microcomputer system was implemented for real-time on-location subsurface target identification using the techniques developed in this dissertation. The system was found to yield practical single-look identification performance with a 10.5 second identification time (see Chapter IX).

B. Conclusions

We have now provided a successful method for the identification of subsurface targets at shallow depth. The method is based on single radar returns and is simple to implement. Based on this method a microcomputer system has been implemented for on-location identification of subsurface targets in real time. Some modifications have to be made for the microcomputer identification radar system to be practical, the most important being a method to calibrate the ground parameters (ε,μ,σ) in real time and to adjust the resonances of the desired target accordingly for real-time subsurface target identification in different ground conditions. This is now being implemented and is expected to be incorporated in the final system.

C. Recommendations for Future Work

The subject of subsurface target characterization and identification is in its infancy. The results obtained in this study represents a significant step forward, but much remains to be done. The following items are highly recommended for future research:

1. The taks of automatic on-location tuning of the subsurface radar to the ground condition is crucial to the problem of subsurface target identification. The consideration of the waveform values of the on-surface wire waveforms suggests a feasible way to solve this problem.

2. The relationships between the extracted resonances of the targets and the various system parameters such as target size, depth, antenna pattern, air-ground interface, etc., need to be exploited for a better understanding and interpretation of the extracted resonances.

3. Application of the characterization and identification technique to deeper targets needs to be expanded. In this regard very little deep electromagnetic probing has been done.

4. Identification of subsurface targets in the presence of other objects.

REFERENCES

1. Jonathan D. Young and Ross Caldecott, "Underground Pipe Detector," United States Patent No. 3967282 and 4062010.

2. Arthur C. Eberle and Jonathan D. Young, "The Development and Field Testing of a New Locator for Buried Plastic and Metallic Utility Lines," Transportation Research Board Fifty-Sixth Annual Meeting, Washington, D.C., January 1977. Also published in Transportation Research Record 631 published by Transportation Research Board, Commission on Sociotechnical Systems, National Research Council, National Academy of Sciences, Washington, D.C., pp. 47-52, Library of Contress JE7.H5, No. 631 (TE 175) 380.5' 08S[625.7].

3. J.D. Young and R. Caldecott, "A Portable Detector for Plastic Pipe and Other Underground Object,s" Report 404X-1, September 1973, The Ohio State University ElectroScience Laboratory, Department of Electrical Engineering; prepared for the Columbia Gas System Service Corporation, Columbus, Ohio.

4. D.L. Moffatt and R.J. Puskar, "A Subsurface Electromagnetic Pulse Radar," Geophysics, Vol. 41, No. 3, June 1976, pp. 506-518.

5. N. Barakat and L.T. Dolphin, Jr., et al., "Electromagnetic Sounder Experiments at the Pyramids of GIZA," Report prepared for the NSF Grant No. FG-38767 by Joint ARE-USA Research Team of AIN SHAMS University, Cairo, A.R.E., and the Stanford Research Institute, California, U.S.A., May 1975.

6. "Terrascan, Underground Utility Locator," Commercial Product Division, Microwave Associates, Inc., Burlington, Massachusetts.

7. C.E. Baum, "Emerging Technology for Transient and Broad-Band Analysis and Synthesis of Antennas and Scatterers," Proc. IEEE, Vol. 64, No. 11, November 1976.

8. C.E. Baum, "On the Singularity Expansion Method for the Solution of Electromagnetic Interaction Problems," Interaction Note 88, December 11, 1971.

9. D.L. Moaffatt, "Radar Target Detection and Discrimination," Short Course Notes for Radar Target Identification, 1977, The Ohio State University, Department of Electrical Engineering, 1976 and 1977.

10. D.L. Moffatt and R.K. Mains, "Detection and Discrimination of Radar Targets," IEEE Trans. on Antennas and Propagation, Vol. AP-23, No. 3, May 1975.

11. C.W. Chuang and D.L. Moffatt, "Natural Resonances of Radar Targets Via Prony's Method and Target Discrimination," IEEE Trans. on Aerospace and Electronic Systems, Vol. AES-12, No. 5, September 1976, pp. 583-589.

12. R. Prony, "Essai expérimental et analytique sur les lois de la dilatabilité de fluides elastiques et sur celles del la force expansive de la vapeur de l'alkool, a differentes témperatues," J. l'Ecole Polytech, (Paris), Vol. 1, No. 2, 1795, pp. 24-76.

13. R.N. McDonough, "Matched Exponents for the Representation of Signals." D:Eng., Dissertation, 1963, The Johns Hopkins University, Department of Electrical Engineering.

14. M.L. Van Blaricum and R. Mittra, "A Technique for Extracting the Poles and Residues of a System Directly from Its Transient Response," IEEE Trans. on Antennas and Propagation, Vol. AP-23, No. 6, November 1975, pp. 777-781.

15. M.L. Van Blaricum, "Techniques for Extracting the Complex Resonances of a System Directly from Its Transient Response," Ph.D. Dissertation, 1976, University of Illinois at Urbana-Champaign, Department of Electrical Engineering.

16. B.S. Melton, "Electromagnetic Prospecting Method," United States Patent 2,077,707, April 29, 1937.

17. L. Statham, "Electric Earth Transients in Geophysical Prospecting," Geophysics, Vol. I, 1936, pp. 271-277.

18. P.F. Hawley, "Transients in Electrical Prospecting," Geophysics, Vol. 3, 1938, pp. 247-257.

19. C.W. Horton, "On the Use of Electromagnetic Waves in Geophysical Prospecting," Geophysics, Vol. 11, 1946, pp. 505-518.

20. R.M. Lerner, "Ground Radar System," United States Patent 3,831,173 August 20, 1974.

21. W.B. Sullivan, "Short Pulse Measurements of Targets Immersed in a Lossy Half-Space," M.Sc. Thesis, The Ohio State University ElectroScience Laboratory, Department of Electrical Engineering, 1970.

22. L.C. Chan, "A Digital Processor for Transient Subsurface Radar Target Identification," Report 479X-3, December 1975, The Ohio State University ElectroScience Laboratory, Department of Electrical Engineering; prepared for Columbia Gas System Service Corporation, Columbus, Ohio.

23. L.C. Chan, D.L. Moffatt and L. Peters, Jr., "A Characterization of Subsurface Radar Targets," Special Issue on Exploration Geophysics, Proc. of IEEE, MID-1979, to be published.

24. C.W. Davis, III, "The Design and Analysis of a Transient Electromagnetic Antenna for Subsurface Radar Applications," M.Sc. Thesis, The Ohio State University ElectroScience Laboratory, Department of Electrical Engineering, June 1975.

25. G.V. Keller and F.C. Frischknecht, Electrical Methods in Geophysical Prospecting, Pergammon Press, 1966.

26. D.C. Gates and R.A. Armistead, "The Use of Advanced Technologies for Locating Underground Obstacles," Stanford Research Institute, June 1974.

27. "Antennas for Mine Detection Systems," Report 2857-1, 8 October 1969, The Ohio State University ElectroScience Laboratory, Department of Electrical Engineering; prepared under Contract DAAK02-69-C-0693 for U.S. Army Mobility Equipment Research and Development Command, Ft. Belvoir, Virginia.

28. "Antennas for Mine Detection Systems," Report 2857-2, 20 February 1970, The Ohio State University ElectroScience Laboratory, Department of Electrical Engineering; prepared under Contract DAAK02-69-C-0693 for U.S. Army Mobility Equipment Research and Development Command, Ft. Belvoir, Virginia.

29. "Antennas for Mine Detection Systems," Report 2857-3, 1 June 1970, The Ohio State University ElectroScience Laboratory, Department of Electrical Engineering; prepared under Contract DAAK02-69-C-0693 for U.S. Army Mobility Equipment Research and Development Command, Ft. Belvoir, Virginia.

30 "Antennas for Mine Detection Systems," Report 2857-4, 17 March 1971, The Ohio State University ElectroScience Laboratory, Department of Electrical Engineering; prepared under Contract DAAK02-69-C-0693 for U.S. Army Mobility Equipment Research and Development Command, Ft. Belvoir, Virginia.

31. "Antennas for Mine Detection Systems," Report 2857-5, September 1970, The Ohio State University ElectroScience Laboratory, Department of Electrical Engineering; prepared under Contract DAAK02-69-C-0693 for Research Division, Intrusion Detection and Sensing Laboratory, Mobility Equipment, Research and Development Center, Fort Belvoir, Virginia.

32. "Antennas for Mine Detection Systems," Report 2857-6, 15 March 1971, The Ohio State University ElectroScience Laboratory, Department of Electrical Engineering; prepared under Contract DAAK02-69-C-0693 for Research Division, Intrusion Detection and Sensing Laboratory, Mobility Equipment, Research and Development Center, Fort Belvoir, Virginia.

33. D.A. Irons, Jr., "Characteristic Spectra of the Electromagnetic Fields Scattered by a Buried TMDB Mine," Report 2857-7, 15 March 1971, The Ohio State University ElectroScience Laboratory, Department of Electrical Engineering; prepared under Contract DAAK02-69-C-0693 for Research Division, Intrusion Detection and Sensing Laboratory, Mobility Equipment, Research and Development Center, Fort Belvoir, Virginia.

34. "Microwave Nonmetallic Mine Detection," Report 2857-8, May 1971, The Ohio State University ElectroScience Laboratory, Department of Electrical Engineering; prepared under Contract DAAK02-69-C-0693 for Research Division, Intrusion Detection and Sensing Laboratory, Mobility Equipment, Research and Development Center, Fort Belvoir, Virginia.

35. D.A. Irons, Jr. and W.D. Burnside, "Antennas for Mine Detection Systems," Report 2857-9, May 1971, The Ohio State University ElectroScience Laboratory, Department of Electrical Engineering' prepared under Contract DAAK02-69-C-0693 for Research Division, Intrusion Detection and Sensing Laboratory, Mobility Equipment, Research and Development Center, Fort Belvoir, Virginia.

36. J.D. Echard, J.A. Scheer, E.O. Rausch, et al., "Radar Detection Discrimination, and Classification of Buried Non-Metallic Mines," February 1978, Georgia Institute of Technology.

37. Keinosuke Fuhunaga, Introduction to Statistical Pattern Recognition, Academic Press, New York and London, 1972.

38. Ashok K. Agrawala, Machine Recognition of Patterns, IEEE Press, 1978.

39. Y.T. Lin, "Classification of Objects with Complex Geometric Shape by Means of Low Frequency Electromagnetic Response," Report 3815-1, August 1974, The Ohio State University ElectroScience Laboratory, Department of Electrical Engineering; prepared under Grant AFOSR-74-2611 for Air Force Office of Scientific Research.

40. D.A. Hill, "Electromagnetic Scattering Concepts Applied to the Detection of Targets Near the Ground," Report 2971-1, September 1970, The Ohio State University ElectroScience Laboratory, Department of Electrical Engineering; prepared under Contract F19628-70-C-0125 for Air Force Cambridge Research Laboratories.

41. E.M. Kennaugh and D.L. Moffatt, "Transient and Impulse Response Approximations," Proc. IEEE, Vol. 53, August 1965, pp. 893-901.

42. G.R. Cooper and C.D. McGillam, Method of Signals and System Analysis, Holt, Rinehard and Winston, Inc., 1967.

43. IBM Application Program, System/360 Scientific Subroutine Package, Version III, Programmer's Manual, Program Number 360A-CM-03X, Fifth Edition, August 1970.

44. Ross Caldecott and Julia Li, "Roots of a Polynomial with Complex Coefficients," ESL Computer Laboratory B[illegible]tin No. 8, February 1972.

45. David Muller, "A Method for Solving Algebraic Equations Using an Automatic Computer, Mathematical Tables and Other Aids to Computations, Vol. 10, October 1956.

46. M.L. Van Blaricum, "An Analysis of Existing Prony's Method Techniques," Mini-Symposium of Modal Analysis of Experimental Data, Albuquerque, New Mexico, March 1977.

47. M.L. Van Blaricum and R. Mittra, "Problems and Solutions Associated with Prony's Method for Processing Transient Data," IEEE Trans. on Antennas and Propagation, Vol. AP-26, No. 1, January 1978, pp. 174-182.

48. D.L. Moffatt, L.C. Chan and G.A. Hawisher, "Characterization of Subsurface Electromagnetic Soundings," Report 4490-1, September 1977, The Ohio State University ElectroScience Laboratory, Department of Electrical Engineering; prepared under Grant No. ENG76-04344 for National Science Foundation.

49. L.C. Chan and D.L. Moffatt, "Characterization of Subsurface Electromagnetic Soundings," Report 4490-2, December 1978, The Ohio State University ElectroScience Laboratory, Department of Electrical Engineering; prepared under Grant No. ENG76-04344 for National Science Foundation.

50. L.C. Chan and Leon Peters, Jr., "Electromagnetic Mine Detection and Identification," Report 4722-1, December 1978, The Ohio State University ElectroScience Laboratory, Department of Electrical Engineering; prepared under Contract DAAK70-77-C-0114 for U.S. Army Mobility Equipment Research and Development Command, Fort Belvoir, Virginia

51. Uwe Dibbern, "Speech Analysis by Wiener Filtering with Interpolation, 1974, Philips Forschungslaboratorium Hamburg GmbH, 2 Hamburg, Germay 54.

52. L.C. Chan, Unpublished Notes.

53. J.D. Markel and A.H. Gray, Jr., Linear Prediction of Speech, Springer-Verlag, 1976.

54. James A. Cadzow, Discrete Time Systems, Prentice-Hall, 1973.

55. Alan V. Oppenheim and Ronald W. Schafer, Digital Signal Processing, Prentice-Hall, Inc., 1975.

56. Lawrence R. Rabiner and Bernard Gold, Theory and Application of Digital Signal Processing, Prentice-Hall, Inc., 1975.

57. L.C. Chan, Unpublished Notes.

58. P.K. Hayes, M.Sc. Thesis, The Ohio State University ElectroScience Laboratory, Department of Electrical Engineering, to be published.

59. L.W. Wald, "Modification of the HFW Underground Antenna Based on Experimental Studies," Report 4722-2, January 1979, The Ohio State University ElectroScience Laboratory, Department of Electrical Engineering; prepared under Contract DAAK70-77-C-0114 for U.S. Army Mobility Equipment Research and Development Command, Fort Belvoir, Virginia.

60. INTEL MCS 80 Design Kit User's Guide, INTEL Corporation, 1976.

61. J.F. Kaiser, "Nonrecursive Digital Filter Design Using the I_0-SINH Window Function, 1974 IEEE Int. Symposium on Circuits and Systems, April 22-25, 1974, pp. 20-23.

62. Fredrick M. Tesche, "On the Analysis of Scattering and Antenna Problems Using the Singularity Expansion Technique," IEEE Transactions on Antennas and Propagation, Vol. AP-21, No. 1, January 1973.

63. J.A. Stratton, Electro-Magnetic Theory, McGraw-Hill, New York, 1941

64. E.O. Brigham, The Fast Fourier Transform, Prentic-Hall, Inc. 1974.

65. J.S. Bendat and A.G. Piersol, Random Data: Analysis and Measurement Procedures, Wiley Interscience, 1971.

66. C.A. Tribuzi, "An Antenna for Use in an Underground (HFW) Radar System," Report 4460-4, November 1977, The Ohio State University ElectroScience Laboratory, Department of Electrical Engineering; prepared under Contract DAAG53-76-C-0179 for U.S. Army Mobility Equipment Research and Development Command, Fort Belvoir, Virginia.

67. C.W. Davis, III and R. Gaglianello, "A Video Pulse Radar System for Tunnel Detection, Report 784460-9, January 1979, The Ohio State University ElectroScience Laboratory, Department of Electrical Engineering; prepared under Contract DAAG53-76-C-0179 for U.S. Army Mobility Equipment Research and Development Command, Fort Belvoir, Virginia.

68. AM9511 Arithmetic Processing Unit, Advanced Micro Devices, Advanced MOS/LSI, Advance Micro Devices, Inc., 1977.

69. Bharadwaja K. Singaraju, D.V. Giri and Carl E. Baum, "Further Developments in the Application of Contour Integration to the Evaluation of the Zeros of Analytic Functions and Relevant Computer Programs," Mathematics Notes, Note #42, March 1976, Air Force Weapons Laboratory.

APPENDIX A
DERIVATION OF PRONY'S METHOD FOR TRANSIENT WAVEFORMS WITH MULTIPLE-ORDER POLES

This appendix derives Prony's method for the extraction of resonances from waveforms with multiple-order poles.

With multiple-order poles the transient waveform can be expressed as

$$r(t) = \sum_{i=1}^{N} \left(1 + \sum_{j=2}^{M_i} b_{ji} p t^{j-1}\right) a_i e^{s_i t} \tag{61}$$

where

$p = 0$, if $M_i < 2$

$p = 1$, if $M_i \geq 2$

and where M_i is the multiplicity of the ith pole.

The corresponding expression of Equation (61) in the complex frequency domain is

$$\mathcal{L}[r(t)] = \sum_{i=1}^{N} \left(\frac{a_i}{(s-s_i)} + \sum_{j=2}^{M_i} \frac{b_{ji} p}{(s-s_i)^j} \right) \quad . \tag{62}$$

In discrete form, Equation (61) can be written as

$$r(nT) = \sum_{i=1}^{N} \left(1 + \sum_{j=2}^{M_i} b_{ji} p (nT)^{j-1}\right) a_i e^{s_i nT} \quad . \tag{63}$$

With the following z-transform pairs[54]

$$\mathcal{Z}\left[e^{s_i nT}\right] = \frac{1}{1-e^{s_i T} z^{-1}}$$

$$\zeta\left[(nT)e^{s_i nT}\right] = \frac{T\, e^{s_i T} z^{-1}}{\left(1-e^{s_i T} z^{-1}\right)^2}$$

$$\zeta\left[(nT)^2 e^{s_i nT}\right] = \frac{T^2\, e^{s_i T} z^{-1}\; 1+e^{s_i T} z^{-1}}{\left(1-e^{s_i T} z^{-1}\right)^2}$$

$$\vdots$$

$$\zeta\left[(nT)^j e^{s_i nT}\right] = \left(-Tz\,\frac{d}{dz}\right)^j \frac{1}{1-e^{s_i T} z^{-1}} \tag{64}$$

where $\zeta[]$ is the z transform operation. We can transform Equation (63) into the z domain, viz.,

$$\zeta[r(nT)] = \sum_{i=1}^{N}\left(1 + \sum_{j=2}^{M_i} b_{ji}\, p\left(-\, zT\,\frac{d}{dz}\right)^{j-1}\right)\frac{a_i}{1-e^{s_i T} z^{-1}}$$

$$= \sum_{i=1}^{N} a_i\left(\frac{1}{1-e^{s_i T} z^{-1}} + \frac{b_{2i} T\, e^{s_i T} z^{-1}}{\left(1-e^{s_i T} z^{-1}\right)^2} \right.+$$

$$+\frac{b_{3i} T^2\, e^{s_i T} z^{-1}\; 1+e^{s_i T} z^{-1}}{\left(1-e^{s_i T} z^{-1}\right)^3}+$$

$$\left. + \cdots + b_{M,i}\left(Tz\,\frac{d}{dz}\right)^{M_i-1}\left(\frac{1}{1-e^{s_i T} z^{-1}}\right)\right) \; . \tag{65}$$

Each term in the right hand side of Equation (65) is a rational function of z^{-1} with its denominator one degree higher in z^{-1} than the numerator. Thus, when the series is summed, it becomes a rational function of z^{-1} in the form of

$$\zeta(r(nT)) = \frac{c_0+c_1 z^{-1} + \cdots\; C_{L-1} z^{-L+1}}{d_0+d_1 z^{-1} + \cdots\; d_L z^{-L}} \tag{66}$$

where the polynomial of z^{-1} in the denominator is one degree higher than that in the numerator. The denominator polynomial is commonly referred to as the characteristic polynomial and its related to the pole locations s_i by

$$\sum_{i=0}^{L} d_i z^{-i} = \prod_{i=1}^{N} \left(1-e^{s_i T} z^{-1}\right)^{M_i} \quad ; \; L = \sum_{i=1}^{N} M_i \quad . \tag{67}$$

Multiply both sides of Equation (67) by z^L, we obtain

$$\sum_{i=0}^{L} d_i z^{L-i} = \prod_{i=1}^{N} \left(z-e^{s_i T}\right)^{M_i}$$

or

$$\sum_{m=0}^{L} \alpha_m z^m = \prod_{i=1}^{N} (z-z_i)^{M_i} \tag{68}$$

where

$$m = L-i; \quad m = 0,1\cdots L$$

$$\alpha_m = d_i$$

$$z_i = e^{s_i T} \quad . \tag{69}$$

Equation (68) is analogous to Equation (11).

We now proceed to write Equation (66) as

$$d_0+d_1 z^{-1} + \cdots d_L z^{-L})\zeta[r(nT)] = c_0+c_1 z^{-1} + \cdots C_{L-1} z^{-L+1} \quad . \tag{70}$$

With the relationship[54]

$$\zeta^{-1}[z^{-i}\zeta(r(nT))] = r(nT-iT) \tag{71}$$

where $\zeta^{-1}[\ ]$ is the inverse z transform operation. We obtain the inverse z transform of Equation (70)

$$\sum_{i=0}^{L} d_i r(nT-iT) = \zeta^{-1}\left[\sum_{i=0}^{L-1} c_i z^{-i}\right] \quad . \tag{72}$$

Since the right-hand side of Equation (72) is zero for $n \geq L$, hence

$$\sum_{i=0}^{L} d_i r(nT-iT) = 0 \quad ; \quad n \geq L \quad . \tag{73}$$

Now with

$$n = L + K; \quad K = 0,1,2\cdots \quad ,$$

$$m = L-i \qquad \text{and}$$

$$\alpha_m = d_i \quad ,$$

we obtain the desired difference equation,

$$\sum_{m=0}^{L} \alpha_m r_{K+m} = 0; \quad K = 0,1,2\cdots \tag{74}$$

where $r_{K+m}=r(KT+mT)$. This difference equation is identical to the Prony difference equation in Equation (12) except for the change of order. Thus, the sample values of a transient waveform with the presence of multiple-order poles satisfies a Prony difference equation of order L, where

$$L = \sum_{i=1}^{N} M_i \quad . \tag{75}$$

With Equation (74) we can solve for the coefficients α_m's, and subsequently solve for the s_i by Equation (67). We can also solve for the poles s_i, as was done in the simple-pole case, by solving Equations (12) and (11) with N changed to L. Thus, the same procedure taken to solve for the pole locations in the simple-pole case can also be used in the multiple-order-pole case. However the procedure for the calculation of the residues requires a slight modification.

The calculation of the residues is done by solving Equation (63), which differs from Equation (8) because of the presence of the terms involving (nT), and the fact that there are L unknowns rather than N. With the assumption that the ith pole is of order M_i, Equation (63) can be written as

$$r_0 = a_1 + a_2 + \cdots + \overbrace{0 + + \cdots + 0 +}^{M_i \text{ terms}} \cdots \quad \cdots + a_N$$

$$r_1 = a_1 z_1 + a_2 z_2 + \cdots + a_i z_i + \overbrace{T(b_{2i} a_i) z_i + T^2 (b_{3i} a_i) z_i + \cdots + T^{M_i - 1} (b_{M_i i} a_i) z_i}^{M_i \text{ terms}} + \cdots + a_N z_N$$

$$r_2 = a_1 z_1^2 + a_2 z_2^2 + \cdots + a_i z_i^2 + \overbrace{T(b_{2i} a_i) z_i^2 + T^2 (b_{3i} a_i) z_i^2 + \cdots + T^{M_i - 1} (b_{M_i i} a_i) z_i^2}^{M_i \text{ terms}} + \cdots + a_N z_N^2$$

$$\vdots \tag{75}$$

From Equation (75), we see that, in solving for the residues in the presence of multiple-order poles, the matrix Equation (15) must be modified as follows

$$DE = F$$

where

$$D = \begin{array}{c} \begin{array}{ccccccccccc} & & & & \text{ith Column} & (i+1)\text{th} & & (i+M_i-1)\text{th} & & & \end{array} \\ \begin{bmatrix} 1 & 1 & 1 & \cdots & 0 & 0 & \cdots & 0 & 1 & \cdots & 1 \\ z_1 & z_2 & z_3 & \cdots & z_i & z_i & \cdots & z_i & z_{i+1} & \cdots & z_N \\ z_1^2 & z_2^2 & z_3^2 & \cdots & z_i^2 & z_i^2 & \cdots & z_i^2 & z_{i+1}^2 & \cdots & z_N^2 \\ \vdots & \vdots & \vdots & & \vdots & \vdots & & \vdots & \vdots & & \vdots \\ z_1^{L-1} & z_2^{L-1} & z_3^{L-1} & \cdots & z_i^{L-1} & z_i^{L-1} & \cdots & z_i^{L-1} & z_{i+1}^{L-1} & \cdots & z_N^{L-1} \end{bmatrix} \end{array}$$

$$E = \begin{bmatrix} a_1 \\ a_2 \\ \vdots \\ a_i \\ a_i b_{2i} \\ a_i b_{3i} \\ \vdots \\ a_i b_{M_i i} \\ a_{i+1} \\ \vdots \\ a_N \end{bmatrix} = \begin{bmatrix} a_1' \\ a_2' \\ \vdots \\ a_i' \\ a_{i+1}' \\ a_{i+2}' \\ \vdots \\ a_{i+M_i-1}' \\ a_{i+M_i}' \\ \vdots \\ a_L' \end{bmatrix}$$

$$F = \begin{bmatrix} r_0 \\ r_1 \\ \vdots \\ r_{i-1} \\ r_i \\ r_{i+1} \\ \vdots \\ r_{i+M_i-2} \\ r_{i+M_i-1} \\ \vdots \\ r_{L-1} \end{bmatrix}$$

APPENDIX B
DERIVATION OF PRONY'S METHOD AND ITS VARIATIONS

This appendix derives the variations of Prony's method due to the constraints $\alpha_i=1$ (Interpolation method) and

$$\sum_{m=0}^{N} \alpha_m^2=1$$

(Eigenvalue method). Computer codes (in Fortran Language) for these methods are also included.

A. The Interpolation Method

In the interpolation method, the Prony difference equation can be written as

$$\alpha_0 r(t)+\alpha_1 r(t+T)+\cdots\alpha_{i-1} r(t+(i-1)T)+\cdots\alpha_{i+1} r(t+(i+1)T)+\cdots$$
$$+ \alpha_N r(t+NT) = - \alpha_i r(t+iT) \qquad . \qquad (76)$$

Thus the matrices A, B and C shown in Equation (13) need to be modified as

$$AB = C \qquad (77)$$

where

$$A = \begin{bmatrix} r_0 & r_1 & \cdots & r_{i-1} & r_{i+1} & \cdots & r_N \\ r_1 & r_2 & \cdots & r_{i+1} & r_{i+2} & \cdots & r_{N+1} \\ \vdots & \vdots & & \vdots & \vdots & & \vdots \\ r_{M-N} & r_{M-N+1} & \cdots & r_{M-N+i-1} & r_{M-N+i+1} & \cdots & r_M \end{bmatrix}$$

$$B = \begin{bmatrix} \alpha_0 \\ \alpha_2 \\ \cdot \\ \cdot \\ \cdot \\ \alpha_{i-1} \\ \alpha_{i+1} \\ \cdot \\ \cdot \\ \cdot \\ \alpha_N \end{bmatrix}$$

$$C = -\begin{bmatrix} r_i \\ r_{i+1} \\ \cdot \\ \cdot \\ \cdot \\ r_{M-N+i} \end{bmatrix} .$$

Equation (77) can be used to solve for the coefficients $\alpha_0, \alpha_1, \cdots \alpha_{i-1}, \alpha_{i+1}, \cdots \alpha_N$ in the interpolation method. Once the coefficients are known, we can solve for the poles and residues by following the identical procedure outlined in the Classical Method (Chapter III).

B. The Eigenvalue Method

Under the constraint

$$\sum_{m=0}^{N} \alpha_m^2 = 1 \qquad ,$$

the instantaneous error in the error-evaluation process of Prony is modified as follows

$$e(t+NT) = \sum_{m=0}^{N} \alpha_m r_M(t+mT) \quad ; \quad \sum_{m=0}^{N} \alpha_m^2 = 1 \qquad . \tag{78}$$

In matrix form, the instantaneous error can be written as

$$\begin{array}{ccc} \epsilon_1 & A & B \\ \begin{bmatrix} e(t_s+NT) \\ e(t_s+NT+T) \\ \vdots \\ e(t_s+MT-T) \end{bmatrix} = & \begin{bmatrix} r_M(t_s) & r_M(t_s+T) & \cdots & r_M(t_s+NT) \\ r_M(t_s+T) & r_M(t_s+2T) & \cdots & r_M(t_s+NT+T) \\ \vdots & & & \\ r_M(t_s+MT-NT-T) & r_M(t_s+MT-NT) & \cdots & r_M(t_s+MT-T) \end{bmatrix} & \begin{bmatrix} \alpha_0 \\ \alpha_2 \\ \vdots \\ \alpha_N \end{bmatrix} \end{array} \quad (79)$$

The total square error over the fitting interval (t_s, t_s+MT-T) is

$$\begin{aligned} \ell_1 &= \epsilon_1^T \epsilon_1 \\ &= B^T A^T A B \\ &= B^T \Phi B \end{aligned} \quad (80)$$

where ℓ_1 is the total squared error over the fitting interval. $[\ \ ]^T$ denotes the transpose operation. $\Phi \triangleq A^T A$, is the data covariance matix[53].

Solving for Matrix B by minimizing ℓ_1 under the constraint

$$\sum_{m=0}^{N} \alpha_m^2 = 1$$

is a standard eigenvalue problem. Via the eigen-analysis, the solution matrix B is the eigen-vector corresponding to the minimum eigenvalue of the covariance Matirx Φ.

Thus, Equation (80) can be used to solve for the coefficients $\alpha_0, \alpha_1 \cdots \alpha_N$. Once these coefficients are known the identical procedure outlined in the Classical Prony's method can be used to solve for the poles and residues.

Computer codes for the Prony's method and its variations are given below. The program names "SEM1" implements the Prony's method under the constraints of $\alpha_m = 1$, $m = 0, 1, 2 \cdots N$ (See Chapter III). The program "Sem2" implements the Prony's method under the constraint of

$$\sum_{m=0}^{N} \alpha_m^2 = 1 \quad .$$

Both programs are well commented and user oriented.

```
CCC ************************************************************
CCC [illegible] SINGULARITY EXPANSION [illegible]
CCC [illegible]: THIS PROGRAM EXTRACTS THE S[illegible] POLES
CCC              FROM A [illegible] WAVEFORM VIA THE
CCC              CLASSICAL PRONY'S METHOD.
CCC [illegible]:
CCC              [illegible] NO. OF POLES
CCC              [illegible] INTERVAL BETWEEN SAMPLES
CCC              [illegible] STARTING PT. OF THE FITTING
CCC                INTERVAL
CCC              [illegible] NO. OF SAMPLES USED IN THE FITTING
CCC                PROCESS
CCC OUTPUT:
CCC        1) [illegible] PARAMETERS AND THE ERRORS FOR
CCC          THE [illegible]
CCC ************************************************************
CCC
CCC 1)    INITIALIZATIONS
CCC *********************
CCC
        OPTIO[illegible]
        OPTIO[illegible]
        INCLUDE [illegible]
        INCLUDE [illegible]
        INCLUDE [illegible]
        INCLUDE [illegible]
        DIMENSION [illegible](2),IUSER(2),[illegible](256),[illegible](265)
       [illegible](256),[illegible],ALPHA[illegible](256)
       [illegible](256),[illegible](15),[illegible](15)
       [illegible],ALPHA(90),ALPOT(90),[illegible]
       [illegible](15),[illegible](15),SF(15),[illegible],CC1(15,15)
       [illegible],SF[illegible],F(256),S1
       [illegible],[illegible]OTT([illegible])
       [illegible](5)
       [illegible]
        DATA [illegible]
        [illegible]=3.[illegible]
        CALL S[illegible](1)
        CALL S[illegible](2)
        CALL S[illegible]
        CALL S[illegible]
        CALL S[illegible](5)
        CALL S[illegible]
        CALL S[illegible](7)
        CALL S[illegible]
        CALL S[illegible]
        CALL S[illegible]
        CALL [illegible]
CCC
CCC 2) INPUT
CCC ********
CCC
        [illegible]
        [illegible]
        CALL [illegible]
```

```
        WRITE(1,9001)
 9001   FORMAT(1X,'[illegible] ')
        CALL [illegible](1,1)
        I=(1,S[illegible]T,'),SHIFT,=1
        IA[illegible]=1
        IA[illegible]
        IF(1.SHIFT.=16.[illegible].SHIFT.=16)GO TO [illegible]
        IA[illegible]=1
        IF(1.SHIFT.=16.[illegible].SHIFT.=16)GO TO 90[illegible]
        WRITE(1,9012)
 9012   FORMAT(1X,'?')
        GO TO [illegible]
 9014   [illegible]=1.
        WRITE(1,505)
 505    FORMAT('[illegible],IFILT=')
        READ([illegible]) I[illegible],IFILT
        CALL [illegible]
        [illegible]=40
        KK1=17
        DO 9004 [illegible]=1,[illegible]
        IF([illegible]) GOTO 250
        IF([illegible]) GOTO 250
        IF([illegible].5) GOTO 250
        IF([illegible].15) GOTO 259
        IF([illegible].32) GOTO 259
        IF([illegible].59) GOTO 259
        IF([illegible].44) GOTO 259
        DO 9005 III=1,I[illegible]
        IF([illegible].1) GOTO 9995
        IA[illegible]=0
        IF(II[illegible].2) IA[illegible]=1
 9995   [illegible]=1.
        CALL [illegible](I[illegible],0,IFILE,IUSER,I[illegible],IFUP)
        [illegible]=[illegible]
        IF([illegible].1) GOTO 590
        [illegible]=0.0
        [illegible]=1.0
CCC
CCC   1) PREPROCESSING
CCC   ****************
CCC
CCC   3-1) [illegible] AMPLITUDE OFFSET
CCC   ******************************
CCC
        DO 21 KK=1,KK1
        DO 211 I=1,3
        IAK=KK+I-1
 2110   XSH(I)=T[illegible](IKK)
        IF(XSH(2).LT.XSH(1).[illegible].XSH(2).LT.XSH(3)) GOTO 21
        IF(XSH(2)-XSHTH) 21,2112,2112
 21     CONTINUE
 2112   [illegible]=KK-1
        DO 22 [illegible]=1,256
 22     [illegible]=[illegible]
        DO 23 [illegible]=1,[illegible]
```

```
25     TWF(KK)=0.0
       DO 24 KK=JJ,256
       TWF(KK)=W(JJ)
24     JJ=JJ+1
       IF(III.NE.1) GOTO 9006
       DO 9007 JJ=1,256
9007   TWFO(JJ)=TWF(JJ)
9006   CONTINUE
CCC
CCC 4-2) 90-DEGREE DIFFERENCE
CCC ************************
CCC
       DO 29 I=1,256
29     TWF(I)=(TWFO(I)-TWF(I))/2.
999    FN=1.
       YOFF=0.0
       DO 27 I=1,10
27     YOFF=YOFF+TWF(I)/10.
       DO 28 I=1,256
28     TWF(I)=TWF(I)-YOFF
CCC
CCC 4-3) FILTERING
CCC **************
CCC
       IF(IFILT.EQ.0) GOTO 1999
       DO 30 I=1,256
30     FTWF(I)=CMPLX(TWF(I),0.0)
       NN1=1
       NN2=1
       NN3=128
       NN4=128
       CALL FFT(FTWF,8,S,-1,IFRR)
       DO 35 I=1,128
35     FTWF(I)=(1./([illegible]-1.))*(I-1)*FTWF(I)
       FTWF(129)=CMPLX(0.0,0.0)
       DO 40 I=1,127
       II=I+1
       J=257-I
40     FTWF(J)=CONJG(FTWF(II))
       CALL FFT(FTWF,8,S,1,IFRR)
       DO 455 I=1,256
455    TWF(I)=REAL(FTWF(I))
1999   DO 1998 I=1,256
1998   FM(I)=TWF(I)
       FMAX=-1.E10
CCC
CCC 4-4) PEAK DETECTION
CCC ********************
CCC
       T=0./256.
       DO 9100 I=1,256
       IF(ABS(FM(I)).GT.FMAX) IFU=I
       IF(ABS(FM(I)).GT.FMAX) FMAX=ABS(FM(I))
9100   CONTINUE
CCC
```

```
CCC 4) FURTHER INITIALIZATIONS
CCC ***************************
CCC
      MEND=ITO+100
      T=0.7255.
      MEND1=MEND+1
      DO 8101 I=1,N
      ERROR(I)=0.0
8101  ERRORM(I)=1.E10
      WRITE(2,8000) (F(I),I=1,256)
8000  FORMAT(5F10.3)
      IF(IMB.GT.0) GOTO 8200
      WRITE(2,8300) IFILE,IUSER,ITO,MEND,IMODE,IFILT,NH1,NH2,NH3,
     &NH4
8300  FORMAT(////,2A3,' ',' ',2X,2A5,5X,'ITO=',I5,3X,'MEND=',I4
     &,3X,'IMODE=',I5,3X,'IFILT=',I5,3X,'NH=',4I4)
      GOTO 8100
8200  WRITE(2,8400) IFILE,IUSER,ITO,MEND,IMODE,IFILT,NH1,NH2,NH3,
     &NH4
8400  FORMAT(////,2A3,'B',2X,2A5,5X,'ITO=',I5,3X,
     &'MEND=',I4,3X,'IMODE=',I5,3X,'IFILT=',I5,3X,'NH=',4I4)
8100  PR=1.
      NROOTS=6
      NROOTE=14
      IBSS=4
      IBSE=10
      IIIS=1
      IIIE=9
      NMS=2
      NME=4
      WRITE(2,8102) NROOTS,NROOTE,IBSS,IBSE,IIIS,
     &IIIE,NMS,NME
8102  FORMAT(/,'RANGE OF PARAMETERS',2X,'N=',2I4,
     &3X,'IB=',2I4,3X,'ITS=',2I4,3X,'N OF SAMPLES=',2I4)
CCC
CCC 5) SETTING THE ITH COEFFICIENT=1
CCC ********************************
CCC
      DO 8102 IROOT=1,NROOT1
      WRITE(2,8105) IROOT
8105  FORMAT(////////,I5,'TH COEFFICIENT=1')
      DO 808 I=1,N
808   ERRORM(I)=1.E10
CCC
CCC 6) VARY THE 4 PARAMETERS
CCC ************************
CCC
      DO 45 NROOT=NROOTS,NROOTE
      NROOT1=NROOT+1
      IF(IROOT1.LT.IROOT) GOTO 45
      DO 45 III=IIIS,IIIE
      DO 45 NM=NMS,NME
      DO 45 IBS=IBSS,IBSE
      NROOT3=NROOT1-IROOT1
      NROOT2=NROOT1-NROOT1
```

```
CCC
CCC 7) SOLVE FOR THE ALPHAS
CCC ************************
CCC
      KK=   ITE+(III-1)*1
      KK=KK+(NROOT-1)*IBS
      IF(KK.GT.NM) GOTO 45
      DO 50 II=1,NROOT2
      III=KK+(NROOT+II-2)*IBS
      A1(II)=-R(III)
      DO 50 I=1,NROOT1
      JJ=1
      IF(I.EQ.IROOT) GOTO 50
      IF(I.GT.IROOT) JJ=I-1
      JJJ=KK+(II+I-2)*IBS
      A1(II,JJ)=R(JJJ)
 50   CONTINUE
      CALL MATRA(A,A1,M1,NROOT2,NROOT,A11,0.9,.15)
      EPS=1.E-2
      CALL GELG(R,A,NROOT,1,EPS,IER)
CCC
CCC 8)  SOLVE FOR XI: SI=(1/T)*LN(YI)=FCU
CCC *************************************
CCC
      DO 55 I=1,NROOT1
      JJ=1
      IF(I.EQ.IROOT) GOTO 55
      IF(I.GT.IROOT) JJ=I-1
      ALPHA(I)=CMPLX(R(JJ),0.0)
 55   CONTINUE
      ALPHA(IROOT)=CMPLX(1.,0.0)
      ALPHA1=0.
      DO 300 I=1,NROOT1
      ALPHA1=ALPHA1+(ABS(REAL(ALPHA(I))))**2
 300  CONTINUE
      ALPHA1=SQRT(ALPHA1)
      DO 305 I=1,NROOT1
      ALPHA(I)=ALPHA(I)/ALPHA1
 305  RALPHA(I)=REAL(ALPHA(I))
      ALPHA2=-1.E10
      DO 306 I=1,NROOT1
      IF(ABS(RALPHA(I)).LT.ALPHA2) GOTO 306
      MALPHA=I
      ALPHA2=ABS(RALPHA(I))
 306  CONTINUE
      FRSUM=0.0
      FLSUM=0.0
      FROU2(I)=0.0
      ISAMPL=NPL-LROOT*IBS
      DO 310 I=KK,NROW
      FR=0.0
      IF(I.GT.ISAMPL) GOTO 312
      DO 311 II=1,NROOT1
      II0=KK+(II-1)*IBS
 311  FR=FR+RALPHA(II)*RX(IIJ)
```

```
      E[illegible]OR(I)=E[illegible]OR(I)+ERR**2
  312 F[illegible]SUM=F[illegible]SUM+F[illegible](I)**2
      FCSUM=FCSUM+F[illegible](I)**2-2.*F[illegible](I)*ERR+ERR**2
  310 CONTINUE
      ERROR([illegible])=ERR[illegible](1)/SQRT(FMSUM*FCSUM)
      ERROR([illegible])=ERROR(1)/FMSUM
      ERROR([illegible])=ERROR(1)/(FMSUM+FCSUM)
      ERROR([illegible])=ERROR(1)/(NSAMPL-NRR+1)
      CALL MULLER(NROOT,NROOT1,1,1.E-10,400,ALPHA,X,NTOL,IFLAG)
CCC
CCC 9) SOLVE FOR THE POLES
CCC ********************
CCC
      DO 65 I=1,NROOT
      S(I)=(1./(I[illegible]*T))*CLOG(X(I))
   65 CONTINUE
CCC
CCC 10) SOLVE FOR THE RESIDUES
CCC ************************
CCC
      DO 75 I=1,NROOT2
      K=NRR+(I-1)*INC
      ALPHA(I)=CMPLX(FM(K),0.0)
      DO 75 II=1,NROOT
      CC(I,II)=X(II)**(I-1)
   75 CONTINUE
      CALL C[illegible](CC1,CC,ALPHA,NROOT2,NROOT,CCT,UD,.9E-15)
      CALL C[illegible](CC1,RL,NROOT,RS)
CCC
CCC 11) CALCULATE THE TOTAL SQUARE ERROR
CCC ************************************
CCC
      ERR1=0.0
      FMSUM=0.0
      FCSUM=0.0
      DO 95 I=[illegible]
      II=[illegible]
      FC=0.0
      DO 100 J=1,NROOT
  100 FC=FC+REAL(RL(J)*CEXP(II*T*S(J)))
      FMSUM=FMSUM+FM(I)**2
      FCSUM=FCSUM+FC**2
   95 ERR1=ERR1+(FM(I)-FC)**2
      ERROR(6)=ERR1/(FMSUM+FCSUM)
      ERROR(7)=ERR1/FMSUM
      ERROR([illegible])=ERR1/SQRT(FMSUM*FCSUM)
      ERROR(5)=ERR1/(NSAMPL-NRR+1)
      DO 76 I=1,8
      IF(ERROR(I).GT.ERRORM(I)) GOTO 76
      ERRORM(I)=ERROR(I)
      NROOTM(I)=NROOT
      I[illegible](I)=I[illegible]
      IIT[illegible](I)=II
      [illegible](I)=[illegible]
      INROT1(I)=[illegible]
```

```
      DO 77 II=1,NROOT
      Z=(1.0-(S(II))/(2.0*PI))
      C=REAL(S(II))
      SP(II,I)=CMPLX(C,Z)*1.E0
77    COM(II,I)=RO(II)
      ALPHOR=0.
      DO 778 II=1,NROOT
      ALPHOR=ALPHOR+ALPHA(II)**2
778   ALPHA2(II,I)=ALPHA(II)
      ALPHOR(I)=ALPHOR
76    CONTINUE
65    CONTINUE
CCC
CCC OUTPUTS FOR THE MINIMUM ERROR CASE
CCC ***********************************
CCC
      DO 70 I=1,P
      WRITE(2,79)
79    FORMAT(/////)
      WRITE(2,80) I,ERROR(I),TROOTI(I)
80    FORMAT(/,'MIN ERROR CASE',I3,5X,'MIN ERROR='
     &,E15.7,5X,'NO. OF COEFF=',I)
      WRITE(2,81) NROOT(I),IOSC(I),ITN(I),NS(I),ENERGY(I)
81    FORMAT(/,'N=',I5,5,'IOS=',I7,5X,'ITS=',I4,2X
     &,'NO OF SAMPLES USED=',I3,5X,'FILTER ENERGY=',E15.7)
      WRITE(2,85)
85    FORMAT(2X,'POLE(REAL)',11X,'POLE(IMAG)',11X,
     &'RESIDUE(REAL)',11X,'RESIDUE(IMAG)')
      NR=NROOT(I)
      NR1=NR+1
      DO 83 II=1,NR
83    WRITE(2,84) SP(II,I),COM(II,I)
84    FORMAT(E15.7,5X,E15.7,6X,E15.7,7X,E15.7)
      WRITE(2,86)
86    FORMAT('0',5X,'COEFFICIENTS:')
      WRITE(2,82) (ALPHA2(II,I),II=1,NR1)
82    FORMAT(   E20.7)
70    CONTINUE
6172  CONTINUE
      CLOSE 2
257   IN=(15+4)/2
      IF(IN.EQ.0) GOTO 258
      IN=1
      GOTO 9003
258   IN=2
      CALL IOFIL(IFILE,IUSE)
9003  CONTINUE
      CALL EXIT
      END
```

```
CCC
CCC SUBROUTINES FOR THE PROGRAM SEMI
CCC ************************************
CCC
      OPTIONS ...
      SUBROUTINE GELG(R,A,M,N,EPS,IER)
      DIMENSION A(1),R(1)
      IF(M)23,23,1
C
C     SEARCH FOR GREATEST ELEMENT IN MATRIX A
    1 IER=0
      PIV=0.
      MM=M*M
      NM=N*M
      DO 3 L=1,MM
      TB=ABS(A(L))
      IF(TB-PIV)3,3,2
    2 PIV=TB
      I=L
    3 CONTINUE
      TOL=EPS*PIV
C
C     A(I) IS PIVOT ELEMENT. PIV CONTAINS THE ABSOLUTE VALUE OF A(I).
C
C     START ELIMINATION LOOP
      LST=1
      DO 17 K=1,M
C
C     TEST ON SINGULARITY
      IF(PIV)23,23,4
    4 IF(IER)7,5,7
    5 IF(PIV-TOL)6,6,7
    6 IER=K-1
    7 PIVI=1./A(I)
      J=(I-1)/M
      I=I-J*M-K
      J=J+1-K
C     I+K IS ROW-INDEX, J+K COLUMN INDEX OF PIVOT ELEMENT
C
C     PIVOT ROW REDUCTION AND ROW INTERCHANGE IN RIGHT HAND SIDE R
      DO 8 L=K,NM,M
      LL=L+I
      TB=PIVI*R(LL)
      R(LL)=R(L)
    8 R(L)=TB
C
C     IS ELIMINATION TERMINATED
      IF(K-M)9,18,18
C
C     COLUMN INTERCHANGE IN MATRIX A
    9 LEND=LST+M-K
      IF(J)12,12,10
   10 II=J*M
      DO 11 L=LST,LEND
   11 TB=A(L)
```

```
      LL=L+II
      A(L)=A(LL)
   11 A(LL)=PIV
C
C     ROW INTERCHANGE AND PIVOT ROW REDUCTION IN MATRIX A
   12 DO 13 L=LST,LEND,M
      LL=L+I
      TB=PIVI*A(LL)
      A(LL)=A(L)
   13 A(L)=TB
C
C     SAVE COLUMN INTERCHANGE INFORMATION
      A(LST)=FLOAT(J)
C
C     ELEMENT REDUCTION AND NEXT PIVOT SEARCH
      PIV=0.
      LST=LST+1
      J=0
      DO 16 II=LST,LEND
      PIVI=-A(II)
      IST=II+M
      J=J+1
      DO 15 L=IST,MM,M
      LL=L-J
      A(L)=A(L)+PIVI*A(LL)
      TB=ABS(A(L))
      IF(TB-PIV)15,15,14
   14 PIV=TB
      I=L
   15 CONTINUE
      DO 16 L=K,NM,M
      LL=L+J
   16 R(LL)=R(LL)+PIVI*R(L)
   17 LST=LST+M
C     END OF ELIMINATION LOOP
C
C     BACK SUBSTITUTION AND BACK INTERCHANGE
   18 IF(M-1)23,22,19
   19 IST=MM+M
      LST=M+1
      DO 21 I=2,M
      II=LST-I
      IST=IST-LST
      L=IST-M
      L=IFIX(A(L)+0.5)
      DO 21 J=II,NM,M
      TB=R(J)
      LL=J
      DO 20 K=IST,MM,M
      LL=LL+1
   20 TB=TB-A(K)*R(LL)
      K=J+L
      R(J)=R(K)
   21 R(K)=TB
   22 RETURN
```

```
C
C     ERROR RETURN
   29 IER=1
      RETURN
      END
      SUBROUTINE CSIMQ(A,B,N,KS)
C     CSIMQ IS A VERSION OF THE SSP SUBROUTINE SIMQ FOR COMPLEX NUMBERS
      COMPLEX A(1),B(1),SAVE,BIGA
C
C     FORWARD SOLUTION
C
      TOL=0.0
      KS=0
      JJ=-N
      DO 65 J=1,N
      JY=J+1
      JJ=JJ+N+1
      BIGA=(0.0,0.0)
      IT=JJ-J
      DO 30 I=J,N
C
C     SEARCH FOR MAXIMUM COEFFICIENT IN COLUMN
C
      IJ=IT+I
      IF(CABS(BIGA)-CABS(A(IJ)))20,30,30
   20 BIGA=A(IJ)
      IMAX=I
   30 CONTINUE
C
C     TEST FOR PIVOT LESS THAN TOLERANCE (SINGULAR MATRIX)
C
      IF(CABS(BIGA)-TOL)35,35,40
   35 KS=1
      RETURN
C
C     INTERCHANGE ROWS IF NECESSARY
C
   40 I1=J+N*(J-2)
      IT=IMAX-J
      DO 50 K=J,N
      I1=I1+N
      I2=I1+IT
      SAVE=A(I1)
      A(I1)=A(I2)
      A(I2)=SAVE
C
C     DIVIDE EQUATION BY LEADING COEFFICIENT
C
   50 A(I1)=A(I1)/BIGA
      SAVE=B(IMAX)
      B(IMAX)=B(J)
      B(J)=SAVE/BIGA
C
C     ELIMINATE NEXT VARIABLE
C
```

```
      IF(J-1)55,70,55
   55 IW=N*(J-1)
      DO65IX=J,N
      IXJ=IW+IX
      IJ=J-1
      DO60JX=JY,N
      IXJX=N*(JX-1)+IX
      JJX=IXJX+IJ
   60 A(IXJX)=A(IXJX)-(A(IXJ)*A(JJX))
   65 B(IX)=B(IX)-(B(J)*A(IXJ))
C
C     BACK SOLUTION
C
   70 NY=N-1
      IT=N*N
      DO80J=1,NY
      IA=IT-J
      IB=N-J
      IC=N
      DO80K=1,J
      B(IB)=B(IB)-A(IA)*B(IC)
      IA=IA-N
   80 IC=IC-1
      RETURN
      END
      SUBROUTINE MATRA(B,C,S,NROOT2,NROOT,CTEMP,SS,M,N)
      DIMENSION C(N,M),S(N),CTEMP(M,N),SS(NROOT),B(NROOT,NROOT)
      DO 500 I=1,NROOT2
      DO 500 J=1,NROOT
  500 CTEMP(J,I)=C(I,J)
      DO 505 L=1,NROOT
C     MULTIPLY THE TWO MATRICES
      DO 505 I=1,NROOT
      B(L,I)=0.
      DO 505 J=1,NROOT2
  505 B(L,I)=CTEMP(L,J)*C(J,I)+B(L,I)
      DO 510 I=1,NROOT
      SS(I)=0.
      DO 510 J=1,NROOT2
  510 SS(I)=CTEMP(I,J)*S(J)+SS(I)
      RETURN
      END
      SUBROUTINE CMATRA(FT,CFT,CS,NROOT2,NROOT,TCFT,S,M,N)
      COMPLEX CFT(N,M),CS(N),TCFT(M,N),S(NROOT),FT(NROOT,NROOT)
      DO 600 I=1,NROOT2
      DO 600 J=1,NROOT
  600 TCFT(J,I)=CFT(I,J)
      DO 605 L=1,NROOT
      DO 605 I=1,NROOT
      FT(L,I)=(0.,0.)
      DO 605 J=1,NROOT2
  605 FT(L,I)=TCFT(L,J)*CFT(J,I)+FT(L,I)
      DO 610 I=1,NROOT
      S(I)=(0.,0.)
      DO 610 J=1,NROOT2
```

```
  610 S(I)=R*E(I+1)*L(I+J)+S(I)
      RETURN
      END
      SUBROUTINE MULLER (NL,M,TOL,ITER,RT,ROUT,RTOL,IFLAG)
      COMPLEX RT(1),ROUT(NL)
      COMPLEX Z,Z1,Z2,Z3,FZ1,FZ2,FZ3,Z32,Z21,L1,D1,C1,G1,LN,LD,LDPOS
      COMPLEX LDNEG,LDMAX,L,ZO,FZ,SAVE
      DIMENSION RTOL(NL)
      [illegible]=1
      IFLAG=0
      DO 4 I=1,M
    4 ROUT(I)=RT(I)
      DO 51 NRT=1,M
      IF(CABS(RT(NRT)).NE.0.)GO TO 2
      Z=(0.,0.)
      RTOL(NRT)=0.
      GO TO 14
    2 CONTINUE
      KOUNT=0
      Z1=CMPLX(-1.,0.)
      Z3=(0.,0.)
      Z2=(1.,0.)
      FZ3=RT(NRT)
      FZ2=RT(NRT)+RT(NRT+1)+RT(NRT+2)
      FZ1=RT(NRT)-RT(NRT+1)+RT(NRT+2)
    1 DO 52 I=1,ITER
      Z32=Z3-Z2
      Z21=Z2-Z1
      L1=Z32/Z21
      D1=1.+L1
      C1=L1*(L1*FZ1-D1*FZ2+FZ3)
      G1=C1+D1*(FZ3-FZ2)
      LN=-2.*D1*FZ3
      LD=CSQRT(G1**2+2*LN*C1)
      LDPOS=G1+LD
      LDNEG=G1-LD
      LDMAX=LDPOS
      IF(CABS(LDNEG).GT.CABS(LDPOS))LDMAX=LDNEG
      IF(CABS(LDMAX).EQ.0.0)LDMAX=(1.,0.)
      L=LN/LDMAX
    7 Z=Z3+Z32*L
      ZO=Z
      IF(CABS(Z).EQ.0.)ZO=Z3
      RTOL(NRT)=CABS(Z-Z3)/CABS(ZO)
      IF(RTOL(NRT).LT.TOL)GO TO 13
      IF(I.EQ.1)GO TO 19
      IF(RTOL(NRT).LT.RTOL2)GO TO 19
      KOUNT=KOUNT+1
      IF(KOUNT.LE.20)GO TO 19
      IFLAG=NRT
      GO TO 30
   19 RTOL2=RTOL(NRT)
      FZ=RT(NRT)
      IF(CABS(Z).EQ.0.0)GO TO 10
      FZ=RT(1)
```

```
      DO 53 J=M,ITEM
      LL=NN+J
   53 F2=RT(LL)+F *Z2
   16 CONTINUE
      IF(CABS(F2).LT.(1E.*CABS(F23)))GO TO 12
      I=I+G.
      GO TO 7
   12 Z1=Z2
      Z2=Z3
      Z3=Z
      F21=F22
      F22=F23
   52 F23=F2
      IFLAG= 01
   30 DO 60 I=N,ITEMP
   60 RT(I)= OUT(I)
      ROOT(J,I)=Z
      RETURN
   14 DO 54 I=M,ITEM
      LL=NN+IN
      JJ= N+I+NT
   54 RT(LL)=RT(LL)+RT(JJ)*Z
   14 RT(NP)=RCOL(R1)
      ROOT(  I)=.
   51 CONTINUE
      SAVE=ROOT(J)
      ROOT(  )=-(RT(NP))/RT( )
      RT(NP)=SAVE
      ROOL(  )=0.0
      RETURN
      END
```

```
CCC *****************************************************
CCC PROGRAM: (NEW SEM (SINGULARITY EXPANSION BY PRONY)
CCC DESCRIPTION: THIS PROGRAM EXTRACTS THE SEM POLES
CCC                 FROM A TIME DOMAIN WAVEFORM VIA THE
CCC                 EIGENVALUE METHOD.
CCC REQUIRES:
CCC               1)VARIES NUM OF POLES
CCC               2)VARIES INS=INTERVAL BETWEEN SAMPLES
CCC               3)VARIES NRRESTARTING PT. OF THE FITTING
CCC                 INTERVAL
CCC               4)VARIES NUM OF SAMPLES USED IN THE FITTING
CCC                 PROCESS
CCC OUTPUT:
CCC          1)POLES,RESIDUES,PARAMETERS AND ERRORS FOR THE
CCC            [illegible] CASES
CCC *****************************************************
CCC
CCC 1)    INITIALIZATIONS
CCC *********************
CCC
         OPTIONS S,P
         OPTION LP
         INCLUDE SOL 2[illegible]
         INCLUDE FCNTH,LIC[illegible]
         INCLUDE [illegible]
         INCLUDE FLS [illegible]
         DIMENSION IFI[illegible](2),IUSER(2),TH[illegible](2),TWF(256),AA(225)
        &,[illegible](256),S(54),ALPHA(16,8),EIG[illegible],A11(256)
         DIMENSION [illegible](256),[illegible]15,15),[illegible](15,90),[illegible](15)
        &,[illegible](15),ALPHA(15),ALP[illegible](90),[illegible]
         COMPLEX ALPHA(90),Y(15),S(15),GF(15),C(9,25),CC1(15,15)
        &,[illegible](15),SPA(25,8),[illegible](15,8),FTWF(256),S1
         DIMENSION [illegible](6),[illegible]NORM(5),[illegible]TM(8),IRSM(8)
        &,[illegible]
         COMMON/[illegible],A1,A,A1T,[illegible]
         DATA [illegible]       /,IA,IB/1HA,1HB/
         PI=3.141592
         CALL SUPERH(1)
         CALL SUPERH(2)
         CALL SUPERH(3)
         CALL SUPERH(4)
         CALL SUPERH(5)
         CALL SUPERH(6)
         CALL SUPERH(7)
         CALL SUPERH(12)
         CALL SUPERH(13)
         CALL SUPERH(14)
         CALL ASSIGN([illegible],0,0,2)
CCC
CCC 2) INPUT
CCC ********
CCC
         WRITE(1,5)
      5  FORMAT(/1X,'[illegible] INPUT')
  [illegible] CALL [illegible](IFILE,IUSER)
```

```
      WRITE(6,9001)
 9001 FORMAT(1X,'[illegible]')
      CALL [illegible]
      IF(I.S[illegible]).SHIFT=1
      [illegible]=1
      I[illegible]=
      IF(I.SHIFT.[illegible].SHIFT.[illegible]) GO TO 9006
      I[illegible]=1
      IF(I.SHIFT.[illegible].SHIFT.[illegible]6) GO TO 9006
      WRITE(6,9002)
 9002 FORMAT(1X,'?')
      GO TO [illegible]
 9006 [illegible]=1.
      WRITE(6,505)
  505 FORMAT('[illegible]FILE=')
      READ(5,*) [illegible]
      CALL [illegible]
      [illegible]
      [illegible]=17
      XSHT[illegible]
      DO 500 [illegible]
      IF([illegible]) [illegible]
      DO 99[illegible] III=1,[illegible]
      IF([illegible]) GO TO [illegible]
      IAM=0
      IF(III.[illegible]) IAM=1
 999A [illegible]=1.
      CALL [illegible](I,[illegible],IFILE,IUSER,I[illegible],IERR)
      XSHT=[illegible]
      IF(I[illegible]) GO TO 999
      [illegible]
CCC
CCC A) PREPROCESSING
CCC ***************
CCC
CCC A-1) TIME AND AMPLITUDE OFFSET
CCC ****************************
CCC
      DO 21 [illegible]
      DO 211[illegible] I=1,3
      [illegible]
 2110 XSH(I)=T[illegible]
      IF(XSH(2).[illegible].XSH(1).OR.XSH(2).LT.XSH(3)) GOTO 21
      IF(XSH(2)-XSHT[illegible]) 21,2112,2112
   21 CONTINUE
 2112 JJ=I[illegible]-1
      DO 22 [illegible]
   22 [illegible]
      DO 23 [illegible]
   23 T[illegible](KK)=0.0
      DO 2[illegible]
      T[illegible](KK)=[illegible]
   24 JJ=JJ+1
      IF([illegible]) [illegible]
      DO 99[illegible] JJ=1,[illegible]
```

```
9097  TWFU(JJ)=TWF(JJ)
9096  CONTINUE
CCC
CCC 4-2) [illegible] DIFFERENCE
CCC ************************
CCC
      DO 29 I=1,256
29    TWF(I)=(TWFU(I)-TWF(I))/2.
999   RN=1.
CCC
CCC 3-2) FILTERING
CCC **************
CCC
      IF(IFILT.NE.1) GOTO 1999
      DO 30 I=1,256
30    FTWF(I)=CMPLX(TWF(I),0.0)
      M1=1
      M2=11
      M4=128
      M5=12
      CALL FORT(FTWF,M,SS,-1,IERR)
      DO 35 I=1,MM2
35    FTWF(I)=(1./(MM2-1.))*(I-1)*FTWF(I)
      FTWF(129)=CMPLX(0.0,0.0)
      DO 40 I=1,127
      II=I+1
      J=257-I
40    FTWF(J)=CONJG(FTWF(II))
      CALL FORT(FTWF,M,S,1,IERR)
      DO 455 I=1,256
455   TWF(I)=REAL(FTWF(I))
1999  DO 1998 I=1,256
      FM(I)=TWF(I)+1.E-10
      IF(I.GT.128) FM(I)=(TWF(I)+1.E-9)*0.1
1998  CONTINUE
      FMAX=-1.E10
CCC
CCC 3-4) PEAK DETECTION
CCC ********************
CCC
      DO 9100 I=1,128
      IF(ABS(FM(I)).GT.FMAX) ITU=I
      IF(ABS(FM(I)).GT.FMAX) FMAX=ABS(FM(I))
      IF(ABS(FM(I)).GT.0.1) NEMU=I
9100  CONTINUE
CCC
CCC 4) FURTHER INITIALIZATIONS
CCC ***************************
CCC
      NEMU=256
      T=50./256.
      NEMU1=NEMU+1
      DO 9111 I=1,6
      FMOOR(I)=1.0
9111  FMOOR(I)=1.E10
```

```
      WRITE(6,6000) (HEAD(I),I=1,20)
 6000 FORMAT(1X,[illegible])
      IF(IY.EQ.1) GOTO 6200
      WRITE(6,6300) IFILE,IUSER,ITMO,IDAY,IYEAR,IFILT,NH1,NH2,NH3,
     *NH4
 6300 FORMAT(////,1X,'A',2X,2A4,5X,'ITMO=',I4,5X,'FILE=',I4
     *,5X,'HOUR=',I3,3X,'IFILT=',I3,3X,'NH=',4I4)
      GOTO 6100
 6200 WRITE(6,6400) IFILE,IUSER,ITMO,IDAY,IYEAR,IFILT,NH1,NH2,NH3,
     *NH4
 6400 FORMAT(////,1X,2A4,2X,2A4,5X,'ITMO=',I5,5X,
     *'[illegible]',I3,3X,'HOUR=',I3,3X,'IFILT=',I3,3X,'NH=',4I4)
 6100 NN=1
      NROOTS=4
      NROOTE=16
      IBSS=4
      IBSE=8
      IITS=1
      IITE=5
      NS=2
      NE=5
      WRITE(6,6101) NROOTS,NROOTE,IBSS,IBSE,IITS,
     *IITE,NS,NE
 6101 FORMAT(//,'RANGE OF PARAMETERS',2X,'N=',2I4,
     *2X,'IB =',2I4,3X,'IITS=',2I4,3X,'# OF SAMPLES=',2I4)
CCC
CCC 4) VARY THE 4 PARAMETERS
CCC ************************
CCC
      DO 45 NROOT=NROOTS,NROOTE
      NROOT1=NROOT+1
      DO 45 III=IITS,IITE
      DO 45 [illegible]
      DO 45 IBS=IBSS,IBSE
      [illegible]
      NROOT2=[illegible]-NROOT1
CCC
CCC 5) SOLVE FOR THE ALPHAS
CCC ***********************
CCC
      [illegible]
      [illegible]
      IF([illegible]) GOTO 45
      DO 50 II=1,NROOT2
      DO 50 I=1,NROOT1
      JJJ=[illegible]
      A1(II,I)=[illegible](JJJ)
   50 CONTINUE
      DO 2122 I=1,NROOT1
      DO 2122 J=1,NROOT1
      A(I,J)=0.
      DO 2122 K=1,NROOT2
 2124 A(I,J)=A(I,J)+A1(K,I)*A1(K,J)[illegible]
 2122 CONTINUE
      [illegible]=1.0E-1
```

```
      II=0
      DO 211 J=1,NROOT1
      DO 211 I=1,N
      II=II+1
  211 AA(II)=A(I,J)
      CALL EIGEN(AA,AAI,NROOT1,0)
      NN=(NROOT1*(NROOT1+1))/2
      EIGENM=AA(NN)
      DO 52 I=1,NROOT1
      NN=NROOT1*NROOT1+I
   52 W(I)=AAI(NN)
CCC
CCC A)  SOLVE FOR XI: SI=(1/T)*LN(XI)=POLE
CCC ***************************************
CCC
      DO 55 I=1,NROOT1
      ALPHA(I)=CMPLX(W(I),0.0)
   55 CONTINUE
      ALPHA1=0.0
      DO 300 I=1,NROOT1
  300 ALPHA1=ALPHA1+(ABS(REAL(ALPHA(I))))**2
      ALPHA1=SQRT(ALPHA1)
      DO 303 I=1,NROOT1
      ALPHA(I)=ALPHA(I)/ALPHA1
  303 RALPHA(I)=REAL(ALPHA(I))
      ALPHA2=-1.E10
      DO 301 I=1,NROOT1
      IF(ABS(RALPHA(I)).LT.ALPHA2) GOTO 301
      NALPHA=I
      ALPHA2=ABS(RALPHA(I))
  301 CONTINUE
      EMSUM=0.0
      ECSUM=0.0
      ERROR(1)=0.0
      NSAMPL=NEND-NROOT*IHS
      DO 310 I=NFFF,NEND
      ERR=0.0
      IF(I.GT.NSAMPL) GOTO 312
      DO 311 II=1,NROOT1
      IITU=I+(II-1)*IHS
  311 ERR=ERR+RALPHA(II)*EM(IITU)
      ERROR(1)=ERROR(1)+ERR**2
  312 EMSUM=EMSUM+EM(I)**2
      ECSUM=ECSUM+EM(I)**2-2.*EM(I)*ERR+ERR**2
  310 CONTINUE
      ERROR(2)=ERROR(1)/SQRT(EMSUM*ECSUM)
      ERROR(3)=ERROR(1)/EMSUM
      ERROR(4)=ERROR(1)/(EMSUM+ECSUM)
      ERROR(1)=ERROR(1)/(NSAMPL-NRV+1)
      CALL MULLER(NROOT,NROOT1,1,E-10,400,ALPHA,X,ATOL,IFLAG)
CCC
CCC B) SOLVE FOR THE POLES
CCC **********************
CCC
      DO 60 I=1,NROOT
```

```
          [illegible]
   85     CONTINUE
CCC
CCC (1) SOLVE FOR THE RESIDUES
CCC ************************
CCC
          DO 75 I=1,[illegible]
          [illegible]
          ALPHA(I)=CMPLX([illegible],0.0)
          DO 75 II=1,NROOT
          CC(I,II)=[illegible]**(I-1)
   75     CONTINUE
          CALL [illegible](CC1,CC,ALPHA,[illegible],NROOT,CCT,CD,[illegible])
          CALL [illegible](CC1,[illegible],NROOT,RS)
CCC
CCC (2) CALCULATE THE TOTAL SQUARE ERROR
CCC ********************************
CCC
          [illegible]=0.0
          [illegible]=0.0
          FCSUM=0.0
          DO 95 I=[illegible]
          II=I-[illegible]
          FC=0.0
          DO 100 J=1,NROOT
  100     FC=FC+[illegible](CD(J)*CEXP(II*[illegible]*S(J)))
          [illegible]**2
          [illegible]=[illegible]+FC**2
   95     [illegible]+(Y(I)-FC)**2
          [illegible]=[illegible]/(FCSUM*FCSUM)
          [illegible]
          [illegible]
          [illegible]
          DO 76 I=1,[illegible]
          IF([illegible]) GOTO 76
          [illegible]
          [illegible]=NROOT
          [illegible]
          [illegible]=III
          [illegible]
          [illegible]
          DO 77 II=1,NROOT
          [illegible]
          [illegible]
          [illegible]
   77     [illegible]
          DO 76 II=[illegible]
          ALPHA[illegible]=ALPHA(II)
   76     CONTINUE
   85     CONTINUE
CCC
CCC (3) [illegible] FOR THE [illegible]
CCC ************************************
CCC
          DO 78 I=1,[illegible]
```

```
      WRITE(6,79)
79    FORMAT(/////)
      WRITE(6,80) I,EIGM(I),ERROR(I)
80    FORMAT(/,' ERROR CASE',I3,5X,'MIN EIGENVALUE= ',F15.7
     &,5X,'MIN ERROR=',E15.7)
      WRITE(6,81) NPOLE(I),NSM(I),ITR(I),NS(I),ALPHA1
81    FORMAT(/,'N=',I3,5X,'NS=',I3,5X,'ITS=',I3,5X
     &,'NO OF SAMPLES USED=',I3,5X,'FILTER ENERGY=',E15.7)
      WRITE(6,85)
85    FORMAT(6X,'POLE(REAL)',11X,'POLE(IMAG)',11X,
     &'RESID(REAL)',11X,'RESID(IMAG)')
      NN=NROOTS(I)
      ...=NN...
      DO 83 II=1,NN
83    WRITE(6,84) SEM(II,1),...(II,I)
84    FORMAT(E15.7,5X,E15.7,6X,E15.7,7X,E15.7)
      WRITE(6,...)
838   FORMAT('COEFFICIENTS:')
70    WRITE(6,82) (ALPHA(II,I), II=1,NP1)
82    FORMAT(5E20.7)
      CLOSE ...
253   IAP=(IAP+1)/2
      IF(IAP.EQ.0) GOTO 256
      IAP=1
      GOTO 2?3
256   IAP=0
      CALL ICFIL(IFILE,ICLSE)
9003  CONTINUE
      CALL EXIT
      END
```

```
CCC
CCC [illegible] SUBROUTINES FOR [illegible]
CCC ***********************************
      [illegible]
      SUBROUTINE CSIMQ(A,B,N,KS)
C     CSIMQ IS A VERSION OF THE SSP SUBROUTINE SIMQ FOR COMPLEX NUMBERS
      COMPLEX A(1),B(1),SAVE,BIGA
C
C     FORWARD SOLUTION
C
      TOL=0.
      KS=0
      JJ=-N
      DO 65 J=1,N
      JY=J+1
      JJ=JJ+N+1
      BIGA=(0.0,0.0)
      IT=JJ-J
      DO 30 I=J,N
C
C     SEARCH FOR MAXIMUM COEFFICIENT IN COLUMN
C
      IJ=IT+I
      IF(CABS(BIGA)-CABS(A(IJ)))20,30,30
   20 BIGA=A(IJ)
      IMAX=I
   30 CONTINUE
C
C     TEST FOR PIVOT LESS THAN TOLERANCE (SINGULAR MATRIX)
C
      IF(CABS(BIGA)-TOL)35,35,40
   35 KS=1
      RETURN
C
C     INTERCHANGE ROWS IF NECESSARY
C
   40 I1=J+N*(J-2)
      IT=IMAX-J
      DO 50 K=J,N
      I1=I1+N
      I2=I1+IT
      SAVE=A(I1)
      A(I1)=A(I2)
      A(I2)=SAVE
C
C     DIVIDE EQUATION BY LEADING COEFFICIENT
C
   50 A(I1)=A(I1)/BIGA
      SAVE=B(IMAX)
      B(IMAX)=B(J)
      B(J)=SAVE/BIGA
C
C     ELIMINATE NEXT VARIABLE
C
      IF(J-N)55,70,55
```

```
   55 IU=(U+(J-1))
      [illegible]
      IX=I[illegible]+1X
      IIX=I*
      DO [illegible]X=J,N
      IAJX=N*(JX-1)+IX
      JJY=(X-1)*1)
   6  S(I,J)=A(I,JY)-(A(I,J)*A(JJY))
   65 A(I)=(IX)-(B(J)*A(IXJ))
C
      BACK SECTION
C
   70 IY=N-1
      II=N*N
      DO 80J=1,NY
      IA=II-N
      IB=N-J
      IC=N
      DO 80K=1,J
      B(IB)=B(IB)-A(IA)*B(IC)
      IA=IA-N
   80 IC=IC-1
      RETURN
      END
      SUBROUTINE CMATMA(FT,CFT,CW,NROOT2,NROOT,TCFT,S,M)
      COMPLEX CFT(N,M),CW(N),TCFT(M,N),S(NROOT),FT(NROOT,NROOT)
      DO 600 I=1,NROOT2
      DO 600 J=1,NROOT
  600 TCFT(J,I)=CFT(I,J)
      DO 605 L=1,NROOT
      DO 605 I=1,NROOT
      FT(L,I)=(0.,0.)
      DO 605 J=1,NROOT2
  605 FT(L,I)=TCFT(L,J)*CFT(J,I)+FT(L,I)
      DO 610 I=1,NROOT
      S(I)=(0.,0.)
      DO 610 J=1,NROOT2
  610 S(I)=CFT(I,J)*CW(J)+S(I)
      RETURN
      END
      SUBROUTINE MULLER (NC,MTOL,ITER,RT,ROOT,RTOL,IFLAG)
      COMPLEX RT(N),ROOT(N)
      COMPLEX Z,Z1,Z2,Z3,FZ1,FZ2,FZ3,Z322,Z221,L1,D1,C1,B1,L,LD,LPOS
      COMPLEX LNEG,LPOS,L,Z0,FZ,SAVE
      DIMENSION RTOL(N)
      IX=N-1
      IFLAG=
      DO 4 I=1,N
    4 ROOT(I)=RT(I)
      DO 51 I=1,
      IF(CABS(RT(NT))).GT.0.)GO TO 2
      Z=(0.,0.)
      [illegible]
      GO TO 10
    2 [illegible]
```

```
      [illegible]
      Z1=CMPLX(-1.,0.)
      Z3=(0.,0.)
      Z2=(1.,0.)
      FZ1=RT(1,N1)
      FZ2=RT([illegible]N1)+RT([illegible]N1+1)+RT([illegible]N1+2)
      FZ3=RT([illegible]N1)+RT([illegible]N1+1)+RT([illegible]N1+2)
    1 DO 52 I=1,ITER
      Z32=Z3-Z2
      [illegible]=Z[illegible]
      [illegible]=Z32/(Z2[illegible])
      [illegible]=1.+[illegible]
      [illegible]=L1*(L1*[illegible]1-D1*FZ2+FZ3)
      [illegible]=C1*[illegible]*(FZ3-FZ2)
      [illegible]=2.*[illegible]
      [illegible]=CSQRT([illegible]**2+2*[illegible]*C1)
      [illegible]=[illegible]
      [illegible]=[illegible]
      [illegible]
      IF(C[illegible]
      IF(C[illegible]=(1.,0.)
      L=[illegible]
    7 Z=Z3+[illegible]*L
      ZL=Z
      IF(CA[illegible]
      [illegible]
      IF([illegible]GO TO 13
      IF([illegible]GO TO 14
      IF([illegible]GO TO 14
      [illegible]
      IF([illegible]GO TO 1[illegible]
      IFLAG=[illegible]
      GO TO [illegible]
   1[illegible] [illegible]
      FZ=RT([illegible])
      IF(CA[illegible](Z)[illegible]GO TO 1[illegible]
      FZ=RT([illegible])
      DO 5[illegible]
      [illegible]
   5[illegible] FZ=RT([illegible])+FZ*Z
   1[illegible] [illegible]
      IF(CA[illegible](FZ)[illegible]CABS(FZ3))[illegible]GO TO 1[illegible]
      L=L*[illegible]
      GO TO 7
   1[illegible] Z1=Z2
      Z2=Z3
      Z3=Z
      FZ1=FZ[illegible]
      FZ2=FZ[illegible]
   52 FZ3=FZ
      IFLAG=[illegible]
   [illegible] [illegible]
   [illegible] [illegible](I)=[illegible](I)
      [illegible]
      RETURN
```

```
   1. DO 50 I=N,1,-1
      ILANG=I+1
      SUM=0.
   4. =I(LL)AN(LL)+B(JJ)*Z
   16 [illegible]
      ROOT( I)=C
   51 CONTINUE
      SAVE=C(I)
      ROOT( )=(-T(M))/A(N)
      A(I)=SAVE
      R(L( )=0.
      RETURN
      END
C
C.................................................
C
C SUBROUTINE EIGEN
C
C COMPUTE EIGENVALUES AND VECTORS OF A REAL SYMMETRIC MATRIX
C CALL EIGEN (A,R,N,MV)
C       A=ORIGINAL MATRIX, DESTROYED IN COMPUTATION, REAL AND SYMMETRIC
C         RESULTANT EIGENVALUES ARE DEVELOPED IN DIAGONAL OF A IN DESCENDING
C
C       R=RESULTANT MATRIX OF EIGENVECTORS(STORED COLUMN WISE,
C         IN SAME SEQUENCE AS EIGENVALUES
C
C       N=ORDER OF MATRICES A AND R
C
C       MV=INPUT CODE
C          0 COMPUTE EIGENVALUES AND EIGENVECTORS
C          1 COMPUTE VALUES ONLY(R NEED NOT BE DIMENSIONED
C            BUT STILL APPEAR IN CALL SEQUENCE
C
C
C
C
      SUBROUTINE EIGEN(A,R,N,MV)
      DIMENSION A(1), R(1)
C
C     GENERATE I
C
    5 RANGE=1.0E-6
      IF(MV-1)10,25,10
   10 IQ=-N
      DO 20 J=1,N
      IQ=IQ+N
      DO 20 I=1,N
      IJ=IQ+I
      R(IJ)=0.0
      IF(I-J)20,15,20
   15 R(IJ)=1.0
   20 CONTINUE
C
C     COMPUTE INITIAL AND FINAL NORM
C
```

```
   25 ANORM=0.0
      DO 35 I=1,N
      DO 35 J=1,N
      IF(I-J)30,35,30
   30 IA=I+(J*J-J)/2
      ANORM=ANORM+A(IA)*A(IA)
   35 CONTINUE
      IF(ANORM)165,165,40
   40 ANORM=1.414*SQRT(ANORM)
      FN=1.0*N
      ANRMX=ANORM*RANGE/FN
C
C     INITIALIZE INDICATORS AND COMPUTE THRESHOLD, THR
C
      IND=0
      THR=ANORM
   45 THR=THR/FN
   50 L=1
   55 M=L+1
C
C     COMPUTE SIN AND COS
C
   60 MQ=(M*M-M)/2
      LQ=(L*L-L)/2
      LM=L+MQ
   62 IF(ABS(A(LM))-THR)130,65,65
   65 IND=1
      LL=L+LQ
      MM=M+MQ
      X=0.5*(A(LL)-A(MM))
   68 Y=-A(LM)/SQRT(A(LM)*A(LM)+X*X)
      IF(X)70,75,75
   70 Y=-Y
   75 SINX=Y/SQRT(2.0*(1.0+(SQRT(1.0-Y*Y))))
      SINX2=SINX*SINX
   78 COSX=SQRT(1.0-SINX2)
      COSX2=COSX*COSX
      SINCS=SINX*COSX
C
C     ROTATE L AND M COLUMNS
C
      ILQ=N*(L-1)
      IMQ=N*(M-1)
      DO 125 I=1,N
      IQ=(I*I-I)/2
      IF(I-L)80,115,80
   80 IF(I-M)85,115,90
   85 IM=I+MQ
      GO TO 95
   90 IM=M+IQ
   95 IF(I-L)100,105,105
  100 IL=I+LQ
      GO TO 110
  105 IL=L+IQ
  110 X=A(IL)*COSX-A(IM)*SINX
```

```
          B(IM)= (IL)*SINX+B(IM)*COSX
          B(IL)=Y
    115   IF(MV-1)120,125,120
    120   ILR=ILQ+I
          IMR=IMQ+I
          X=B(ILR)*COSX-B(IMR)*SINX
          B(IMR)=B(ILR)*SINX+B(IMR)*COSX
          B(ILR)=X
    125   CONTINUE
          X=2.0*A(LM)*SINCS
          Y=A(LL)*COSX2+A(MM)*SINX2-X
          X=A(LL)*SINX2+A(MM)*COSX2+X
          A(LM)=(A(LL)-A(MM))*SINCS+A(LM)*(COSX2-SINX2)
          A(LL)=Y
          A(MM)=X
C
C         TESTS FOR COMPLETION
C
    130   IF(M-N)135,140,135
    135   M=M+1
          GO TO 60
    140   IF(L-(N-1))145,150,145
    145   L=L+1
          GO TO 55
    150   IF(IND-1)160,155,160
    155   IND=0
          GO TO 50
    160   IF(THR-ANRMX)165,165,45
    165   IQ=-N
          DO 185 I=1,N
          IQ=IQ+N
          LL=I+(I*I-I)/2
          JQ=N*(I-2)
          DO 185 J=I,N
          JQ=JQ+N
          MM=J+(J*J-J)/2
          IF(A(LL)-A(MM)) 170,185,185
    170   X=A(LL)
          A(LL)=A(MM)
          A(MM)=X
          IF(MV-1)175,185,175
    175   DO 180 K=1,N
          ILR=IQ+K
          IMR=JQ+K
          X=R(ILR)
          R(ILR)=R(IMR)
    180   R(IMR)=X
    185   CONTINUE
          RETURN
          END
```

APPENDIX C

This appendix tabulates the extracted resonances of the mine-like target at different antenna locations in icy ground. The poles, residues as well as the minimum-error-case parameters associated with the Prony Process are given. These parameters are N, IBS, III, and M and are defined as follows.

N = Number of poles

IBS = Interval between samples, i.e., $T = IBS \times T_B$

III = The start time of the fitting interval in the Prony process is $t_s + (III-1) \times 2 \times T_B$

M = Number of samples used in the fitting interval is MxN.

TABLE 17
EXTRACTED RESONANCES OF THE MINE-LIKE TARGET
AT VARIOUS ANTENNA LOCATIONS IN ICY GROUND

ANTENNA LOCATION = CENTER — N=11, IBS=5, III=5, M=3, ϵ=0.632E-2

POLE (REAL PART)	POLE (IMAG PART)	RESIDUE (REAL PART)	RESIDUE (IMAG PART)
-.6165323E8	±.5980379E8	.1627237E0	±.2203193E0
-.9816088E8	±.1153422E9	-.1200819E0	±.4662508E-1
-.2972145E9	±.3199646E9	-.6727021E0	±.2528001E-1
-.2574395E9	±.4525337E9	-.2245525E0	±.9734140E-1

15 cm EAST OF CENTER — N=11, IBS=7, III=1, M=2, ϵ=0.604E-3

POLE (REAL PART)	POLE (IMAG PART)	RESIDUE (REAL PART)	RESIDUE (IMAG PART)
-.7955556E9	±.7207162E8	-.3441590E0	∓.5773295E0
-.9747022E8	±.1327517E9	-.2914887E-1	±.4185661E0
-.2185998E9	±.1964866E9	.1786104E1	±.6787741E0
-.2235657E9	±.2570622E9	.1210215E1	±.1496749E1
-.2108089E9	±.3265433E9	-.2914887E-1	∓.4185661E0

15 cm SOUTH OF CENTER — N=10, IBS=4, III=2, M=2, ϵ=0.375E-2

POLE (REAL PART)	POLE (IMAG PART)	RESIDUE (REAL PART)	RESIDUE (IMAG PART)
-.4419169E8	±.5302244E8	-.1283107E0	±.2668165E0
-.1687482E9	±.1862940E9	.1938946E0	±.4774533E0
-.1866233E9	±.2797166E9	.2234024E-1	±.5512929E0
-.3106326E8	±.3993629E9	-.5570095E-1	±.4816288E0
-.4141821E9	±.5571886E8	.7225376E0	∓.9451689E0

* Real and imaginary parts of the extracted resonances are in Nepers/s and Hz, respectively.

TABLE 17 (Cont.)

15 cm WEST OF CENTER		N=7, IBS=9, III=3, M=3 ϵ=0.448E-2	
POLE (REAL PART)	POLE (IMAG PART)	RESIDUE (REAL PART)	RESIDUE (IMAG PART)
-.8252691E8	±.7159227E8	.4703710E0	±.2550093E0
-.6366100E8	±.1213223E9	.2435532E-1	∓.1370926E0
-.2474290E9	±.2123833E9	.3750488E0	∓.2747979E0
-.1196715E9	±.2833333E9	.1486354E9	0.0000000

15 cm NORTH OF CENTER		N=12, IBS=6, III=5, M=2 ϵ=0.287E-3	
POLE (REAL PART)	POLE (IMAG PART)	RESIDUE (REAL PART)	RESIDUE (IMAG PART)
-.1238699E9	±.5956967E8	-.7568201E0	∓.4133825E0
-.1455328E9	±.1044725E9	.4427186E0	±.3773904E0
-.2976452E9	±.2543575E9	.1651730E0	±.4133825E0
-.3582517E9	±.3319750E9	.3949756E0	∓.7346425E0
-.3250828E9	±.4250000E9	.2408422E0	0.0000000

30 cm EAST OF CENTER		N=11, IBS=6, III=4, M=2 ϵ=0.247E-2	
POLE (REAL PART)	POLE (IMAG PART)	RESIDUE (REAL PART)	RESIDUE (IMAG PART)
-.9395545E8	±.7131887E8	-.3951318E0	∓.1237333E1
-.1369431E9	±.1220007E9	-.1243418E1	±.8057936E-1
-.3187709E9	±.2553445E9	-.1835029E1	∓.6562829E0
-2052859E9	±.3777737E9	.1061165E0	±.9037383E-1
-.2686828E9	±.4250000E9	-.2203826E0	0.0000000

30 cm SOUTH OF CENTER		N=13, IBS=6, III=2, M=2 ϵ=0.406E-3	
POLE (REAL PART)	POLE (IMAG PART)	RESIDUE (REAL PART)	RESIDUE (IMAG PART)
-.7440484E8	±.5768431E8	.2634359E0	±.3522781E0
-.2734229E9	±.1749879E9	-.5841965E0	∓.1580445E1
-.2451866E9	±.2385293E9	.1394630E1	∓.1721972E0
-.2480318E9	±.2889975E9	.6811801E0	±.1354053E1
-.2653034E9	±.3814169E9	-.6790937E0	±.1187006E1

TABLE 17 (Cont.)

30 cm WEST OF CENTER		N=13, IBS=6, III=3, M=2 ε=0.685E-2	
POLE (REAL PART)	POLE (IMAG PART)	RESIDUE (REAL PART)	RESIDUE (IMAG PART)
-.1174326E9	±.9037581E8	-.7656702E0	∓.8719310E0
-.2722184E9	±.1783297E9	.3367912E0	∓.1380838E0
-.2442735E9	±.3781778E9	-.2437025E0	±.4363209E-1

30 cm NORTH OF CENTER		N=12, IBS=6, III=2, M=2 ε=0.171E-2	
POLE (REAL PART)	POLE (IMAG PART)	RESIDUE (REAL PART)	RESIDUE (IMAG PART)
-.3929171E8	±.6274667E8	.3064080E0	∓.2378655E-2
-.3953903E8	±.1162181E9	-.8984933E-1	±.4503131E-1
-.2863506E9	±.1847860E9	-.2726371E1	∓.3413519E0
-.2130829E9	±.2626060E9	-.1131884E1	∓.7116251E0
-.3845860E9	±.2977974E9	.2613163E1	∓.2442230E1
-.3482679E9	±.3921698E9	.1288635E1	±.1489745E1

AVERAGE	
POLE (REAL PART)	POLE (IMAG PART)
-.7493116E8	±.6347621E8
-.9981995E8	±.1146405E9
-.2416503E9	±.2535799E9
-.2809195E9	±.3074991E9
-.2885261E9	±.4076659E9

APPENDIX D

This appendix tabulates the average extracted resonances of mine-like target waveforms obtained using the 12m long antenna.

Table 18
AVERAGE EXTRACTED RESONANCES OF THE MINE-LIKE TARGET WAVEFORMS OBTAINED USING THE 12m LONG ANTENNA

POLE (REAL)*	POLE (IMAG)
-242.9760E6	±144.3435E6
-381.1344E6	±233.9871E6
-407.1770E6	±319.0055E6
-373.7482E6	±413.1869E6

*Real and imaginary parts of the extracted resonances are in Nepers/s and Hz, respectively.

APPENDIX E

This appendix lists the Fortran program for performing the target identification process (SRTID2), it also tabulates some of the target identification results described in Chapter IV. Detail correlation coefficient values are given.

```
CCC *****************************************************
CCC
CCC PROGRAM NAME: SUTIDE
CCC                  SUBSURFACE RADAR TARGET IDENTIFICATION
CCC
CCC FUNCTION: PERFORMS THE PREDICTION-CORRELATION
CCC            IDENTIFICATION
CCC
CCC *****************************************************
      OPTIONS  +
      INCLUDE FORTH,LIMZ
      INCLUDE FLSYS,AONC
      INCLUDE FESYS,SYSM
      DIMENSION THF(256),IBLCK(2),THFD(256),W(256)
      DIMENSION EROR(50),ERROR(50),DELTA(50),DELTAT(50)
      COMPLEX FILES(15),A(15,15),R(15),FISF(256)
      DIMENSION IPFIL(2),ITFILE(2),IFUSER(2),ITUSER(2)
     &,ITFIL(2),S(60),XSH(3),XMAXT(15),ALPHA(15,20)
      INTEGER AA,BB
      DATA IBLEK/5H     /,IA,IB/1HA,1HB/
CCC
CCC
CCC 2) INITIALIZATIONS
CCC ******************
CCC
CCC
CCC   IF NTOPT .EQ. 0 ==>PAST AND FUTURE VALUES ARE USED
CCC   IF NTOPT .NE. 0 ==>ONLY PAST VALUES ARE USED
CCC   IF IPLOT .EQ. 1 ==>RHO IS PLOTTED
CCC   IF IPLOT .NE. 1 ==>EROR IS PLOTTED
      CALL SUPERK(3)
      NTOPT=
      IPLOT=
CCC
CCC
CCC 3) I/O SPECIFICATIONS
CCC *********************
CCC
CCC
      WRITE(6,15)
15    FORMAT(//)
      WRITE(6,10)
10    FORMAT(1X,'OUTPUT FILE NAME: ')
      READ(5,20)OUTFIL
20    FORMAT(A6)
      CALL ASSIGN(OUTFIL,6,6,1)
      IAUMN=IBLCK(1)
      WRITE(6,50)
50    FORMAT('1',NOPF,IFILT= ')
      READ(5,*) NOPF,IFILT
      WRITE(6,2)
2     FORMAT(1X,'FILE INPUT')
      CALL OPEN(IPFIL,IPUSER)
      DO 100 NF=1,1
      CALL ASSIGN(IPFIL,IPUSER,2)
```

```
      READ(5,1)T
      READ(5,4)FILE
    2 FORMAT(I5)
      DO 6 J=1,FILE
      READ(5,30)POLES(J)
    4 DO 1100 F
      DO 6 J=1,FILE
      R=REAL(POLES(J))
      X=AIMAG(POLES(J))*2.*3.141592
    6 POLES(J)=CMPLX(R,X)
      CLOSE
      IF(OP.EQ.1) GOTO 8
      WRITE(6,5)
    5 FORMAT(/1X,'ACCEPTED INPUT')
 9000 CALL ASFILE(ITFILE,ITUSER)
      WRITE(6,9001)
 9001 FORMAT(1X,'7 OR 15 ')
      CALL R.FATS(I,1)
      I=(I.SHIFT.1).SHIFT.-1
      IARR=1
      IAR=0
      IF(I.SHIFT.-16.EQ.1A.SHIFT.-16)GO TO 9004
      IAR=1
      IF(I.SHIFT.-16.EQ.1N.SHIFT.-16)GO TO 9004
      WRITE(6,9002)
 9002 FORMAT(1X,'?')
      GO TO 9000
 9004 DO 77 II=1,2
   77 ITFIL(II)=ITFILE(II)
      IAR1=IAR
      CALL OPNSEI
    8 DO 9 II=1,2
    9 ITFILE(II)=ITFIL(II)
      IAR=IAR1
CCC
CCC
CCC A) PREPROCESSING OF SIGNALS
CCC ****************************
CCC
CCC
      I = 1
      DO 9999 IW=1,NUM
      DO 9909 III=1,TRUE
      IF(IPO.EQ.1) GOTO 9998
      IAR=0
      IF(III.LE.2) IAR=1
 9998 IRAN=1.
      CALL READBL(ITWE,256,I,G,ITFILE,ITUSER,IAR,0,IERR)
      SUM=0.0
      DO 1010 I=1,7
 1010 SUM=SUM+TWE(I)/7.
      DO 1020 I=1,256
 1020 TWE(I)=TWE(I)-SUM
 9901 FORMAT(1X,F10.5)
      IF(I.EQ.1) GOTO 990
```

```
CCC
CCC
CCC B) HORIZONTAL AND VERTICAL OFFSET
CCC *********************************
CCC
CCC
      CALL GETCP(IS)
      YSMIN=1.0
      YSM=0.0
      DO 11 KK=1,7
11    YSM=YSM+TAB(KK)/7.
      DO 12 KK=1,256
12    TAB(KK)=TAB(KK)-YSM
      YSMAX=0.0
      JJM=1
      KKS=25
      DO 21 IK=1,KKS
      DO 2110 I=1,3
      IKK=IK+I-1
2110  XSH(I)=TAB(IKK)
      IF(XSH(2).LT.XSH(1).OR.XSH(2).LT.XSH(3)) GOTO 21
      IF(XSH(2)-XSMAX) 21,2112,2112
21    CONTINUE
2112  JJ=IK+1
      DO 22 KK=1,256
22    Y(KK)=TAB(KK)
      DO 23 KK=1,256
23    TAB(KK)=0.0
      DO 24 KK=JJ,256
      TAB(KK)=Y(JJ)
24    JJ=JJ+1
      IF(III.NE.1) GOTO 9006
      DO 9007 JJ=1,256
9007  TABO(JJ)=TAB(JJ)
9006  CONTINUE
      DO 29 I=1,256
29    TAB(I)=(TABO(I)-TAB(I))/2.
999   BKM=1.
      DO 27 I=1,12
27    TAB(I)=0.0
      DO 28 I=247,256
28    TAB(I)=0.0
CCC
CCC C) PRE-FILTERING
CCC ***************
CCC
      IF(IFILT.LT.0) GOTO 9997
      GOTO 9996
      DO 330 I=1,256
330   FILF(I)=CMPLX(TAB(I),0.0)
      NO1=1
      NO2=1
      M=21
      FMM=1.5
      CALL FFT(FILF,M,M,S,-1,IFMK)
```

```
      DO 3422 I=M1,MM2
3422  F(I)=(F(I)*(I-M1))/(MM2-M1)
      DO 3423 I=M3,MM4
3423  F(I)=(F(I)*(I-(M4+120.)))/(120.-M3)
      DO 3440 I=1,128
      I1=I+1
      J=257-I
3440  FTMP(I)=CMPLX(F(I),F(J))
      CALL FOURT(FTMP,8,-1,1,ERR)
      DO 3445 I=1,256
3445  TMF(I)=REAL(FTMP(I))
CCC
CCC
CCC 6) PEAK DETECTION(BEFORE FILTERING)
CCC ********************************
CCC
CCC
9997  MAXM=1.
      TMAX=-1.E10
      DO 3100 I=1,256
3100  F(I)=F(I)*31.2/2.5+1.E-10
      DO 3101 I=1,128
      J=I+2
3101  TMF(I)=F(J)
      DO 3102 I=129,256
3102  TMF(I)=0.0
      DO 7 I=1,128
      IF(TMAX.LT.ABS(TMF(I))) MM=I
      IF(TMAX.LT.ABS(TMF(I))) TMAX=ABS(TMF(I))
      IF(ABS(TMF(I)).GT.0.1) NN=I
7     CONTINUE
      DELTA=T/256.
      NB=MM*100
      ICNT1=0.
      ICNT=0.
CCC
CCC
CCC 7) ERROR AND PEAK-AMPLITUDE THRESHOLD DETECTOR
CCC **********************************************
CCC
CCC
1556  ICNT=1.0
      [illegible]
      [illegible]
      TMAX1=0.975
      TMAXN=0.75
      LIMIT=5.0
      MAXIT=45
      ADJS=1.0
      IF(... .LT.14) ADJS=.25
      IF(... .LT.17) ADJS=.25
      IF(... .LT.7) ADJS=.25
      IF(... .LT.40) ADJS=4.0
      IF(... .LT.44) ADJS=4.0
      [illegible]
```

```
      ENGY=0.0
      DO 2000 I=AA,BB
 2000 ENGY=ENGY+F(I)**2*ADJS
      ENGY=ENGY/(BB-AA+1.)
      WRITE(3,600)
      IF(AA.GE.LIMITS.AND.AA.LE.ULIMITS) GOTO 2001
      WRITE(3,2002)
 2002 FORMAT('PEAK TIMING OUT OF RANGE')
 2001 ERRR=1.0
      IF(TMAX.GE.TMAXMI.AND.TMAX.LE.TMAXMA) GOTO 2003
      WRITE(3,2004)
 2004 FORMAT('MAXIMUM AMPLITUDE OUT OF RANGE')
 2003 ERRR=1.0
      IF(ENGY.GE.EMIN.AND.ENGY.LE.EMAX) GOTO 2007
      WRITE(3,2006)
 2006 FORMAT('ENERGY OUT OF RANGE')
CCC
CCC 4) POST-FILTERING
CCC ****************
CCC
CCC
 2007 ERRR=1.0
      IF(IFILT.EQ.0) GOTO 1999
      IF(IW.GT.1) GOTO 45
      DO 30 I=1,64
   30 FTWF(I)=CMPLX(1.0,0.0)
      NH1=1
      NH2=6
      NH3=11
      NH4=16
      NH5=NH4+1
      ATTN=60.
      ALPHAA=0.1102*(ATTN-8.7)
      TAU=15.
      DO 31 I=1,NH1
   31 FTWF(I)=CMPLX(0.0,0.0)
      DO 222 I=NH1,NH2
  222 FTWF(I)=(FTWF(I)*(I-NH1))/(NH2-NH1)
      DO 223 I=NH3,NH4
  223 FTWF(I)=(FTWF(I)*(-I+NH4))/(NH4-NH3)
      DO 224 I=NH5,65
  224 FTWF(I)=CMPLX(0.0,0.0)
      DO 225 I=1,64
  225 FTWF(I)=FTWF(I)*(-1)**(I-1)
      DO 40 I=1,63
      II=I+1
      J=129-I
   40 FTWF(J)=CONJG(FTWF(II))
      CALL FFT(FTWF,7,S,1,IERR)
      DO 45 I=1,128
   45 W(I)=REAL(FTWF(I))
      SUM=0.0
      DO 32 I=1,128
      IF(ABS(W(I)).GT.SUM) SUM=ABS(W(I))
   32 CONTINUE
```

```
      DO 33 I=1,128
 33   X(I)=X(I)/2.0
      DO 34 I=1,46
 34   X(I)=0.0
      DO 35 I=84,128
 35   X(I)=0.0
      Y=ALPHA1
      CALL AIFU(Y,U)
      Y1=X
      DO 36 I=47,83
      Y=ALPHA*SQRT(1.-((I-65)/1[illegible])**2)
      CALL A[illegible](Y,U)
      Y=[illegible]/Y1
 36   X(I)=X(I)*Y
      SUM=0.0
      DO 37 I=47,83
 37   SUM=SUM+X(I)/37.
      DO 38 I=47,83
 38   X(I)=X(I)-SUM
      WRITE(3,1[illegible])
 39   PK=1.
      DO 241 I=1,256
 241  TAPE(I)=X(I)
      DO 239 I=A[illegible],[illegible]
      KK=I-1[illegible]
      SUM=0.
      DO 240 J=47,83
      IF(KK.LT.1) GOTO 240
      SUM=SUM+X(J)*TAPE(KK)
 240  KK=KK+1
 239  TAP(I)=SUM
 1999 [illegible]K=1.
CCC
CCC
CCC 01 [illegible]
CCC ************
CCC
CCC
      [illegible]
C     DELTA IS THE SAMPLING TIME INTERVAL.
      ISAMPL=[illegible]
      [illegible]
      IF(L[illegible].1.ISAMPL) ISAMPL=IMAX
      ISAMPL=ISAMPL
      DO 400 LL=1,ISAMPL
      DELTA=DELTA*[illegible]
      DDELTA(LL)=DELTA
      DO 150 I=1,NPOLE
 150  Z(I)=[illegible](POLES(I)*DELTA)
C     A(I,J) ARE THE COEFFICIENTS OF THE LINEAR DIFFERENCE EQ.
      A(1,1)=Z(1)
      DO 160 I=2,NPOLE
      I1=I-1
      A(I,1)=A(I1,1)+Z(I)
 160  A(I,2)=A(I1,I)*Z(I)
```

```
      DO 170 I=2,NPOLE
      II=I-1
      DO 170 J=2,II
      JJ=J-1
  170 A(I,J)=A(II,JJ)*B(I)+A(II,J)
      AMAX=0.
      DO 161 I=1,NPOLE
      AMAGN=REAL(A(NPOLE,I))
      AMAG=ABS(AMAGN)
      IF(AMAG.GT.AMAX) KMAX=I
      IF(AMAG.GT.AMAX) AMAX=AMAG
  161 CONTINUE
      IF(NUM.LT.3) GOTO 171
      RAKMAX=REAL(A(NPOLE,KMAX))
      IF(AMAX.LT.1.) NOUT=1
      IF(AMAX.LT.1) KMAX=0
      IF(AMAX.LT.1) RAKMAX=1.0
      NPOLE1=NPOLE+1
      IF(LO.LT.4.OR.LO.GT.8) GOTO 171
      II=LO-3
      KMAXI(II)=NPOLE-KMAX
      DO 175 I=1,NPOLE
      J=NPOLE1-I
  175 ALPHA(II,I)=((-1)**(J+KMAX))*REAL(A(NPOLE,J))
     &/RAKMAX
      ALPHA(II,NPOLE1)=((-1)**(KMAX))/RAKMAX
  171 NN=1
CCC
CCC
CCC TF CORRECTION
CCC ***************
CCC
CCC
      IF(NTOUT.LE.0) KMAX=0
      RAKMAX=1.
      IF(NTOUT.EQ.0)RAKMAX=REAL(A(NPOLE,KMAX))
      JLIMIT=LENG(NPOLE-KMAX)
      JBEGIN=1+NCP*LO*KMAX
      SUM1=0.
      SUM2=0.
      SUM3=0.
      DO 190 J=JB,ITOTAL
      JPLK=J+LL*KMAX-1+NN
      SUM=0.
      IF(NTOUT.EQ.0)
     &SUM=((-1)**(KMAX+1))*TSF(JPLK)/RAKMAX
      DO 180 I=1,NPOLE
      IF(I.EQ.KMAX) GO TO 180
      JPLKI=J+LL*(KMAX-I)-1+NN
      SUM=SUM+((-1)**(I+KMAX+1))*REAL(A(NPOLE,I))*
     &TSF(JPLKI)/RAKMAX
  180 CONTINUE
      JJJ=J-1+NN
      SUM1=SUM1+(TSF(JJJ)-SUM)**2
      SUM2=SUM2+TSF(JJJ)**2
```

```
      [illegible] (1000)**,**[illegible]
  190 CONTINUE
      [illegible](L)=1.-[illegible]/SUM2
      [illegible](L)=1.-SUM1/SUM3
      IF(L.GT.[illegible]) GOTO 800
      [illegible]SUM1=[illegible]+[illegible](L)
      [illegible]SUM2=[illegible]+[illegible](L)
  800 CONTINUE
      [illegible]SUM1=[illegible]/[illegible].
      [illegible]SUM2=[illegible]/[illegible].
      CALL [illegible] (IE)
      ISECOND=[illegible]*(IE-15)
CCC
CCC
CCC 11) OUTPUTS
CCC ***********
CCC
CCC
 1002 FORMAT(1X,' SECONDS OF CPU TIME=',I10)
      WRITE(1,801) IPFIL(1),IPFIL(2),IPUSER(1),IPUSER(2)
  801 FORMAT(1X,'POLE FILE: ',2A6,5X,2A3)
      WRITE(1,810) ITFILE(1),ITFILE(2),IAG,ITUSER(1),ITUSER(2)
  810 FORMAT(1X,'TAPE FILE: ',2A6,2X,I2,2X,2A3)
      WRITE(1,815)
      WRITE(1,820)[illegible]
  820 FORMAT(1X,'     T     = ',1PE13.5)
      WRITE(1,830)ISAMPL
  830 FORMAT(1X,'  ISAMPL = ',I6)
      WRITE(1,840)AA,BB
  840 FORMAT(1X,'     AA    = ',I6/1X,'     BB    = ',I6)
      WRITE(1,815)
  815 FORMAT(1X,'   ')
      WRITE(1,870)
  870 FORMAT(6X,'    I    ',5X,'RROOT',11X,'IROOT')
      DO 50 I=1,ISAMPL
      WRITE(1,880)I,RROOT(I),IROOT(I)
   50 CONTINUE
  890 FORMAT([illegible],I5,5X,2E15.3)
      WRITE(1,895)IFLOT
  895 FORMAT(1X,'IFLOT= ',I5)
      WRITE(1,897)RCSUM1,RCSUM2,EMAX,EMAX
  897 FORMAT(1X,'[illegible] VALUE= ',F10.5,5X,F10.5
     &,5X,'[illegible] ERROR= ',E15.7,5X,'[illegible]= ',E15.7)
      WRITE(1,1002)ISECOND
      IF(L.EQ.[illegible]) GOTO 9999
      WRITE(1,802)
  802 FORMAT(/////)
      WRITE(1,1110) NPOLE
 1110 FORMAT(/,'NO. OF POLES=',I4)
      DO 1111 I=1,N
      J=I+3
      WRITE(1,1112) [illegible]X1(I)
 1112 FORMAT(/,'[illegible]',I4,'[illegible]',[illegible]=',I4)
      WRITE(1,1113)
 1113 FORMAT([illegible])
```

```
      WRITE(3,1114) (ALPHA(I,II),II=1,NPOLE1)
 1114 FORMAT(5E20.7)
 1111 CONTINUE
CCC
CCC
CCC 1e) ADVANCE WAVEFORM AND POLE FILENAME
CCC *****************************************
CCC
CCC
 9991 IAP=(IAP+1)/2
      IF(IAP.NE.0) GOTO 9008
      IAP=1
      GOTO 9991
 9008 CALL ICHAL(ITFILE,ITUSER)
      IAP=0
 9999 CONTINUE
      CALL ICHIL(IPFIL,IPUSER)
 1000 CONTINUE
      WRITE(3,1001) TABLE,IFILT,NH1,NH2,NH3,NH4
 1001 FORMAT('1MODE,IFILT= ',2I4,5X,'NH1,2,3,4= ',4I4)
      CALL EXIT
      END
CCC
CCC
      SUBROUTINE BIFO(X,B)
CC    X GETAKEN 0..20.
      Y=X/2.
      T=1.E-6
      E=1.
      DE=1.
      DO 1 I=1,25
      DE=DE*Y/I
      SDE=DE*DE
      E=E+SDE
      IF(E*T-SDE) 1,1,2
    1 CONTINUE
    2 B=E
      X=Y
      RETURN
      END
```

TABLE 19
VALUES OF THE CORRELATION COEFFICIENT FOR THE IDENTIFICATION OF THE MINE-LIKE TARGET IN WET GROUND

WAVEFORM	ANTENNA LOCATION	$\rho(9T_B)$
MINE-LIKE TARGET	E,S	.593
	C	.167
	C	.785
	C	.363
	15 cm,E	.170
	15 cm,S	.596
	15 cm,W	.382
	15 cm,N	.296
	30 cm,E	.183
	30 cm,S	.294
	30 cm,W	.766
	30 cm,N	.288
	45 cm,E	-.478
	45 cm,S	.678
BRASS CYLINDER	C	-.678
	15 cm,S	-.380
	30 cm,S	-.448
	45 cm,W	-.447
ALUMINUM SPHERE	7 cm,S	-.337
	22 cm,S	-.387
	37 cm,S	-.061
COPPER SHEET	7 cm,N	-.727
	10 cm,S	-.384
	25 cm,S	-.026
	13 cm,NE	-.065
	28 cm,NE	-.183

TABLE 20
VALUES OF THE CORRELATION COEFFICIENT FOR THE IDENTIFICATION OF THE MINE-LIKE TARGET IN DRY GROUND

WAVEFORM	ANTENNA LOCATION	$\rho(9T_B)$
MINE-LIKE TARGET	C	.575
	15 cm,E	.685
	15 cm,S	.709
	15 cm,W	.483
	15 cm,N	.538
BRASS CYLINDER	C	-.779
ALUMINUM SPHERE	7 cm,S	-.080
COPPER SHEET	10 cm,S	-.291

TABLE 21
VALUES OF THE CORRELATION COEFFICIENTS FOR THE IDENTIFICATION OF THE MINE-LIKE TARGET AND THE BRASS CYLINDER IN DRY GROUND

WAVEFORM	ANTENNA LOCATION	DESIRED TARGET = MINE-LIKE TARGET $\rho(8T_B)$	DESIRED TARGET = BRASS CYLINDER $\rho(5T_B)$
MINE-LIKE TARGET	C	.525	.648
	15 cm,E	.434	.646
	15 cm,S	.423	.491
	15 cm,W	.477	.651
	15 cm,N	.837	.922
	30 cm,E	.687	.738
	30 cm,S	.535	.168
	30 cm,W	.396	.831
	30 cm,N		
BRASS CYLINDER	C	-.266	.954
	15 cm,SN	.228	.983
	30 cm,SN	.146	.951
	15 cm,EW	.228	.979
	30 cm,EW	-.049	.991

TABLE 22
DETERMINING THE DETECTION AND IDENTIFICATION THRESHOLDS FOR THE IDENTIFICATION OF THE MINE-LIKE TARGET. R_{ID} = 30 cm

ANTENNA LOCATION	C	15 cm,S	30 cm,S	15 cm,N	30 cm,N	15 cm,E	30 cm,E	15 cm,N	30 cm,N	MINIMUM $\rho_{T_{Oi}} = \rho_{THi}$
$\rho(5T_B)$	.445	.969	.984	.527	.921	.890	.832	.894	.939	.445
$\rho(6T_B)$	-.0213	.800	.795	.184	.394	-.365	-.488	-.379	.0136	-.488
$\rho(7T_B)$	.536	.875	.827	.487	.707	.373	.253	.127	.206	.127
$\rho(8T_B)$	.561	.936	.813	.433	.687	.453	.450	.322	.243	.243
$\rho(9T_B)$	.658	.902	.705	.293	.386	.321	.679	.533	.289	.289
$\rho(10T_B)$	.822	.952	.727	.221	.426	.464	.749	.593	.542	.221
$\rho(11T_B)$	.922	.902	.821	.436	.522	.545	.832	.517	.504	.436
$\rho(12T_B)$	.0424	-.194	-.243	-.177	-.259	-.0213	.236	.177	.240	-.259
$\langle\rho(5T_B\text{-}12T_B)\rangle$	.49554	.76761	.67871	.30050	.47297	.33235	.44311	.34789	.38204	.30050
t_{MAX}*	38	41	68	39	28	28	69	40	27	RANGE=27,69
MAX**	2.82380	2.53884	1.84263	2.14075	1.73829	3.14312	1.66354	2.57983	2.18490	RANGE=1.66354,2.82380
E_M***	.20548	2.6127	.32341	.25412	.21247	.69875	.16681	3.0058	.59804	RANGE= .16681,3.4058

*t_{MAX} is in units of T_B

**MAX is in units of 200 mv

***E_M is in units of $(200\ mv)^2$

TABLE 23

DETERMINING THE DETECTION AND IDENTIFICATION THRESHOLDS FOR THE IDENTIFICATION OF THE BRASS CYLINDER. R_{ID} = 30 cm

ANTENNA LOCATION	C	15 cm,S	30 cm,S	15 cm,N	30 cm,N	15 cm,E	30 cm,E	15 cm,W	30 cm,W	MINIMUM $\rho T_{Ci} = \rho_{Thi}$
$\rho(5T_B)$	.997	.996	.905	.993	.610	.990	.992	.995	.989	.610
$\rho(6T_B)$	.994	.967	.582	.983	.510	.949	.953	.969	.891	.510
$\rho(7T_B)$	.981	.841	.746	.959	.614	.806	.875	.861	.765	.614
$\rho(8T_B)$	.947	.859	.562	.949	.386	.643	.725	.640	.772	.386
$\rho(9T_B)$	.915	.574	-.139	.940	.0432	.554	.587	.556	.857	-.139
$\rho(10T_B)$	.984	.867	.848	.978	.543	.820	.868	.882	.941	.543
$\rho(11T_B)$	.985	.834	-.854	.933	-.322	.759	.904	.896	.906	-.854
$\rho(12T_B)$	.989	.881	.---	.893	.---	.712	.691	.937	.711	.691
$\langle\rho(5T_B-12T_B)\rangle$	.97278	.83346	.37853	.95342	.34073	.78409	.82445	.84224	.67933	.34073
t_{MAX}*	60	63	93	92	65	73	81	75	85	RANGE=60,93
MAX**	7.17425	4.41336	1.13819	1.18190	6.65543	3.13931	1.44120	2.50931	.7448	RANGE=.74148,7.17425
E_M***	5.25863	2.08050	.12844	.15091	3.09266	.95062	.18457	.61825	.07016	RANGE=.07016,5.25808

* t_{MAX} is in units of T_B

** MAX is in units of 200 mV

***E_M is in units of $(200\ mV)^2$

TABLE 24
DETERMINING THE DETECTION AND IDENTIFICATION THRESHOLDS FOR THE IDENTIFICATION OF THE ALUMINUM SPHERE. R_{ID} = 37 cm

ANTENNA LOCATION*	E,S	15 cm,S	30 cm,S	E,N	15 cm,N	30 cm,N	E,E	15 cm,E	30 cm,E	E,W	15 cm,W	30 cm,W	MINIMUM $\epsilon_{Toi} = \epsilon_{THi}$
$\epsilon(5T_B)$	.523	.691	.825	.197	.603	.762	.764	.732	.812	.401	.924	.708	.197
$\epsilon(6T_B)$	.481	.746	.746	.631	.727	.786	.678	.783	.735	.745	.922	.803	.481
$\epsilon(7T_B)$	.751	.882	.840	.600	.943	.752	.772	.832	.666	.790	.879	.765	.600
$\epsilon(8T_B)$	.708	.837	.813	.123	.936	.580	.623	.743	-.106	.361	.661	.571	-.106
$\epsilon(9T_B)$	.621	.852	.825	.345	.870	.603	.277	.312	.637	.250	.218	.219	.218
$\epsilon(10T_B)$	.810	.896	.926	.444	.629	.823	.730	.830	.666	.189	.709	.792	.189
$\epsilon(11T_B)$	.590	.723	.945	.541	.103	.794	.826	.828	.648	.395	.722	.795	.103
$\epsilon(12T_B)$	.596	.617	.818	.365	.0464	.802	.837	.376	.624	.341	.584	.650	.341
$<\epsilon(5T_B-12T_B)>$	.66711	.77723	.85132	.44250	.64822	.76397	.71905	.66172	.62796	.42042	.73454	.66985	.42942
t_{MAX}**	35	22	29	36	43	29	43	31	25	33	31	29	RANGE=22,43
MAX***	2.79707	1.15359	2.05633	1.89583	2.41714	1.87024	2.53899	2.91758	1.51643	2.91588	2.08713	2.92536	RANGE=1.15359,2.92536
E_M****	.16526	.05072	.11075	.06707	.18438	.12757	.13554	.38887	.11729	.17206	.21727	.20153	RANGE= .11075, .38887

* Antenna Location here is referenced to edge of sphere

** t_{MAX} is units of T_B

*** MAX is units of 200 mV

**** E_M is units of $(200\ mV)^2$

APPENDIX F

This appendix tabulates the average extracted resonances of the different-size, different-depth cylinders and the thin wires (discussed in Chapter V).

TABLE 25
AVERAGE EXTRACTED RESONANCES OF THE DIFFERENT-
SIZE DIFFERENT-DEPTH CYLINDERS

DEPTH \ LENGTH	30 cm		90 cm		150 cm		300 cm	
	POLE (REAL)*	POLE (IMAG)	POLE (REAL)	POLE (IMAG)	POLE (REAL)	POLE (IMAG)	POLE (REAL)	POLE (IMAG)
30 cm	-169.5610911E6	± 68.75855222E6	-184.1313250E6	± 60.16855375E6	-197.8829273E6	± 69.73136636E6	-193.5835556E6	± 66.46100889E6
	-195.4250778E6	±111.39225110E6	-207.8996333E6	±143.92506670E6	-176.1866725E6	±119.59008750E6	-154.2036429E6	±127.38822860E6
	-160.8158800E6	±211.93096000E6	-193.9141500E6	±331.50570000E6	-260.8286500E6	±181.60040000E6	-251.3500333E6	±222.62823330E6
	- 71.6164723E6	±306.11995110E6	-226.3574500E6	±425.82118000E6	-228.9907834E6	±318.30021660E6	-102.6181290E6	±330.53312500E6
	-140.6709863E6	±451.30661250E6			-334.3826200E6	±409.26970000E6	-255.9519000E6	±406.93393300E6
90 cm	-206.3700178E6	± 66.86268111E6	-184.7466769E6	± 70.05995769E6	-144.4792900E6	± 69.24613667E6	-123.66685750E6	± 62.08320525E6
	-192.9582500E6	±112.32885000E6	-210.5452500E6	±163.58552000E6	-137.9945538E6	±108.60655250E6	- 73.59138167E6	±146.25415000E6
	-140.7524250E6	±205.95595000E6	-167.9889964E6	±347.76115000E6	-211.8574367E6	±176.39561430E6	-139.94530000E6	±206.81345000E6
	-157.2407367E6	±302.79635560E6			- 99.9779283E6	±351.19955000E6	-109.05371000E6	±335.78052500E6
150 cm	-169.6732957E6	± 57.32631430E6	-144.7749275E6	± 68.29041250E6	-132.5029220E6	± 62.19726500E6	-113.5388433E6	± 62.54994778E6
	-112.6025029E6	±136.18361430E6	- 93.6473850E6	±163.11830000E6	- 98.3763786E6	±125.84105710E6	-104.2920900E6	±147.55353330E6
	- 64.2650300E6	±229.34780000E6	-140.0411350E6	±308.61637500E6	-104.2604350E6	±173.43510000E6	-126.5257850E6	±230.83195000E6
	-162.8578020E6	±335.84088000E6			-104.7832783E6	±310.54561670E6	- 80.1101950E6	±298.63620000E6

* Real Part in Nepers/s, Imaginary Part in Hz.

TABLE 26
AVERAGE EXTRACTED RESONANCES OF THE 5cm DEEP
DIFFERENT-LENGTH THIN WIRES

DEPTH \ LENGTH	30 cm		45 cm		60 cm	
	POLE (REAL)*	POLE (IMAG)	POLE (REAL)	POLE (IMAG)	POLE (REAL)	POLE (IMAG)
5 cm	-239.256800E6	± 70.72278E6	-154.0950000E6	± 66.85459000E6	- 83.8039850E6	± 55.8029517E6
	-134.151920E6	±110.25438E6	- 98.1801729E6	± 82.37259857E6	- 81.8100535E6	± 73.6336200E6
	-144.240780E6	±224.25932E6	-148.2810333E6	±157.00765000E6	-186.4533000E6	±137.0595800E6
	-143.758252E6	±304.80154E6	-163.7349333E6	±260.42380000E6	-154.2790000E6	±208.5681333E6
					- 77.1887280E6	±298.3121600E6

* Real Part in Nepers/s, Imaginary Part in Hz

APPENDIX G

This appendix tabulates the average extracted resonances of the waveforms from the two models of the mine-like target and the small-antenna mine-like target waveforms.

TABLE 27
AVERAGE EXTRACTED RESONANCES OF THE MINE-LIKE TARGET

	POLE (REAL)*	POLE (IMAG)
MINE-LIKE TARGET MODEL NO. 1 0.6m ANTENNA	-1.75363970E8 -5.73125538E7 -2.87494683E8 -1.82908509E8 -9.76454733E7	±6.61019133E7 ±1.32122486E8 ±2.27030133E8 ±3.07411043E8 ±4.28447900E8
MINE-LIKE TARGET MODEL NO. 2 0.6m ANTENNA	-1.49959862E8 -9.64557560E7 -2.09351880E8 -1.91461498E8 -1.91729062E8	±7.56869867E7 ±1.64502020E8 ±2.27711640E8 ±2.89778957E8 ±4.14181320E8
MINE-LIKE TARGET MODEL NO. 1 0.15m ANTENNA	-6.90468500E7 -2.80111200E8 -2.35432000E8 -5.03972000E7 -1.22024400E8	±1.31552700E8 ±2.22590300E8 ±2.69826400E8 ±2.99420800E8 ±4.04685600E8

*Real Part in Nepers/s, Imaginary Part in Hz.

APPENDIX H

This appendix tabulates the identification results for identification of the mine-like target with the small-antenna system.

TABLE 28
DETERMINING THE DETECTION AND THE IDENTIFICATION THRESHOLDS
FOR THE IDENTIFICATION OF THE MINE-LIKE TARGET
WITH THE SMALL ANTENNA SYSTEM. R_{ID}=45 cm

ANTENNA LOCATION	15 cm,N	30 cm,N	15 cm,E	30 cm,E	15 cm,W	30 cm,W	45 cm,W	45 cm,N	45 cm,S	15 cm,S	45 cm,E	30 cm,S	C	MINIMUM $\rho_{Toi}=\rho_{THi}$
$\rho(4T_B)$	.615	.821	.930	.885	.806	.956	.960	.770	.743	.640	.654	.859	.629	.615
$\rho(5T_B)$	.630	.786	.303	.551	.627	.915	.889	.672	.410	.675	.166	.569	.625	.166
$\rho(6T_B)$	.873	.962	.670	.763	.615	.922	.971	.978	.917	.759	.870	.788	.974	.615
$\rho(7T_B)$	.938	.954	.775	.456	.751	.964	.978	.952	.964	.825	.861	.943	.994	.456
$\rho(8T_B)$	.863	.935	.724	.520	.718	.960	.979	.881	.904	.767	.420	.882	.867	.420
$\langle\rho(4T_B\text{-}8T_B)\rangle$	.78795	.89153	.66039	.63496	.70538	.94319	.95557	.85055	.78754	.73322	.59436	.80828	.85786	.59436
t_{MAX}*	75	73	76	71	75	76	76	71	63	83	66	76	58	RANGE=58,83
MAX**	3.72266	.89136	3.72363	1.20459	3.70801	.71973	.29724	.39099	.98535	3.72266	1.59570	1.51758	2.06456	RANGE=0.29724,3.72363
E_N***	1.4184	.04407	.94246	.08919	.99642	.04637	.00993	.00709	.05818	.50583	.15287	.09946	.25444	RANGE= 0.00709,1.42

* t_{MAX} = Peak Timing, in units of T_B

** MAX = Peak Magnitude, in units of 400 mv

*** E_N = Waveform Energy, in units of $(400\ mv)^2$

TABLE 29
FIR FILTER COEFFICIENTS USED IN THE PREPROCESSOR
OF THE MICROCOMPUTER IDENTIFICATION SYSTEM

```
H( 0)=  -.1502785E  -1
H( 1)=  -.1652442E  -1
H( 2)=  -.1905340E  -1
H( 3)=  -.2152655E  -1
H( 4)=  -.2544619E  -1
H( 5)=  -.2841376E  -1
H( 6)=  -.3457116E  -1
H( 7)=  -.3810196E  -1
H( 8)=  -.4696953E  -1
H( 9)=  -.5059113E  -1
H(10)=  -.6269651E  -1
H(11)=  -.6575464E  -1
H(12)=  -.8052841E  -1
H(13)=  -.7266609E  -1
H(14)=  -.9761710E  -1
H(15)=  -.5022250E  -1
H(16)=  -.1101347E   0
H(17)=   .3453146E   0
H(18)=   .9862565E   0
H(19)=   .3453146E   0
H(20)=  -.1101347E   0
H(21)=  -.5022250E  -1
H(22)=  -.9761710E  -1
H(23)=  -.7266609E  -1
H(24)=  -.8052841E  -1
H(25)=  -.6575464E  -1
H(26)=  -.6269651E  -1
H(27)=  -.5059113E  -1
H(28)=  -.4696953E  -1
H(29)=  -.3810196E  -1
H(30)=  -.3457116E  -1
H(31)=  -.2841376E  -1
H(32)=  -.2544619E  -1
H(33)=  -.2152655E  -1
H(34)=  -.1905340E  -1
H(35)=  -.1652442E  -1
H(36)=  -.1502785E  -1
```

TABLE 30
DETERMINING THE IDENTIFICATION THRESHOLDS FOR THE IDENTIFICATION OF THE MINE-LIKE TARGET WITH THE SMALL-ANTENNA SYSTEM BASED ON FIR FILTERING

ANTENNA LOCATION / $\rho(T_{oi})$	15 cm,N	30 cm,N	15 cm,E	30 cm,E	15 cm,W	30 cm,W	45 cm,W	45 cm,N	45 cm,S	15 cm,S	45 cm,E	30 cm,S	C	MINIMUM $\rho_{T_{oi}}=\rho_{Th}$
$\rho(4T_B)$	.579	.794	.919	.866	.750	.951	.659	.625	.804	.594	.965	.753	.714	.570
$\rho(5T_B)$	.568	.779	.365	.527	.533	.917	.725	.166	.448	.800	.601	.638	.343	.166
$\rho(6T_B)$	.85[illegible]	.957	.751	.761	.524	.925	.852	.872	.698	.971	.720	.981	.912	.524
$\rho(7T_B)$	.935	.950	.870	.471	.686	.967	.903	.881	.936	.993	.831	.949	.958	.471
$\rho(8T_B)$	.885	.939	.851	.543	.519	.969	.746	.423	.818	.856	.724	.872	.890	.423
$\bar{\rho}(4T_B-8T_B)$	.76206	.88358	.75106	.63344	.60214	.94563	.77706	.59332	.74069	.84274	.80818	.83843	.76338	.59332

APPENDIX I

This appendix gives detail descriptions of the APU[68] and the micro-program that implements the various system control and target identification processes.

A. The APU and Its Interface with the SDK-80

The connection diagram of the APU is given in Figure 58.

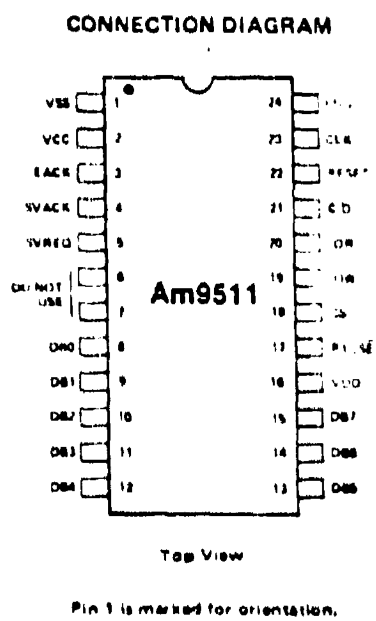

Figure 58. Connection diagram for the APU.

Interfacing the APU with the SDK-80 requires the generation of the various control signals. In this study, the APU is interfaced to the SDK-80 as a memory location, and the control signals are generated as follows:

1. $\overline{CS}$: chip select

   The chip-select signal is generated by using address lines A13, A14, and A15 of the 8080A processor in the SDK-80. The signal generation circuit is shown in Figure 59. The chip-select signal $\overline{CS}$ is low when the address lines A13, A14, A15 are all high.

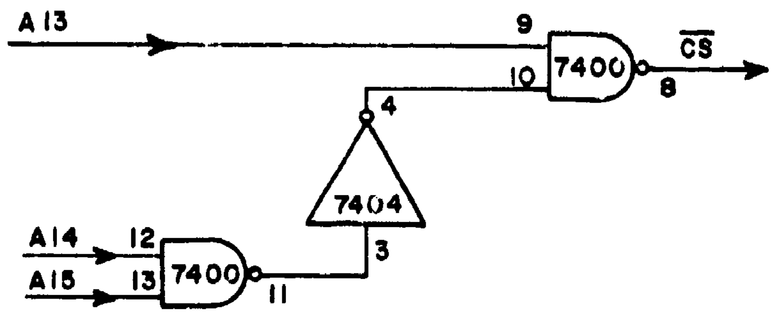

Figure 59. The chip-select ($\overline{CS}$) signal for the APU.

2. C/$\overline{D}$: command/data

   The C/$\overline{D}$ signal is tied directly to the address line Aϕ of the 8080A processor.

3. $\overline{IOR}$: tied directly to $\overline{MEMR}$ of the 8080A processor.

4. IOW: tied directly to $\overline{MEMW}$ line of the 808A processor.

5. $\overline{PAUSE}$: tied directly to the ready line of the 8080A processor.

6. CLK: tied directly to ϕ2 of the 8080A processor.

7. $\overline{EACK}$, $\overline{SVACK}$, SVREQ, RESET, $\overline{END}$: unused.

8. To eliminate possible loading problem, two additional signals are generated to inhibit the ROM's and RAM's of the SDK-80 when the APU is being addressed. These two control signals (E1 and E3) are given in Figure 60.

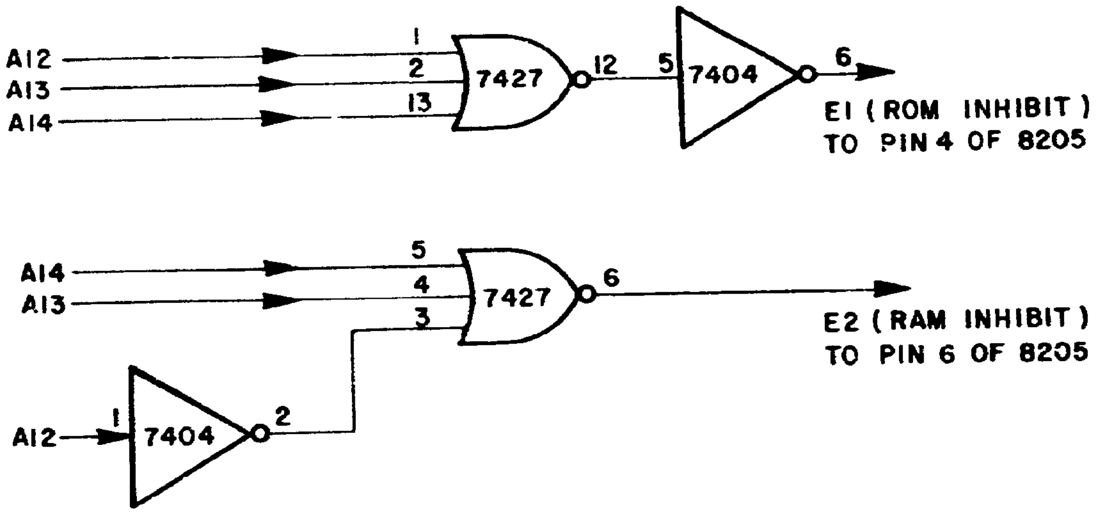

Figure 60. The ROM-inhibit (E1) and RAM-inhibit (E2) signals.

A summary of the APU commands is given in Table 31.

TABLE 31
APU COMMAND SUMMARY

Command Code 7	6	5	4	3	2	1	0	Command Mnemonic	Command Description (1)
FIXED POINT SINGLE PRECISION									
R	1	1	0	1	1	0	0	SADD	Adds TOS to NOS. Result to NOS. Pop Stack.
R	1	1	0	1	1	0	1	SSUB	Subtracts TOS from NOS. Result to NOS. Pop Stack.
R	1	1	0	1	1	1	0	SMUL	Multiplies NOS by TOS. Result to NOS. Pop Stack.
R	1	1	0	1	1	1	1	SDIV	Divides NOS by TOS. Result to NOS. Pop Stack.
FIXED POINT DOUBLE PRECISION									
R	0	1	0	1	1	0	0	DADD	Adds TOS to NOS. Result to NOS. Pop Stack.
R	0	1	0	1	1	0	1	DSUB	Subtracts TOS from NOS. Result to NOS. Pop Stack.
R	0	1	0	1	1	1	0	DMUL	Multiplies NOS by TOS. Result to NOS. Pop Stack.
R	0	1	0	1	1	1	1	DDIV	Divides NOS by TOS. Result to NOS. Pop Stack.
FLOATING POINT									
R	0	0	1	0	0	0	0	FADD	Adds TOS to NOS. Result to NOS. Pop Stack.
R	0	0	1	0	0	0	1	FSUB	Subtracts TOS from NOS. Result to NOS. Pop Stack.
R	0	0	1	0	0	1	0	FMUL	Multiplies NOS by TOS. Result to NOS. Pop Stack.
R	0	0	1	0	0	1	1	FDIV	Divides NOS by TOS. Result to NOS. Pop Stack.
DERIVED FLOATING POINT FUNCTIONS (2)									
R	0	0	0	0	0	0	1	SQRT	Square Root of TOS. Result in TOS.
R	0	0	0	0	0	1	0	SIN	Sine of TOS. Result in TOS.
R	0	0	0	0	0	1	1	COS	Cosine of TOS. Result in TOS.
R	0	0	0	0	1	0	0	TAN	Tangent of TOS. Result in TOS.
R	0	0	0	0	1	0	1	ASIN	Inverse Sine of TOS. Result in TOS.
R	0	0	0	0	1	1	0	ACOS	Inverse Cosine of TOS. Result in TOS.
R	0	0	0	0	1	1	1	ATAN	Inverse Tangent of TOS. Result in TOS.
R	0	0	0	1	0	0	0	LOG	Common Logarithm (base 10) of TOS. Result in TOS.
R	0	0	0	1	0	0	1	LN	Natural Logarithm (base e) of TOS. Result in TOS.
R	0	0	0	1	0	1	0	EXP	Exponential (e^x) of TOS. Result in TOS.
R	0	0	0	1	0	1	1	PWR	NOS raised to the power in TOS. Result to NOS. Pop Stack.
DATA MANIPULATION COMMANDS (3)									
R	0	0	0	0	0	0	0	NOP	No Operation
R	0	0	1	1	1	1	1	FIXS	Converts TOS from floating point to single precision fixed point format.
R	0	0	1	1	1	1	0	FIXD	Converts TOS from floating point to double precision fixed point format.
R	0	0	1	1	1	0	1	FLTS	Converts TOS from single precision fixed point to floating point format.
R	0	0	1	1	1	0	0	FLTD	Converts TOS from double precision fixed point to floating point format.
R	1	1	1	0	1	0	0	CHSS	Changes sign of single precision fixed point operand on TOS.
R	0	1	1	0	1	0	0	CHSD	Changes sign of double precision fixed point operand on TOS.
R	0	0	1	0	1	0	1	CHSF	Changes sign of floating point operand on TOS.
R	1	1	1	0	1	1	1	PTOS	Push single precision fixed point operand on TOS to NOS.
R	0	1	1	0	1	1	1	PTOD	Push double precision fixed point operand on TOS to NOS.
R	0	0	1	0	1	1	1	PTOF	Push floating point operand on TOS to NOS.
R	1	1	1	1	0	0	0	POPS	Pop single precision fixed point operand from TOS. NOS becomes TOS.
R	0	1	1	1	0	0	0	POPD	Pop double precision fixed point operand from TOS. NOS becomes TOS.
R	0	0	1	1	0	0	0	POPF	Pop floating point operand from TOS. NOS becomes TOS.
R	1	1	1	1	0	0	1	XCHS	Exchange single precision fixed point operands TOS and NOS.
R	0	1	1	1	0	0	1	XCHD	Exchange double precision fixed point operands TOS and NOS.
R	0	0	1	1	0	0	1	XCHF	Exchange floating point operands TOS and NOS.
R	0	0	1	1	0	1	0	PUPI	Push floating point constant "π" onto TOS. Previous TOS becomes NOS.

Notes: 1. NOMENCLATURE: TOS = Top Of Stack, NOS = Next On Stack.
2. All derived floating point functions destroy the contents of the stack. Only the result can be counted on to be valid upon command completion.
3. Format conversion commands (FIXS, FIXD, FLTS, FLTD) require that floating point data format be specified (command bits 5 and 6 must be 0).

B. The Microprogram for the Microcomputer System

The various functions of the microcomputer systems are implemented as commands listed in Table 32. The microprogram that implements the various commands is given following Table 32.

TABLE 32
TABLE OF COMMANDS IMPLEMENTED IN
THE MICROCOMPUTER SYSTEM

COMMAND CODE	DESCRIPTIONS
F	Restart
A	Display a memory waveform on the Oscilloscope
8	Branch to another ROM
7	Displays data values of interest
6	Change or enter the number of waveform taken to form an average waveform
H	Change or enter number of samples per waveform
2	Change or enter the sequence number for the next waveform
1	Initiate Recording sequence via the push button
Ø	Record a waveform, and perform the identification process
B	Dump memory onto tape
D	Check if data transmission to recorder is error-free

```
ASM80 SDKTRA.TXT OBJECT(:F1:SDKTRA.OBJ) PRINT(:F1:SDKTRA.LST) NOPAGING
ISIS-II 8080/8085 MACRO ASSEMBLER, V1.0        SDKTRA                          PAGE
 1
  LOC  OBJ          SEQ          SOURCE STATEMENT
                      0 ;***************************
                      1 ;       THIS IS THE CASSETTE TAPE RECORDING VERSION OF
                      2 ;       THE SDK PORTABLE MICROCOMPUTER SYSTEM PROGRAM.
                      3 ;       IT IS USED WITH THE MODIFIED TERRASCAN UNIT
                      4 ;       TO RECORD 148 POINT WAVEFORMS.
                      5 ;       IT HAS THE ABILITY TO DO DATA PROCESSING USING
                      6 ;       AN AM9511 APU CHIP.
                      7 ;       THE TERRASCAN PROVIDES A STROBE PULSE FOR THE
                      8 ;       A/D CONVERTER, THEN THE 'END OF CONVERSION'
                      9 ;       SIGNAL STROBES THE INTERRUPT BIT PC4.
                     10 ;       A NEGATIVE TRUE SIGNAL ON PC1 (BOW) SIGNALS THE
                     11 ;       PROGRAM THAT THE TERRASCAN IS AT THE BEGINNING
                     12 ;       OF A WAVEFORM.
                     13 ;***************************
                     14 ;
                     15 ;       **** MODULES WHICH LINK WITH SDKTRA ARE:
                     16 ;               SDKID   ;TARGET IDENTIFICATION ROUTINE.
                     17 ;               IFLP    ;CONSTANTS FOR USE BY SDKID.
                     18 ;
                     19         NAME    SDKTRA
                     20 ;
                     21         EXTRN   SRTID,DSTAT
                     22         PUBLIC  BGPTR,STRPTR
                     23         PUBLIC  NAVGS,NAVG      ;NAVGS=2**NAVG
                     24         PUBLIC  ALARM,UPDISP,DSPLTC,SEGNO
                     25         PUBLIC  NEGML
                     26 ;
                     27         STKLN   1AH     ;ALLOTTED STACK LENGTH.
                     28 ;
                     29 ;
                     30 ;       *** IDADD IS THE NUMBER OF BYTES ADDED TO A
                     31 ;       *** WAVEFORM DATA RECORD BY IDENTIFICATION
                     32 ;       *** ROUTINE 'SRTID'.
  0019               33 IDADD   EQU     6*4+1
  0000               34 ROAD    EQU     0
  04C0               35 ROM1    EQU     40CH
  0800               36 ROM2    EQU     800H
  0C00               37 ROM3    EQU     0C00H
                     38 ;       *** 8251 USART ***
  00FA               39 LINR    EQU     0FAH
  00FB               40 LINCMD  EQU     0FBH
  0040               41 RESET   EQU     40H
  000C               42 SYMODE  EQU     0CH
  0020               43 WAITCM  EQU     20H
  00CD               44 ASMODE  EQU     0CDH    ;X1 CLOCK,2 STOP BITS
  0021               45 TXEN    EQU     21H
  0001               46 LINST   EQU     1
  0004               47 TXEMPT  EQU     4
  005A               48 ASYN1   EQU     5AH
  00E5               49 ASYN2   EQU     0E5H
  00AC               50 SYN1    EQU     0ACH
```

```
0067                   STB2    EQU     67H
                       ;       *** 8279 KEYBOARD/DISPLAY INTERFACE ***
00DF                   KBCNTR  EQU     0DFH
00DE                   KEYBD   EQU     0DEH
00DE                   DISPLY  EQU     0DEH
000F                   FUINST  EQU     0FH
                       ;       *** 8255 I/O PORT (LEFT HAND SOCKET=A4) ***
00EF                   DATCNT  EQU     0EFH    ;CONTROL
00EC                   RCVDAT  EQU     0ECH    ;PORT A (DATA)
00ED                   RAMP    EQU     0EDH    ;PORT B
00EE                   MRAST   EQU     0EEH    ;PORT C
0009                   INTREN  EQU     9
                       ;       *** 8255 I/O PORT (RIGHT HAND SOCKET=A3)
00F7                   PICNTR  EQU     0F7H
00F4                   PIA     EQU     0F4H
00F5                   PIB     EQU     0F5H
00F6                   PIC     EQU     0F6H
                       ;       ***
0080                   ROW     EQU     80H
0040                   ROSTAT  EQU     40H
003F                   CUTMSK  EQU     3FH
0040                   MRBUIT  EQU     40H
000E                   CLR7    EQU     0EH
000F                   SET7    EQU     0FH
                       ;       *** PROGRAM INTENDED TO RESIDE IN ROM0 ***
                               CSEG    ;CODE SEGMENT.
                       ;
0000 F3                START:  DI
0001 310000    S               LXI     SP,STACK
0004 210040                    LXI     H,4000H
0007 220000    D               SHLD    DBUFTP  ;INITIALIZE TOP OF BUFFER POINT

                       ;       *** INITIALIZE DEFAULT SYSTEM PARAMETERS ***
                       ;           8 AVG.    128 PTS/WAVEFORM
000A 3E08                      MVI     A,08H
000C 320000    D               STA     NAVGS
000F 3E80                      MVI     A,80H
0011 320000    D               STA     NPTS
0014 210000                    LXI     H,0
0017 220000    D               SHLD    SYSFLG  ;RESETS SYSFLG AND FLAG.
                       ;       *** INITIALIZE DATA BUFFER POINTERS
001A 210000                    LXI     H,DBUF0
001D 220000    D               SHLD    STRPTR  ;STORE POINTER
                       ;       *** INITIALIZE PARALLEL PORT A4 ***
0020 3EB1                      MVI     A,0B1H
0022 D3EF                      OUT     DATCNT  ;DATA CONTROL PORT
                                               ;(RCVD DATA + RAMP)
                       ;       *** INITIALIZE SEQUENCE NUMBER TO 0 ***
0024 AF                        XRA     A
0025 320000    D               STA     SEQNO
0028 3E09                      MVI     A,INTREN        ;INTERRUPT ENABLE
002A D3EF                      OUT     DATCNT  ;SET BIT PC4
                       ;INITIALIZE NPT & NAVG TO DEFAULT VALUES
002C 210000                    LXI     H,(8000H+[illegible])   ;NO. PTS/RECORD 256*8+[illegible]
                       END
```

```
002F 221400   C   104          SHLD   NPT
0032 3E02         105          MVI    A,2      ;2**2 AVGS
0034 C33E00   C   106          JMP    AROUND
                  107 ;     ***************
                  108 ;     DON'T FORGET 38H IS INTERRUPT LOCATION
                  109 ;     ***************
0038              110          ORG    38H
0038 C37100   C   111          JMP    INTRPT   ;INTERRUPT VECTOR
                  112 ;     *** INITIALIZE 8279 KEYBOARD + DISPLAY
003B 321600   D   113 AROUND:  STA    NAVG
003E 3E34         114          MVI    A,20H+20D        ;PRESCALE FOR CLOCK = 2
0040 D3CF         115          OUT    KDCNTR
0042 3E02         116          MVI    A,2      ;LEFT ENTRY,ENCODED N-KEY ROLLO
ER
0044 D3CF         117          OUT    KDCNTR
                  118 ;        *** INITIALIZE 8251 (USART) ***
0046 AF           119          XRA    A        ;CLEAR AND RESET LINK
0047 D3F9         120          OUT    LINCMD   ;CLEAR UNDEFINED STARTUP STATE
0049 D3F9         121          OUT    LINCMD
004B D3F9         122          OUT    LINCMD
004D 3E40         123 SETSYN:  MVI    A,RESET
004F D3F9         124          OUT    LINCMD   ;ASYNCHRONOUS MODE
0051 3ECE         125          MVI    A,ASMODE
0053 D3F9         126          OUT    LINCMD
0055 3E21         127          MVI    A,TXEN   ;ENABLE TRANSMITTER
0057 D3F9         128          OUT    LINCMD
0059 CDC000   C   129 COMMLP:  CALL   CLRDSP
                  130 ;        *** COMMAND LOOP ***
005C 310000   S   131 CMDLP:   LXI    SP,STACK
005F CD2A00   C   132          CALL   BEEP
0062 CD0000   C   133          CALL   RDKB     ;READ AND DISPLAY KEYPRESS
0065 CDEA00   C   134          CALL   DISP1
0068 FE0F         135          CPI    0FH
006A CA0000   C   136          JZ     START    ;RESTART
006D FE0E         137          CPI    0EH
006F CA0000   C   138          JZ     DPUNT    ;DUMP MEMORY ONTO TAPE
0072 FE0A         139          CPI    0AH
0074 CA0000   C   140          JZ     WAVOUT   ;DISPLAY A WAVEFORM VIA D/A
0077 FE08         141          CPI    8
0079 CA0000   C   142          JZ     RENCH    ;BRANCH TO ANOTHER ROM
007C FE07         143          CPI    7
007E CA0000   C   144          JZ     TUNEUP   ;DISPLAY DATA VALUES OF INTEREST
0081 FE06         145          CPI    6
0083 CA0000   C   146          JZ     NAVRD    ;READ NO. OF WAVEFORMS TO BE AVE
RAGED.
0086 FE02         147          CPI    2
0088 CA2100   C   148          JZ     SEQSET   ;SET SEQUENCE NUMBER
008B FE00         149          CPI    0
008D CC0001   C   150          CZ     ROM
0090 C35C00   C   151          JMP    CMDLP
                  152 ;
                  153 ;        ***********
                  154 ;
0093 CD0000   C   155 RONCHI:  CALL   RDKB
0096 CDEA00   C   156          CALL   DISP1
```

```
0099 FE03             CPI     0
009B CA0000           JZ      ROM0
009E FE02             CPI     2
00A0 CA0000           JZ      ROM2
00A3 FE03             CPI     3
00A5 CA0000           JZ      ROM3
00A8 C3DC00     C     JMP     CMDLP       .
                    ;
                    ;         **********
                    ;
                    ;         *** FOR EACH INCOMING WAVEFORM COMPUTE AND
                    ;         *** DISPLAY AVG. VALUE, PEAK VALUE (ABOVE
                    ;         *** OR BELOW 1/2 FULL SCALE), AND POSITION
                    ;         *** OF THIS PEAK (0 TO 7FH).
00AB CD0400     C     TUNEUP: CALL    TUNE
00AE 3A1A00     D             LDA     TPEAK   ;FETCH PEAK VALUE
00B1 0600                     MVI     B,0     ;SELECT LEFTMOST 2 DIGITS
00B3 CDF500     C             CALL    DPDISP  ;DISPLAY 2 CONSECUTIVE DIGITS
00B6 3A1C00     C             LDA     TTIME   ;FETCH TIME OF PEAK
00B9 CDFA00     C             CALL    DSPCTR  ;DISPLAY IN CENTER 2 DIGITS
00BC 3A1E00     C             LDA     TAVG    ;FETCH AVG. VALUE
00BF CDFA00     C             CALL    DSPRTR  ;DISPLAY IN RIGHTMOST 2 DIGITS
00C2 DB0F                     IN      KBCNTR  ;FIFO STATUS WORD
00C4 E60F                     ANI     0FH     ;ANY KEYPRESSES ?
00C6 CAAB00     C             JZ      TUNEUP  ;IF NO STAY IN TUNEUP MODE
00C9 CDE000     C             CALL    KIN     ;IF YES FETCH VALUE OF KEYPRESS
00CC FE0C                     CPI     0CH
00CE C2AB00     C             JNZ     TUNEUP  ;JUMP IF NOT 'C'
00D1 C39900     C             JMP     CMDCLR  ;IF 'C' CLEAR DISPLAY &
                                              ;ENTER COMMAND LOOP
00D4 AF               TUNE:   XRA     A       ;INITIALIZE RAMP COUNT
00D5 320A00     C             STA     RMPSTR
00D8 320A00     C             STA     FLAG    ;RESET RUN FLAG
00DB 67                       MOV     H,A
00DC 6F                       MOV     L,A
00DD 221E00     C             SHLD    TAVG
00E0 3E80                     MVI     A,80H   ;1/2 FULL SCALE
00E2 321A00     C             STA     TPEAK
00E5 321C00     C             STA     TPPEAK
00E8 CD0000     C             CALL    WSYNC   ;WAIT FOR BEG. OF WAVEFORM
00EB FB               TLOOP:  EI
00EC 3A0E00     D     TWAIT:  LDA     SYSFLG  ;WORD READ LATELY
00EF E680                     ANI     RDSTAT
00F1 CAEC00     C             JZ      TWAIT   ;JUMP IF NO
00F4 3A0E00     D             LDA     SYSFLG
00F7 E67F                     ANI     NOT RDSTAT
00F9 320E00     C             STA     SYSFLG  ;RESET READ FLAG
00FC 3A0000     C             LDA     DAVG
00FF 4F                       MOV     C,A
0100 3A1A00     C             LDA     TPEAK
0103 B9                       CMP     C
0104 D21100     C             JNC     TMIN    ;JUMP IF NEW DATA NOT > TPEAK
0107 79                       MOV     A,C     ;NEW DATA IS GREATER THAN
0108 321A00     C             STA     TPEAK   ;OLD DATA, SO UPDATE
010B 3A0A00     C             LDA     RMPSTR
```

```
010E 321?0?   C   212          STA    TTIME     ;SAVE   POSITION OF THE +PEAK
0111 3A1C0?   C   213 TMIN1    LDA    TPKNEG
0114 B9           214          CMP    C
0115 DA220?   C   215          JC     TAVER     ;JUMP IF NEW DATA PT < TPKNEG
0118 79           216          MOV    A,C       ;NEW DATA IS SMALLER
0119 321C0?   C   217          STA    TPKNEG    ;THAN OLD TPKNEG
011C 3A0A0?   C   218          LDA    RMPSTR
011F 3210??   C   219          STA    TIMNEG    ;SAVE POS. OF THE -PEAK
0122 0600         220 TAVER1   MVI    B,0       ;BC HAS DATA
0124 2A180?   C   221          LHLD   TAVG
0127 09           222          DAD    B
0128 221?0?   C   223          SHLD   TAVG      ;UPDATE SUM
012B 210A0?   C   224          LXI    H,RMPSTR
012E 34           225          INR    M         ;INCREMENT RAMP COUNT
012F 3A0?0?   C   226          LDA    NPTS      ;# OF PTS/WAVEFORM
0132 BE           227          CMP    M         ;RAMP DONE ?
0133 C2??0?   C   228          JNZ    LOOP      ;IF NOT CONTINUE DATA TAKING
0136 3A1C0?   C   229          LDA    TPKNEG    ;IS (+) OR (-) PEAK LARGER
0139 4F           230          MOV    C,A
013A 3A1A0?   C   231          LDA    TPEAK
013D 81           232          ADD    C
013E DA??0?   C   233          JC     FIXAVG    ;CARRY SET IF TPEAK IS LARGER
0141 79           234          MOV    A,C
0142 321A0?   C   235          STA    TPEAK     ;LET TPKNEG, TIMNEG
0145 3A1?0?   C   236          LDA    TIMNEG    ;BE DISPLAYED
0148 321?0?   C   237          STA    TTIME
014B 0E07         238 FIXAVG   MVI    C,7
014D 2A1?0?   C   239          LHLD   TAVG      ;SUM OF DATA VALUES
0150 C??F0?   C   240          CALL   HLSHF?    ;DIVIDE H,L BY
0153 221?0?   C   241          SHLD   TAVG      ;# OF PTS/WAVEFORM
0156 F3           242          DI
0157 C9           243          RET
                  244 ;
                  245 ;        ****************
                  246 ;
0158 2A??0?   C   247 DUMP     LHLD   STRPTR
015B C???0?   C   248          CALL   NEGHL
015E EB           249          XCHG
015F 2A0?0?   C   250          LHLD   DBLFTP
0162 19           251          DAD    D         ;# OF PTS LEFT IN BUFFER IN HL
0163 EB           252          XCHG             ;NOW IN D,E
0164 2A140?   C   253          LHLD   NPT
0167 C???0?   C   254          CALL   NEGHL
016A 19           255          DAD    D         ;SUBTRACT # OF PTS/RECORD FROM
                  256                           ;# OF PTS LEFT IN BUFFER
016B DA??0?   C   257          JMP    ALARM     ;IF NO SPACE LEFT, DUMP BUFFER
NTO TAPE
016E AF           258          XRA    A
016F FA?3         259          CPI    ?         ;SET RUN AND TAPE WAVEFORM FLAG
0171 320F0?   C   260          STA    FLAG
                  261 ;PUSH PREAMBLE ONTO STACK
0174 C???0?   C   262          CALL   PRE??
0177 2A??0?   C   263          LHLD   STRPT?
017A 22??0?   C   264          SHLD   BGPTR     ;SAVE BEGINNING OF DATA ADDRES.
                  265 ;CLEAR OUT BUFFER
```

```
0170 0E00          266          MVI    C,0
0172 2A0000   C    267          LHLD   STRPTR
0175 AF            268          XRA    A
0183 77            269 CLRLP:   MOV    M,A
0184 23            270          INX    H
0185 0D            271          DCR    C
0186 C20301   C    272          JNZ    CLRLP
0189 3A1500   C    273 RUPGI:   LDA    SEQNO    ;FETCH SEQUENCE NUMBER
018C 0602          274          MVI    B,2
018E CDF302   C    275          CALL   UPDISP   ;DISPLAY 2 DIGITS (CENTER)
0191 3A0000   C    276          LDA    NAVGS
0194 4F            277          MOV    C,A
0195 3A0000   C    278          LDA    SYSFLG
0198 E6C1          279          ANI    NOT CNTMSK       ;CLEAR OUT OLD # OF AVG.
019A B1            280          ORA    C        ;REPLACE WITH NEW #
019B 320000   C    281          STA    SYSFLG
019E E63F          282          ANI    CNTMSK   ;LEAVE ONLY # OF AVGS.
01A0 CDF700   C    283          CALL   DSPEIC   ;DISPLAY IN DIGITS 4 + 5
01A3 CD0000   C    284 RLOOP:   CALL   BEEP
01A6 AF            285          XRA    A        ;RESET RAMP COUNTER
01A7 320000   C    286          STA    RMPSTR
01AA CD3300   C    287          CALL   SYNCH
01AD 3A0000   C    288 STWAT:   LDA    SYSFLG   ;WORD READ LATELY ?
01B0 E640          289          ANI    RDSTAT
01B2 CA0001   C    290          JZ     STWAT    ;JUMP IF NO
01B5 3A0000   C    291          LDA    SYSFLG
01B8 E6BF          292          ANI    NOT RDSTAT       ;CLEAR WORD FLAG
01BA 320000   C    293          STA    SYSFLG
                   294 ;INTEGRATE CURRENT DATA FROM RADAR SYSTEM
01BD 2A0000   C    295          LHLD   DAVG     ;FETCH DATA
01C0 EB            296          XCHG
01C1 2A0000   C    297          LHLD   STRPTR   ;FETCH ADDR OF SUM
01C4 4E            298          MOV    C,M      ;LOW ORDER BYTE OF SUM
01C5 23            299          INX    H
01C6 46            300          MOV    B,M      ;HIGH ORDER BYTE
01C7 EB            301          XCHG            ;DATA NOW IN HL
01C8 3A0000   C    302          LDA    FLAG
01CB E602          303          ANI    2        ;CHECK WHETHER 'A' OR 'B' SWEEP
01CD C2D301   C    304          JNZ    RUN1     ;JUMP IF 'A'
01D0 CD0000   C    305          CALL   NEGHL    ;WAVEFORM 'B' (-DATA IN HL)
01D3 09            306 RUN1:    DAD    B        ;ADD DATA TO SUM.
01D4 EB            307          XCHG
01D5 2A0000   C    308          LHLD   STRPTR   ;FETCH ADDR OF SUM
01D8 73            309          MOV    M,E      ;SAVE LOW ORDER BYTE
01D9 23            310          INX    H
01DA 72            311          MOV    M,D      ;SAVE HIGH ORDER BYTE
01DB 23            312          INX    H
01DC 220000   C    313          SHLD   STRPTR   ;SAVE ADDRESS OF NEXT SUM
                   314 ;INCREMENT RAMP
01DF 3A0000   C    315          LDA    RMPSTR
01E2 3C            316          INR    A
01E3 320000   C    317          STA    RMPSTR
01E6 4F            318          MOV    C,A
01E7 3A0000   C    319          LDA    NPTS     ;GET # OF PTS/WAVEFORM
01EA B9            320          CMP    C        ;RAMP DONE ?
```

```
0IEB C?F201    C   321             JZ      RMPDUN   ;JUMP IF YES
0IEE FB            322             EI
0IEF C3A301    C   323             JMP     STWAT
01F2 F3            324 RMPDUN:     DI
01F3 2A0200    D   325             LHLD    BGPTR
01F6 220000    D   326             SHLD    STRPTR
01F9 3A0E00    D   327             LDA     SYSFLG
01FC 3D            328             DCR     A
01FD 320E00    D   329             STA     SYSFLG
0200 0604          330             MVI     B,4
0202 E63F          331             ANI     CNTMSK
0204 CDF302    C   332             CALL    UPDISP
0207 3A0E00    D   333             LDA     SYSFLG
020A E63F          334             ANI     CNTMSK
020C C2A301    C   335             JNZ     RLOOP
020F 3A0F00    D   336 RMPDON:     LDA     FLAG
0212 E602          337             ANI     2           ;WAVEFORM 'A' OR 'B' ?
0214 CA3000    C   338             JZ      DONE        ;FINISHED IF 'B'
0217 3A0F00    D   339             LDA     FLAG
021A E601          340             ANI     1           ;RESET 'A' WAVEFORM FLAG
021C 320F00    D   341             STA     FLAG        ;SAVE IT.
021F CDC000    C   342             CALL    CLRLSP      ;CLEAR EARLIER KEYPRESSES.
0222 CD2A03    C   343 RMPDN1:     CALL    BEEP
0225 CD0A00    C   344             CALL    KPIN
0228 FE00          345             CPI     0           ;PRESS '0' FOR 90DEG POLARZ.
022A CA9001    C   346             JZ      RUPU
022D C32200    C   347             JMP     RMPDN1
                   348 ;
0230 2A0000    D   349 DONE:       LHLD    STRPTR
0233 1601          350             MVI     D,1
0235 1E00          351             MVI     E,0
0237 19            352             DAD     D
0238 220000    D   353             SHLD    STRPTR
                   354 ;           *** SPTID ROUTINE ADDS 'IDADD' BYTES TO
                   355 ;           *** BUFFER, INCREMENTING STRPTR ACCORDINGLY.
023B CD0000    E   356             CALL    SPTID       ;PERFORM IDENTIFICATION.
                   357 ;
                   358 ;           PUSH POSTAMBLE UNTO STACK
                   359 ;           (CHECKSUM / DELAY)
023E CD7403    C   360             CALL    CHEKSM
0241 2A1100    D   361             LHLD    CHKSUM
0244 CD7303    C   362             CALL    NEGHL
0247 221100    D   363             SHLD    CHKSUM
024A 211100    D   364             LXI     H,CHKSUM
024D 0E02          365             MVI     C,2
024F CD6300    C   366             CALL    STKWAT
0252 3EFF          367             MVI     A,0FFH      ;INTER RECORD GAP
0254 CD5303    C   368             CALL    UPUSH
0257 3A1300    D   369             LDA     SEQNO
025A 3C            370             INR     A
025B 321300    D   371             STA     SEQNO       ;UPDATE SEQUENCE NUMBER
025E 2A0000    D   372             LHLD    STRPTR
0261 420600    D   373             SHLD    ENDPTR      ;STORE END OF DATA POINTER
                   374 ;           *** IF TARGET DETECTED, SET OFF ALARM.
0264 210000    E   375             LXI     H,DSTAT
```

```
0267 7E                        MOV     A,M
0268 E640                      ANI     40H     ;CODE FOR SUCCESSFUL DETECTION.
026A C2BE04    C               JNZ     ALARM
                        ;
026D C02A05    C               CALL    BEEP
0270 C9                        RET
                        ;
                        ;              ****************************************
                        ;
                        ;INTERRUPT PROCESSING ROUTINE ADDS INCOMING DATA
                        ;TO THE TEMP BUFFER DAVG
                        ;              **********
0271 F3                 INTRPT: DI
0272 F5                        PUSH    PSW
0273 DBEE                      IN      MRPST   ;READ C PORT. MUST READ ASAP
                                               ;AFTER INTERUPT TO CATCH BOW.
0275 E5                        PUSH    H
0276 C5                        PUSH    B
                        ;      READ BEGINNING OF WAVEFORM (BOW) FLAG
0277 0F                        RRC
0278 0F                        RRC
0279 2F                        CMA             ;BOW SIGNAL IS NEGATIVE TRUE
027A E680                      ANI     BOW
027C 4F                        MOV     C,A
027D 3A0E0         C           LDA     SYSFLG
0280 E67F                      ANI     NOT BOW ;CLEAR OLD BOW BIT
0282 B1                        ORA     C       ;INSERT NEW BOW BIT
0283 320E0         C           STA     SYSFLG
0286 DBEC                      IN      RCVDAT  ;READ DATA PORT.
                                               ;RESETS INTERRUPT TO CPU
0288 4F                        MOV     C,A     ;SAVE DATA
0289 3A0E0         C           LDA     SYSFLG
028C E640                      ANI     RDSTAT
028E C24F0         C           JNZ     DOUT    ;JUMP IF LAST RESULT WAS NOT
                                               ;SERVICED, LOSS OF DATA!!!!!!
                        ;ADD DATA TO DAVG
0291 2600                      MVI     H,0
0293 69                        MOV     L,C
0294 3A0F0         C           LDA     FLAG
0297 E601                      ANI     1
0299 CA         C              JZ      INTION  ;IF IN TUNEUP KEEP MAGNITUDES
029C 1EFF                      MVI     E,0FFH
029E 1E80                      MVI     E,80H
02A0 19                        DAD     D       ;CONVERT TO SIGNED NUMBERS
02A1 220B0         C    TIIRP1: SHLD   DAVG
                        ;SET DATA READY FLAG
02A4 3A0E0         C           LDA     SYSFLG
02A7 F640                      ORI     RDSTAT
02A9 320E0         C           STA     SYSFLG
02AC C1                        POP     B
02AD E1                        POP     H
02AE F1                        POP     PSW
02AF FB                        EI
02B0 C9                        RET
02B1 CD0           C    DAVRDY: CALL   RDT
```

```
0244 FE06                    CPI     6
0246 D28102      C           JNC     NAVRD     ;LOOP IF INVALID
0249 32180 1     C           STA     NAVG
024C 3C                      INR     A
024D 4F                      MOV     C,A
024E 3E80                    MVI     A,80H
0250 07          AVROT:      RLC               ;CHANGE 0,1,2,3,4,5
0251 0D                      DCR     C
0252 C2C002      C           JNZ     AVRO
0255 32C00       C           STA     NAVGS     ;TO 1,2,4,8,16,32
0258 C35901      C           JMP     CCMPLP
025B 3EC1        CLRDSP:     MVI     A,0C1H    ;CLEAR ALL STATUS AND DISPLAY
025D D30F                    OUT     KDCNTR
025F DB0F        CLRWT:      IN      KDCNTR    ;WAIT FOR CLEAR TO FINISH
0261 17                      RAL
0262 DACF02      C           JC      CLRWT
0265 C9                      RET
                 ;           ***********
                 ;           READ DIGIT FROM 16 KEY KEYPAD
                 ;           THE KEYBOARD INTERFACE HAS AN INTERNAL FIFO.
0266 DB0F        KRIN:       IN      KDCNTR    ;FIFO STATUS WORD
0268 E60F                    ANI     KBINST
026A CA0E02      C           JZ      KRIN      ;LOOP IF FIFO EMPTY
026D CD2A0       C           CALL    BELP
02E0 3E40        KIN1:       MVI     A,40H     ;SPECIFY FIFO READ
02E2 D30F                    OUT     KDCNTR
02E4 DB0E                    IN      KEYBD
02E6 E63F                    ANI     3FH       ;CHANGE SCAN/RETURN CODE
02E8 0F                      RRC               ;INTO HEX VALUE
02E9 C9                      RET
                 ;           DISPLAY VALUE IN LEFTMOST LED
02EA F5          DISP1:      PUSH    PSW
02EB 3E90                    MVI     A,90H     ;SELECT LEFTMOST DIGIT
02ED D30F                    OUT     KDCNTR
02EF F1                      POP     PSW
02F0 D30E                    OUT     DISPLY
02F2 C9                      RET
                 ;           ***********
                 ;           DISPLAY 2 HEX DIGITS FROM 'A' REG IN LED'S
                 ;           STARTING WITH CELL SPECIFIED BY 'B' REG.
                 ;           ***********
02F3 4F          UPDISP:     MOV     C,A
02F4 3E90                    MVI     A,90H     ;WRITE DISPLAY RAM
02F6 80                      ADD     B         ;0,1,2,3,4,5
02F7 D30F                    OUT     KDCNTA
02F9 79                      MOV     A,C
                 ;ENTER HERE TO DISPLAY AT NEXT
                 ;TWO RAM ADDRESSES.
02FA 4F          DSPETC:     MOV     C,A
02FB 1F                      RAR
02FC 1F                      RAR
02FD 1F                      RAR
02FE 1F                      RAR
02FF E60F                    ANI     0FH
0301 D30E                    OUT     DISPLY    ;WRITE HIGH ORDER DIGIT
```

```
0303 79                486              MOV     A,C
0304 E60F              487              ANI     0FH
0306 D30E              488              OUT     DISPLY  ;WRITE LOW ORDER DIGIT
0308 C9                489              RET
                       490 ;
                       491 ;            READ TWO DIGITS FROM KEYBOARD & PACK INTO 'A' RE
                       492 ;
0309 CD0603    C       493 TWODIG:      CALL    KBIN
030C 47                494              MOV     B,A     ;SAVE 1ST (HI ORDER) DIGIT
030D 07                495              RLC
030E 07                496              RLC
030F 07                497              RLC
0310 07                498              RLC
0311 D30E              499              OUT     DISPLY  ;ZERO 2ND DIGIT
0313 4F                500              MOV     C,A
0314 CD0603    C       501              CALL    KBIN
0317 B1                502              ORA     C
0318 F5                503              PUSH    PSW
0319 78                504              MOV     A,B     ;RETRIEVE 1ST (HI ORDER) DIGIT
031A CDEA03    C       505              CALL    DISP1   ;PUT INTO LEFTMOST LED
031D F1                506              POP     PSW
031E D30E              507              OUT     DISPLY  ;2ND DIGIT INTO 2ND LE
0320 C9                508              RET
                       509 ;
                       510 ;SEQSET ALLOWS THE SEQUENCE # TO BE SPECIFIED.
                       511 ;THE SEQUENCE # IS INCREMENTED EVERY TIME 'RUN'
                       512 ;SEQUENCE IS EXECUTED.
                       513 ;
0321 CD0903    C       514 SEQSET:      CALL    TWODIG
0324 321300    D       515              STA     SEQNO
0327 C3[illegible]    C       516              JMP     CONSLP
                       517 ;
                       518 ;TRIGGER ALARM SO THAT IT 'BEEPS'
                       519 ;BEEPER CONTROLLED BY BIT PC7
                       520 ;
032A F5                521 BEEP:        PUSH    PSW
032B 3E0E              522              MVI     A,CLR7
032D D3EF              523              OUT     DATCNT
032F 3E0F              524              MVI     A,SET7
0331 D3EF              525              OUT     DATCNT
0333 F1                526              POP     PSW
0334 C9                527              RET
                       528 ;
                       529 ;
                       530 ;
0335 3EAC              531 PREAMB:      MVI     A,STX1
0337 CD5A[illegible]    C       532              CALL    UPUSH
033A 3E67              533              MVI     A,STX2
033C CD5A[illegible]    C       534              CALL    UPUSH
033F 3A[illegible]    D       535              LDA     NPTS    ;# OF DATA PTS & # OF AVG'SS
0342 CD5A[illegible]    C       536              CALL    UPUSH
0345 3A15[illegible]    D       537              LDA     NAVG    ;STORE NAVG NOT NAVGS!!!!!!
0348 CD5A[illegible]    C       538              CALL    UPUSH
034B 3A13[illegible]    D       539              LDA     SEQNO
```

```
0346 CD5003   C   540         CALL    DPUSH
0349 2A00D0   L   541         LHLD    STRPTR
034C 22020D   L   542         SHLD    BGPTR   ;STORE BEGINNING OF DATA POINTER
034F C9           543         RET
                  544 ;
                  545 ;PUSH BYTE ONTO THE STACK
                  546 ;
0350 E5           547 DPUSH:  PUSH    H
0351 C5           548         PUSH    B
0352 2A00D0   D   549         LHLD    STRPTR
0355 77           550         MOV     M,A
0356 23           551         INX     H
0357 2200D0   L   552         SHLD    STRPTR
035A C1           553         POP     B
035B E1           554         POP     H
035C C9           555         RET
                  556 ;
                  557 ;       PUSH (C) CONSECUTIVE WORDS ONTO DATA STACK
                  558 ;
035D 7E           559 STRWRT: MOV     A,M
035E CD5003   C   560         CALL    DPUSH
0361 23           561         INX     H
0362 0D           562         DCR     C
0363 C25D03   C   563         JNZ     STRWRT
0366 C9           564         RET
                  565 ;
                  566 ;       SHIFT H&L RIGHT (C) TIMES
                  567 ;
036F B7           568 HLSHFR: ORA     A       ;CLEAR  CARRY
0370 7C           569         MOV     A,H
0371 1F           570         RAR
0372 67           571         MOV     H,A
0373 7D           572         MOV     A,L
0374 1F           573         RAR
0375 6F           574         MOV     L,A
0376 0D           575         DCR     C
0377 C26F03   C   576         JNZ     HLSHFR
037A C9           577         RET
                  578 ;
                  579 ;       ROUTINE ADDS CONTENTS OF HL TO CHKSUM
                  580 ;
037B 210000       581 CHEKSM: LXI     H,0
037E 22110D   D   582         SHLD    CHKSUM  ;RESET CHECKSUM
0381 2A020D   L   583         LHLD    BGPTR   ;FETCH BEGINNING OF DATA ADDR
0384 0E80         584         MVI     C,80H   ;128 DATA PTS
0386 E5           585 CHKSM0: PUSH    H
0387 5E           586         MOV     E,M     ;FETCH DATA
0388 1600         587         MVI     D,0
038A 2A110D   D   588         LHLD    CHKSUM  ;FETCH TOTAL
038D 19           589         DAD     D       ;ADD THEM TOGETHER
038E 22110D   D   590         SHLD    CHKSUM  ;SAVE THE RESULT
0391 E1           591         POP     H
0392 23           592         INX     H
0393 0D           593         DCR     C
0394 C28603   C   594         JNZ     CHKSM0  ;KEEP LOOPING IF HAVEN'T
```

```
                                        ;REACHED END OF DATA
0397 C9                         RET
                        ;
                        ;       NEGATE H+L REGISTER
                        ;
0398 7C                 NEGHL:  MOV     A,H
0399 2F                         CMA
039A 67                         MOV     H,A
039B 7D                         MOV     A,L
039C 2F                         CMA
039D 6F                         MOV     L,A
039E 23                         INX     H
039F C9                         RET
                        ;
                        ;
                        ;
                        ;       **** CONTINUOUSLY OUTPUT WAVEFORM TO D/A FOR
                        ;       **** VIEWING ON A MONITOR SCOPE.
                        ;
03A0 CD0500     C       WAVOUT: CALL    TVDAT
03A3 321000     C               STA     SGNO
03A6 214924                     LXI     H,MHLFB
03A9 110600                     LXI     D,0006
03AC 1A                 WVOUT1: LDAX    D               ;GET POSITION OF S.GNO.
03AD 220300     C               SHLD    DAVG            ;SAVE IT.
03B0 CD9803     C               CALL    NEGHL
03B3 EB                         XCHG
03B4 2A0000     C               LHLD    STPPTR
03B7 19                         DAD     D               ;SEE IF WE HAVE GONE
                                                        ;PAST GOOD DATA.
03B8 D25900     C               JNC     CCMPLE          ;JUMP IF YES
03BB 2A0300     C               LHLD    DAVG
03BE 4E                         MOV     C,M             ;FETCH SEG NO
03BF 3A1000     C               LDA     SGNO
03C2 B9                         CMP     C
03C3 2A1400     C               LHLD    NPT
03C6 EB                         XCHG
03C7 2A0300     C               LHLD    DAVG
03CA C2AC03     C               JNZ     WVOUT1          ;IF NOT TRY NEXT RECORD
03CD 2A0300     C       WVOUT2: LHLD    DAVG            ;DAVG POINTS AT SEGNO
03D0 2B                         DCX     H               ;SUBTRACT 1 TO POINT AT THE HIGH
T DAVG
03D1 7E                         MOV     A,M
03D2 321700     C               STA     WFAVG           ;WFAVG CONTAINS THE RIGHT WAVG
03D5 23                         INX     H               ;AND 2 TO POINT AT THE FIRST BYT
E OF DATA
03D6 23                         INX     H
03D7 AF                         XRA     A
                        ;       *  OUTPUT TOP & BOTTOM FULL SCALE
                        ;       *  FOR SCOPE SYNCHING PURPOSES!
03D8 D3E0                       OUT     WAVE
03DA CD0C34     C               CALL    DELY
03DD 2F                         CMA
03DE D3E0                       OUT     WAVE
03E0 0680                       MVI     B,80H   ;128 PTS/WAVEFORM ALWAYS
```

```
03E2 5E           648 WVLP:   MOV     L,M     ;FETCH LOW ORDER BYTE
03E3 23           649         INX     H
03E4 56           650         MOV     D,M     ;FETCH HIGH ORDER BYTE
03E5 EB           651         XCHG
03E6 3A1C00   C   652         LDA     NAVG
03E9 C601         653         ADI     1       ;ADD 1 TO COMPENSATE FOR 50-DEG
DIFF
03EB 4F           654         MOV     C,A
03EC CDEF03   C   655         CALL    HLSHFR  ;DIVIDE BY NUMBER OF AVGS.
03EF 7D           656         MOV     A,L     ;ONLY LOW ORDER BYTE
                  657                         ;HAS GOOD DATA
03F0 C680         658         ADI     80H     ;CONVERT BACK TO MAGNITUDES
03F2 D3E0         659         OUT     HAMP
03F4 EB           660         XCHG            ;GET ADDRESS BACK IN HL
03F5 23           661         INX     H
03F6 05           662         DCR     B
03F7 C2E203   C   663         JNZ     WVLP
                  664 ;
03FA DBDF         665         IN      KBCNTR  ;KEY PRESSED LATELY?
03FC E6FF         666         ANI     KBINST
03FE CAC003   C   667         JZ      WVOUT2
0401 CDE000   C   668         CALL    KIN     ;YES
0404 FE0C         669         CPI     0CH     ;WAS IT A 'C' ?
0406 CA5900   C   670         JZ      CCMDLP  ;IF SO BACK TO COMMAND LOOP
0409 C3C003   C   671         JMP     WVOUT2  ;IF NOT CONTINUE OUTPUTING
                  672 ;
                  673 ;       **** D/A HAS 30 MICROSECOND SETTLING TIME
                  674 ;       **** CALL=8.5 , DELY=15.5 MICROSECONDS
                  675 ;
040C C5           676 DELY:   PUSH    B
040D C1           677         POP     B
040E C9           678         RET
                  679 ;
                  680 ;       ***************
                  681 ;
040F 21          682 TPWRT:  LXI     H,DABUFO ;BEGINNING OF DATA
0412 DB          683 TPWRT0: IN      LINCML  ;CASSETTE LINK READY?
0414 E601         684         ANI     LINST
0416 CA1204   C   685         JZ      TPWRT0
0419 7E           686         MOV     A,M
041A D3FA         687         OUT     LINA
041C 23           688         INX     H
041D E5           689         PUSH    H
041E CD5000   C   690         CALL    NEGHL
0421 EB           691         XCHG
0422 2A0000   C   692         LHLD    ENDPTR
0425 19           693         DAD     D               ;HAVE WE REACHED THE
                  694                                 ;END OF THE DATA YET?
0426 E1           695         POP     H
0427 DA1204   C   696         JC      TPWRT0  ;KEEP GOING IF NOT
042A 21          697         LXI     H,DABUFO
042D 22       C   698         SHLD    STRPTR  ;RESET STORAGE POINTER
0430 C35900   C   699         JMP     CCMDLP
                  700 ;       BEFORE READING DATA, FIRST SYNCH UP TO BEGINNING
                  701 ;       OF THE WAVEFORM, NOW (BEGINNING OF WAVEFORM)
```

```
                    ;       IS SET BY INTERRUPT ROUTINE.
0433 FB             KSTNUP: EI
0434 76                     HLT
0435 3A0E00    C    SYNUP:  LDA     SYSFLG
0438 E6FE                   ANI     NOT RDSTAT      ;RESET READ FLAG
043A 320E00    C            STA     SYSFLG
043D E601                   ANI     EOW     ;EOW ENCOUNTERED?
043F CA3504    C            JZ      SYNUP   ;NO
0442 3E0F                   MVI     A,SET7  ;CLEAR ALARM
0444 D3EF                   OUT     LATCH
0446 3A0E00    C            LDA     SYSFLG
0449 F6??                   ORI     RDSTAT  ;SET READY FLAG
044B 320E00    C            STA     SYSFLG
044E C9                     RET
                    ;       ********************
                    ;
044F C1             GOLTI:  POP     B
0450 E1                     POP     H
0451 F1                     POP     PSW
0452 3A0F00    C            LDA     FLAG
0455 B7                     ORA     A       ;CHECK RUN FLAG
0456 CA6E04    C            JZ      ALARM   ;JUMP IF IN TUNEUP
0459 3A1300    C            LDA     SEGNO   ;RESET SEQUENCE NUMBER
045C 3C                     LCP     A
045D 321300    C            STA     SEGNO
0460 2A0200    C            LHLD    BGPTR   ;RESET STPPTR
0463 110300                 LXI     D,5
0466 EB                     XCHG
0467 CD9A04    C            CALL    NEGHL
046A 19                     DAD     D       ;RESULT IN HL
046B 220000    C            SHLD    STRPTR
046E 3E0E           ALARM:  MVI     A,CLR7
0470 D3EF                   OUT     LATCNT  ;SET OFF ALARM.
0472 CD0000    C    ALARM0: CALL    KBIN    ;KEYPRESS CLEARS ALARM.
0475 3E0E                   MVI     A,0EH
0477 D3DE                   OUT     DISPLY  ;PUT 'E' IN 2ND LED.
0479 CD0000    C    ALARM1: CALL    KBIN    ;2ND KEY PRESS.
047C FECE                   CPI     0EH     ; RESTARTS AND
047E C27904    C            JNZ     ALARM1  ;  CLEARS DISPLAY.
0481 C38900    C            JMP     CENCLP
                    ;
                    ;       ********************
                    ;
                            DSEG    ;DATA SEGMENT
0000           C    STRPTR: DS      2
0002           C    BGPTR:  DS      2
0004           C    UHUPTR: DS      2
0006           C    FOUPTR: DS      2
0008           C    CAVG:   DS      2
000A           C    RMFSTP: DS      1
000B           C    FPTS:   DS      2
000D           C    AAVGS:  DS      1
000E           C    SYSFLG: DS      1
000F           C    FLAG:   DS      1
0010           C    SEGNO:  DS      1
```

```
  0011          C    757 CHKSUM: DS       2
  0013          C    758 SEGNO:  DS       1
  0014          C    759 FPT:    DS       4
  0018          C    760 NAVG:   DS       1
  0017          C    761 WNAVG:  DS       1
  0018          C    762 TAVG:   DS       2
  001A          C    763 TPEAK:  DS       1
  001B          C    764 TTIME:  DS       1
  001C          C    765 THNEG:  DS       1
  001D          C    766 TIMEFG: DS       1
                     767 ;
                     768 ;
                     769         ASEG     ;ABSOLUTE SEGMENT
  2000               770         ORG      2000H
                     771 ;       *** STORAGE FOR IDENTIFICATION ROUTINES.
                     772 ;       ***  THESE MUST BE DUPLICATED IDENTICALLY IN *
 RING,
  2000               773 DATA:   DS       512
  2200               774 DATA1:  DS       5?0
                     775 ;       BEGINNING OF DATA BUFFER
  2440               776 DBUFD:  DS       1
  0000          C    777         END      START
PUBLIC SYMBOLS
ALARM  C 046?     DPTR  D 0002     DSPETC C 02FA     NAVG   D 0016     NAVGS  D 0·
?      NEGHL  C 0597     SEGNO  D 0013
STRPTR D 000?     UPDISP C 02F3
EXTERNAL SYMBOLS
DSTAT  E 000?     SPTTO  E 0000
USER SYMBOLS
ALARM  C 046?     ALARMU C 0472     ALARM1 C 0479     ARGUPD C 0036     ASCODE A 0·
?      ASYN1  A 00F?     ASYN2  A 00F?
AVNO   C 02C?     BEEP  C 032A     BGPTR  D 0002     BOX    A 00B0     CCNDLP C 0·
?      CHKSM  C 037?     CHKSMO C 03??
CHKSM  D 0011     CLF7  A 00FE     CLRUSR C 020?     CLRLP  C 0103     CLRWT  C 0··
F      CPULP  C 00??     CNTMSK A 00FF
DATA   A 2000     DATA1 A 2200     DATCNT A 00FF     DAVG   D 0006     DBUFD  A 244
B      DBUFIP D 00?4     DELY  C 04?C
DISP1  C 02E?     DISPLY A 00FE    DONE   C 0230     DPUSH  C 0?E8     DSPETC C 02F
A      DSTAT  E 0000     ENDPTH D 0104
FIXAVG C 01?0     FLAG  D 000F     GOUT   C 0?0F     HLSHFR C 03FF     IDAUD  A 0·
?      I1?PD  C ??8?     INTREN A 0000
INTREF C 0271     KBIN  C 02?5     KBIOST A 00?F     KBCNTR A 01?F     KEYBD  A 0·
F      KIN    C 02E?     LINCPD A 01F0
LINK   A 00F?     LIMST A 0001     MRBIT  A 00?0     MRKST  A 00CE     NAVG   D 00·
A      NAVGS  D 00?0     NAVHU C 02F1
NEGHL  C 0597     NPT   D 0014     NPTS   D 000?     PIA    A 00F4     PIB    A 00·
B      PIC    A 00F?     PICNTR A 00F7
PREAK  C 045?     RAMB  A 00ED     RCVDAT A 00EC     RDSTAT A 0040     RESET  A 0·
0      REDUP  C 0163     RDROUN C 020F
RMRON1 C 02??     RMRDUN C 01F2     REPSTR D 000?     ROM0   A 0000     ROM1   A 0·
?      ROM2   C 0?0?     ROMA  A 0C00
ROMCH  C 0??5     RON   C 0168     RUNA   C 01?9     RUN1   C 0105     SEGNO  D 0·
3      SEGSET C 00?1     SET7  A 00FF
SETSY  C 0?4?     SGEO  D 0010     SPTIM  E 0000     START  C 0000     STAWPT C 0·
S      STRPTR D 000?     STVAT C 01A?
STYUPE A 000?     SYT1  A 00AC     SYN2   A 00?7     SYNLP  C 0455     SYSFLG D 0·
?      TAVGH  C 01??     TAVG  D 0018
TIMEFG D 001?     TLOOP C 00F0     TMAIN  C 0111     TPEAK  C 001A     THNEG  D 00·
?      TSAMT  C 0??E     TSRTU C 0413
TTIME  D 001?     TUNE  C 0004     TUNELP C 00?9     TWAIT  C 00EC     TWOIN  C 0·
?      TCENT  C 0006     TXEN  A 0121
UPDISP C 02F?     WAITCM A 00?0    WAVOUT C 05?0     WNAVG  D 0017     WSYNUP C 04?
?      WCLP   C 03E?     WVOUT1 C 05AF
WVOUT2 C 05C?
ASSEMBLY COMPLETE, NO ERROR(S)
```

```
ASM80 SORIDR.TXT OBJECT (:F1:SORID2.OBJ) PRINT (:F1:SORID2.LST) NOPAGING
ISIS-II 8080/8085 ASSEMBLER, V1.0       SORID                                PAGE
 1
  LOC  OBJ          SEQ          SOURCE STATEMENT
                      0 ;           PROGRAM SORID IS A MODULE USED WITH SORTR4 A
ND DATA
                      1 ;        LIST IFLP TO PERFORM TARGET IDENTIFICATION PROCE
DURES
                      2 ;        ON EXPERIMENTAL DATA ON-SITE.
                      3 ;
                      4          NAME    SORID
                      5 ;
                      6          EXTRN   BGRIN,STRPTR,ALARM,UPDISP,NSPETC,SEQ?C
                      7          EXTRN   NEGHL,NAVGS,NAVG           ;NAVGS==NAVG
                      8 ;           DATA BUFFER STORAGE SPECIFIED IN 'SORTR4',
                      9 ;           NUM CONSTANTS SPECIFIED IN 'IFLP'.
                     10          EXTRN   NTR,MTO,MU,MMAXMA,MMAXPI,ONE,ZERO,EMIN,
MAX
                     11          EXTRN   AMIN,AMAX,MU,ALPHA,RHOTH,RHOTH
                     12 ;
                     13          PUBLIC  SRTID,OSTAT
                     14 ;
                     15          STKLN   0AH       ;ALLOTTED STACK LENGTH.
                     16 ;
                     17 ;        *** IDADD IS THE NO. OF BYTES ADDED TO
                     18 ;        *** WAVEFORM DATA RECORD OF 'SORTR4' BY
                     19 ;        *** THE IDENTIFICATION ROUTINES.
   00,9              20 IDADD    EQU     8*4+1
                     21 ;
                     22 ;        ENTRY POINT AND INITIALIZATION
                     23 ;****************
                     24 ;
                     25          CSEG    ;CODE SEG EXT
                     26 ;
  0000 21300         27 SRTID:   LXI     H,ENDADR          ;ZERO RAM LOC'S.
  0003 CD0000   E    28          CALL    NEGHL   ;FAST SHUFFLE BECAUSE ENDADR IS
  0006 EB            29          XCHG                 ; RELOCATABLE.
  0007 210000   D    30          LXI     H,I1
  000A 3600          31 ZRAM:    MVI     M,0H
  000C 23            32          INX     H
  000D E5            33          PUSH    H
  000E 19            34          DAD     D
  000F E1            35          POP     H
  0010 D20A00   C    36          JNC     ZRAM
                     37 ;
                     38 ;        *** CLEAN BUFFER AREA.
                     39 ;        *** BEWARE OF BUFFER SIZE CHANGES IN 'SORTR4'.
  0013 01B700        40          LXI     B,-DATA-1C85D   ;-(DATA+512+564-1)
  0016 210000        41          LXI     H,DATA
  0019 3600          42 ZRAM1:   MVI     M,0
  001B 23            43          INX     H
  001C E5            44          PUSH    H
  001D 09            45          DAD     B
  001E E1            46          POP     H
  001F D21900   C    47          JNC     ZRAM1
```

```
                          48 ;
                          49 ; CONVERT DIFF. WAVEFORM TO FLOATING PT FORMAT
                          50 ;  ********************************************
                          51 ;
                          52 ;
0022 2A0000     E         53 CONV1    LHLD    BGPTR
0025 EB                   54          XCHG
0026 CD0000     C         55          CALL    FLTS
0029 110022               56          LXI     D,DATA1
002C 210400     D         57          LXI     H,K1
002F CD7600     C         58          CALL    INDEX
0032 CD3500     C         59          CALL    STORE
0035 2A0000     E         60          LHLD    BGPTR
0038 23                   61          INX     H
0039 23                   62          INX     H
003A 220000     E         63          SHLD    BGPTR
003D 210400     D         64          LXI     H,K1
0040 34                   65          INR     M
0041 7E                   66          MOV     A,M
0042 FE7F                 67          CPI     127D
0044 FA2200     C         68          JM      CONV
0047 210000     D         69          LXI     H,K1
004A 3600                 70          MVI     M,0H
                          71 ;
                          72 ;
                          73 ; DETECTOR
                          74 ; ********
                          75 ;
                          76 ;
                          77 ; SEARCH FOR THE MAXIMUM TIMING
                          78 ; *****************************
                          79 ;
004C 110022               80 TMLOOP: LXI    D,DATA1     ;LOOP TO SEARCH FOR T AX
004F 210400     D         81          LXI     H,K1     ;STARTING ADDR OF D(K)B)=DATA1
0052 CD7600     C         82          CALL    INDEX    ;GET THE CURRENT SAMPLE
0055 EB                   83          XCHG
0056 E5                   84          PUSH    H
0057 46                   85          MOV     B,M      ;CHECK SIGN BIT OF SAMPLE
0058 7E                   86          MOV     A,M      ;SAVE SIGNED SAMPLE BYTE
0059 E67F                 87          ANI     7FH      ;STRIP SIGN BIT FOR ABS VALUE
005B 77                   88          MOV     M,A
005C 23                   89          INX     H
005D 23                   90          INX     H
005E 23                   91          INX     H
005F EB                   92          XCHG    ;PUT UNSIGNED SAMPLE ONTO APU STACK
0060 CD2300     C         93          CALL    PUT
0063 E1                   94          POP     H
0064 70                   95          MOV     M,B      ;RESTORE SIGNED SAMPLE
0065 110900     D         96          LXI     D,WPTR1
0068 CD3800     C         97          CALL    STORE
006B CD2900     C         98          CALL    PUT
006E 111400     D         99          LXI     D,AMPL+3     ;(AMPL)=RUNNING MAX
0071 CD2300     C        100          CALL    PUT
0074 CD5600     C        101          CALL    FSUB
0077 111500     D        102          LXI     D,AMPTEM
```

```
007A CD3800    C   103          CALL   STORE
007D 211500    D   104          LXI    H,AMPTEM
0080 7E            105          MOV    A,M
0081 B7            106          ORA    A
0082 FA9900    C   107          JM     SMALL1    ;SMALL1,UNSIGNED SAMPLE SMALLE
R THAN MAX
0085 110C00    D   108          LXI    D,MPTR1+3
0088 CD2900    C   109          CALL   PUT
008B 111100    D   110          LXI    D,AMPL
008E CD3800    C   111          CALL   STORE     ;UPDATE RUNNING MAX
0091 210400    D   112          LXI    H,K1
0094 7E            113          MOV    A,M      ;UPDATE PEAK TIMING
0095 210500    D   114          LXI    H,KMAX
0098 77            115          MOV    M,A
0099 210400    D   116 SMALL1:  LXI    H,K1
009C 34            117          INR    M
009D 7E            118          MOV    A,M
009E FE7F          119          CPI    127D
00A0 FA0C00    C   120          JM     TALOOP   ;IS SEARCH DONE?
00A3 210400    D   121          LXI    H,K1
00A6 3600          122          MVI    M,0H
00A8 211100    D   123          LXI    H,AMPL   ;ADJUST PEAK AMPL BY THE # OF
ERAGE
00AB 7E            124          MOV    A,M
00AC 17            125          RAL
00AD 210000    D   126          LXI    H,NAVG
00B0 96            127          SUB    M
00B1 96            128          SUB    M
00B2 1F            129          RAR
00B3 211100    D   130          LXI    H,AMPL
00B6 77            131          MOV    M,A
00B7 210500    D   132          LXI    H,KMAX
00BA 7E            133          MOV    A,M
00BB 210400    D   134          LXI    H,K1
00BE 77            135          MOV    M,A
                   136 ;
                   137 ;
                   138 ; ENERGY CALCULATION
                   139 ; ******************
                   140 ;
00BF 110300        141 ENLOOP:  LXI    D,DATA1+3H       ;CAL ENERGY FOR INTERV
00C2 210400    D   142          LXI    H,K1             ; (TMAX-TMAX+100)
00C5 CD7800    C   143          CALL   INDEX
00C8 CD2900    C   144          CALL   PUT
00CB 13            145          INX    D
00CC 13            146          INX    D
00CD 13            147          INX    D
00CE CD2900    C   148          CALL   PUT
00D1 CD6200    C   149          CALL   FMULT
00D4 111900    D   150          LXI    D,ENERGY+3H
00D7 CD2900    C   151          CALL   PUT
00DA CD4E00    C   152          CALL   FADD
00DD CD3800    C   153          CALL   STORE
00E0 210400    D   154          LXI    H,K1
00E3 34            155          INR    M
```

```
00E4 7E                  MOV    A,M
00E5 FE06                CPI    1020
00E7 FA0F0   C           JM     ENOUGH  ;K101027
00EA 21000   C           LXI    H,ENERGY
00ED 7E                  MOV    A,M
00EE 17                  RAL
00EF 210000  E           LXI    H,NAVG
00F2 96                  SUB    M
00F3 96                  SUB    M
00F4 96                  SUB    M
00F5 96                  SUB    M
00F6 1F                  RAR
00F7 21000   D           LXI    H,ENERGY
00FA 77                  MOV    M,A
                  ;
                  ;
                  ; THRESHOLD DETECTION
                  ; ********************
                  ;
00FB 21000   E           LXI    H,KMAXMI              ;ENERGY CAL COMPLETED
00FE 7E                  MOV    A,M                   ;START THRESHOLD DETECT
00FF 21050   D           LXI    H,KMAX
0102 BE                  CMP    M
0103 FA0001  C           JM     DST1    ;KMAX/KMAXMI,OUT OF RANGE
0106 21060   I           LXI    H,DSTAT
0109 34                  INR    M
010A C31D01  C           JMP    AMPCOM
010D 21000   E   DST1:   LXI    H,KMAXMA
0110 7E                  MOV    A,M
0111 21050   C           LXI    H,KMAX
0114 BE                  CMP    M
0115 FA1D01  C           JM     AMPCO   ;IN RANGE
0118 21060   L           LXI    H,DSTAT ;ADJUST THE STATUS REGISTER
011B 34                  INR    M
011C 34                  INR    M
011D 110301  E   AMPCOM: LXI    D,AMIN+3H
0120 CD2900  C           CALL   PUT
0123 111401  L           LXI    D,AMPL+3H
0126 CD2904  C           CALL   PUT
0129 CD3A04  C           CALL   FCMP
012C FA3901  C           JM     DST2
012F 21060   L           LXI    H,DSTAT
0132 7E                  MOV    A,M
0133 C604                ADI    4H
0135 77                  MOV    M,A
0136 C35201  C           JMP    ENCOM
0139 110400  E   DST2:   LXI    H,AMAX+3H
013C CD2901  C           CALL   PUT
013F 111400  D           LXI    D,AMPL+3H
0142 CD2904  C           CALL   PUT
0145 CD3A04  C           CALL   FCMP
0148 FA5201  C           JP     ENCOM   ;IN RANGE,GOTO CMP ENERGY
014B 210601  L           LXI    H,DSTAT
014E 7E                  MOV    A,M
```

```
014F C608          210          ADI    8H
0151 77            211          MOV    M,A
0152 110300   F    212 ENCUM:   LXI    D,EMIN+3H
0155 CD2900   C    213          CALL   PUT
0158 111000   C    214          LXI    D,ENERGY+3H
015B CD2900   C    215          CALL   PUT
015E CD0000   C    216          CALL   FCMP
0161 FA4E01   C    217          JM     USTO
0164 210000   C    218          LXI    H,DSTAT
0167 7E            219          MOV    A,M
0168 C610          220          ADI    10H
016A 77            221          MOV    M,A
016B C38701   C    222          JMP    FILTP
016E 110300   F    223 DST3:    LXI    D,EMAX+3H
0171 CD2900   C    224          CALL   PUT
0174 111000   C    225          LXI    D,ENERGY+3H
0177 CD2900   C    226          CALL   PUT
017A CD0000   C    227          CALL   FCMP
017D F28701   C    228          JP     FILTP    ;IN RANGE,GOTO FILTERING
0180 210000   C    229          LXI    H,DSTAT
0183 7E            230          MOV    A,M
0184 C620          231          ADI    20H
0186 77            232          MOV    M,A
0187 210000   C    233 FILTP:   LXI    H,DSTAT      ;PREFILTERING OPERATION
018A 7E            234          MOV    A,M      ;FILTERED WAVEFORM=(H(0)*F(KTD)
*
018B B7            235          ORA    A      ;+SUM(H(FI)*(R(KTD-FI)+R(KTD+FI))
018C CA0000   C    236          JNZ    OUTMGS      ;FI=1,2,---10
018F 210000        237 FILT:    LXI    H,DATA   ;INDEX FOR FILTERING OPR
0192 220000   C    238          SHLD   WPTR2    ;WPTR2=INDEX FOR R(T)
0195 210000   C    239          LXI    H,KI     ;KI=INDEX FOR KTD
0198 3600          240          MVI    M,0H     ;M=INDEX FOR MT
                   241 ;
                   242 ; FILTERING
                   243 ;**********
                   244 ;
019A 210000   C    245 FILTN:   LXI    H,KDAY   ;CURRENT TIME INDEX
019D 110300        246          LXI    D,DATA1+3H
01A0 CD7A00   C    247          CALL   INDEX
01A3 210000   C    248          LXI    H,KI
01A6 CD7A00   C    249          CALL   INDEX
01A9 EB            250          XCHG
01AA 220000   C    251          SHLD   WPTR1    ;WPTR1=INDEX FOR DATA,
01AD EB            252          XCHG   ;WPTR,=INDEX FOR DATA;THE PROCESSED WA
FORM
01AE CD2900   C    253          CALL   PUT      ;CAL HN(0)*R(KTD)
01B1 110300   F    254          LXI    D,H0+3H
01B4 CD2900   C    255          CALL   PUT
01B7 CD0000   C    256          CALL   FMULT
01BA 2A0000   C    257          LHLD   WPTR2
01BD EB            258          XCHG
01BE CD3400   C    259          CALL   STORE
01C1 210000   C    260 FILTM:   LXI    H,FI     ;FI=INDEX FOR FILTER COEFF(FI)
01C4 34            261          INR    M        ;FI=0,1,2,3---15
01C5 2A0000   C    262          LHLD   WPTR1    ;H=FIR COEFF:H(FI)=H(0),H(1)..
```

```
**HH(19)
    01E8 EB              263           XCHG
    01E9 210700    C     264           LXI     H,FI
    01EC CD7600    C     265           CALL    INDEX
    01EF CD2900    C     266           CALL    PUT       ;PUT R(T+FI) ONTO TOS
    01F2 13              267           INX     D
    01F3 13              268           INX     D
    01F4 13              269           INX     D
    01F5 210700    D     270           LXI     H,FI
    01F8 7E              271           MOV     A,M
    01F9 17              272           RAL                  ;GET 2*FI
    01FA 2F              273           CMA
    01FB C601            274           ADI     1H      ;-2*FI
    01FD 6F              275           MOV     L,A
    01FE 26FF            276           MVI     H,0FFH
    01F0 29              277           DAD     H
    01F1 29              278           DAD     H
    01F2 19              279           DAD     D
    01F3 EB              280           XCHG
    01F4 CD2900    C     281           CALL    PUT       ;FORM R(T+FI)+R(T-FI)
    01F7 CD4E00    C     282           CALL    FADD
    01FA 110300    C     283           LXI     D,HM+4H
    01FD 210700    D     284           LXI     H,FI
    01F0 CD7600    C     285           CALL    INDEX
    01F3 CD2900    C     286           CALL    PUT
    01F6 CD8200    C     287           CALL    FMULT
    01F9 2A0000    D     288           LHLD    WPTR2     ;FORM H(FI)*(R(T+FI)+R(T-FI))
    01FC EB              289           XCHG
    01FD 13              290           INX     D
    01FE 13              291           INX     D
    01FF 13              292           INX     D
    0200 CD2900    C     293           CALL    PUT
    0203 CD4E00    C     294           CALL    FADD      ;FORM RUNNING SUM FOR FILTERED
AMPLE
    0206 CD5900    C     295           CALL    STORE
    0209 210700    D     296           LXI     H,FI
    020C 7E              297           MOV     A,M
    020D FE12            298           CPI     12H
    020F FAC101    C     299           JM      FILTN
    0212 210700    D     300           LXI     H,FI
    0215 3600            301           MVI     M,0H      ;RESET INDICES FOR THE NXT FIL
RED SAMPLE
    0217 210400    D     302           LXI     H,K1
    021A 34              303           INR     M
    021B 2A0000    D     304           LHLD    WPTR2
    021E 23              305           INX     H
    021F 23              306           INX     H
    0220 23              307           INX     H
    0221 23              308           INX     H
    0222 220000    D     309           SHLD    WPTR2
    0225 3E64            310           MVI     A,100H      ;TAKE ALL 101 FILTERED SAMPLE
FORMED
    0227 210400    D     311           LXI     H,K1
    022A BE              312           CMP     M
    022B F29A01    C     313           JP      FILTD   ;NEXT DATA PT
```

```
022E 210400   U   IDENTP: LXI    H,K1      ;RESET INDEX FOR IDENTIFICATIO
0231 3600                 MVI    M,0H      ;K1=TIME INDEX
0233 21042?               LXI    H,DATA+3H
0236 220900   D           SHLD   WPTR1     ;WPTR1=TMAX+DATA+3H
                  ;
                  ; THE IDENTIFICATION PROCESS
                  ; **************************
                  ;
                  ;THE IDENTIFICATION PROCESS
                  ;
                  ;  1) FORM E(KTB+M0*T)=SUM(ALPHA(MT)*RM(KTB+MT))
                  ;     K=0,1,2---100,M=0,1,2----
                  ;
                  ;  2) FORM PROD=RM*(RM-E)
                  ;
                  ;  3) FORM RHO(TUI)=1-(SUM(E*E)/SUM(2*PROD)+SUM(E*E))
                  ;
                  ; ERROR FORMATION LOOP
                  ; ********************
                  ;
0239 110000   D           LXI    D,NTO     ;NTB=NUM ERROR SAMPLES
023C 210000   D           LXI    H,NTO
023F CD7E04   C           CALL   INDEX1
0242 EB                   XCHG
0243 4E                   MOV    C,M       ;(C)=# OF ERROR SAMPLES
0244 0600         MLOOP1: MVI    B,0BH     ;(B)=# OF D.E.COEFF=11
0246 2A0900   D   ELOOP1: LHLD   WPTR1
0249 EB                   XCHG
024A 210500   D           LXI    H,MT      ;MT=INDEX FOR MT,T=ITB
024D CD7E04   C           CALL   INDEX
0250 210400   D           LXI    H,K1      ;K1=INDEX FOR KTB
0253 CD7E04   C           CALL   INDEX
0256 CD2904   C           CALL   PUT
0259 110500   D           LXI    D,ALPHA+3H
025C 210C00   D           LXI    H,I1      ;I1=INDEX OF COEFF FOR DIFF TO
025F CD7E04   C           CALL   INDEX     ;I1=0,44,88,132,176 BYTES
0262 210E00   D           LXI    H,I2      ;I2=INDEX FOR COEFF FOR SAME T
0265 CD7E04   C           CALL   INDEX     ;I2=0,4,8,---40
0268 CD2904   C           CALL   PUT
026B CD6204   C           CALL   FMULT
026E 112400   D           LXI    D,ERROR+3H
0271 CD2904   C           CALL   PUT
0274 CD4E04   C           CALL   FADD
0277 CD5804   C           CALL   STORE
027A 05                   DCR    B         ;ADJUST THE M INDEX
027B CA9502   C           JZ     KLOOP     ;INSTANTANEOUS ERROR FORMED?
027E 110000   D           LXI    D,NTO     ;NTO=NTB+STB---STB
0281 210000   D           LXI    H,NTO
0284 CD7E04   C           CALL   INDEX1
0287 EB                   XCHG
0288 7E                   MOV    A,M
0289 210500   D           LXI    H,MT
028C 86                   ADD    M
028D 77                   MOV    M,A
028E 210100   D           LXI    H,I2      ;NEXT ALPHA
```

```
0291 34                  369          INR    M
0292 C34602        C     370          JMP    FLOOP   ;GET NEXT PROD TERM IN SUMMATI
0295 112400        C     371 FLOOP:   LXI    D,ERROR+3H       ;FORM SQUARE ERROR
0298 CD2904        C     372          CALL   PUT
029B 112400        C     373          LXI    D,ERROR+3H
029E CD2904        C     374          CALL   PUT
02A1 CD6B04        C     375          CALL   FMULT
02A4 111C00        C     376          LXI    D,ERROR2+3H
02A7 CD2904        C     377          CALL   PUT
02AA CD4E04        C     378          CALL   FADD
02AD CD3804        C     379          CALL   STORE   ;1 TERM IN SQUARE ERROR
02B0 110320              380          LXI    D,CATA+3H        ;FORM RM=(RM-ERROR(T))*
PUT
02B3 210400        C     381          LXI    H,K1
02B6 CD7604        C     382          CALL   INDEX
02B9 D5                  383          PUSH   D
02BA 110000        C     384          LXI    D,MO    ;MO=INDEX OF MAX MAG COEF
02BD 210200        C     385          LXI    H,MIO
02C0 CD7604        C     386          CALL   INDEX1
02C3 EB                  387          XCHG
02C4 7E                  388          MOV    A,M
02C5 210800        C     389          LXI    H,FI2
02C8 77                  390          MOV    M,A
02C9 110000        C     391          LXI    D,MIO
02CC 210200        C     392          LXI    H,MIO
02CF CD7604        C     393          CALL   INDEX1
02D2 EB                  394          XCHG
02D3 E5                  395          PUSH   H
02D4 210800        C     396          LXI    H,FI2
02D7 7E                  397          MOV    A,M
02D8 E1                  398          POP    H
02D9 D1                  399          POP    D
02DA E5                  400          PUSH   H
02DB CD7604        C     401 SULOOP:  CALL   INDEX   ;INDEX=(K1*N0+T0)
02DE E1                  402          POP    H     ;THIS LOOP CAL THE RIGHT INDEX
02DF E5                  403          PUSH   H     ;FOR ERROR NORMALIZATION
02E0 3D                  404          DCR    A     ;(INDEX=K1*N0+T0)
02E1 C2DB02        C     405          JNZ    SULOOP
02E4 E1                  406          POP    H          ;THIS KEEPS THE STACK LEVEL AT
P
02E5 CD2904        C     407          CALL   PUT
02E8 13                  408          INX    D
02E9 13                  409          INX    D
02EA 13                  410          INX    D
02EB CD2904        C     411          CALL   PUT
02EE 112400        C     412          LXI    D,ERROR+3H
02F1 CD2904        C     413          CALL   PUT
02F4 CD5304        C     414          CALL   FSUB
02F7 CD6B04        C     415          CALL   FMULT
02FA 112000        C     416          LXI    D,PROD+3H    ;PROD FORMED
02FD CD2904        C     417          CALL   PUT
0300 CD4E04        C     418          CALL   FADD
0303 CD3804        C     419          CALL   STORE
0306 2A0000        C     420          LHLD   ZERO
0309 222100        C     421          SHLD   ERROR
```

```
0310 222301   D   422          SHLD    ERROR+2H         ;RESET PARAMETERS FOR T TERM
030F 21040?   L   423          LXI     H,K1
0312 34           424          INR     M
0313 210100   L   425          LXI     H,I2
0316 3600         426          MVI     M,0
0318 210301   L   427          LXI     H,M1
0318 3600         428          MVI     M,0
0310 00           429          UCP     C
031E CA2405   C   430          JZ      RLOOP1   ;DONE WITH 1 RHO(TO) VALUE
0321 C34402   C   431          JMP     RLOOP1   ;NEXT TERM IN ERROR2
                  432 ;
                  433 ;
                  434 ; LOOP FOR NEXT VALUE OF RHO(TO)
                  435 ; *****************************
                  436 ;
                  437 ;
0324 11030?   F   438 RLOOP1: LXI      D,ONE+3H       ;CAL RHO(TO1)
0327 C02904   C   439          CALL    PUT
032A 111C0?   D   440          LXI     D,ERROR2+3H        ;CAL RHO=ERROR2/(SUM(2 ROM)+ERROR2)
0320 C02900   L   441          CALL    PUT
0330 11200?   D   442          LXI     D,PROD+3H
0333 C02904   C   443          CALL    PUT
0336 112000   I   444          LXI     D,PROD+3
0339 C02904   C   445          CALL    PUT
033C C04E03   C   446          CALL    FADD
033F 111C0?   L   447          LXI     D,ERROR2+3H
0342 C02904   C   448          CALL    PUT
0345 C04E04   C   449          CALL    FADD
0348 C06C04   C   450          CALL    FDIV     ;RHO FORMED
0348 C1583,4  C   451          CALL    FSUB
034E 11230    D   452          LXI     D,RHO
0351 21120?   D   453          LXI     H,MTO
0354 C07A0?   C   454          CALL    INDEX
0357 C05B0?   C   455          CALL    STORE
035A C09E04   C   456          CALL    RHOPP
0350 21020?   L   457          LXI     H,MTO    ;ADD PARAMETERS FOR NEXT RHO(TO)
0360 34           458          INR     M
0361 3E05         459          MVI     A,5H
0363 BE           460          CMP     M
0364 CA0000   C   461          JZ      OUTPUT   ;IF ALL 5 RHO VALUES ARE DONE,OUTPUT
0367 21000?   I   462          LXI     H,I4     ;ADD INDEX FOR NEXT SET OF ALPH
036A 3E0B         463          MVI     A,11D
036C 86           464          ADD     M
0360 77           465          MOV     M,A
036E 2A0007   F   466          LHLD    ZERO
0371 221201   L   467          SHLD    ERROR2
0374 221E0?   D   468          SHLD    ERROR2+2H
0377 221301   I   469          SHLD    PROD
037A 221F0?   I   470          SHLD    PROD+2H
0370 C3420?   C   471          JMP     IDENTH
0380 112301   D   472 OUTPUT: LXI     D,RHO+3H         ;FORM SUM RHO
```

```
0383 CD2904    C   473           CALL    PUT
038E 112C0     C   474           LXI     D,RMO+7H
0389 CD2904    C   475           CALL    PUT
038C CD4E04    C   476           CALL    FADD
038F 11D0      C   477           LXI     D,RMO+0BH
0392 CD2904    C   478           CALL    PUT
0395 11540     C   479           LXI     D,RMO+0FH
0398 CD2904    C   480           CALL    PUT
039B 1153      C   481           LXI     D,RMO+15H
039E CD2904    C   482           CALL    PUT
03A1 CD4E04    C   483           CALL    FADD
03A4 CD4E04    C   484           CALL    FADD
03A7 CD4E04    C   485           CALL    FADD
03AA 11590     C   486           LXI     D,RMO+14H
03AD CD5904    C   487           CALL    STORE
03B0 CD2904    C   488           CALL    PUT
03B3 11170     C   489           LXI     D,RMOTH+17H
03B6 CD2904    C   490           CALL    PUT
03B9 CD8604    C   491           CALL    CMP
                   492 ;
                   493 ;         *** DISPLAY 'DSTAT' ON LED'S.
                   494 ;
03BC FAE903    C   495           JM      OTHER    ;BELOW TO THRESHOLD=OTHER TARG
03BF C3CE03    C   496           JMP     TARGET
                   497 ;
                   498 ;         *** PARAMETERS OUT OF RANGE.
03C2 210600    C   499 OUTRGF:   LXI     H,DSTAT ;DISPLAY 'DSTAT' ON LEDS.
03C5 7E            500           MOV     A,M
03C6 E614          501           ANI     14H      ;CHECK FOR ENERGY AND AMPL TOO
  OW
03C8 C2FA03    C   502           JNZ     NOTARG
03CB C3E903    C   503           JMP     OTHER    ;OTHER TARGET
                   504 ;         *** MESSAGE ON LEDS ...
03CE 0602          505 TARGET:   MVI     B,2
03D0 3ECE          506           MVI     A,0CEH
03D2 CD0000    E   507           CALL    UPDISP
03D5 3EA0          508           MVI     A,0A0H
03D7 CD0000    E   509           CALL    HSPEIC
                   510 ;
03DA 210600    C   511           LXI     H,DSTAT
03DD 7E            512           MOV     A,M
03DE C640          513           ADI     40H
03E0 77            514           MOV     M,A
03E1 C30000    E   515           JMP     RESET
                   516 ;         *** MESSAGE ON LEDS 'EASI'.
03E4 0602          517 OTHER:    MVI     B,2
03E6 3EEA          518           MVI     A,0EAH
03E8 CD0000    E   519           CALL    UPDISP
03EB 3E51          520           MVI     A,051H
03ED CD0000    E   521           CALL    HSPEIC
                   522 ;
03F0 210600    C   523           LXI     H,DSTAT
03F3 7E            524           MOV     A,M
03F4 C680          525           ADI     80H
03F6 77            526           MOV     M,A
```

```
03F7 C30604  C          JMP   RESET
                ;       *** MESSAGE ON LEDS 'SAFE'
03FA 0E02       ROTARG: MVI   C,2
03FC 3E5A               MVI   A,5AH
03FE CD0000  E          CALL  UPDISP
0401 3EFE               MVI   A,0FEH
0403 CD0000  E          CALL  USPETC
                ;
0406 210000  D  RESET:  LXI   H,DSTAT
0409 0E00               MVI   C,0
040B 7E                 MOV   A,M
040C CD0000  E          CALL  UPDISP
040F 46                 MOV   B,M
0410 110000             LXI   D,0
0413 78         TAPE1:  MOV   A,B
0414 2A0000  E          LHLD  STRPTR
0417 77                 MOV   M,A
0418 23                 INX   H
0419 220000  E          SHLD  STRPTR
041C 212500  D          LXI   H,PNO
041F 19                 DAD   D
0420 46                 MOV   B,M
0421 13                 INX   D
0422 7B                 MOV   A,E
0423 FE19               CPI   .DATO
0425 FA1304  C          JM    TAPE1
                ;
0428 C9                 RET         ;RETURN TO SCHTRH
                ;
                ;
                ; SUBROUTINES
                ; ************
                ;
0429 210000     PUT:    LXI   H,0C000H
042C 1A                 LDAX  D           ;PUTS DATA INTO TOS
042D 77                 MOV   M,A         ;USES MEM ADDRESS
042E 1B                 DCX   D
042F 1A                 LDAX  D
0430 77                 MOV   M,A
0431 1B                 DCX   D
0432 1A                 LDAX  D
0433 77                 MOV   M,A
0434 1B                 DCX   D
0435 1A                 LDAX  D
0436 77                 MOV   M,A
0437 C9                 RET
0438 210000     STORE:  LXI   H,0C000H
043B 7E                 MOV   A,M         ;STORES TOS IN MEM LOCATION
043C 12                 STAX  D           ;LOC SPECIFIED BY D
043D 13                 INX   D
043E 7E                 MOV   A,M
043F 12                 STAX  D
0440 13                 INX   D
0441 7E                 MOV   A,M
0442 12                 STAX  D
```

```
0443 13              582        INX   D
0444 7E              583        MOV   A,M
0445 12              584        STAX  D
0446 C9              585        RET
0447 7E              586 WAIT:  MOV   A,M      ;INPUTS STATUS WORD OF 8
0448 E680            587        ANI   80H      ;INTO ACCULATOR AND
044A C24704    C     588        JNZ   WAIT     ;WAITS FOR APU TO FINISH
044D C9              589        RET
044E 2101E0          590 FADD:  LXI   H,0E001H
0451 3E10            591        MVI   A,10H
0453 77              592        MOV   M,A
0454 CD4704    C     593        CALL  WAIT
0457 C9              594        RET
0458 2101E0          595 FSUB:  LXI   H,0E001H
045B 3E11            596        MVI   A,11H
045D 77              597        MOV   M,A
045E CD4704    C     598        CALL  WAIT
0461 C9              599        RET
0462 2101E0          600 FMULT: LXI   H,0E001H
0465 3E12            601        MVI   A,12H
0467 77              602        MOV   M,A
0468 CD4704    C     603        CALL  WAIT
046B C9              604        RET
046C 2101E0          605 FDIV:  LXI   H,0E001H
046F 3E13            606        MVI   A,13H
0471 77              607        MOV   M,A
0472 CD4704    C     608        CALL  WAIT
0475 C9              609        RET
0476 6F              610 INDEX: MOV   L,A      ;((E)+4*((HL)) INTO DE
0477 2600            611        MVI   H,0H
0479 29              612        DAD   H
047A 29              613        DAD   H
047B 19              614        DAD   D
047C EB              615        XCHG
047D C9              616        RET
047E 7D              617 INDEX1: MOV  A,L      ;((DE)+((HL)) INTO DE
047F 83              618        ADD   E
0480 5F              619        MOV   E,A
0481 7A              620        MOV   A,D
0482 CE00            621        ACI   0H
0484 57              622        MOV   D,A
0485 C9              623        RET
0486 2101E0          624 FCMP:  LXI   H,0E001H  ;FIRST BYTE OF (NOS-TOS) I'
     0 A
0489 3E11            625        MVI   A,11H
048B 77              626        MOV   M,A
048C CD4704    C     627        CALL  WAIT
048F 111500    D     628        LXI   D,AMPTEM
0492 2100E0          629        LXI   H,0E000H
0495 CD3A00    C     630        CALL  STORE
0498 211500    D     631        LXI   H,AMPTEM
049B 7E              632        MOV   A,M
049C 07              633        RLC   A
049D C9              634        RET
049E CD2000    C     635 THRPR: CALL  PUT      ;THRESHOLD IDENTIFICATION
```

```
04A1 1185U0   E   636            LXI    D,RHCTH+3H
04A4 210U07   U   637            LXI    H,N10
04A7 CD7604   C   638            CALL   INDEX
04AA CD29,4   C   639            CALL   PUT
04AD CD8A04   C   640            CALL   FCMP
04B0 F7           641            RF
04B1 E1           642            POP    H         ;TEND STACK.
04B2 C3E404   C   643            JMP    OTHER     ;EFLOW THRESHOLD.
                  644 ;
04B5 21006E       645 FLTS:      LXI    H,0E00H
04B8 1A           646            LDAX   D
04B9 77           647            MOV    M,A
04BA 13           648            INX    D
04BB 1A           649            LDAX   D
04BC 77           650            MOV    M,A
04BD 23           651            INX    H
04BE 3E10         652            MVI    A,10H
04C0 77           653            MOV    M,A
04C1 CD4700   C   654            CALL   WAIT
04C4 C9           655            RET
                  656 ;
                  657 ;
                  658            DSEG   ;DATA SEGMENT (RAM)
                  659 ;
0000              660 I1:        DS     1
0001              661 I2:        DS     1
0002              662 FTU:       DS     1
0003              663 VT:        DS     1
0004              664 K1:        DS     1
0005              665 KMAX:      DS     1
0006              666 DSTAT:     DS     1
0007              667 F1:        DS     1
0008              668 F12:       DS     1
0009              669 WPTR1:     DS     2
000B              670 WPTR2:     DS     2
000D              671 ENERGY:    DS     4
0011              672 AMPL:      DS     4
0015              673 AMPTEM:    DS     4
0019              674 ERROR2:    DS     4
001D              675 PROD:      DS     4
0021              676 ERROR:     DS     4
0025              677 RHO:       DS     24
003D              678 ENDADR:    DS     1        ;DUMMY LOC. FOR CLEARING PURPOS
e.
                  679 ;
                  680 ;          *** THE FOLLOWING BUFFERS ARE ALSO FOUND IN
                  681 ;          *** PROGRAM 'POINTER'.
                  682 ;          *** THEY MUST BE THE SAME.
                  683            ASEG   ;ABSOLUTE SEGMENT.
2000              684            ORG    2000H
2000              685            DATA:  DS       512
2200              686            DATA1: DS       504
                  687 ;
                  688 ;          *** THE FOLLOWING CONSTANTS ARE FOUND IN
                  689 ;          *** PROGRAM 'FIELP'.
```

```
          690 1         UTR1      US        5
          691 1         MTA1      US        5
          692 1         MO1       US        5
          693 1         KMAXMA1   US        1
          694 1         KMAXMI1   US        1
          695 1         ONE1      US        4
          696 1         ZERO1     US        2
          697 1         EMIN1     US        4
          698 1         EMAX1     US        4
          699 1         AMIN1     US        4
          700 1         AMAX1     US        4
          701 1         HL1       US        76
          702 1         ALPHA1    US        22
          703 1         RHOTH1    US        2
          704 1         RHOTHA1   US        4
          705           END
PUBLIC SYMBOLS
DSTAT  D 0006    SPTIO  C 0000
EXTERNAL SYMBOLS
ALARM  E 0000    ALPHA  E 0000    AMAX   E 0000    AMIN   E 0000    HUPTR  E 0
USPETC E 0000    EMAX   E 0000
EMIN   E 0000    HN     E 0000    KMAXMA E 0000    KMAXMI E 0000    MO     E 0
MTU    E 0000    FAVG   E 0000    MTU    E 0000    ONE    E 0000    RHOTH  E 0
NAVGS  E 0000    PEGHL  E 0000    SEGNO  E 0000
RHOTHA E 0000    SEGNO  E 0000
STPPTR E 0000    UPLISP E 0000    ZERO   E 0000
USER SYMBOLS
ALARM  E 0000    ALPHA  E 0000    AMAX   E 0000    AMIN   E 0000    AMPCOM C 01
AMPL   D 0011    AMPTEM D 0015
HUPTR  E 0000    CONV   C 0022    DATA   A 2000    DATA1  A 2400    USPETC E 0
DST1   C 0100    DST2   C 0139
DST3   C 0100    DSTAT  D 0006    EMAX   E 0000    EMIN   E 0000    EMCON  C 01
EQUADR D 0120    ENERGY D 0000
ENLOOP C 0000    ERROR  D 0021    ERROR2 D 0019    FAVG   C 044E    FCMP   C 04
FDIV   C 044C    FI     D 0007
FI2    D 0002    FILT   C 01FF    FILTO  C 01FA    FILTH  C 01C1    FILTP  C 01
FITS   C 04B5    FMULT  C 04F2
FSUB   C 045    HN     E 0000    I1     D 0000    I2     D 0001    IUADD  A 0
IPENTP C 0226    INDEX  C 0474
INDEX1 C 0470    K1     D 0004    KLOOP  C 0295    KMAX   D 0006    KMAXMA E 0
KMAXMI E 0000    MO     E 0000
KLOOP  C 0200    LLOOP  C 0246    MLOOP1 C 0264    MT     C 0003    MTU    E 0
NAVG   E 0000    NAVGS  E 0000
PEGHL  E 0000    OUTARG C 05FA    MTU    D 0002    MTH    E 0000    ONE    E 0
OTHER  C 05E4    OUTPUT C 0580
OUTRGL C 04C2    PROD   D 0010    OUT    C 0429    RESET  C 0406    RHO    D 0
RHOPP  C 045C    RHOTH  E 0000
RHOTHA E 0000    RLOOP1 C 0324    SEGNO  E 0000    SMALL1 C 0099    SPTIO  C 0
STORE  C 0430    STPPTR E 0000
TAPE1  C 0413    TARGET C 05CE    TMLOOP C 00CC    UPUISP E 0000    WAIT   C 04
WPTR1  D 0000    WPTR2  D 0000
ZERO   E 0000    ZMAX   C 0000    ZMAX1  C 0019
ASSEMBLY COMPLETE, NO ERROR(S)
```

```
ASM80 IFLP2.TXT OBJECT(:F1:IFLP2.OBJ) PRINT(:F1:IFLP2.LST) NOPAGING
ISIS-II 8080/8085 MACRO ASSEMBLER, V4.0      IFLP                              PAGE
 1
  LOC  OBJ          SEQ          SOURCE STATEMENT
                     1 ;              IFLP CONTAINS THE ROM CONSTANTS FOR USE WI
H THE
                     1 ;           IDENTIFICATION ROUTINE SUBID AND SEKTRN.
                     2 ;
                     3             NAME     IFLP
                     4 ;
                     5             PUBLIC   NTBINT,MC,KMAXMA,KMAXMI,ONE,ZERO,EMIN,E
MAX
                     6             PUBLIC   AMIN,AMAX,HF,ALPHA,RHOTH,RHOTHA
                     7 ;
                     8             CSEG     ;INCLUDE WITH SOURCE CODE IN ROM.
                     9 ; THESE ARE THE ROM CONSTANTS
  0000 3D           10 NTBINT:     DB       61
  0001 33           11             DB       51
  0002 29           12             DB       41
  0003 1F           13             DB       31
  0004 15           14             DB       21
  0005 04           15 MC:         DB       4
  0006 05           16             DB       5
  0007 06           17             DB       6
  0008 07           18             DB       7
  0009 08           19             DB       8
  000A 06           20 NO:         DB       6
  000B 03           21             DB       3
  000C 06           22             DB       6
  000D 06           23             DB       6
  000E 07           24             DB       7
  000F 30           25 KMAXMA:     DB       48
  0010 0E           26 KMAXMI:     DB       14
  0011 01           27 ONE:        DB       001H,000H,000H,000H
  0012 00
  0013 00
  0014 00
  0015 00           28 ZERO:       DB       000H,000H
  0016 00
  0017 0A           29 EMIN:       DB       00AH,09FH,009H,012H
  0018 9F
  0019 09
  001A 12
  001B 11           30 EMAX:       DB       011H,0A6H,0E0H,0B3H
  001C A6
  001D E0
  001E B3
  001F 04           31 AMIN:       DB       004H,0C0H,000H,000H
  0020 C0
  0021 00
  0022 00
  0023 07           32 AMAX:       DB       007H,0A7H,0FFH,0FFH
  0024 A7
  0025 FF
  0026 FF
```

```
 56    0027 D0        33 HIT      DB    0D0H,0FCH,07AH,0E9H
 57    0028 FC
 58    0029 7A
 59    002A E9
 60    002B 7F        34          DB    07FH,080H,0C0H,013H
 61    002C 80
 62    002D C0
 63    002E 13
 64    002F F0        35          DB    0F0H,0E1H,0AEH,040H
 65    0030 E1
 66    0031 AE
 67    0032 40
 68    0033 FC        36          DB    0FCH,0F2H,030H,0FCH
 69    0034 F2
 70    0035 30
 71    0036 FC
 72    0037 F0        37          DB    0F0H,0C7H,0F8H,079H
 73    0038 C7
 74    0039 E8
 75    003A 79
 76    003B F0        38          DB    0F0H,094H,0C1H,0F6H
 77    003C 94
 78    003D C1
 79    003E F6
 80    003F F0        39          DB    0FCH,0A4H,0ECH,012H
 81    0040 A4
 82    0041 EC
 83    0042 12
 84    0043 F0        40          DB    0F0H,052H,091H,0C5H
 85    0044 52
 86    0045 91
 87    0046 C5
 88    0047 F0        41          DB    0F0H,080H,067H,005H
 89    0048 80
 90    0049 67
 91    004A 05
 92    004B FC        42          DB    0FCH,0CEH,066H,0E5H
 93    004C CE
 94    004D 66
 95    004E E5
 96    004F FC        43          DB    0FCH,0C0H,063H,017H
 97    0050 C0
 98    0051 63
 99    0052 17
100    0053 FC        44          DB    0FCH,09CH,010H,0BCH
101    0054 9C
102    0055 10
103    0056 BC
104    0057 FC        45          DB    0FCH,080H,09AH,0C7H
105    0058 80
106    0059 9A
107    005A C7
108    005B F0        46          DB    0F0H,0F5H,0C4H,0CEH
109    005C E5
110    005D C4
```

```
111    005E 0C
112    005F FF          47         DB     0FFH,000H,067H,0F7H
113    0060 00
114    0061 67
115    0062 F7
116    0063 FF          48         DB     0FFH,0ACH,0B4H,0E9H
117    0064 AC
118    0065 B4
119    0066 E9
120    0067 FF          49         DB     0FFH,09CH,015H,0E0H
121    0068 9C
122    0069 15
123    006A E0
124    006B FF          50         DB     0FFH,0A7H,05EH,0E0H
125    006C A7
126    006D 5E
127    006E E0
128    006F FA          51         DB     0FAH,0F6H,037H,094H
129    0070 F6
130    0071 37
131    0072 94
132    0073 7B          52 ALPHA:  DB     07BH,001H,06FH,0F2H
133    0074 01
134    0075 6F
135    0076 F2
136    0077 F0          53         DB     0F0H,090H,0BBH,005H
137    0078 90
138    0079 BB
139    007A 05
140    007B 7E          54         DB     07EH,0D2H,0BBH,0C7H
141    007C D2
142    007D BB
143    007E C7
144    007F FF          55         DB     0FFH,0BAH,02EH,0BAH
145    0080 BA
146    0081 2E
147    0082 BA
148    0083 D0          56         DB     0D0H,093H,0D2H,0D9H
149    0084 93
150    0085 D2
151    0086 D9
152    0087 A0          57         DB     0A0H,0CCH,0D4H,014H
153    0088 CC
154    0089 D4
155    008A 14
156    008B 00          58         DB     000H,0FFH,0FFH,0FFH
157    008C FF
158    008D FF
159    008E FF
160    008F A0          59         DB     0A0H,0F0H,0EAH,042H
161    0090 F0
162    0091 EA
163    0092 42
164    0093 00          60         DB     000H,0E2H,07AH,076H
165    0094 E2
```

```
166    0095 7D
167    0096 76
168    0097 6C           61          DB        080H,0A8H,061H,0E9H
169    0098 86
170    0099 61
171    009A E9
172    009B 7F           62          DB        07EH,0FEH,080H,099H
173    009C F5
174    009D B4
175    009E 39
176    009F 7C           63          DB        07CH,0E3H,002H,005H
177    00A0 E9
178    00A1 62
179    00A2 09
180    00A3 7D           64          DB        07BH,0CFH,0B4H,0A9H
181    00A4 CF
182    00A5 B4
183    00A6 A9
184    00A7 7F           65          DB        07EH,0A8H,0EFH,0FFH
185    00A8 A8
186    00A9 EF
187    00AA FF
188    00AB 7D           66          DB        07DH,0E8H,098H,06CH
189    00AC E8
190    00AD 99
191    00AE 6C
192    00AF 7F           67          DB        07FH,0A7H,000H,069H
193    00B0 A7
194    00B1 09
195    00B2 69
196    00B3 7E           68          DB        07EH,0E2H,021H,04FH
197    00B4 E2
198    00B5 21
199    00B6 4F
200    00B7 00           69          DB        000H,093H,001H,047H
201    00B8 93
202    00B9 01
203    00BA 47
204    00BB 7E           70          DB        07EH,0BFH,090H,0AFH
205    00BC 6F
206    00BD 51
207    00BE 3F
208    00BF 0C           71          DB        000H,0FFH,0FFH,0FFH
209    00C0 FF
210    00C1 FF
211    00C2 FF
212    00C3 F8           72          DB        0F8H,0C4H,0F8H,06DH
213    00C4 C4
214    00C5 FA
215    00C6 6D
216    00C7 0C           73          DB        000H,0F6H,04BH,0C3H
217    00C8 F6
218    00C9 4B
219    00CA C3
220    00CB 7B           74          DB        07BH,09EH,006H,004H
```

```
221   00CC 9E
222   00CD 6A
223   00CE 64
224   00CF 7D         75        DB      07CH,0ECH,0ACH,04BH
225   00D0 6F
226   00D1 6D
227   00D2 49
228   00D3 7F         76        DB      07EH,099H,06AH,0B5H
229   00D4 93
230   00D5 6A
231   00D6 65
232   00D7 7F         77        DB      07FH,090H,07DH,069H
233   00D8 6D
234   00D9 77
235   00DA E9
236   00DB 7F         78        DB      07FH,099H,049H,0EFH
237   00DC 09
238   00DD 45
239   00DE EF
240   00DF 0A         79        DB      00FH,09AH,066H,0BAH
241   00E0 9A
242   00E1 6A
243   00E2 6F
244   00E3 0F         80        DB      00FH,0C3H,0B0H,09EH
245   00E4 C3
246   00E5 6F
247   00E6 9E
248   00E7 00         81        DB      000H,0F2H,0FAH,00DH
249   00E8 F2
250   00E9 FA
251   00EA 0D
252   00EB 00         82        DB      000H,0FFH,0FFH,0FFH
253   00EC FF
254   00ED FF
255   00EE FF
256   00EF 00         83        DB      000H,0E1H,064H,076H
257   00F0 E1
258   00F1 64
259   00F2 76
260   00F3 00         84        DB      000H,09AH,07EH,01FH
261   00F4 9A
262   00F5 7E
263   00F6 1F
264   00F7 79         85        DB      079H,0C0H,0C0H,04FH
265   00F8 C0
266   00F9 C0
267   00FA 4F
268   00FB 7C         86        DB      07CH,0B0H,0B8H,092H
269   00FC B0
270   00FD B8
271   00FE 92
272   00FF 7C         87        DB      07CH,0D8H,0A1H,0BEH
273   0100 D8
274   0101 A1
275   0102 BE
```

```
0103 7E        88     DB    07EH,0E8H,0B8H,086H
0104 E8
0105 B8
0106 86
0107 7F        89     DB    07FH,0CBH,0A7H,01BH
0108 CB
0109 A7
010A 1B
010B 00        90     DB    000H,099H,090H,0A7H
010C 99
010D 90
010E A7
010F 00        91     DB    000H,0CFH,0EFH,095H
0110 CF
0111 EF
0112 95
0113 00        92     DB    000H,0FAH,0D1H,0A7H
0114 FA
0115 D1
0116 A7
0117 00        93     DB    000H,0FFH,0FFH,0FFH
0118 FF
0119 FF
011A FF
011B 00        94     DB    000H,08FH,072H,065H
011C 8F
011D 72
011E 65
011F 7F        95     DB    07FH,0A1H,03DH,086H
0120 A1
0121 3D
0122 86
0123 7E        96     DB    07EH,0ADH,08DH,0A7H
0124 AD
0125 8D
0126 A7
0127 7B        97     DB    07BH,097H,0CCH,0A5H
0128 97
0129 CC
012A A5
012B 7D        98     DB    07DH,08EH,03BH,06FH
012C 8E
012D 3B
012E 6F
012F 7E        99     DB    07EH,08AH,037H,08BH
0130 8A
0131 37
0132 8B
0133 7F        100    DB    07FH,0D5H,094H,043H
0134 D5
0135 94
0136 43
0137 00        101    DB    000H,096H,03AH,085H
0138 96
0139 3A
```

```
013A 65
013B 00        102           DB     000H,004H,040H,041H
013C 04
013D 41
013E 41
013F 00        103           DB     000H,0FFH,0FFH,0FFH
0140 FF
0141 FF
0142 FF
0143 00        104           DB     000H,0F7H,090H,089
0144 3?
0146 89
0147 00        105           DB     000H,0AAH,082H,0DCH
0148 AA
0149 82
014A DC
014B 7F        106           DB     07FH,083H,089H,0B0H
014C 83
014D 89
014E B0
014F 00        107 RHOTH1:   DB     000H,085H,0A1H,0CAH
0150 85
0151 A1
0152 CA
0153 00        108           DB     000H,0C3H,0DFH,056H
0154 C3
0155 DF
0156 56
0157 00        109           DB     000H,090H,070H,0A3H
0158 90
0159 70
015A A3
015B 00        110           DB     000H,0A0H,04FH,0DFH
015C A0
015D 4F
015E DF
015F 00        111           DB     000H,0C7H,0AEH,014H
0160 C7
0161 AE
0162 14
0163 02        112 RHOTHA:   DB     002H,0F0H,05DH,0CCH
0164 F0
0165 5D
0166 CC
               113           END
PUBLIC SYMBOLS
ALPHA  C 0073   AMAX   C 0023   AMIN   C 001F   EMAX   C 0018   EMIN   C 0?
?      HA     C 0027   KMAXMA C 000F
KMAXM1 C 001?   KO     C 000A   MTU    C 0005   NTB    C 0000   ONE    C 0?
1      RHOTH  C 014F   RHOTHA C 0163
ZERO   C 001?
EXTERNAL SYMBOLS
USER SYMBOLS
ALPHA  C 0073   AMAX   C 0023   AMIN   C 001F   EMAX   C 0018   EMIN   C 0
7      HA     C 0027   KMAXMA C 000F
KMAXM1 C 001?   KO     C 000A   MTU    C 0005   NTB    C 0000   ONE    C 0
1      RHOTH  C 014F   RHOTHA C 0163
ZERO   C 001?
ASSEMBLY COMPLETE, NO ERROR(S)
```

C. Details in Obtaining the Second Set of Identification Data With the Microcomputer System

1. Difference equation coefficients

Table 33 tabulates the difference equation coefficients used in the microcomputer system for identification of the mine-like target.

2. Detection thresholds (R_{ID}=30 cm)

t_{MAX} RANGE = 14,49 (T_B)

MAX RANGE = 12,82

E_M RANGE = 0.639, 0.862

The same detection thresholds were used for identification of the mine-like target in both ground conditions.

3. Identification thresholds (R_{ID}=30 cm)

Table 34 tabulates the identification thresholds for identification of the mine-like target in the two different ground conditions.

TABLE 33
DIFFERENCE EQUATION COEFFICIENTS USED IN THE MICROCOMPUTER SYSTEM FOR IDENTIFICATION OF THE MINE-LIKE TARGET

T[illegible]	[illegible]		[illegible]		[illegible]		71E		8TE	
[illegible]	[illegible]		[illegible]		[illegible]		[illegible]		7	
ALPHA(0)	[illegible]	-1	[illegible]	-1	.19[illegible]341[illegible]	-1	.5[illegible]022[illegible]3[illegible]	-2	.2650342[illegible]	-2
ALPHA(1)	-.77[illegible]267[illegible]	-1	.25[illegible]72E	-1	.69[illegible]44[illegible]E	-1	.3455644E	-1	.1653016[illegible]	-1
ALPHA(2)	[illegible]	[illegible]	.167[illegible]77E	[illegible]	.14[illegible]915[illegible]	0	.1057155E	0	.6544963[illegible]	-1
ALPHA(3)	[illegible]	[illegible]	.11[illegible]	[illegible]	.27[illegible]336[illegible]	0	.2269002E	0	.1799[illegible]	0
ALPHA(4)	[illegible]	[illegible]	.32776[illegible]	[illegible]	.42[illegible]922[illegible]	[illegible]	.3977593E	0	.3565959[illegible]	0
ALPHA(5)	[illegible]	[illegible]	[illegible]	[illegible]	[illegible]	[illegible]	.5936[illegible]55E	0	.5868457[illegible]	[illegible]
ALPHA(6)	.1[illegible]	1	.5774121[illegible]	[illegible]	.7[illegible]6775[illegible]	[illegible]	.[illegible]124438[illegible]	0	.[illegible]2931[illegible]	0
ALPHA(7)	-.951[illegible]	[illegible]	.1[illegible]737[illegible]	[illegible]	[illegible]9[illegible]	[illegible]	.9797616E	0	.100[illegible]	1
ALPHA(8)	[illegible]	[illegible]	.100[illegible]	1	.1[illegible]	1	.1000[illegible]09E	1	.567[illegible]	0
ALPHA(9)	-.5[illegible]	[illegible]	-.[illegible]	-1	.[illegible]4697[illegible]	[illegible]	.7476412E	0	.6[illegible]	0
ALPHA(10)	[illegible]	[illegible]	.[illegible]2[illegible]47[illegible]	0	.5878[illegible]2[illegible]	[illegible]	.3149249E	0	.2[illegible]056[illegible]	0

TABLE 34
IDENTIFICATION THRESHOLDS FOR THE IDENTIFICATION OF THE MINE-LIKE TARGET WITH THE MICROCOMPUTER SYSTEM

$\rho_{T_{oi}}$ / GROUND	$\rho_{T_{01}}$ $T=4T_B$	$\rho_{T_{02}}$ $T=5T_B$	$\rho_{T_{03}}$ $T=6T_B$	$\rho_{T_{04}}$ $T=7T_B$	$\rho_{T_{05}}$ $T=8T_B$	$<(\rho_{T_0})>$
CONDITION 1 (TUNED)	.522	.801	.615	.677	.780	.79177
CONDITION 2 (UNTUNED)	.500	.500	.250	.125	.500	.40000

APPENDIX J

Table 35 tabulates the extracted resonances and their corresponding residues of the thin-wire (30cm long, 5cm deep) waveform.

Table 35
EXTRACTED RESONANCES FROM THE 30cm LONG, 5cm DEEP THIN WIRE
ANTENNA LOCATION = CENTER OF WIRE

POLE * (REAL)	POLE (IMAG)	RESIDUE (REAL)	RESIDUE (IMAG)
-.1308792E 9	-.2243403E 9	-.1708435E 0	.6741198E-1
-.4685945E 9	.2800813E 9	.1377038E 1	-.2542809E 1
-.2156001E 9	.7260306E 8	.2210962E 0	.1263321E 1
-.4685945E 9	-.2800813E 9	.1377038E 1	.2542809E 1
-.2156001E 9	-.7260306E 8	.2210962E 0	-.1263321E 1
-.1708076E 9	.3030841E 9	.5459014E-1	.2335131E 0
-.1209931E 9	.1126777E 9	-.9631155E 0	-.2862594E 1
-.1209931E 9	-.1126777E 9	-.9631167E 0	.2862594E 1
-.1708073E 9	-.3030841E 9	.5459009E-1	-.2335131E 0
-.1308792E 9	.2243403E 9	-.1708435E 0	-.6741193E-1
-.6272871E 0	.1839096E-2	-.2458968E-1	-.4475425E-7

PARAMETERS: N=11, IBS=7, M=2, III=4, ε=0.391E-2

Two pairs of poles appear to have dominant residues, namely the pole pairs at 280 MHz and 112 MHz. However, the pole pair at 280 MHz has a much more negative real part, thus, in the late-time region, only the pole pair at 112 MHz is dominant.

Table 36 tabulates the extracted resonances and their corresponding residues from the 30cm long on-surface wire.

In the early-time region, the pole pair at 302 MHz is dominant.

---

* Real Part in Nepers/s. Imaginary part in Hz.

TABLE 36
EXTRACTED RESONANCES AND FROM THE ON-SURFACE THIN WIRE
(30cm LONG). ANTENNA LOCATION = CENTER OF WIRE

POLE* (REAL)	POLE (IMAG)	RESIDUE (REAL)	RESIDUE (IMAG)
-.1462028E10	.0000000E 1	.2469165E 1	.6242044E-7
-.3449277E 9	-.3023622E 9	.1591370E 1	-.1711432E 1
-.3449277E 9	.3023622E 9	.1591370E 1	.1711432E 1
-.1003984E 9	-.2404006E 9	-.1003876E 0	.1049173E-1
-.2344375E 9	.4529953E 9	-.2735412E 0	.1113815E-1
-.4641263E 8	.6872750E 8	-.6308170E-1	.7273762E-1
-.2344375E 9	-.4529953E 9	-2.035411E 0	-.1113816E-1
-.1003984E 9	.2404006E 9	-.1003877E 0	-.1049174E-1
-.3901977E 8	-.1401513E 9	-.2077824E-1	-.2096944E-1
-.3901977E 8	.1401513E 9	-.2077823E-1	.2096944E-1
-.3232055E 9	.3787546E 9	-.3689420E 0	-.6241565E 0
-.3232055E 9	-.3787546E 9	-.3680420E 0	.6241565E 0
-.4641263E 8	-.6872750E 8	-.6308171E-1	-.7273761E-1

PARAMETERS: N=13, IBS=5, M=2, III=1, ε=0.3839075E-3

*Real part in Nepers/s. Imaginary part in Hz.